Characterisation of a family of novel glycosyltransferases from enteropathogenic *Escherichia coli* and *Salmonella*

by

Tania Wong Fok Lung

Submitted in total fulfillment of the requirements of the degree of Doctor of Philosophy

June 2016

(Produced on archival quality paper)

Department of Microbiology and Immunology at the Peter Doherty Institute for Infection and Immunity

The University of Melbourne

I dedicate this thesis to my parents, Benoit and Gloria Wong.

Abstract

Enteropathogenic *Escherichia coli* (EPEC) is a diarrhoeal pathogen of children that utilises a type III secretion system (T3SS) to inject virulence effector proteins into enterocytes during infection. NleB1 is a novel glycosyltransferase effector from EPEC that catalyses the addition of a single GlcNAc moiety in an *N*-glycosidic linkage to arginine. NleB1 modifies arginine-117 (Arg^{117}) of the Fas associated death domain (DD) protein, FADD, which prevents assembly of the canonical death inducing signalling complex (DISC) and inhibits FasL-induced cell death. NleB1 also modifies the equivalent arginine residues in the DD proteins, tumour necrosis factor receptor type 1 (TNFR1)-associated death domain (TRADD) and receptor-interacting protein kinase 1 (RIPK1).

Apart from the DxD catalytic motif of NleB1, little is known about other functional sites in the protein and the regions required for substrate binding and specificity. Here a library of 22 random transposon-based, in-frame, linker insertion mutants of NleB1 were tested for their ability to block caspase-8 activation in response to FasL during EPEC infection. Immunoblot analysis of caspase-8 cleavage products showed that 14 mutant derivatives of NleB1 no longer inhibited caspase-8 activation, including the catalytic DxD mutant. Regions of interest around the linker insertion sites were examined further with multiple or single amino acid substitutions. Coimmunoprecipitation studies of 34 site-directed mutants showed that the NleB1 derivatives with the E253A, Y219A, and PILN(63– 66)AAAA (in which the PILN motif from residues 63 to 66 was changed to AAAA) mutations bound to but did not GlcNAcylate FADD. A further mutant derivative, the PDG(236 –238)AAA mutant, did not bind to or GlcNAcylate FADD. Further testing of these mutants with TRADD and RIPK1, showed that NleB1 bearing the mutations E253A and Y219A could still bind to FADD and RIPK1 but not to TRADD. Infection of mice with the EPEC-like mouse pathogen *Citrobacter rodentium* expressing $NleB_{E253A}$ and $NleB_{Y219A}$ showed that these 2 strains were attenuated, indicating the importance of the residues E253 and Y219 in NleB1 virulence *in vivo*. In summary, we identified new amino acid

residues critical for NleB1 activity and confirmed that FADD GlcNAcylation was critical for NleB1 function.

Close homologues of NleB1 are found in *Salmonella enterica* serovar Typhimurium and these are termed SseK1, SseK2 and SseK3. We hypothesized that the SseK effectors would also bind to DD proteins and inhibit apoptotic or inflammatory signalling. The SseK effectors did not appear to play a strong role in the inhibition of death receptor signaling given that we could not detect binding of the SseK effectors to the death domain proteins FADD, TRADD and RIPK1, which are targets of NleB1. A further survey of DD proteins revealed that SseK3 bound to TNFR1. However *S.* Typhimurium did not appear to inhibit TNF-induced IL-8 production and the biological significance of this interaction is still unknown. We conclude that the SseKs have an alternative function during *S.* Typhimurium infection to NleB1 in EPEC.

Declaration

This is to certify that:

i. The thesis comprises only my original work towards the Ph.D except where indicated in the Preface,
ii. Due acknowledgement has been made in the text to all other material used,
iii. The thesis is fewer than 100 000 words in length, exclusive of tables, maps, bibliographies, and appendices.

……

Tania Wong Fok Lung, B.Biomed., B.Sc. Honours
Department of Microbiology and Immunology at the
Peter Doherty Institute for Infection and Immunity,
The University of Melbourne

Preface

In accordance with the regulations of The University of Melbourne, I acknowledge that some of the work presented in this thesis was collaborative.

In chapter 3, Kristina Creuzburg assisted with the construction of the transposon mutants.

In chapters 3 and 5, Michelle Kelly made the constructs pET28a-FADD, pGEX-NleB1 and pEGFP-C2-SseK1. Cristina Giogha constructed pET28a-TRIM32 and pGEX-SseK3 and assisted with the protein purification of His-FADD, GST-NleB1, GST-NleB1 mutants, His-TRIM32 and GST-SseK3. The constructs pEGFP-C2-NleB1$_{DxD(221\text{-}223)AxA}$ and pEGFP-C2-NleB2$_{DxD(221\text{-}223)AAA}$ were made by Jaclyn Pearson. Rohan Teasdale donated the construct pcDNA-TRIM32. Wild type *Salmonella* Typhimurium SL1344 and the derivatives Δ*sseK1*, Δ*sseK2*, Δ*sseK3*, Δ*sseK1/2/3* were provided by Nathaniel Brown. Dick Strugnell donated the *Salmonella* Typhimurium SL1344 derivatives Δ*invA* and Δ*ssaR*.

In chapters 4 and 5, the constructs pGADT7-DD TRADD, pGADT7-DD MyD88, pGADT7-DD IRAK1 and pGADT7-DD IRAK4 were made by Clare Oates and the *Citrobacter rodentium* Δ*nleB* mutant was constructed by Valérie Crepin. Sze Ying Ong, Ka Yee Fung and Jaclyn Pearson assisted with the infection of mice. Georgina Pollock assisted with the caspase-8 immunoblot in Figure 4.10.

In chapter 5, André Mu and Danielle Ingle constructed the phylogenetic trees.

The remainder of this thesis comprises only my original work.

List of publications arising from this thesis

This thesis contains material that is published or is currently in preparation for publication:

Pearson, JS, Giogha, C, Ong, SY, Kennedy, CL, Kelly, M, Robinson, KS, **Wong Fok Lung, T**, Mansell, A, Riedmaier, P, Oates CVL, Zaid, A, Mühlen, S, Crepin, VF, Marchès, O, Ang CS, Williamson, NA, O'Reilly, LA, Bankovacki, A, Nachbur, U, Infusini, G, Webb, AI, Silke, J, Strasser, A, Frankel, G and Hartland, EL (2013) A type III effector antagonises death receptor signalling during bacterial gut infection. *Nature* 501:247-251

Giogha, C, **Wong Fok Lung, T**, Pearson, JS and Hartland, EL (2014) Inhibition of death receptor signaling by bacterial gut pathogens. *Cytokine & Growth Factor Reviews* 25:235-243

Wong Fok Lung, T, Pearson, JS, Schuelein, R and Hartland, EL (2014) The cell death response to enteropathogenic *Escherichia coli* infection. *Cellular Microbiology* 16:1736-1745

Yang, Z, Soderholm, A, **Wong Fok Lung, T**, Giogha, C, Hill, MM, Brown, NF, Hartland EL and Teasdale, RD (2015) SseK3 is a novel *Salmonella* effector that binds TRIM32 and modulates the host pro-inflammatory immune response. *PLoS ONE* 10(9): e0138529

Wong Fok Lung, T, Giogha, C, Creuzburg, K, Ong, SY, Pollock, GL, Zhang, Y, Fung, KY, Pearson, JS and Hartland, EL (2016) Mutagenesis and functional analysis of the bacterial arginine glycosyltransferase effector NleB1 from enteropathogenic *Escherichia coli*. *Infection and Immunity* doi 10.1128/IAI.01523-15

Other publications arising from candidature:

Giogha, C, **Wong Fok Lung, T,** Mühlen, S, Pearson, JS and Hartland, EL (2015) Substrate recognition by the zinc metalloprotease effector NleC from enteropathogenic *Escherichia coli*. *Cellular Microbiology* doi: 10.1111/cmi.12469

In preparation:

Pearson, JS, Mühlen, S, Giogha, C, Nachbur, U, **Wong Fok Lung, T**, Oates, CV, Ingle, D, Hilderbrand, J, Dagley, L, Bankovacki, A, Schroeder, G, Frankel, G, Masters, S, Vince, J, Webb, A, Silke, J and Hartland, EL (2016) A bacterial cysteine protease effector cleaves RHIM proteins to block necroptosis and inflammation. *In preparation for Nature*

Acknowledgements

I would first like to thank my supervisor, Liz, for giving me the opportunity to work in her laboratory over the last few years. Her enthusiasm and sharpness in the challenging field of bacterial pathogenesis have inspired me and motivated me in my research. Thank you for your confidence in my abilities, for giving me carte blanche when I needed to go overseas to take care of my ailing father and for welcoming me back with open arms after my leave of absence. It was comforting to know that I did not have to worry about my work during those trying times.

I would also like to thank my co-supervisor, Roy. His vast knowledge and positive outlook on everything, be it on science or life in general, have always been very refreshing. Thank you for all I have learnt during my honours year in your laboratory. The knowledge and experience I have gained during my training in the Robins-Browne laboratory have been instrumental for me in terms of my education as a hands-on scientist. Thank you for the support and encouragement during my PhD.

I am grateful to all the members of the Hartland laboratory, past and present, for their scientific advice and friendship. I would especially like to thank Jac for giving me the chance to work alongside her on exciting projects outside my own work, for providing me with technical help and for her funny impromptu karaokes to Laura Branigan's 80s hit 'Gloria'. Special thanks to Kristina Creuzburg, who helped me finish the construction of my library of transposon mutants while I was on my leave of absence. I will be forever grateful. I would also like to thank Cristina Giogha, my confidante and closest friend in the lab, Ka Yee Fung, Ying Ong, Ying Zhang, Yoghi Srikantha and Gina Pollock for lending me a shoulder to cry on and for their continuous encouragement and assistance. I am also thankful to Sau Fung Lee for sharing with me her invaluable knowledge on yeast two-hybrid screening, to Josh Newson, Clare Oates, Ralf Schuelein, Catherine Kennedy, Sabrina Mühlen, Abdou Hachani, Bettina Wright, Simon Belluzzo, Vicky Bennett-Wood and Patrice Newton for their technical assistance and friendship.

I would like to extend my thanks to the members of the BioResource Facility, particularly Tom Cumming and Alison Rotherham for keeping an eye on my mice, to Nat Brown and Tim Scott for answering my numerous *Salmonella*-related questions, to Rebecca Whitsed Short for all the administrative paperwork and encouragement, to my PhD committee members Dick Strugnell and Sammy Bedoui for their feedback at every meeting, to Danielle Ingle for helping me with the phylogenetic trees and to the teaching staff who gave me the opportunity to teach. I am also thankful to Zhe Yang and Rohan Teasdale from the University of Queensland for a wonderful and fruitful collaboration.

I am grateful to my dearest friends. André Mu, Toshiki Sekiya, Michelle Nguyen and Edin Mifsud, thank you for all the dinners and drinks we have had together and for our friendship that dates back to undergraduate days or Honours year. It is comforting to know that we have each other's back. Inês Sa Almeida and Tony Svasek, whom I met at my dance school over three years ago, thank you for all the wonderful times we have shared at the dance studio, for your consistent encouragement, for buying me hot chocolates and cocktails and for putting up with me especially during this past year.

Above all, I would like to thank my family, who from the other side of the world, have been unwavering in their support, patience and encouragement. Mum and Dad, I will be forever grateful for all the sacrifices you have both made to send me to Australia so I could do what makes me happy. To my Dad, who is now watching over me from a better place, thank you for raising me to be an independent woman, for believing in me and in all I undertake and for being my number one fan! To my Mum, thank you for all the pep talks and for being an example of courage by rising up to all of life's challenges after losing Dad. A special mention to my brother Tim who has taken good care of me and cooked me delicious meals when I was busy doing lab work until late. Thank you Tim for your support. And finally, I would like to thank John for patiently listening to my concerns and fears, for talking me through my insecurities and for believing in me.

Abbreviations

The following abbreviations have been used throughout the thesis:

%	Percentage
°C	Degrees celsius
A/E	Attaching and effacing
AA	Aggregative adherence
AAF	Aggregative adherence fimbria
Ade	Adenine
aEPEC	Atypical enteropathogenic *Escherichia coli*
Amp	Ampicillin
Arp	Actin-related protein
ATP	Adenosine triphosphate
Bfp	Bundle-forming pilus
BI	Bax inhibitor
BLAST	Basic Local Alignment Search Tool
BSA	Bovine serum albumin
cDNA	Complementary deoxyribonucleic acid
CF	Colonisation factor
CFA	Colonisation factor antigen
CFTR	Cystic fibrosis transmembrane conductance regulator
CFU	Colony forming unit
cIAP	Cellular inhibitor of apoptosis protein
Cm	Chloramphenicol
CMP	Cytidine 5'-monophosphate
CRKL	v-Crk sarcoma virus CT10 oncogene-like protein
CSN5	COP9 signalosome subunit 5
DAEC	Diffusely adherent *Escherichia coli*
DAF	Decay-accelerating factor
DC	Dendritic cell

DD	Death domain
DDO	Double drop out
DISC	Death inducing signaling complex
DMEM	Dulbecco's modified Eagle's medium
DMSO	Dimethyl sulfoxide
DNA	Deoxyribonucleic acid
DR	Death receptor
DTT	Dithiothreitol
EAEC	Enteroaggregative *Escherichia coli*
EAST	Enteroaggregative *Escherichia coli* ST
EDTA	Ethylenediaminetetraacetic acid
eEF1A	Eukaryotic translation elongation factor 1 alpha 1
EF	Elongation factor
EGFP	Enhanced green fluorescent protein
EHEC	Enterohaemorrhagic *Escherichia coli*
EIEC	Enteroinvasive *Escherichia coli*
EPEC	Enteropathogenic *Escherichia coli*
ER	Endoplasmic reticulum
ERK	Extracellular signal-regulated kinase
ETEC	Enterotoxigenic *Escherichia coli*
F	Forward
F-actin	Actin filament or filamentous actin
FADD	Fas-associated protein with death domain
FAK	Focal adhesion kinase
FAS	Fluorescent actin staining
FASP1	FAPP-1 associated protein 1
FBOX22	F-box only protein 22
FBS	Foetal bovine serum
Fuc	Fucose
g	Gram

Gal	Galactose
GalNAc	*N*-acetyl galactosamine
GALT	Gut-associated lymphoid tissue
GAP	GTPase-activating protein
GAPDH	Glyceraldehyde 3-phosphate dehydrogenase
Gb3	Globotriosylceramide
Gb4	Globotetraosylceramide
gDNA	Genomic deoxyribonucleic acid
GDP	Guanosine diphosphate
GEF	Guanine nucleotide exchange factor
GFP	Green fluorescent protein
Glc	Glucose
GlcNAc	*N*-acetyl glucosamine
GST	Glutathione S-transferase
GT	Glycosyltransferase
h	Hours
H_20	Water
HC	Haemorrhagic colitis
His	L-histidine
HIV	Human immunodeficiency virus
HPLC-ESI	High performance liquid chromatography-electrospray ionisation
HRP	Horseradish peroxidase
HUS	Haemolytic uraemic syndrome
IE	Integrative element
IFN	Interferon
IFNG/IFNγ	Interferon gamma
IKK	IκB kinase
IL	Interleukin
ILK	Integrin-linked kinase
IP	Immunoprecipitation or immunoprecipitate

IPTG	Isopropyl β-D-1 thiogalactopyranoside
IRAK1	Interleukin-1 receptor-associated kinase 1
IRAK4	Interleukin-1 receptor-associated kinase 4
ITIM	Immunoreceptor tyrosine-based inhibitory motif
IκB	Inhibitor of NF-κB
JAB1	Jun activation domain-binding protein 1
JNK	c-Jun N-terminal kinase
Kan	Kanamycin
LB	Luria-Bertani
LDS	Lithium dodecyl sulphate
LEE	Locus of enterocyte effacement
Leu	L-leucine
Lgt	*Legionella pneumophila* glucosyltransferase
LPS	Lipopolysaccharide
LT	Heat-labile toxin (ETEC) or lethal toxin (*C. difficile*)
M	Molar
Man	Mannose
MAPK	Mitogen-activated protein kinase
MAPKK	MAPK kinase
MAPKKK	MAPKK kinase
MEGA5	Molecular Evolutionary Genetic Analysis 5
Met	L-methionine
min	Minutes
ml	Millilitre
MLKL	Mixed lineage kinase domain-like
MLN	Mesenteric lymph node
mm	Millimetre
mM	Millimolar
MMP	Mitochondrial membrane potential
MOI	Multiplicity of infection

mRNA	Messenger ribonucleic acid
MS	Mass spectrometry
MyD88	Myeloid differentiation primary response 88
N-WASP	Neural Wiskott-Aldrich syndrome protein
NAD	Nicotinamide adenine dinucleotide
Nal	Nalidixic acid
NC	Needle complex
NCBI	National Centre for Biotechnology Information
NEMO	NF-κB essential modulator
NeuAc	N-acetylneuraminic acid
NF-κB	Nuclear factor-κB
ng	Nanogram
NGT	*N*-linked asparagine glycosyltransferase
NIK	NF-κB-inducing kinase
NK	Natural killer
NKT	Natural killer T
Nle	Non-LEE encoded
NLR	NOD-like receptor
NLS	Nuclear localisation signal
nm	Nanometre
NMR	Nuclear magnetic resonance
NOD	Nucleotide-binding oligomerisation domain
Nramp1	Natural resistance-associated macrophage 1
NTS	Non-typhoidal *Salmonella*
NZF	Npl4 zinc finger domain
OD	Optical density
OGT	*O*-GlcNAc transferase
OI	O-island
ORF	Open reading frame
PAI	Pathogenicity island

PAMP	Pathogen associated molecular pattern
PaTox	*Photorhabdus asymbiotica* protein toxin
PBS	Phosphate buffered saline
PCR	Polymerase chain reaction
pEAF	EPEC adherence factor plasmid
PEG	Polyethylene glycol
PFA	Paraformaldehyde
PIPES	Piperazine-N, N'-bis (2-ethanesulfonic acid)
PMN	Polymorphonuclear neutrophil
PP	Prophage
PRR	Pattern recognition receptor
psi	Pounds per square inch
QDO	Quadruple drop out
R	Reverse
RAxML	Randomized Axelerated Maximum Likelihood
RBS	Ribosome binding site
REPEC	Rabbit specific EPEC
RHIM	Receptor-interacting protein homotypic interaction motif
RHIM	RIP homotypic interaction motif
RIG	Retinoic acid-inducible gene
RIPA buffer	Radioimmunoprecipitation assay buffer
RIPK1	Receptor- interacting protein kinase 1
RIPK3	Receptor- interacting protein kinase 3
RNA	Ribonucleic acid
rpm	Revolution per minutes
rRNA	Ribosomal ribonucleic acid
RT	Room temperature
SCV	*Salmonella* containing vacuole
SD	Synthetic dextrose
SDS	Sodium dodecyl sulphate

ShET1	*Shigella* enterotoxin 1
Sif	*Salmonella*-induced filament
Skp1	S-phase kinase-associated protein 1
SOB	Super optimal broth
SOC	Super optimal broth with catabolite repression
SPF	Specific pathogen free
ssDNA	Single stranded deoxyribonucleic acid
Sse	*Salmonella* secreted effector
ST	Heat-stable toxin
STEC	Shiga toxin-producing *Escherichia coli*
Strep	Streptomycin
Stx	Shiga toxin
T3SS	Type III secretion system
TAB	TAK1-binding protein
TAD	Transcription activation domain
TAE	Tris-acetate-EDTA
TAK1	TGF-β-activated kinase 1
TBS	Tris buffered saline
TDO	Triple drop out
Tet	Tetracycline
Tir	Translocated intimin receptor
TLR	Toll-like receptor
TNF	Tumour necrosis factor
TNFR	TNF receptor
TPR	Tetratricopepetide repeat
TRADD	Tumour necrosis factor receptor type 1-associated death domain
TraDIS	Transposon-directed insertion site-sequencing
TRAF	TNFR-associated factor
TRAIL	Tumour necrosis factor-related apoptosis-inducing ligand
TRAIL-R	TRAIL receptor

TRIM32	Tripartite motif 32
Trp	L-tryptophan
U	Units
UDP	Uridine diphosphate
Ura	Uracil
UV	Ultraviolet
v/v	Volume by volume
VTEC	Verotoxigenic *Escherichia coli*
w/v	Weight by volume
WCL	Whole cell lysate
XIAP	X-linked inhibitor of apoptosis
Y2HS	Yeast two-hybrid screen
YMM	Yeast nitrogen minimal medium
YPD	Yeast extract peptone dextrose
µg	Microgram
µl	Microlitre
µm	Micrometre

Table of contents

List of figures

List of tables

Chapter 1

Literature review

Chapter 1: Literature review

1.1 Introduction

Pathogen exposure can result in a variety of infections. Diarrhoea, which arises from gastrointestinal infections, is a major cause of morbidity and mortality, particularly in young children in developing countries (1, 2). According to a recent study, an estimated 6.3 million children worldwide died before the age of 5 in 2013, with the majority of deaths occurring in sub-Saharan Africa and southern Asia (3). Roughly half of those deaths were associated with infectious diseases, of which diarrhoea was the second leading cause (1).

The aetiologic agents of diarrhoea include a wide array of pathogens ranging from viruses to bacteria and parasites that are transmitted from the stool of an infected individual to the mouth of another individual (4). This is termed the faecal to oral transmission. Among the most common bacterial enteric pathogens are *Escherichia coli*, *Salmonella* species, *Shigella* species, *Campylobacter jejuni* and *Vibrio cholerae*. These differ in their pathogenic mechanisms and in the number of organisms needed to cause disease (infectious dose). For example, *Shigella* species are resistant to low pH and have an infectious dose as low as 10 organisms (5, 6). In contrast, *Vibrio cholerae* is acid sensitive and a larger infectious dose is required to cause illness. An early study by Cash *et al*. showed that 10^8 *V. cholerae* were required to cause illness in volunteers and that higher doses up to 10^{11} organisms were required when volunteers were not fed sodium bicarbonate (7).

1.1.1 *Escherichia coli* and 'summer diarrhoea'

Escherichia coli is a Gram-negative, facultative anaerobic bacillus belonging to the family of Enterobacteriaceae from the class of Gammaproteobacteria. It was first described by Theodore Escherich, in 1885 as *Bacterium coli commune* and believed to be the predominant microorganism in the human gut (reprinted in English (8)). It is now known that *E. coli* constitutes 0.1% of the human gut microbiome (9, 10), which

benefits humans by providing additional nutrition and by acting as a barrier against gut pathogens (11). Escherich showed that *E. coli* could cause disease in rabbits but failed to demonstrate its role as a human pathogen (8). However in 1889, Laurelle suggested that *E. coli* was a gastrointestinal pathogen (12) and in 1897, Lesage suggested that there were both pathogenic and non-pathogenic strains of *E. coli* (13).

Diarrhoea decimated the young population of Europe during the summer months in the 17th century and was termed 'summer diarrhoea', 'cholera infantum' or 'griping of the guts' (14). 'Summer diarrhoea' was characterised by apparently stable infants becoming critically ill and on the verge of death within hours. Physician Benjamin Rush reported similar cases in 1773 in America and this was considered the first written report of 'summer diarrhoea' (14). The cause of 'summer diarrhoea' and its high infectivity in children under the age of two was completely unknown for decades (15). The aetiology of the disease was suspected to be of bacterial nature but attempts to isolate a recognised bacterial pathogen were unsuccessful. However, a characteristic seminal smell from the 'summer diarrhoea' patients was observed by English paediatrician Dr Beavan (16), which prompted his colleague, John Bray to associate *Escherichia coli* with 'summer diarrhoea'. It was only in 1945 that Bray proved in a landmark paper that *E. coli,* then known as *Bacterium coli*, was the cause of 'summer diarrhoea' (17). Bray observed that culture plates of *Bacterium coli* from 'summer diarrhoea' patients, which was then considered as normal flora, also had this characteristic smell (16). No dysentery bacilli or *Salmonella* were recovered from these patients (16). Bray was able to raise antisera against this specific *Bacterium coli* that agglutinated bacteria isolated from faecal samples of infants with 'summer diarrhoea' but not bacteria from healthy infants (17). Bray and Beavan then developed a method to differentiate pathogenic from non-pathogenic *E. coli* using antibodies raised from an infant suffering from 'summer diarrhoea' in slide agglutination assays (18).

1.1.2 Typing scheme for *E. coli*

Bray's discovery was corroborated by other groups, establishing *E. coli* as the causative agent of 'summer diarrhoea' in infants (19-22). However, as more pathogenic strains of *E. coli* were discovered, they were annotated differently, resulting in confusion and underlying the need for a standardised annotation scheme. This was resolved when Kauffmann established a serotyping scheme for *E. coli* based on the surface O (somatic) and H (flagellar) antigens (23). The O antigen refers to the oligossacharides of the lipopolysaccharide (LPS) and the H antigen is based on the flagellar proteins. A combination of O and H antigens defines the serotype of the *E. coli*. At present, more than 180 O and 60 H serogroups have been recognised. This typing scheme was originally designed by Kauffmann and White to type *Salmonella enterica* strains (24). The *Salmonella* typing scheme has been revised and updated to avoid confusion and make it amenable to the large number of *Salmonella enterica* strains that have been isolated to this date (25, 26). Eventually the strain of *E. coli* identified by Bray was found to belong to serogroup O111. The *E. coli* serotyping scheme proved to be useful given that various *E. coli* strains that have been isolated from cases of infantile diarrhoea in the 1940s belonged to only a small number of O serogroups. These serogroups were O26, O55, O111, O119, O127, O128 and O142 (21, 27, 28).

The term 'enteropathogenic *E. coli*' (EPEC) was coined in 1955 by Neter *et al*. to refer to *E. coli* strains that caused gastrointestinal disease and that were not isolated from faeces of healthy patients (29). Owing to a lack of identifiable virulence markers, biochemical and microbiological assays could not be used to distinguish what was then known as EPEC from the strains of normal flora and the use of serotyping was the only means of identifying *E. coli* until the 1970s when Cravioto *et al.*, showed that most EPEC strains adhered to HEp-2 cells *in vitro* (30). Scaletsky *et al.*, further demonstrated a localised adherence pattern, whereby the bacteria form microcolonies at the site of adherence (31). In 1969, Staley *et al*. were the first to use electron microscopy to study gut tissues from piglets infected with an O55:H7 EPEC

isolate (32). This study revealed characteristic histological changes of the intestinal cells, including the loss of microvilli at sites of bacterial attachment and the formation of pedestal-like structures. These ultrastructural changes were confirmed with rabbit ileal loops (33) and suckling rabbits (34, 35) and the histological lesions were termed attaching and effacing (A/E) lesions (34, 36). The formation of A/E lesions *in vivo* in humans was confirmed by ultrastructural studies of biopsy materials from human patients with EPEC diarrhoea (36-40). The actin-rich pedestals can be visualised by scanning electron microscopy or a fluorescent actin staining (FAS) test that has been extensively used to distinguish A/E pathogens in the 1980s (41). Furthermore, in the 1980s, different diarrhoeagenic strains of *E. coli* that possessed virulence factors such as heat labile and heat stable toxins were discovered, starting the advent of laboratory tests (42). These included molecular diagnostic techniques involving the use of DNA probes (43) to detect the presence of specific virulence genes, which were then replaced by polymerase chain reaction (PCR) methods (44).

1.2 Diarrhoeagenic *Escherichia coli*

Pathogenic *E. coli* has evolved through the acquisition of virulence factors by horizontal gene transfer to adapt to new environmental conditions and can cause one of three disease outcomes: diarrhoeal disease, urinary tract infections and sepsis or meningitis (45). Strains of *E. coli*, which cause diarrhoea in humans, have been classified into at least six distinct pathotypes (45, 46). These include enteropathogenic *E. coli* (EPEC), enterohaemorrhagic *E. coli* (EHEC), enterotoxigenic *E. coli* (ETEC), enteroagggregative *E. coli* (EAEC), enteroinvasive *E. coli* (EIEC) and diffusely adherent *E. coli* (DAEC) (47). Each pathotype carries characteristic virulence factors that enable bacteria of the particular pathotype to cause infections with distinctive clinical, pathological and epidemiological features.

EPEC and EHEC share major pathogenic mechanisms and a common ancestor (28, 48-50). However, the production of Shiga toxin (Stx) by EHEC can result in more severe disease outcomes such as diarrhoea that can progress to haemorrhagic colitis or

the haemolytic uraemic syndrome (HUS). Given that EPEC is the focus of this study, both pathotypes will be discussed more thoroughly in the following sections.

ETEC is an important cause of infantile diarrhoea in developing countries (51, 52). It is also the most common aetiologic agent of traveller's diarrhoea, which is defined as the passing of three or more unformed stools within 24 hours by a traveller (53, 54). This diarrhoeagenic *E. coli* pathotype causes disease by colonising the small intestine using one or more fimbrial and afimbrial (fibrillar) colonisation factors (CFs) (51, 52). Fimbrial adhesins consist of linear homopolymers or heteropolymers whereas afimbrial adhesins consist of single proteins or homotrimers. More than 22 antigenically different CFs among human ETEC strains have been discovered (55). Studies using animals as well as humans have shown that CF-positive ETEC but not their isogenic CF-negative mutants colonise the gut and induce diarrhoea (55-58). In spite of the wide array of CFs, epidemiological studies indicate that the majority of human ETEC strains express the fimbrial colonisation factor antigens I, II or IV (CFA/I, CFA/II or CFA/IV) (59).

Other virulence factors of ETEC include the heat-labile toxin (LT) and the heat-stable toxin (ST) (45, 51, 52). ETEC can express only an LT or an ST or both (45). The structure of LT is closely related to that of cholera toxin from *V. cholerae* (60). LT is a multimeric protein complex consisting of 1 A subunit and 5 B subunits (AB_5 arrangement) which are encoded on a plasmid (60, 61). The B subunits bind to the GM1 gangliosides on the host cell surface and the A subunit is internalised and activated (60). Upon reaching the basolateral membrane, the A subunit transfers an ADP-ribosyl moiety from nicotinamide adenine dinucleotide (NAD) to the α-subunit of the stimulatory G protein, a component of the trimeric GTP-binding protein that activates adenylate cyclase (60). This locks the adenylate cyclase in an active form, resulting in an increase in cAMP levels within the host cell. This in turn activates cAMP-dependent kinases that phosphorylate the chloride channel, cystic fibrosis transmembrane conductance regulator (CFTR), resulting in Cl^- secretion from secretory crypt cells into the gut lumen and subsequently diarrhoea (62). On the other

hand, when ST is secreted, it binds to and activates guanylate cyclase on the apical surface of epithelial cells, leading to increased cGMP levels in epithelial cells (45, 62). The increase in cGMP levels also results in Cl^- secretion and the inhibition of Na^+ absorption from the gut lumen. The net accumulation of sodium chloride in the gut lumen leads to an outpouring of diarrhoea by osmosis (45, 62). Interestingly, ST structurally resembles the host peptide guanylin, which regulates electrolyte homeostasis and it has been suggested that ST functions by molecular mimicry (63).

EAEC is distinguished from other diarrhoeagenic *E. coli* pathotypes by its distinctive adherence to HEp-2 cells in an aggregative stacked brick-like pattern (64). While this pathotype has first been associated with diarrhoea among infants in developing countries in 1987 (65), more recent studies have implicated diarrhoea in different settings; EAEC is responsible for infantile diarrhoea as well as for diarrhoea in adults in industrialised countries (66-68) and causes persistent diarrhoea among human immunodeficiency virus (HIV)-acquired immunodeficiency syndrome patients and traveller's diarrhoea (69-71). Laboratory studies have attributed the aggregative adherence (AA) phenotype to the carriage of a plasmid called pAA (72). Following this finding, a fragment of the plasmid was used as a DNA probe to distinguish EAEC from other *E. coli* (73, 74). However, this only identifies a portion of the strains that display the AA pattern. In 1995, Nataro *et al.* proved that only one of 4 AA probe-positive EAEC strains (strain 042) elicited diarrhoea in adult volunteers, confirming that not all EAEC strains, as defined by being AA probe-positive, are equally pathogenic (75).

The pathogenesis of EAEC infections is believed to begin with colonisation of the lower gastrointestinal tract followed by secretion of toxins such as Pic, *Shigella* enterotoxin 1 (ShET1), enteroaggregative *E. coli* ST (EAST1) and Pet (64). This is then followed by the induction of mucosal inflammation (76, 77). Pic is an autotransporter with mucinolytic activity while Pet, another autotransporter, leads to cytoskeletal changes and epithelial cell rounding by cleaving the host protein spectrin

(78, 79). However, the function of shET1 is poorly understood (80) and the role of EAST1 in virulence remains controversial due to its presence in many commensal *E. coli* isolates (81, 82). EAEC strain 042 adheres to the intestinal mucosa using fimbrial structures known as aggregative adherence fimbriae (AAFS) (72, 83, 84). At least 4 variants of AAFs exist but the adherence of EAEC is not restricted to the expression of an AAF, suggesting the existence of as yet uncharacterised adhesins. AggR, an AraC-like regulator, regulates expression of the AAF adhesins (84). Interestingly, like the *aggR* gene, the genes encoding the AAFs and other virulence factors such as Aap (dispersin) (85) and its Aat transport system are encoded on the pAA plasmid (86) and form part of the AggR regulon (87). Colonic biopsies using wild type EAEC 042 and its isogenic Δ*aap* mutant showed a hyperaggregative adherence pattern of the mutant compared to the AA pattern observed with the wild type strain (85). This suggested that upon secretion, Aap aids in intestinal dispersal of the bacteria, partially counteracting the aggregation mediated by the AAFs.

Jiang *et al.* found that significantly higher levels of IL-8 were observed in the faecal samples of patients infected with EAEC strains expressing the AggR regulon compared to EAEC strains lacking those virulence factors (88). This was supported by *in vitro* IL-8 assays in HCT-8 intestinal epithelial cells by Huang *et al* (66). EAEC is emerging as a human pathogen of considerable threat (66). The contribution of a multidrug resistant EAEC strain in uropathogenesis (89) and the role of an EAEC strain that acquired a Shiga toxin on a prophage in the 2011 outbreak of diarrhoea and haemolytic uraemic syndrome in Europe (90), highlight the ability of EAEC to adapt to new environments.

EIEC is closely related to *Shigella* species in terms of biochemistry, genetics and pathogenesis (91). In fact, *Shigella* are essentially non-lactose fermenting *E. coli* (92, 93). EIEC may ferment lactose late or not at all (94). EIEC pathogenesis like that of *Shigella* includes invasion of colonic epithelial cells (95, 96), lysis of the endocytic vacuole, intracellular replication, cytoplasmic actin based motility and spread to

adjacent epithelial cells (95, 97). EIEC can cause dysentery, like *Shigella* species, although in most cases this diarrhoeagenic *E. coli* pathotype causes watery not bloody diarrhoea (98). EIEC shares many virulence factors with *Shigella* species including carriage of a large virulence plasmid (99-101) that encodes a Type III secretion system (T3SS) (101-104) and virulence effectors proteins such as IpaA, IpaB and IpaC (99, 105-107). The virulence plasmid is responsible for much of the pathogenesis of EIEC and *Shigella*.

DAEC induces a diffuse adherence pattern to HEp2-cell monolayers (31, 108). One of the virulence factors of DAEC is the fimbrial adhesin F1845 which belongs to the Dr family of adhesins (109-111). Members of the Dr family of adhesins bind to and cluster a cell surface protein called decay-accelerating factor (DAF), leading to the activation of signal transduction cascades, such as PI-3 kinase activation, that ultimately causes the development of long cellular extensions around the adherent bacteria (112). DAEC strains have been found to cause diarrhoea in children above 12 months of age (47, 113). However, the implication of DAEC in causing diarrhoeal illness is still debatable. Some studies have found that DAEC strains are not involved in causing illness in adults and rather form part of the asymptomatic intestinal microbiota strains in children and adults (114).

1.3 Attaching and effacing pathogens

EPEC and EHEC are a subset of diarrhoeagenic *E. coli* that induces a characteristic intestinal histopathology known as A/E lesions while remaining extracellular. A/E lesions are typified by intimate bacterial adherence to enterocytes, the formation of actin-rich pedestals adjacent to the sites of bacterial attachment and localised destruction of brush border microvilli (36) (Figure 1.1). A/E lesions are believed to lead to a loss of absorptive capacity of intestinal cells, which contributes to diarrhoea. Other A/E pathogens include the rabbit specific EPEC (REPEC) and the mouse pathogen *Citrobacter rodentium*. The ability of these A/E pathogens to form A/E lesions is encoded by genes present on a pathogenicity island (PAI) called the locus of

enterocyte effacement (LEE). This PAI contains genes that encode a Type III secretion system (T3SS) as well as *eae* encoding an outer membrane adhesin known as intimin and *tir* encoding the translocated intimin receptor (Tir). The LEE PAI and the formation of A/E lesions will be discussed later in more detail.

1.3.1 Enterohaemorrhagic *E. coli*: epidemiology, disease and treatment

EHEC was first recognised as a diarrhoeagenic *E. coli* pathotype following two epidemiologic observations in 1982. Riley *et al*., investigated two outbreaks of a distinctive gastrointestinal illness designated as haemorrhagic colitis (HC) that was associated with the consumption of undercooked hamburgers at a fast food restaurant chain (115). HC was characterised by watery diarrhoea followed by bloody diarrhoea, severe abdominal pain and little or no fever (115, 116). A previously uncharacterised *E. coli* serotype O157:H7 was isolated from the faeces of patients from both outbreaks. Secondly, Karmali *et al*. reported the association of haemolytic uraemic syndrome (HUS) with the presence of cytotoxins and cytotoxin-producing *E. coli* in stools of patients. HUS, which is defined as acute renal failure, thrombocytopenia and haemolytic anaemia, is preceded by a bloody diarrhoea indistinguishable from HC (117, 118). The *E. coli* O157:H7 strain was subsequently found to produce Stx that was responsible for both the HC and HUS (119). Stx is encoded on a bacteriophage in the *E. coli* strain O157:H7 and other *E. coli* serotypes (120-122). Shiga toxin-producing *E. coli* (STEC), also known as verotoxigenic *E. coli* (VTEC) refers to *E. coli* that produce the Shiga toxin. In general, EHEC strains are classed as a subset of STEC/VTEC. This means that in addition to producing Stx, EHEC strains can induce A/E lesions that are not a typical feature of STEC/VTEC infection. In fact, presence of the LEE PAI together with *stx* characterises the EHEC pathotype.

Shiga toxins, like cholera toxin and LT from ETEC, consist of 5 B subunits and an A subunit (120, 121). The cellular receptors for Shiga toxins are globotriosylceramide (Gb3) and globotetraosylceramide (Gb4) (123). Following binding of the Shiga toxin to its receptor, the A subunit is internalized by endocytosis and cleaved into A1 and

A2 (124, 125). The A1 subunit is a 28s rRNA *N*-glycosidase that cleaves the 28s rRNA component of the eukaryotic 60s ribosomal subunit (126), thereby disrupting protein synthesis and resulting in cell death (124). Many cell types are sensitive to these toxins, including enterocytes, renal and brain endothelial cells, cells of the monocytic lineage and platelets and erythrocytes (127).

EHEC causes sporadic and potentially fatal infections in children and adults worldwide. Canada and the United States appear to be more affected by sporadic EHEC O157:H7 infections, especially during summer (128). EHEC infections have also been reported in the Southern hemisphere, where non-O157:H7 strains are more prevalent (47). The predominant reservoir of EHEC is domestic cattle, in which EHEC does not cause disease but rather forms part of the normal gut flora (129, 130). Wild animals also excrete EHEC in their faeces. EHEC is transmitted by the faecal to oral route, through the consumption of undercooked ground beef, unpasteurised milk or contaminated vegetables or water. Furthermore, the estimated infectious dose for EHEC from outbreak investigations is only 10 to 100 organisms (131, 132). Due to the possibility of severe complications following EHEC infection, studies involving human volunteers to directly determine the infectious dose for EHEC were deemed unethical and were not conducted. Therefore, the infectious dose estimate was calculated by using the highest most probable number of *E. coli* O157:H7 detected per gram of contaminated meat linked with the EHEC outbreaks and the quantity of meat consumed by patients suffering from EHEC infection (131, 132). The low infectious dose is similar to that of *Shigella* infection and is consistent with numerous reports of person-to-person transmission during outbreaks (130, 133-135).

Treatment of EHEC infections is primarily focused on supportive therapy, mainly rehydration. The use of antibiotics in the treatment of EHEC, particularly the O157:H7 strain, is not recommended due to the increased risk of developing HUS after antibiotic treatment (136, 137). In addition, the use of trimethoprim, furazolidone and the quinolones favours the release of Stx from EHEC O157:H7,

possibly due to bacterial cell lysis and release of stored toxins (138). The use of anti-motility agents that inhibit peristalsis is also not recommended because of the increased risk of developing HUS (139, 140).

1.3.2 Enteropathogenic *E. coli*: epidemiology, disease and treatment

EPEC was initially described as a collection of *E. coli* strains that induced diarrhoea in young patients and that could be recovered from their faeces but not from the stools of healthy children. Some particular *E. coli* serotypes were most commonly associated with EPEC (141). However, current classification of *E. coli* strains within the EPEC pathotype relies on the presence or absence of specific genetic virulence markers. Molecular techniques to detect these specific virulence factors revealed that strains identified by serology as EPEC prior to 1960 and isolated from infants suffering from diarrhea are in fact EPEC (142). By definition, all EPEC strains possess the LEE PAI but lack the gene encoding the Shiga toxin (143). The presence of the EPEC adherence factor plasmid (pEAF) subdivides EPEC into two distinct subsets, typical and atypical EPEC (aEPEC) (143). The latter subset lacks the pEAF plasmid (143). This plasmid encodes the bundle-forming pili (Bfp) (144) and the transcriptional activator, Per, that upregulates the expression of genes on the LEE PAI (145, 146). The *eae* gene forms part of the core LEE PAI. Therefore *E. coli* strains that are *eae*+ *bfpA*+ *stx*− are typical EPEC and *E. coli* strains that are *eae*+ *bfpA*− *stx*− are aEPEC. It should be noted that aEPEC causes a mild but more prolonged diarrhoea in children in industrialised and developing countries (147-150). For the purpose of this study, typical EPEC will be referred to as EPEC.

EPEC has been a significant cause of morbidity and mortality primarily in children under two years of age in developed and developing countries (1, 2, 151). In an epidemiological study of diarrhoeal disease in young children in the US from 1964 to 1966, EPEC infection accounted for 16% of infantile diarrhoea (152). However, the mortality rate due to EPEC infection in the developed world has dropped significantly from the early 1900s to the 1970s. Today, EPEC infection is no longer regarded as a

clinical problem in developed countries although it remains an important public health problem in developing countries mostly due to poor sanitation (153, 154). Several studies have shown a strong correlation between the isolation of EPEC from infants with diarrhoea compared to healthy infants. This correlation is strongest in infants below 6 months of age (152). In children older than 2 years, EPEC can be isolated from both healthy and sick individuals, but no statistically significant correlation with disease was observed (152). The reason for this age specificity remains poorly understood although it has been suggested to be due to age-related intestinal cell surface receptors (47). Nevertheless, adults may develop diarrhoea due to EPEC infection provided a large inoculum size is ingested. In fact, due to ethical reasons, volunteer studies using EPEC are carried out on adults and these require an infective dose around 10^8 to 10^{11} organisms (28). This does not reflect the dose required to cause illness in children. The infectious dose in naturally transmitted infection among infants is believed to be much lower (47). Interestingly, the induction of diarrhoea in adult volunteers fed with EPEC helped to alleviate any doubts raised in the 1960s and 1970s about the pathogenicity of EPEC considering that EPEC was not found to be invasive or to produce toxins.

As with all gastrointestinal pathogens, transmission of EPEC occurs via the faecal to oral route, usually from contaminated hands, food or fomites (152). The reservoir of EPEC infection is believed to be symptomatic or asymptomatic children and asymptomatic adult carriers such as mothers or adults caring for young infants (152). Epidemiologic studies in many countries have shown significant levels of asymptomatic carriage with 17 to 20% of healthy infants below two years of age shedding EPEC strains in their faeces for up to two weeks after symptoms of the disease have ceased (152, 155).

Following ingestion and passage in the stomach, EPEC colonises the small intestine (156). Infection with EPEC results in acute or persistent diarrhoea that is non-bloody and mucoid (47). The diarrhoea can be accompanied by fever and vomiting. The

outcome of EPEC infection, ranging from subclinical infection to acute gastroenteritis, presumably depends on host factors. In most cases, if recovery from EPEC infection occurs, the bacteria are cleared.

The main goal of treatment of EPEC infection is to prevent dehydration by correcting fluid and electrolyte imbalances. Oral rehydration is usually sufficient for mild cases while parenteral rehydration is required for more severe cases. Antibiotics have been used to treat EPEC infection and have proved useful in many instances although they are now considered a last recourse considering that multiple antibiotic resistance is common for EPEC (157). Additionally, recent studies have shown that antibiotics may prolong disease caused by pathogenic *E. coli* due to the depletion of normal gut microflora and may prolong the shedding of EPEC in faeces which increases the risk of transmission (158, 159).

1.3.3 Genome sequence of the prototypic EPEC strain E2348/69

EPEC was the first *E. coli* pathotype to be associated with diarrhoeal illness. The EPEC strain E2348/69 serotype O127:H6 (EPEC lineage 1, phylogroup B2) was first isolated in 1969 from an infant suffering from loose stools in a residential nursery in Taunton, England (160). Following the onset of disease symptoms seen in that infant, 14 out of the 17 infants in the nursery suffered from diarrhoea. This EPEC strain was then used in adult volunteer studies and proved to be a true human diarrhoeagenic pathogen. It then became the prototypic EPEC strain for the study of EPEC biology and pathogenesis. Studies using EPEC E2348/69 have enabled landmark discoveries including discovery of the LEE. In spite of all the research conducted on this strain, the complete genome sequence of EPEC E2348/69 was only published in 2008 (161).

The E2348/69 genome consists of three main components: a circular chromosome (4,965,553 bp), the pEAF plasmid (pMAR2; 97,978 bp) and a small drug resistant plasmid (pE2348-2; 6,147 bp) (161). When compared with the genomes of 6 other pathogenic *E. coli* including EHEC O157:H7 strain Sakai (phylogroup E) and ETEC

strain E24377A (phylogroup B1), a commensal *E. coli* strain and a laboratory *E. coli* strain, the chromosomal content of E2348/69 was highly conserved with the chromosomes of these other *E. coli* strains; approximately 70% of the 4,488 E2348/69 genes are conserved in all strains examined (161). Spread throughout these conserved regions however, were many strain specific sequences, mostly found in mobile genetic elements; of the 424 EPEC E2348/69-specific genes, the majority (349/424) are located in prophages (PPs) and integrative elements (IEs) (319 genes) and plasmids (30 genes) (161). E2348/69 encodes 13 PPs (PPs1-13), and eight IEs (IE1a, IE1b, IE2-6 and the LEE) (161). Interestingly, the LEE encoded by EPEC is simpler than that of EHEC O157:H7 Sakai, yet the genes encoding the structural components of the T3SS are largely conserved (162). Of the EPEC strains examined and compared to EHEC strain Sakai, EPEC E2348/69 has the smallest LEE which encodes 41 open reading frames (ORFs) (161, 163). The varying size of the LEE is dependent on the integrated genetic elements in sequences flanking the core LEE (162, 164). For example, the larger LEE of EHEC O157:H7 Sakai is due to additional genes carried on a P4-like prophage designated 933L flanking the core LEE region (162).

Additionally, when compared with the incomplete genomes of EPEC strains B171, E22 and E110019 that encode at least 28 (plus 12 effector pseudogenes), 40 (plus 6 effector pseudogenes) and 24 (plus 13 effector pseudogenes) effectors respectively or with the complete genome sequence of EHEC strain Sakai that encodes 50 (plus 12 effector pseudogenes), the genome of EPEC E2348/69 revealed that E2348/69 has the smallest T3SS effector repertoire of 21 effectors and 6 effector pseudogenes (161). Twelve of the T3SS effectors of E2348/69 are encoded by lambda-like PPs (PP2, PP4 and PP6), 7 are encoded by IEs (IE2, IE5, IE6) and 7 are encoded by the LEE (161) (Figure 1.2).

1.3.4 Animal models of EPEC infection

EPEC strains are considered human and age specific. Consequently, research to determine the virulence factors of EPEC causing diarrhoea in young children is limited because the use of children in such studies is unethical. Although adult

volunteers have been used in the past to study EPEC infection, such studies are costly and largely impractical. Furthermore, EPEC does not colonise laboratory mice efficiently and does not cause disease in mice (165-167). In fact, oral inoculation of human EPEC into mice results in a commensal rather than a pathogenic relationship (166). To date, there is no known murine specific EPEC strain although other animal-specific EPEC strains exist and can be used as models of human EPEC infection. One example is the use of REPEC which causes a similar disease in young rabbits to that seen in children.

1.3.5 *Citrobacter rodentium*

A growing number of studies have found that infection of mice with the natural murine bacterial pathogen *Citrobacter rodentium* provides a convenient small animal model to investigate both the molecular and cellular aspects of infections with EPEC (165, 166, 168). This is because *C. rodentium* shares common virulence determinants with EPEC including the LEE PAI and numerous non-LEE encoded T3SS effectors (169). In fact, *C. rodentium*, which was initially termed *C. freundii* biotype 4280, is a member of the Enterobacteriaceae family that is genetically highly similar to EPEC and is believed to have evolved convergently with human EPEC (169-171). Both pathogens produce virtually indistinguishable A/E lesions in the intestinal epithelium. LEE-encoded virulence factors such as intimin and Tir of EPEC, EHEC and *Citrobacter rodentium* are functionally interchangeable, further demonstrating the genetic relatedness of these pathogens (172, 173). In mice, *C. rodentium* causes colonic epithelial hyperplasia that is not a feature of EPEC infection in humans (168). On the other hand, oral infection of susceptible mice with *C. rodentium* is often accompanied by the passing of softened faeces, which is reminiscent of diarrhoea caused by EPEC in humans (165, 168). Therefore, studies on the virulence of *C. rodentium* are likely to provide insights onto the pathogenesis of infections with EPEC. *C. rodentium* strains such as DBS100, ICC168, ICC169 (a spontaneous nalidixic acid resistant strain of ICC168) are clonal in nature and hence highly similar (174).

Interestingly, some mouse strains are more susceptible to *C. rodentium* infection than others. For example, C57BL/6, NIH Swiss and BALB/c mice infected with high inocula (10^8-10^9 CFU), show minimal mortality and are capable of clearing the bacteria by 21-28 days post infection (175). However, C3H/HeJ mice, which are defective in TLR4 signaling, are highly susceptible to *C. rodentium* infection (176). These latter mice exhibit higher bacterial load and more severe colonic hyperplasia accompanied with mucosal ulceration and apoptosis. Nevertheless, studies have demonstrated that the TLR4 defect in the C3H/HeJ mice does not make them more susceptible to *C. rodentium* infection, although a genetic basis for the pronounced phenotype seen in C3H/HeJ mice has not been identified to date (176). The related mouse strains C3H/HeN and C3H/HeOuJ, which have an intact TLR4 signaling system, also display increased susceptibility to *C. rodentium* infection (176).

1.4 Invasive enteric pathogens

Unlike A/E pathogens that remain extracellularly attached to the apical membrane of intestinal cells, invasive enteric pathogens such as *Salmonella*, *Shigella*, *Yersinia* and some *E. coli* species invade the intestinal cells as part of their colonising strategy. For example, *Salmonella* species invade intestinal epithelial cells (Figure 1.3) or macrophages and this contributes to their systemic spread within the host. *Salmonella* remains in modified phagosomes called *Salmonella* containing vacuoles (SCVs), depending on the host specificity of the strain while *Shigella* species destroy the infected epithelial cells and elicit mucosal inflammation upon bacterial invasion. Different invasive enteric pathogens employ particular strategies to survive and multiply within the host after breaching the intestinal epithelium.

1.4.1 *Salmonella* species

Salmonella species are Gram-negative, facultative anaerobic bacilli of the Enterobacteriaceae family like *Escherichia* species. In fact, *Salmonella* and *Escherichia* are genetically related and diverged into separate lineages around 140 million years ago (177, 178). The complexity of *Salmonella* nomenclature is reflected

in the numerous revisions it has undergone during the 20th century. Following Kaufmann and White's serological classification of *Salmonella* species and biochemical analyses, it was suggested that *Salmonella* be divided into several species. However, DNA hybridization studies revealed that members of the *Salmonella* genus were more closely related than previously thought which resulted in the proposal of a single species, *Salmonella enterica* in 1987, with many formerly classified species becoming subspecies and serovars (179). It was only in 2002 that the *Salmonella* genus was finally classified into two species, *S. enterica* and *S. bongori* (180, 181), with only the former species being capable of causing disease in mammals (182). *S. enterica* is further divided into 6 subspecies and the majority of pathogenic serovars belong to the subspecies *enterica* (182). In this thesis, *Salmonella enterica* subspecies *enterica* serovar Typhimurium, which will be studied, is abbreviated as *S.* Typhimurium.

1.4.2 Disease outcomes from *Salmonella* infections and epidemiology

S. enterica causes two types of disease in humans: a systemic enteric fever known as typhoid fever and diarrhoea. *S. enterica* serovars causing typhoid fever are termed typhoidal *Salmonella* whereas those that cause self-limiting gastroenteritis are termed non-typhoidal *Salmonella* (NTS).

Typhoid fever is caused by the human specific *S. enterica* serovar Typhi and paratyphoid fever is caused by *S. enterica* serovar Paratyphi (183, 184). Typhoid fever and paratyphoid fever are clinically indistinguishable (183, 184). The occurrence of typhoid fever is predominant in children in developing countries of Asia and Africa (183). The clinical symptoms include a mild to high fever accompanied by influenza-like muscular aches, headaches and abdominal pains (185).

In contrast to typhoidal serovars, NTS serovars are not human-specific. NTS serovars that are largely host-adapted such as *S. enterica* serovars Gallinarum (poultry), Abortusovis (sheep) and Choleraesuis (swine) seldom cause disease in other hosts,

including humans (186). However, some NTS serovars such as Enteritidis and Typhimurium are capable of infecting a broader range of species and can cause gastrointestinal disease in humans (186, 187). NTS are also spread by the faecal to oral route. The most common clinical symptoms are diarrhoea, abdominal pain, nausea and vomiting, fever and muscular aches (186, 188). Symptoms usually last 4-7 days and treatment includes oral rehydration and rest (186). However, *Salmonella* infections may be fatal in young infants and immunocompromised patients. Antibiotics are not usually recommended since they prolong the shedding of *Salmonella* in faeces (189).

1.5 Innate host response to EPEC and *Salmonella*

The host innate immune system is characterised by rapid non-specific immune responses against pathogens that have breached the first line of defence such as the skin or the mucosal barrier. The gastrointestinal epithelium utilises a plethora of innate immune defence mechanisms to fight enteric pathogens. The host intestinal epithelium is composed of enterocytes, mucus-secreting goblet cells, enteroendocrine cells, microfold M cells and Paneth cells and lies above the lamina propria where lymphocytes and other immune cells reside. All these cell types play a vital role in sensing bacterial pathogens through recognition of pathogen associated molecular patterns (PAMPs) by a range of pattern recognition receptors (PRRs) including Toll-like receptors (TLRs), nucleotide-binding oligomerisation domain (NOD)-like receptors (NLRs), retinoic acid-inducible gene (RIG)-I like helicases and C-type lectin receptors (190).

TLRs recognise a range of bacterial strutctures. For example, TLR2 recognises peptidoglycan (191-193), TLR4 senses bacterial LPS (194-196), TLR5 senses flagellin (197) while TLR9 senses bacterial DNA motifs (198, 199). The cytosolic PRRs such as NLRs comprise a family of at least 20 receptors that recognise cytosolic PAMPs (200, 201) and form part of large protein complexes called inflammasomes that activate caspase-1 (202). Caspase-1 activation ultimately induces a form of cell

death called pyroptosis (203) that shares features of apoptosis and necrosis and also leads to the maturation of the proinflammatory cytokines IL-1β and IL-18 (204). Amongst the 5 inflammasomes that have been discovered thus far (204-209), the NLRP3 and NLRC4 inflammasomes are the best studied. The former responds to LPS, peptidoglycan and bacterial or viral nucleic acids in the presence of ATP whereas the latter recognises cytosolic flagellin (210).

PRR stimulation leads to a cascade of signaling events that ultimately results in the production of inflammatory cytokines, infiltration of inflammatory immune cells and/or death of the infected cell. Both EPEC and *Salmonella* activate the host innate immune system and will be described in further details in subsequent sections.

1.5.1 Inflammatory signaling

Nuclear factor-κB (NF-κB) signaling is considered the prototypical inflammatory signaling pathway based on the activation of NF-κB in response to the proinflammatory cytokines such as TNF and IL-1 or stimulation of PRRs and the subsequent effect of NF-κB on the expression of other proinflammatory cytokines such as IL-8 (211). The mammalian NF-κB proteins consist of RELA (also known as p65), RELB, c-REL, NF-κB p105 which is subsequently cleaved into the subunit p50, NF-κB p100 which is cleaved into the subunit p52 which are members of the Rel domain-containing protein family (212). Rel proteins can form homodimers or heterodimers through the conserved N-terminal Rel-homology domain to mediate transcription of genes (213, 214). The C-terminal transcription activation domains (TADs) of p65, c-REL and RELB are important for controlling the activation of target gene transcription (214).

NF-κB proteins are tightly regulated. Under normal physiological conditions, NF-κB dimers are held inactive in the cytoplasm by a direct interaction with inhibitors of NF-κB (I_KB) such as $I_KBα$, $I_KBβ$ and $I_KBε$ which mask the nuclear localisation signal (NLS) of the NF-κB dimers (213). Upon stimulation of TLRs by PAMPs or cytokine

receptors such as IL-1 receptor (IL-1R) or TNF receptor 1 (TNFR1), a signaling cascade involving multiple adaptor proteins such as TNFR-associated factors (TRAFs), Myeloid differentiation primary response protein 88 (MyD88), receptor-interacting proteins kinases (RIPKs) and IL-1R-associated kinases (IRAKs) that eventually lead to the degradation of $I_KB\alpha$, exposing the NLS and enabling NF-κB to translocate to the nucleus (Figure 1.4) (215, 216). Upon receptor stimulation, the different signaling pathways converge to the activation of the I_KB kinase (IKK) complex, consisting of IKKα, IKKβ and a regulatory subunit called NF-κB essential modulator (NEMO or IKKγ). IKKβ and NEMO are activated first and activate IKKα, which leads to the phosphorylation and proteasomal degradation of $I_KB\alpha$ (Figure 1.4) (217). The above NF-κB signaling pathway is the canonical pathway. An alternative pathway exists based on the IKK subunits that are activated. For example, upon stimulation of the lymphotoxin-β receptor, IKKα is activated by NF-κB-inducing kinase (NIK) and cleaves p100 to p52 that ultimately forms a heterodimer with RELB (213) (218-220).

Similar to NF-κB signaling, mitogen-activated protein kinase (MAPK) signaling also controls inflammation. MAPK signaling is a three-tier kinase module whereby MAPK is activated upon phosphorylation by a MAPK kinase (MAPKK), which in turn is activated upon phosphorylation by a MAPKK kinase (MAPKKK) (Figure 1.5). To date, at least 6 groups of mammalian MAPKs have been identified: extracellular signal-regulated kinase 1 or 2 (ERK1/2), ERK3/4, ERK5, ERK7/8, Jun N-terminal kinase 1, 2 or 3 (JNK1/2/3) isoforms and the p38 isoforms (221-223). MAPKs are enzymes that phosphorylate serines or threonines of their protein targets (224). ERK1/2, ERK5, p38 and JNK1/2/3 are the classical MAPKs (225). ERK1/2 is usually activated by the MAPKK MEK1/2 which is activated by the MAPKKK Raf (226). ERK1/2 activation is followed by the activation of transcription factors that aid in mounting a proinflammatory response (Figure 1.5). The initial signaling for the activation of p38 or JNK starts with the activation of one of the MAPKKKs, TGF-β-activated kinase 1 (TAK1), MEKK1-4 and ASK1 (224) (Figure 1.5). However to

activate p38, the MAPKKs, MKK3 and MKK6, are required whereas the MAPKKs, MEK4 or 7 (MEK4/7), are specific for JNK activation (224, 227, 228) (Figure 1.5). The MAPK p38 can directly activate transcription of proinflammatory genes. JNK activates the transcription factor c-Jun, which is a member of the AP-1 family of transcription factors along with c-Fos, FosB, FOSL1/2, JunB, JunD and c-MAF (229, 230). These form heterodimers or homodimers and translocate to the nucleus to transcribe proinflammatory genes.

1.5.2 Cell death and signaling

In response to microbial infections, multicellular hosts can also induce the death of infected cells by one of the following cell death modalities namely apoptosis, necrosis and pyroptosis (231). Host cell death forms part of the intrinsic innate immune system (232). For example, apoptosis is usually induced in response to bacterial infections to eliminate infected cells during the early stage of infection and to recruit dendritic cells which will engulf, process and expose the bacterial antigens to MHC class I molecules to mount an adaptive immune response (233). However, bacterial pathogens have evolved an array of intricate strategies to manipulate host cell death and survival pathways to enhance colonisation and survival within the host. For example, *Shigella* can induce both necrosis and apoptosis upon infection of intestinal epithelial cells (234-236). However, *Shigella* activates the host cell pro-survival signaling pathway NOD1/RIPK2/ NF-κB /Bcl-2 and delays cell death signaling to allow the bacteria to replicate and disseminate (234). The different strategies employed to modulate host cell death depends on the pathogen and the cell type infected. Modulation of NF-κB pro-survival and apoptotic signaling by bacterial pathogens is widely observed.

1.6 Characteristics of apoptosis

Apoptosis is the best studied mode of cell death and early morphological changes include cell shrinkage and pyknosis (chromatin condensation) (237). Extensive plasma membrane blebbing is also observed followed by karyorrhexis (nuclear fragmentation) and the separation of cell fragments into small, round apoptotic

bodies. These contain tightly packed organelles, with or without a nuclear fragment, and are surrounded by an intact plasma membrane. These bodies are subsequently phagocytosed by macrophages (238). Phosphatidylserine which is normally sequestered in the inner leaflet of the plasma membrane is moved to the outer leaflet during apoptosis and aids in the recognition of apoptotic cells by phagocytes (239). The apoptotic process and the accompanying removal of the cell do not usually trigger inflammation because the apoptotic cells do not release their cellular contents into the interstitial space, and phagocytic cells do not produce anti-inflammatory cytokines upon uptake of apoptotic bodies (240, 241). Although there is a wide range of stimuli capable of triggering apoptosis, all result in the activation of a group of cysteine aspartic-specific proteases, termed caspases, which mediate a complex signaling cascade that bridges the initial stimulus to cell death (242).

Whereas apoptosis is an energy-dependent process, necrosis is a passive mode of cell death that occurs in response to tissue injury. During necrosis, cells swell and release their cytoplasmic contents into the interstitial space eventually causing inflammation (243). Other forms of cell death share processes in common with apoptosis and necrosis, including necroptosis, pyroptosis and autophagy and which induce inflammation to varying extents (244).

Apoptosis can be stimulated by either intracellular ligands, known as the intrinsic or mitochondrial pathway, or by extracellular ligands, known as the extrinsic or death receptor pathway. Both pathways converge at the point of activation or cleavage of the executioner caspase, caspase-3, resulting in the late morphological changes of apoptosis (245).

1.6.1 Death receptor mediated apoptosis

The extrinsic pathway of apoptosis involves a family of transmembrane receptors termed death receptors that are members of the tumour necrosis factor receptor (TNFR) superfamily. Members of this family have conserved cysteine rich regions in

the extracellular ligand binding domain and a cytoplasmic domain of about 80 amino acids called the death domain (DD) (246). A functional member of the TNFR superfamily is typically a trimeric complex that is stabilised by intracysteine disulfide bonds formed between the cysteine rich regions of individual subunit members (247). However, TNFRs can also exist in the soluble form (248). The death domain of death receptors is essential for relaying the death signal from the cell surface to the intracellular signaling pathway via a range of adaptor molecules that ultimately results in activation of the initiator caspase, caspase-8. The best-characterised death receptors include Fas/CD95/APO-1, TNFR1/p55/CD120a, TNF-related apoptosis-inducing ligand receptor 1 (TRAIL-R1)/DR4 and TRAIL-R2/DR5/Apo2/KILLER and their respective ligands are FasL, TNF, and TRAIL/Apo2L (for TRAIL-R1 and TRAIL-R2) (246, 249-252). These trimeric ligands belong to the TNF family of cytokines and are mainly expressed as transmembrane proteins although they can also be released as soluble cytokines by proteolytic cleavage. The apoptosis-inducing capacity of the soluble forms has been shown to be lower than the membrane-bound forms. For example, soluble FasL can bind to Fas but is not capable of activating the downstream apoptotic signaling events unless the ligands are cross-linked (253). Recent studies have demonstrated that only the membrane-bound form of FasL possesses significant apoptosis-inducing capacity (254).

Fas is expressed ubiquitously and although it is particularly abundant in lymphoid tissues and on activated mature T lymphocytes, functional Fas is also expressed on the basolateral membrane of intestinal epithelial cells (255-257). In contrast to the ubiquitous expression of Fas, FasL is expressed on a selective cellular pool including activated cytotoxic T cells, Natural Killer (NK) cells and Natural killer T (NKT) cells. Upon stimulation of Fas by FasL, there is an aggregation of pre-assembled Fas trimers at the plasma membrane, which leads to internalisation of Fas (258). Fas can then recruit the adaptor protein, Fas-associated protein with death domain (FADD), via homotypic interactions between death domains found in both the cytoplasmic region of Fas and the C-terminus of FADD. FADD then recruits procaspase-8 via a second

homotypic interaction, this time involving the death effector domain (DED) of FADD and procaspase-8. The interaction between Fas, FADD, and procaspase-8 forms the death-inducing signaling complex (DISC), resulting in proximity-induced activation (cleavage) of caspase-8 (259). Activated caspase-8 can then cleave and activate the executioner caspase-3 leading to apoptotic cell death. In certain cell types, including epithelial cells, FasL stimulation induces apoptotic cell death through caspase-8 mediated cleavage of a pro-apoptotic Bcl-2 homology 3 (BH3)-only protein called Bid (260, 261) (262). Bid is a member of the Bcl-2 family of proteins, which is involved in the mitochondrial cell death pathway and so its activation by caspase-8 is an example of a cross-talk between the intrinsic and extrinsic pathways of apoptosis (260, 261).

The death receptors, TRAIL-R1 and TRAIL-R2, have extensive tissue distribution whereas the ligand, TRAIL, is expressed mainly on NK cells, NKT cells and macrophages. TRAIL induces apoptosis by binding to either TRAIL-R1 or TRAIL-R2, although TRAIL-R2 is more important in inducing apoptosis. Receptor binding of TRAIL leads to recruitment of FADD via homotypic DD interactions, which in turn recruits procaspase-8 via DED interactions to the DISC and leads to activation of a caspase cascade in a similar manner to the FasL-induced apoptotic cell death pathway (263).

Two different TNFRs exist, TNFR1 and TNFR2. Although both receptors share sequence similarity in their extracellular ligand-binding region, their cytoplasmic region sequences are different, thereby accounting for their different signaling activities (264-266). Both TNFR1 and TNFR2 can bind to TNF. However, only TNFR1 is involved in death receptor signaling as TNFR2 lacks an intracellular death domain. TNFR1 is expressed ubiquitously and is required for TNF-induced apoptosis of pathogen-infected cells (267, 268). Upon stimulation of TNFR1 by TNF, TNFR1 translocates to lipid rafts (269) whereupon receptor-interacting protein kinase 1 (RIPK1), tumour necrosis factor receptor type1-associated death domain protein

(TRADD), TNF receptor-associated factor 2 (TRAF2) and cellular inhibitor of apoptosis protein 1 and 2 (c-IAP1/2) are recruited to form the membrane bound receptor complex I (Figure 1.6) (270, 271). Upon deubiquitination by deubiquitinating enzymes, the receptor complex is internalised by endocytosis (272) during which RIPK1, TRAF2 and TRADD dissociate from TNFR1 enabling the DD of TRADD to bind to the DD of FADD. This in turn recruits procaspase-8 via homotypic DED interactions to the newly formed cytosolic complex IIa (Figure 1.6) (271, 273). Activated caspase-8 then cleaves the executioner caspases leading to cell death by apoptosis. If caspase-8 is depleted or inhibited, complex IIb cannot induce apoptotic cell death and instead TNFR1 stimulation leads to a recently described form of cell death known as programmed necrosis or necroptosis which relies on receptor-interacting protein kinase 3 (RIPK3) and mixed lineage kinase domain-like (MLKL) (Figure 1.6) (274, 275).

Even though TNFR1 stimulation can lead to cell death, the primary function of TNFR1 is in inflammation. In this pathway, RIPK1 in membrane bound receptor complex I is polyubiquitinated at Lysine-377 by the E3 ubiquitin ligases, cIAP-1/2 (276, 277). Polyubiquitinated RIPK1 recruits TAK1 and the associated TAK1-binding proteins 1/2/3 (TAB1/2/3) (277). TAK1 then activates the IKK complex leading to phosphorylation of the NF-κB inhibitory protein, IκB, which is then ubiquitinated and degraded enabling nuclear translocation of NF-κB and transcriptional activation of NF-κB-dependent genes including pro-inflammatory and anti-apoptotic genes (Figure 1.6) (278). In fact, inhibiting the NF-κB pathway or protein synthesis sensitises cells to TNF-induced apoptosis (279).

1.6.2 The intrinsic or Bcl-2 pathway of apoptosis

The intrinsic pathway of apoptosis is stimulated by a range of non-receptor mediated stimuli such as DNA damage, endoplasmic reticulum (ER) stress or viral infection which ultimately induce the release of signaling factors from the mitochondria (280, 281). A number of intrinsic stimuli activate the BH3-only proteins, which promote

cell death by antagonising the inhibitory effects of the anti-apoptotic Bcl-2 proteins. BH3-only proteins also activate the proapoptotic Bcl-2 family members such as Bax and Bak in the outer mitochondrial membrane resulting in the release of cytochrome *c* into the cytoplasm (281). Cytochrome *c* stimulates the formation of a multimeric protein complex called the apoptosome that includes Apaf-1 and procaspase-9 (282). Activation of the initiator caspase, caspase-9, leads to cleavage of the executioner caspases resulting in apoptotic cell death.

1.7 Immune responses during infection with EPEC and *C. rodentium*

Cytokine production in response to EPEC *in vitro* infection results from the activation of NF-κB and MAPK signaling pathways following recognition by TLRs and NLRs. Culture supernatant from EPEC E2348/69 but not from the flagellin (Δ*fliC*) mutant induces IL-8 production from cultured colonic epithelial cells showing that flagellin is an important PAMP to induce inflammation (283). This is supported by animal infection studies, which show EPEC infection is accompanied by infiltration of inflammatory cells in the intestinal lamina propria and transmigration of inflammatory cells across the intestinal epithelium into the gut lumen (284, 285). Although TLR5 is only expressed at the basolateral epithelial surface (286), A/E pathogens, which are extracellular pathogens, are believed to gain access to TLR5 by compromising the epithelial barrier and cell polarity (287, 288). Moreover, lamina propria dendritic cells that sample luminal contents also express TLR5 (289).

Interestingly, IL-8 production in epithelial cells via TLR5-independent mechanisms was also observed although at a later stage of infection, indicating that bacterial factors other than flagellin also contribute to the activation of the host innate immune system (290). Activation of NF-κB signaling has been demonstrated *in vivo* during infection of mice with the non-flagellated mouse A/E pathogen, *C. rodentium* (290, 291). *C. rodentium* does not activate TLR5 but triggers an inflammatory response via a T3SS-dependent manner or via LPS/TLR4 signaling. *In vivo* studies using *C. rodentium* have shown that infection of TLR4-/- mice that are insensitive to LPS

resulted in lower levels of cytokine production and a decreased infiltration of inflammatory cells at the infection site, suggesting that LPS is an important bacterial inflammatory stimulus during infection with A/E pathogens. *E. coli* or *Salmonella* LPS was also recently discovered to activate a non-canonical inflammasome through direct sensing by caspase-4 (292). Hence there are multiple mechanisms leading to an inflammatory response.

C. rodentium-infected mice display increased colonic expression of genes encoding IL-1β, IL-12, IL-17, IL-22, TNF and IFNγ (293, 294). This shows the importance of a Th1/Th17 response to *C. rodentium* infection; Th1 cells produce IFNγ whereas Th17 cells secrete large amounts of IL-17 and IL-22 (295). The Th17 response triggered in mice within two weeks following *C. rodentium* infection requires NOD1/NOD2 signaling and the production of IL-6 (294, 296). The importance of IL-6 during gut infection is further demonstrated by the fact that IL-6 deficient mice develop increased mucosal ulcerations (297). An increase in the faecal levels of TNF and IL-6 was associated with better resolution of EPEC infection in young children from Mexico that were enrolled in a randomised study (298). This was consistent with the role of these cytokines in clearing *C. rodentium in vivo*.

While IL-6 is vital for IL-17 production, it is not required for maximal production of IL-22. Instead IL-23 induces IL-22 production during infection with *C. rodentium* (299). More recent studies have shown that several innate lymphoid cell populations (300-302) and natural killer cell subsets secrete IL-22 (303-306). Furthermore, colon-infiltrating neutrophils and colonic macrophages produce IL-22 in response to IL-23 and TNF signaling (294). *In vivo* studies have shown that *C. rodentium*-infected IL-22 knockout mice display severe intestinal damage, systemic bacterial load and mortality, highlighting the importance of this cytokine in host defence against *C. rodentium* (294). It was suggested that IL-22 induces the production of antimicrobial peptides of the Reg family of proteins from intestinal epithelial cells (294, 307). However, there is no evidence proving that the Reg proteins kill

C. rodentium in vivo, even though exogenous mouse or human RegIIIγ significantly improved the survival of IL-22 knockout mice following *C. rodentium* infection. Additionally, the use of *C. rodentium* in diverse immune-deficient mouse strains demonstrates the importance of the adaptive immune response including $CD4^+$ T cells, B cells and *C. rodentium* specific antibodies in the clearance of the pathogen (307, 308). IL-22 is thought to mediate the cross talk between immune cells and the intestinal epithelial cells during infection with A/E pathogens (294, 307).

1.8 Immune response during *Salmonella* infection

Infection of intestinal epithelial cells and macrophages with *Salmonella* also results in large changes to host cytokine expression *in vitro* and *in vivo* (309). For example, *in vitro* studies have shown that infected epithelial cells display increased expression of many proinflammatory cytokines, including IL-8 (309). Activation of NF-κB is vital in mediating the epithelial inflammatory response to *Salmonella* infection (310). Flagellated *Salmonella* induces IL-8 secretion at the basolateral side of the infected epithelial cells, whereby the bacterial flagella engage TLR5 (286, 311, 312). Additionally, in *Salmonella*-infected macrophages, the flagella subunit, flagellin, is translocated into the host cell cytosol via T3SS1, resulting in NLRC4 inflammasome activation, IL-18 and IL-1β secretion and caspase-1-mediated cell death (pyroptosis) (209, 244, 313, 314). Furthermore, macrophage exposure to *Salmonella* results in an increased transcription of proinflammatory cytokine genes such as those encoding IL-1, IL-6 and TNF *in vivo* (309).

Mouse infection studies have shown protective roles for IL-1α, TNF, IFN-γ, IL-12 and IL-18 whereas IL-4 and IL-10 impaired host defense against *Salmonella* (309). Treatment of mice with IL-1α or TNF increases host survival after *Salmonella* infection (315). Additionally, a decrease in the level of TNF by using anti-TNF antibodies or TNF knock-out mice increases the severity of *Salmonella* infection and decreases host survival (316, 317). In response to *Salmonella* infection, the expression of *IFNG* is upregulated in the intestinal mucosa, Peyer's patches, mesenteric lymph

nodes, liver and spleen (318, 319). Impairment of IFN-γ using antibodies or knock-out mice increases the bacterial load in the liver and spleen and decreases survival of the host (316, 317, 320). Since only T cells and NK cells express IFN-γ, this suggests other cells that have direct contact with *Salmonella* induce IFN-γ production by these cells. IL-12 and IL-18 are two cytokines produced by macrophages that can induce IFN-γ production. Neutralisation of IL-12 increases the bacterial load in the spleen and decreases host survival whereas treatment with IL-12 increases host survival (321). Importantly, treatment of *Salmonella*-infected mice with anti-IL12 is accompanied by a decrease in splenic IFN-γ mRNA expression and serum IFN-γ levels compared to untreated, infected mice (322). Similarly, infected mice treated with anti-IL18 have lower serum IFN-γ levels and an increased bacterial load in the liver and spleen (323, 324).

The expression of the cation transporter natural resistance-associated macrophage 1 (Nramp1) in late phagosomes confers resistance to infection with intracellular pathogens including *S. enterica* in mice (325). Nramp1 acts primarily as a transporter for cations such as manganese and iron (325, 326). Nramp1 expression has been linked with iron efflux out of phagosomes, depriving intracellular pathogens of iron (327). Additionally Nramp1 modulates the expression of cytokines including TNF and IL-1β (325). $Nramp1^{+/+}$ mice had lower levels of *S.* Typhimurium colonisation in the caecum compared to $Nramp1^{-/-}$ mice and developed more pronounced colitis, which was characterised with higher secretion of proinflammatory cytokines such as TNF and infiltration of neutrophils and macrophages (328, 329). Furthermore, the mouse strain 129 SvJ is resistant to *S.* Typhimurium infection unlike C57BL/6 mice. This is because 129 SvJ mice have an intact *Nramp1* allele whereas C57BL/6 mice are homozygous for a mutant *Nramp1* allele (*Nramp1G169D*) (329).

1.9 Pathogenesis of A/E pathogens

1.9.1 Initial adherence

In addition to inducing the characteristic A/E lesions in the gut, EPEC strains adhere to intestinal cells in two distinct patterns termed localised and diffuse adherence,

depending on the presence or absence of the pEAF plasmid (pMAR2 in EPEC E2348/69) (31, 108). Typical EPEC, which carry the pEAF plasmid, exhibit a localised adherence pattern whereas atypical EPEC lacking the pEAF plasmid exhibit a diffuse adherence pattern (31). Human volunteer studies have revealed that the carriage of the pEAF plasmid correlated with but was not essential for the ability of EPEC to cause disease (108). For example, atypical EPEC lacking the pEAF plasmid (143) and typical EPEC cured of the pEAF plasmid (330) could still induce A/E lesions and cause diarrhoea.

Bfp, a type IV fimbria, encoded by genes on the pEAF plasmid is the virulence factor used by typical EPEC to mediate bacterial clustering (microcolony formation) resulting in localised adherence and non-intimate attachment to intestinal cells. Bfp reversibly aggregates into rope-like bundles that support interbacterial interactions (331, 332). The introduction of a 14 *bfp* gene cluster from the pEAF plasmid together with an additional fragment of the plasmid consisting of regulatory genes in a laboratory *E. coli* strain is sufficient for Bfp biogenesis and the ability to induce the localised adherence phenotype (333, 334). *bfpA* encodes the major pilin subunit called prebundlin (or BfpA) while other *bfp* genes encode products homologous to proteins involved in the biogenesis of other type IV pili (334, 335). For example, *bfpP* codes for a prepilin peptidase which is homologous to other prepilin peptidases in other type IV pilus sytems and cleaves prebundlin into the mature form (336). The importance of Bfp in EPEC virulence was demonstrated in a human volunteer study whereby a Δ*bfpA* mutant was unable to produce Bfp and induced significantly less diarrhoea than wild type EPEC (144).

While Bfp is known to mediate aggregation and localised adherence, it has also been shown to mediate bacterial dispersal in the gut (144, 337). Thus Bfp is believed to allow the bacteria to adhere and multiply early in infection and then disperse individual progeny to colonise other mucosal sites. This paradigm is demonstrated by a study that showed that EPEC carrying a mutation in one of the *bfp* genes (*bfpF*)

encoding a protein involved in pilus retraction failed to disperse from bacterial aggregates on tissue culture cells *in vitro* and was about 200 fold less virulent than the wild type when used to infect volunteers (144). To date, a protein or glycoprotein receptor for Bfp has not been identified although Bfp does have an affinity for phosphatidylethanolamine (338).

1.9.2 The locus of enterocyte effacement pathogenicity island

A 36 kb chromosomal locus, termed the locus of enterocyte effacement (LEE), is vital for the formation of A/E lesions (339). The LEE PAI is found in all A/E pathogens despite minor variations (339, 340). For example, the LEE of EPEC O127:H6 E2348/69 consists of 41 predicted open reading frames (ORFs) while the LEE of EHEC O157:H7 EDL933 consists of 54 ORFs (341, 342). The additional 13 ORFs are carried on the P4-like prophage 933L, which in the latter strain integrated into the very end of the core LEE (342). This prophage exists in other EHEC and EPEC strains but not in EPEC O127:H6 E2348/69 (342).

The *LEE* genes are organised in five polycistronic operons *LEE1*, *LEE2*, *LEE3*, *LEE4* and *LEE5* (Figure 1.2B). Many genes, termed *esc*, encode the components for a T3SS while other genes encode secreted proteins that form a translocation apparatus (*esp*), translocated effector proteins, T3SS chaperones, an outer membrane adhesin intimin (*eae*) and the translocated intimin receptor Tir (*tir*) as well as gene regulators (341). Genes coding for T3SS components are highly conserved across A/E pathogens whereas those coding for components involved in cell interactions such as the Esp proteins are more variable (145).

1.9.3 The T3SS

Many pathogenic Gram-negative bacteria including A/E pathogens, as well as *Yersinia*, *Salmonella* and *Shigella* species use a T3SS to inject virulence effector proteins directly into host cells that modulate host cell biology for the benefit of the pathogen. The T3SS consists of more than 20 proteins (343) (Figure 1.7). Many

components of the T3SS of EPEC, *S.* Typhimurium and *S. flexneri* are highly conserved and share structural similarity with components of the flagellar basal body complex (344, 345). The core of the T3SS is referred to as the needle complex (NC). The NC consists of a needle structure that projects from the bacterial outer membrane through which effector proteins are injected, as well as a cylindrical basal body which functions as a channel and spans the bacterial inner and outer membranes as well as the periplasmic region (346) (Figure 1.7A). The basal body of the T3SS is subdivided into three portions; an inner ring, an outer ring and a central rod which builds the channel connecting the inner and outer rings (347).

Although the EPEC NC is similar to that of *Salmonella* and *Shigella*, a unique expandable sheath-like structure exists at the tip of the thin needle (neck portion) (348). EscF is the major component of the thin needle and is required for secretion of Esp proteins (349). This is supported by the fact that *Salmonella* Δ*prgI* and *Shigella* Δ*mxiH* mutants are secretion-defective (347, 350). EscF homologues in *Salmonella* and *Shigella* are PrgI (24% identity) and MxiH (25% identity) respectively. The sheath-like structure of the EPEC NC comprises a polymer of EspA arranged in a helical fashion into a filamentous structure (351) (Figure 1.7B). EspB and EspD are secreted via the NC to form a pore in the host membrane (352). The EPEC NC can extend beyond 600 nm and is around 10 times longer than that of *Shigella* (348). The outer ring of the basal body of the T3SS consists of EscC, which is a member of the secretin superfamily (353). EscC is synthesised as a preprotein with a signal sequence. Following its export through the bacterial inner membrane via a Sec-dependent pathway, the signal sequence is cleaved off (353). EscC associates with EscD (354). EscJ is another preprotein that is transported across the inner membrane via the Sec pathway (352). Mature EscJ oligomerises to form the EPEC T3SS inner ring, along with EscR, EscS, EscT and EscU. T3SSs utilise a highly conserved ATPase to provide the energy for the transport of effectors into host cells (355-357). The EPEC or EHEC ATPase is known as EscN. EscN homologues in *Yersinia*, and *Salmonella* are known as YscN and InvC respectively (355, 357). EscN is located in the bacterial

inner membrane attached to the NC and is able to associate with effectors and chaperones via a C-terminal domain (353, 358). While the components of T3SSs are generally conserved, the effectors translocated by each T3SS apparatus are not conserved (343, 359).

1.9.4 T3SS effectors

The T3SS effectors of EPEC that are directly translocated into the host cell cytosol are encoded either within the LEE, or outside the LEE where they are termed non-LEE encoded (Nle) effectors. The T3SS effectors subvert multiple host cell functions through binding and/or modification of host cell target proteins ((360)). The role of several of these effectors in EPEC pathogenesis will be discussed briefly in the following sections.

1.9.5 Intimate attachment, actin rearrangement and pedestal formation

EPEC, EHEC and *C. rodentium* induce the formation of A/E lesions on the intestinal epithelia that are characterised by intimate bacterial attachment and the formation of actin-rich pedestals. The rearrangement of actin underneath adherent bacteria requires the translocation of the LEE-encoded effector Tir by the T3SS. Tir inserts into the host cell plasma membrane in a hairpin loop topology (361), where the central extracellular domain between the two transmembrane domains functions as a receptor for the bacterial outer membrane protein intimin (362-364), thereby mediating intimate attachment of the bacteria (365). The N- and C-terminal ends of Tir are located in the host cell cytosol (366).

Actin assembly is dependent on the host proteins actin-related protein 2/3 (Arp2/3) and the nucleation-promoting factor called neural Wiskott-Aldrich syndrome protein (N-WASP) (367, 368). Actin rearrangement by EPEC O127:H6 Tir requires phosphorylation of tyrosine residue 474 (Y474) located in the cytosolic C-terminal domain of Tir (364, 369, 370). This modification is vital for Tir to induce actin polymerisation following infection of epithelial cells *in vitro* (364). Y474

phosphorylation leads to the recruitment of the host adaptor protein Nck that recruits N-WASP (Figure 1.8). N-WASP in turn activates the actin polymerising activity of the Arp2/3 complex. *C. rodentium* Tir induces actin rearrangement by recruitment of the same host adaptor proteins (172). However, actin polymerisation by a Nck-independent mechanism involving Tir oligomerisation and phosphorylation of Y454 and Y474 has also been discovered (369, 370) (Figure 1.8).

Interestingly, EHEC Tir lacks Y474 and therefore is not tyrosine-phosphorylated in host cells (371-373). EHEC Tir induces actin polymerisation using a bacterial proline-rich effector protein called $EspF_U$/TccP that is translocated into host cells via the T3SS. Translocated TccP associates with Tir and N-WASP which then activates the Arp2/3 complex for actin polymerisation (371). EHEC O157:H7 Tir is unable to restore the ability of EPEC O127:H6 or *C. rodentium* Δ*tir* mutants to form actin-rich pedestals on cultured cells (172, 373, 374).

1.9.6 EPEC modulates host inflammation and cell death

Whilst the effacement of microvilli by EPEC may indeed contribute to the development of diarrhoea, the timing of these lesions (31) does not correlate with the rapid onset of diarrhoea seen in volunteer studies (47, 375), implying that the model of EPEC pathogenesis is considerably more complex than attachment to intestinal epithelial cells and the induction of intestinal histopathology. EPEC has evolved to modulate host cell inflammatory signaling pathways and to modulate cell death using several T3SS effectors. An overview of some well characterised effectors involved in the modulation of host inflammation and cell death is given below.

1.9.6.1 Inhibition of NF-κB-induced inflammation by EPEC

The T3SS effector NleE inhibits NF-κB activation upon TNF and IL-1β stimulation (376, 377). NleE is encoded on O-island (OI)-122 in EHEC and on integrative element IE6 in EPEC (161). Initial studies have shown that ectopically expressed NleE inhibits IκB degradation and subsequently p65 nuclear translocation upon

stimulation of cultured epithelial cells with TNF or IL-1β (376, 377). Consistently, infection of epithelial cells with EPEC expressing NleE resulted in a marked decrease in IL-8 production compared to cells infected with EPEC lacking NleE (377). In addition, NleE inhibited NF-κB activation in dendritic cells and subsequent secretion of IL-8, IL-6 and TNF (378). Recently, NleE was shown to bind to and modify the host adaptor proteins TAB2 and TAB3 upstream of IκB in the NF-κB signaling pathway (379). NleE functions as a novel cysteine methyltransferase which transfers a methyl group to a zinc coordinating cysteine residue located in the Npl4 zinc finger domain (NZF) of TAB2 and TAB3 (379). This modification results in an inability of TAB2 and TAB3 to recognise ubiquitin chains on TRAF2 and TRAF6, the ubiquitin ligases involved in TLR, TNFR and IL-1R signaling (379).

The activation of IKK in the NF-κB signaling pathway requires an upstream kinase complex consisting of TAK1, TAB1, TAB2 and TAB3. TRAF2 and TRAF6 polyubiquitinate and activate TAK1 whereas TAB2 and TAB3 are receptors of lysine-63 (K^{63})-linked polyubiquitin chains via their NZF domains (380). By modifying TAB2 and TAB3, TAK1 and IKK activation is abolished. In spite of *in vitro* studies demonstrating that NleE is a potent inhibitor of inflammation, the importance of NleE in virulence *in vivo* has been hard to define. During *C. rodentium* infection of mice, a Δ*nleE* mutant only showed a marginal attenuation compared to wild type *C. rodentium*, which could be due to redundancy with other anti-inflammatory T3SS effectors (381, 382).

Interestingly, both NleH1 and NleH2 are also associated with the inhibition NF-κB activation in response to TNF stimulation (383). NleH1 and NleH2 are present in EPEC and EHEC whereas *C. rodentium* possesses only one NleH protein which is functionally similar to NleH1 (384, 385). The mechanism by which NleH inhibits NF-κB activation is not fully understood as one study implicated the kinase activity of NleH (383), while a kinase-independent mechanism was proposed by others (384, 386). In the former study, Royan *et al*. showed that NleH1 and NleH2 inhibited IκB

degradation following TNF stimulation due to their proposed kinase activity although the precise mechanism of this inhibition is unknown (383). The NleH-mediated inhibition of IκB degradation upon TNF stimulation was disproved by other studies, which proposed a kinase-independent mechanism involving the ribosomal protein S3 (RPS3), a coactivator of NF-κB. RPS3 is phosphorylated by IKKβ and translocated into the nucleus to aid gene transcription (384). Gao *et al*. found that both NleH1 and NleH2 are capable of binding the N-terminus of RPS3 via their N-terminal region but only NleH1 inhibited IKKβ-mediated phosphorylation of RPS3 and subsequent nuclear translocation (387). Furthermore, although NleH1 and NleH2 are autophosphorylated serine/threonine kinases, they were unable to phosphorylate RPS3 and their binding to RPS3 was independent of their kinase activity (384). More recently, Pham *et al*. identified a v-Crk sarcoma virus CT10 oncogene-like protein (CRKL) as a kinase substrate of EHEC NleH1, which was required for NleH1 to inhibit RPS3 phosphorylation by IKKβ (388). More work will need to be performed to fully understand how NleH1 inhibits the RPS3/NF-κB pathway.

Infection studies using *C. rodentium* and the susceptible mouse strain C3H/HeJ mice showed that deleting *nleH* resulted in attenuation compared to the wild type strain as a higher survival rate was observed in Δ*nleH*-infected mice (385). Complementation of Δ*nleH* with EHEC NleH1 restored virulence in mice while complementation with EHEC NleH2 reduced virulence, which is consistent with the proposed opposing functions of NleH1 and NleH2 (385). The kinase activity of NleH1 was found to be important for virulence *in vivo* (389). In addition, *C. rodentium* Δ*nleH*-infected mice displayed higher colonic levels of the proinflammatory cytokine TNF (390). This colonic level of TNF was reduced to wild type levels upon expression of NleH1 but not NleH2 (390).

NF-κB activation is also inhibited by NleC which is encoded on OI-36 in EHEC and prophage PP4 in EPEC (161). NleC from EPEC and EHEC are identical on the amino acid level and share 95% similarity with NleC from *C. rodentium* (161, 391). This

effector functions as a zinc metalloprotease that directly cleaves the NF-κB subunits p50 and p65 (392-395). The direct cleavage of p65 by NleC has been shown using recombinant proteins (392, 395) and during EPEC infection (394). NleC carrying mutations in the conserved zinc metalloprotease motif ^{183}HEXXH^{187} loses its ability to cleave the NF-κB subunits, indicating that this motif is vital for proteolytic activity (396). The NF-κB subunit p65 is cleaved at the N-terminus within the Rel homology domain (392, 395). Different cleavage sites have been proposed (392, 395), although this has now been resolved to be after amino acid residue C38 (397, 398). In addition, a recent molecular study identified two regions in the Rel homology domain of p65 that serve as binding sites for NleC (399). While the deletion of *nleC* in *C. rodentium* does not result in a decreased colonising ability compared to wild type *C. rodentium*, increased colitis was observed in these mice, thereby supporting a role for NleC in the inhibition of inflammation (381, 396, 400).

Ectopic expression of the T3SS effector NleB1 in cultured cells also inhibits NF-κB activation but only upon TNF and not IL-1β stimulation suggesting NleB1 interfered with death receptor signaling (377). However, NleB1 does not inhibit production of the proinflammatory cytokine IL-8 during EPEC infection (401). Apart from the above-mentioned Nle effectors, the LEE-encoded effector Tir has also been implicated in inhibiting host innate immune signaling. Tir possesses immunoreceptor tyrosine-based inhibitory motifs (ITIMs), which are features of host proteins, at the N-terminus (402). ITIM-containing proteins are phosphorylated at conserved tyrosines. This in turn allows binding to the tyrosine phosphatases SHP-1 and SHP-2 and down regulation of host innate immune responses (403, 404). For example, Tir phosphorylation at Y483 and Y511 leads to the interaction of Tir with SHP-1 and decreased TNF and IL-6 expression (402, 405). Additionally, Tir has been reported to inhibit TNF-induced NF-κB signaling by targeting the host adaptor protein TRAF2 (406).

1.9.6.2 Inhibition of MAPK-induced inflammation by EPEC

NleD is another zinc metalloprotease effector of A/E pathogens. NleD is encoded on OI-36 in EHEC and prophage PP4 in EPEC downstream of *nleC*. NleD contains the conserved zinc metalloprotease motif ^{141}HEXXH^{145} and directly cleaves the c-Jun N-terminal kinase (JNK) and mitogen activated protein kinase (MAPK), p38 (392). In response to stimulation of Toll-like receptors (TLRs), interleukin 1 receptor (IL-1R) or TNFR, several mitogen activated protein 3 kinases (MAP3Ks) are activated that can in turn activate JNK which can then phosphorylate c-Jun, a member of the AP-1 group of transcription factors regulating cell proliferation, apoptosis and inflammation (407, 408). JNK activation involves phosphorylation on threonine-183 and tyrosine-185 located in the activation loop (409) and NleD cleaves JNK and p38 in this activation loop (392). The combined inactivation of JNK and p38 by NleD is linked with suppression of the inflammatory response via inhibition of IL-8 expression as infection of epithelial cells with a Δ*nleBECD* mutant of EPEC resulted in higher levels of IL-8 secretion compared to cells infected with a Δ*nleBEC mutant*.

1.9.6.3 Inhibition of inflammasome activation by EPEC

Pathogenic *E. coli* and *C. rodentium* are known to elicit activation of the NLRP3 inflammasome in epithelial cells and macrophages resulting in the production of IL-1β and inflammation (410-412). Recently, NleA was shown to inhibit the secretion of IL-1β from infected THP-1 cells (413). This inhibition was not due to the inhibition of NF-κB activation but rather on the direct binding of NleA to NLRP3 (413). The interaction of NleA to NLRP3 interrupted the de-ubiquitination of NLRP3, which is required for the assembly of the NLRP3 inflammasome. Hence, by binding to NLRP3, NleA limited the formation of NLRP3 inflammasome foci following EPEC infection and negatively regulated IL-1β secretion (413). NleA is the first reported EPEC effector that is involved in the suppression of inflammasome activation in macrophages.

1.9.7 EPEC infection and host cell viability

A number of studies have shown that EPEC surface properties and some translocated effectors can activate apoptotic signaling *in vitro*; purified outer membrane EPEC proteins induce TNF expression and activate caspase-3 induced apoptosis (414, 415) and EPEC strains expressing bundle forming type IV pili (Bfp) induce cell death in cultured epithelial cells more readily than strains that lack Bfp suggesting that attachment plays a role in triggering cell death (416). The modes of cell death triggered by EPEC infection have not been fully elucidated and some inconsistencies exist in the analysis of caspase activation (416-418).

Additionally, some individual effector proteins have been directly implicated in inducing cell death. T3SS effectors such as EspF and Map compromise mitochondrial and tight junction integrity leading to increased apoptotic cell death (287, 419-425). EspF is a LEE encoded effector with a multitude of attributed functions ranging from microvillus effacement, disruption of the epithelial barrier, depletion of host cell DNA mismatch repair (MMR) proteins and the induction of apoptosis (426, 427). EspF triggers intrinsic apoptosis by disrupting the mitochondrial membrane potential (MMP), resulting in the release of cytochrome *c* into the host cell cytosol and caspase-9 activation (421). EspF also binds the host protein Abcf2 within mitochondria and in the presence of EspF, the level of Abcf2 in cells decreases while caspase-9 cleavage increases (422). Furthermore, cells treated with siRNA to *abcf2* show increased caspase-3 activation when stimulated with staurosporine, suggesting that Abcf2 may be involved in apoptosis (422). Given the localisation of Map to the mitochondria, this effector has also been implicated in reduced host cell survival, although the precise role of Map in cell death remains to be determined.

Another EPEC effector, Cif, affects host cell cycle progression inducing a delayed form of apoptosis (428-430). More recently Cif was found to target NEDD8, a ubiquitin-like protein involved in cell cycle control (431). Cif harbours a papain-like cysteine protease domain that deamidates NEDD8 and thereby compromises the activity of neddylated Cullin-RING ubiquitin ligases leading to defective ubiquitin-

dependent degradation of multiple host cell proteins and increased cytotoxicity (432). EspH also induces a cytotoxic effect and induces caspase-3 cleavage, which is related to disassembly of focal adhesions (433, 434). EspH binds the DH-PH domain in multiple RhoGEFs, which prevents activation of Rho and therefore Rho-dependent events such as phagocytosis as well as disruption of the host actin cytoskeleton structure (434).

1.9.7.1 Anti-apoptotic effectors of EPEC

Despite the fact that some effectors have been associated with cytotoxic effects and/or activation of executioner caspases, in general cells infected with EPEC do not display characteristic late apoptotic features such as membrane blebbing, nuclear condensation and cell shrinkage. In addition, *in vivo* studies report that apoptosis was not observed in tissues from humans infected with EPEC (37, 38, 435) or in tissues from C57BL/6 mice infected with *C. rodentium* (176). Hence apoptosis is not a characteristic feature of EPEC infection. In fact, compared to *Salmonella*, *Shigella* and *Yersinia*, three genera of invasive enteric bacteria, EPEC was experimentally much weaker in its ability to cause cell death (418, 436, 437).

The first EPEC T3SS effectors associated with the inhibition of cell death were NleH1 and NleH2. Δ*nleH1/H2* double mutants of EPEC are highly cytotoxic for cells, which can be complemented by the reintroduction of either *nleH1* or *nleH2* (390). Further investigation of NleH1 showed that this effector inhibits caspase-3 activation/cleavage even when cells are treated with a wide range of proapoptotic compounds including staurosporine, tunicamycin and brefeldin A. Caspase-3 inhibition was independent of NleH predicted kinase activity (390). The exact mechanism by which NleH1 blocks apoptosis has not been fully elucidated although NleH1 interacts with an anti-apoptotic protein called Bax inhibitor-1 (BI-1) (390). BI-1 is an ER protein that when overexpressed in mammalian cells suppresses apoptosis induced by a variety of stimuli including the proapototic protein Bax, deprivation of growth factor, treatment with the anti-cancer agent, etoposide as well as staurosporine

(438). NleH1 also blocks cell death induced by the TcdB toxin from *Clostridum difficile*. TcdB is a glucosyltransferase that inactivates Rho family proteins causing disruption of the cell cytoskeleton and cell death (439). The modification of Rho by TcdB is detected by a newly described pyrin-containing inflammasome (440) that activates caspase-1 and induces cell death. More work is needed to elucidate the mechanism by which NleH blocks cell death, especially given the ability of NleH1 to inhibit cell death from such a diverse range of intrinsic stimuli involving different caspases.

The effector NleD which was found to inhibit MAPK signaling is also believed to promote cell survival given that the cleavage of JNK in the activation loop can block JNK-mediated apoptosis (392).

1.9.7.2 Inhibition of the extrinsic cell death response

EPEC has also evolved an ability to block death receptor induced apoptosis using NleB. EPEC and EHEC express two homologues of the T3SS effector NleB while *C. rodentium* expresses only one. Initial studies in EPEC identified a role for NleB1 in the inhibition of NF-κB activation upon TNF but not IL-1β stimulation (376, 377), yet despite this, NleB1 does not inhibit IL-8 production during EPEC infection (401). Instead recent studies have demonstrated that NleB1 inhibits the extrinsic apoptotic pathway by modifying DD-containing proteins including FADD, RIPK1 and TRADD (401, 441). The role of RIPK1 and TRADD in the TNFR1 receptor complex likely explains the inhibition of NF-κB activation under certain experimental conditions (3, 377)

NleB1 is a glycosyltransferase (442) that binds to and modifies the DD of FADD by adding a single GlcNAc moiety at arginine-117 (Arg^{117}), thereby inhibiting TNF or FasL-induced DISC formation and subsequent caspase-8 activation and apoptotic cell death. Arg^{117} in FADD is essential for Fas-FADD as well as TRADD-FADD DD interactions (443, 444). The critical role of this conserved residue in apoptosis is

evident in the embryonic lethality of mice carrying an R117Q mutation (445). NleB1 also GlcNAcylates TRADD at the equivalent arginine residue (Arg^{235}), preventing recruitment of TRADD, TRAF2 and ubiquitinated RIPK1 to TNFR1 (441). NleB1 also inhibits TRAIL-induced DISC formation and apoptosis (441).

The role of NleB1 *in vivo* has been investigated using *nleB* deletion mutants of *C. rodentium*. *nleB* mutants are attenuated for colonisation (381) and mice infected with *C. rodentium* lacking *nleB* show increased numbers of cells positive for cleaved caspase-8 (401), suggesting that death receptor signaling controls bacterial load. The importance of the FasL-Fas signaling pathway during *C. rodentium* infection was demonstrated by infecting Fas-deficient ($Fas^{lpr/lpr}$) and FasL-deficient ($Fas^{gld/gld}$) mice with *C. rodentium* (401). Both strains develop severe, watery diarrhoea and showed increased colitis in response to *C. rodentium* compared to wild-type mice. Although the source of FasL during infection is unclear, this model suggests that FasL-positive immune cells recognise and delete infected cells by inducing apoptosis, thereby controlling pathogen load. In the presence of NleB, this cell death response is thwarted and the bacteria maintain their attachment to a viable enterocyte (Figure 1.9).

While NleB1 is specific for the extrinsic apoptotic pathway, NleF has been implicated in the inhibition of apoptosis stimulated by both the intrinsic and extrinsic pathways (446). Due to the ability of NleF to bind and inhibit caspase-9 activation, the main focus of work on NleF has been the inhibition of intrinsic apoptosis. However, NleF also prevents TRAIL-induced apoptosis in HeLa cells by binding to and inhibiting caspase-8 (446). NleF-mediated inhibition results from insertion of the carboxy terminal end of NleF into the active site of the caspase (446). However, the role of NleF in apoptosis inhibition during infection is still unclear and may be secondary to effectors such as NleB1, as no significant differences were observed in the activation of downstream executioner caspases-3 and 7 in HeLa cells infected with wild-type EPEC or a Δ*nleF* EPEC derivative (446). NleF also binds to caspase-4 which was

recently described as an innate sensor of intracellular LPS (447). The CARD domain of caspase-4 binds directly to LPS leading to stimulation of pyroptosis. Hence during infection the role of NleF may be to counteract inflammasome formation in infected enterocytes.

1.9.7.3 Protecting epithelial integrity

Two further T3SS effector proteins influence cell survival through maintaining cellular junctions. EspZ (SepZ) is a LEE encoded effector protein that promotes maintenance of intestinal epithelium by stabilising focal adhesions during infection (448-450). Epithelial cells infected with an EPEC Δ*espZ* mutant exhibit increased cytotoxicity compared to cells infected with wild type EPEC and EspZ-mediated protection from cytotoxicity has been attributed to its ability to bind CD98. CD98 enhances signaling from the β1-integrin receptor, including pro-survival signals from the Akt kinase and focal adhesion kinase (FAK) (451, 452).

Interestingly, the T3SS effector, OspE, from the invasive enteric pathogen *Shigella flexneri* also stabilises focal adhesion sites of host intestinal cells, thereby reinforcing their adherence to the basement membrane and preventing the exfoliation of infected cells into the gut lumen (453). The mechanism of action of OspE is via binding to integrin-linked kinase (ILK), which contributes to the inhibition of focal adhesion disassembly rather than affecting focal adhesion assembly (453). Focal adhesion disassembly is normally accompanied by phosphorylation of focal adhesion kinase (FAK) and paxillin (454). Indeed, the phosphorylation of both FAK and paxillin was significantly reduced in cells expressing OspE and ILK (453). The residue important for OspE binding to ILK was also identified as tryptophan-68 (W68) (453). OspE homologues can be found in strains of EHEC, EPEC and *C. rodentium* where they are termed EspO. W68 is highly conserved among EspO homologues, which also bind to ILK (453). Hence EspO effectors in A/E pathogens may act in concert with EspZ and effectors that regulate the actin cytoskeleton to block sloughing of infected cells in the gut lumen (455).

1.10 Pathogenesis of the invasive pathogen *Salmonella*

Like EPEC infection, *Salmonella* infection is well understood. Much of what is known about *Salmonella* infection and pathogenesis has been determined by a combination of *in vitro* and *in vivo* studies. Mice have been used extensively to model human *Salmonella enterica* infections due to the relatively low cost for the maintenance of mice and the availability of a wide range of transgenic and knockout strains. Interestingly, while *S.* Typhimurium causes gastroenteritis in humans, infection of susceptible mouse strains such as BALB/c and C57BL/6 with *S.* Typhimurium leads to a systemic illness, reminiscent of human typhoid fever and is therefore used to study systemic disease from *Salmonella* infection in humans (456). Mice develop elevated temperatures, ruffled fur and lose weight but do not show symptoms like diarrhoea, with mice succumbing to infection as early as 5 days post infection depending on the mouse strain infected, the *S.* Typhiumurium strain used and the route of infection (456). A streptomycin mouse model has been developed to study intestinal salmonellosis where mice orally pretreated with streptomycin and infected with *S.* Typhimurium display high bacterial colonisation levels in the caecum and colon (10^8-10^{10} CFU/g faeces) accompanied by intestinal inflammation as early as one day post oral infection (457). Mice also develop softened faeces. Streptomycin pretreatment significantly reduces the microbiota density and composition, thereby disrupting the colonisation resistance to enteric pathogens (458).

1.10.1 The intestinal phase of infection and inflammation

Following oral infection (natural route) with *S. enterica*, a small proportion of bacteria can tolerate the acidic environment of the stomach (459) and enter the small intestine. *Salmonella* can switch virulence gene expression in as quickly as 4 minutes upon sensing new environmental conditions (460) such as the anaerobic conditions of the small intestine (461). *Salmonella* is also capable of withstanding destruction by bile salts and attack by local innate immune responses (462, 463), while competing with the normal gut microbiota (464, 465). Early volunteer studies reviewed by Blaser *et al*. indicate that the infectious dose ranges from 10^5 to 10^8 organisms and that this

variation depends on the serovar of the organism (466). The pathogen successfully colonises the host by first invading the intestinal epithelium using a T3SS which will be explained in more detail later.

A key regulator of virulence gene operons that enable invasion of the gastrointestinal epithelium is HilA (467-470). It has been suggested that *Salmonella* preferentially invades the antigen-sampling M cells and translocate to the underlying Peyer's patches (471, 472). It has also been shown that *Salmonella* invades M cells and induces apoptosis of these cells to facilitate access to the Peyer's patches (473, 474). Infection of enterocytes with *Salmonella* also results in the manipulation and disruption of tight junctions to enable the bacteria to reach the lamina propria. Dendritic cells have also been shown to extend through tight junctions and transport *Salmonella* from the gut lumen to the lamina propria and mesenteric lymph nodes (MLNs) (475-477), whereby the bacteria gain access to macrophages, neutrophils and other DCs by macropinocytosis, providing them with an intracellular niche. In humans, NTS serovars such as Typhimurium and Enteritidis remain confined to the intestines. Infection with these serovars results in gut mucosal inflammation triggered by innate immune responses accompanied by neutrophil influx and gastroenteritis (478). More recently, it has been shown that *S.* Typhimurium takes advantage of the host intestinal inflammation to sidestep nutritional competition in the gut (479). *S.* Typhimurium-induced intestinal inflammation stimulates the production of tetrathionate that can be used as an electron acceptor to support anaerobic respiration. Tetrathionate respiration enabled *S.* Typhimurium to utilise ethanolamine, a nutrient that is not readily fermented, thereby providing *S.* Typhimurium with a competitive edge in the inflamed intestines over the microbiota (479).

1.10.2 Invasion of enterocytes by *Salmonella*

Salmonella invasion of host cells is a key virulence factor. Unlike EPEC, which possesses one T3SS, *S. enterica* possesses two virulence-associated systems, T3SS1 and T3SS2. These are differentially regulated and are encoded on two distinct PAIs

known as *Salmonella* pathogenicity islands 1 and 2 (SPI-1 and SPI-2) (178, 480, 481). The T3SS effectors are encoded within as well as outside these PAIs. T3SS1 is activated upon contact with intestinal epithelial cells and translocates at least 15 effectors directly into the host cells (482), whereby many of those T3SS1 effectors such as SipA, SipC, SopB, SopE, SopE2 and SptP induce localised membrane ruffling and bacterial invasion (483). SipA and SipC both bind to actin and collaborate to form actin filaments (F-actin) (484). SipA is not essential for invasion by *S.* Typhimurium but enhances SipC-mediated actin nucleation and bundling of F-actin (485-487). SopE, SopE2 and SopB do not directly bind to actin but mediate the activation of small Rho GTPases that contribute to the formation of F-actin networks. Unlike SopE and SopE2 which directly activate Rho GTPases (488, 489), SopB indirectly activates RhoG through the activation of SH3-containing guanine exchange factor (SGEF) (490). Interestingly, SipA, SopB, SopE and SopE2 also disrupt the tight junctions between epithelial cells. In contrast, SptP terminates the membrane ruffling process following bacterial invasion by inactivating Rho GTPases such as Rac1 and Cdc42, thereby reverting the actin cytoskeleton to its original state (491).

Other T3SS1 effectors activate the MAPK pathways leading to the production of proinflammatory cytokines and recruitment of PMNs (483). Oral infection with *S.* Typhimurium mutants that are defective for secretion via the T3SS1 results in a 10 to 100 fold decrease in virulence in the mouse model of systemic infection (480, 492). The moderately poor attenuation of SPI-1 null mutants reflects the ability of *S. Typhimurium* to spread to the liver and spleen from the intestines through uptake by and survival within transmigrating phagocytic cells (493). Furthermore SPI-1 mutants display no virulence defect upon intraperitoneal infection of mice (480, 492), confirming that the T3SS1 does not have a significant role in bacterial survival in macrophages.

1.10.3 The systemic phase of infection

How *Salmonella* is restricted to the gut and prevented from spreading systemically is

unclear. The development from gut restricted infections to systemic spread with traditionally self-limiting NTS serovars in immunocompromised patients suggests that $CD4^+$ T cells are essential for limiting systemic spread (494-499). Additionally, the innate influx of polymorphonuclear cells and inflammation previously mentioned in *Salmonella* gastrointestinal infections is not seen in human typhoid infection, suggesting that typhoidal *Salmonella* may avoid the early innate intestinal immune response to spread systemically (500). This is supported by the fact that *Salmonella* is not controlled by gut-associated lymphoid tissue (GALT) during infection of mice with *S*. Typhimurium or infection of humans with *S*. Typhi and the bacteria spread via the lymphatic systems to other sites such as the MLN, liver, spleen and bone marrow (501-503).

1.10.4 Intracellular survival in the *Salmonella*-containing vacuole (SCV)

The ability to survive within host cells following invasion is yet another key virulence factor that is fundamental to the success of *Salmonella* as a pathogen. Intracellular survival is vital for virulence in a murine typhoid model. SPI-2 null mutants are profoundly attenuated in the systemic mouse model upon oral or intraperitoneal infection (178, 481, 504). Furthermore, depletion of macrophages, the primary intracellular niche, renders *S*. Typhimurium avirulent (505-507). T3SS2 is responsible for mediating intracellular survival and replication of *Salmonella* (178, 481). This T3SS is found in all subspecies of *S. enterica* but absent from *S. bongori* (508) . Upon invasion into enterocytes or entry into macrophages by macropinocytosis (T3SS1 dependent or independent), *Salmonella* is contained within phagosomes that mature into SCVs. T3SS2 effectors are thought to modulate this maturation to SCVs. The complex biogenesis of SCVs is accompanied by the formation of tubules connected to the SCVs known as *Salmonella*-induced filaments (Sifs) that are most apparent in epithelial cells, extending from the SCV (509).

About 30 T3SS2 effectors have been discovered, many of which seem to mediate late SCV biogenesis including the movement of the SCV to the juxtanuclear region (483,

510). For example, SifA is necessary for Sif formation given that a Δ*sifA* mutant was unable to form Sifs and escaped from the SCV into the cytosol (511). This mutant was also attenuated in mice (512). PipB2 cooperates with SifA in Sif formation whereas SseJ counteracts the effect of SifA and downregulates Sif formation, as a Δ*sifAsseJ* double mutant does not escape the SCV (513-515). More recently, SseF and SseG have been also been found to be essential for the formation of Sifs and perinuclear positioning of the SCV although the mechanism of action is unknown (516, 517). Previously, it was reported that *Salmonella* uses several T3SS2 effectors to block phagosome–lysosome fusion and promote intracellular survival (518). However, several studies have shown that evasion of lysosme fusion is not a major determinant for bacterial survival within the SCVs, given that this can occur in infected phagocytic and non-phagocytic cells (519, 520). To this date, the function of many T3SS2 effectors remains unknown or ill-defined and requires characterisation.

1.10.5 Inhibition of inflammation by *Salmonella* T3SS effectors

Some *S.* Typhimurium T3SS effectors have the ability to inhibit the host inflammatory response, thereby giving the pathogen more time to colonise the host and proliferate before dissemination. For example, GogB, which is encoded on the bacteriophage Gifsy-1 and secreted by both the SPI-1 and SPI-2- encoded T3SSs (521), was recently identified as an anti-inflammatory effector that manipulates the host ubiquitination system (522). GogB targets the Skp, Cullin, F-box (SCF) containing complex by binding to two of its components: S-phase kinase-associated protein 1 (Skp1) and F-box only protein 22 (FBOX22) (522). The SCF complex is a multi-protein E3 ubiquitin ligase which catalyses the addition of ubiquitin moieties to proteins fated for proteasomal degradation, one of which is IκB (523). By targeting the SCF complex, GogB interferes with IκB degradation and inhibits NF-κB activation.

The cellular responses stimulated soon after *S.* Typhimurium entry within host cells such as the reorganisation of actin and inflammation are quickly reversed by the SPI-

1-encoded T3SS effector SptP (524, 525). SptP is a substrate of the SPI-1 T3SS. While the reversion of changes in the actin cytoskeleton is mediated by the GTPase-activating protein (GAP) activity of SptP located within its N terminus (526), the inhibition of inflammation by SptP arises from inhibition of the MAPK ERK (526, 527). SptP inhibits ERK activation by inhibiting Raf1, a process requiring the GAP activity of SptP as well as its tyrosine phosphatase activity which is conferred by its C terminus (527). Inhibition of ERK activation ultimately leads to a decrease in the production of the pro-inflammatory cytokine IL-8 (526).

Another *Salmonella* effector to contribute to the downregulation of IL-8 production after invasion of intestinal epithelial cells is SspH1. SspH1 is encoded by the bacteriophage Gifsy-3 (528) and can be translocated by both the SPI-1 and SPI-2 T3SSs (529). SspH1 has been found to bind to a mammalian serine/threonine protein kinase called PKN1 using its leucine-rich repeat domain (530) which could explain the nuclear localisation of SspH1 as well as its role in the inhibition of NF-κB-dependent gene expression including IL-8 expression (531). More experimental work will need to be performed to clarify how the SspH1-PKN1 interaction inhibits NF-κB signaling. SpvC is yet another *Salmonella* effector with anti-inflammatory properties. SpvC is encoded on a virulence plasmid and is a substrate of both the SPI-1 and SPI-2 T3SSs, although translocation into the cytosol of macrophages occurs via the SPI-2 T3SS (532). SpvC functions as a phosphothreonine lyase, removing phosphate from threonine in the conserved activation motif of MAPK ERK to irreversibly inactivate the kinase (532). In addition, SpvC inactivates p38 and JNK *in vitro* (533, 534) and inhibits the production of pro-inflammatory cytokines *in vivo* (533). It has been suggested that the ability of SpvC to suppress inflammation is by the inactivation of the MAPK signaling pathway (533).

Interestingly, the *Salmonella* effector SseL was also proposed to be anti-inflammatory. SseL was suggested to dampen innate immune defences *in vivo* by deubiquitinating IκB, preventing its proteasomal degradation and interfering with NF-

κB signaling (535). However, recently, a new study reassessed the involvement of SseL in the inhibition of the NF-κB pathway and found no evidence proving that SseL targets the NF-κB pathway (536). Instead, SseL was found to contribute to macrophage cell death (536).

1.10.6 *Salmonella* and cell death

Salmonella can induce host cell death using T3SS-dependent and independent mechanisms depending on the cell type infected (537). *Salmonella* expressing T3SS1 triggers a rapid programmed cell death termed pyroptosis that is dependent on caspase-1 within 1-2 h post infection of macrophages and dendritic cells (244, 313, 538, 539). Caspase-1 activation leads to the activation of Il-1β and IL-18, cell lysis and the release of intracellular contents. Previous studies suggested the T3SS1 effector SipB could bind directly to caspase-1 and induce pyroptosis (540). However, later studies have shown that caspase-1 activation requires NLRC4 inflammasome activation by flagellin or the T3SS rod protein PrgJ, which are both injected in the host cell cytosol (209, 314, 541). Importantly, *Salmonella* grown under conditions repressing T3SS1 expression do not induce pyroptosis in macrophages. However, a delayed macrophage cell death occurs 18-24 h post infection (313, 542-544). This delayed macrophage cell death is also mediated by caspase-1 and is believed to share features of pyroptosis and requires T3SS2 and the effectors SpvB and SseL. During this delayed cell death, *Salmonella* activates the NLRP3 and NLRC4 inflammasomes (545).

In contrast to the rapid onset of cell death in macrophages following *Salmonella* infection, *Salmonella* induces late apoptosis in epithelial cells 12-18 h post infection (546). This delayed apoptosis in epithelial cells requires bacterial entry and replication. Human colon epithelial cells (HT29) infected with an invasion-defective mutant of *S. enterica* serovar Dublin (Δ*invA*) or an Δ*aroA* mutant of *S*. Dublin, which is as invasive as the wild type strain but replicates more slowly inside cells, display reduced apoptosis compared to cells infected with wild type *S*. Dublin (546).

Additionally, TNF and nitric oxide (NO), which are produced during the early inflammatory response upon invasion of epithelial cells, contribute to the late induction of epithelial cell apoptosis (546).

1.10.7 Inhibition of cell death by *Salmonella*

Although less numerous than anti-inflammatory effectors, effectors which have been associated with the inhibition of host cell death will be briefly discussed. SopB, also known as SigD (547), possesses some anti-apoptotic activity in *Salmonell*a-infected epithelial cells. SopB is encoded within SPI-5 (548) and is a SPI-1 T3SS substrate (549). The ability of this effector to inhibit apoptosis is dependent on its phosphoinositide phosphatase activity which is in turn required for the activation of the serine/threonine kinase Akt (550, 551) . Akt is a prosurvival kinase which suppresses apoptosis (552).

While some effectors can either inhibit inflammation or apoptosis, the SPI-1-encoded T3SS effector AvrA (553) can dampen both the inflammatory and apoptotic pathways of a eukaryotic host. AvrA is a substrate of the SPI-1 T3SS (553). AvrA has been reported to target a number of signaling pathways. Initial studies suggested that AvrA blocks the NF-κB pathway downstream of IKK activation; Collier-Hyams *et al*. focused mainly on *in vitro* work showing that ectopically expressed AvrA inhibited the nuclear translocation of the NF-κB subunit p65 in response to TNF as well as TNF-induced activation of an NF-κB-dependent IL-8 reporter in HeLa cells (554). However, Collier-Hyams *et al*. also suggested that AvrA is proapoptotic (554). Later work by Ye *et al*. showed that AvrA inhibited NF-κB signaling and apoptosis both *in vitro* and *in vivo* and proposed that AvrA acts as a deubiquitinase with IκB and β-catenin as suggested targets (555). Deubiquitination of IκB rendered it more stable, preventing NF-κB nuclear translocation whereas deubiquitination of β-catenin led to NF-κB stabilisation and activation of transcription, thereby increasing cell proliferation and inhibiting apoptosis (555). A different biochemical activity was suggested by Jones *et al*., whereby AvrA inhibits inflammation and apoptosis both *in*

vivo and *in vitro* by acetylating the mitogen-activated protein kinase kinases (MAPKKs) MKK4 and MKK7, inhibiting their phosphorylation and blocking the c-JUN N-terminal kinase (JNK) and NFκB signaling pathways (556). Using the streptomycin pretreatment mouse model of enteric salmonellosis, it was then shown that AvrA prevents macrophage cell death and bacterial dissemination by blocking JNK phosphorylation (557). The ability of AvrA to dampen both the inflammatory and the apoptotic pathways is consistent with the fact that *Salmonella* elicits transient inflammation in intestinal epithelial cells without overtly destroying the epithelia which is more characteristic of infections with *Shigella* or EHEC (558).

1.11 Aims of this study

Many Gram-negative bacteria use the T3SS and translocated effector proteins to cause disease in the host. While the role of many of these effectors in virulence has been determined, many effectors remain to be fully characterised. The effectors NleA to G were initially identified when studying the A/E pathogen *C. rodentium* (448). Amongst these effectors, NleB1 is highly conserved across all A/E pathogens and has strong homologues in *Salmonella* species, termed SseKs (559, 560). At the time this study began, NleB1 was only known to inhibit NF-κB activation *in vitro* and to be important for virulence *in vivo* (377, 381). Since then, NleB1 has been characterised as an *N*-acetyl glucosamine transferase that modifies a conserved arginine within death domain proteins, thereby inhibiting extrinsic apoptotic signaling (401, 441). Given the unique arginine glycosyltransferase activity of NleB1 and the unknown targets of SseK1-3, the broad aim of this study was to characterise the NleB/SseK effectors further. The specific aims were to:

i) map the potential functional and substrate binding sites of NleB1,

ii) test the functional impact of these selected regions of NleB1 during EPEC infection *in vitro* and *in vivo* and

iii) characterise the NleB homologues, SseK1-3, in *Salmonella*.

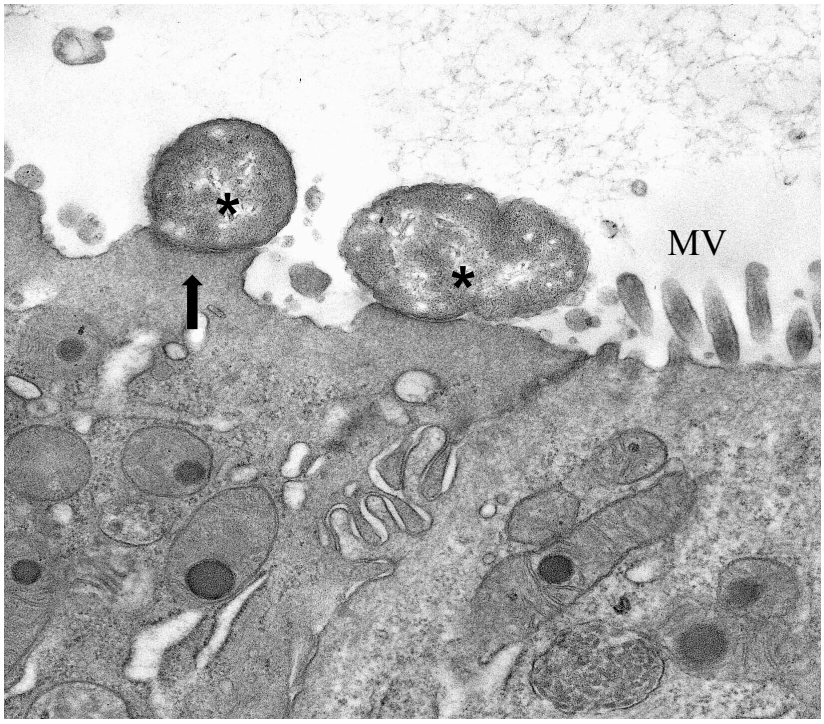

Figure 1.1. Electron micrograph showing an attaching and effacing (A/E) lesion. *Citrobacter rodentium* (asterisk) adheres closely to murine colonic cells, inducing the formation of an actin-rich pedestal (arrow) at the site of the bacterial attachment and effacement of brush border microvilli (MV). *C. rodentium* on the right is undergoing cell division. (Image adapted from (561) - Courtesy of Vicki Bennett-Wood)

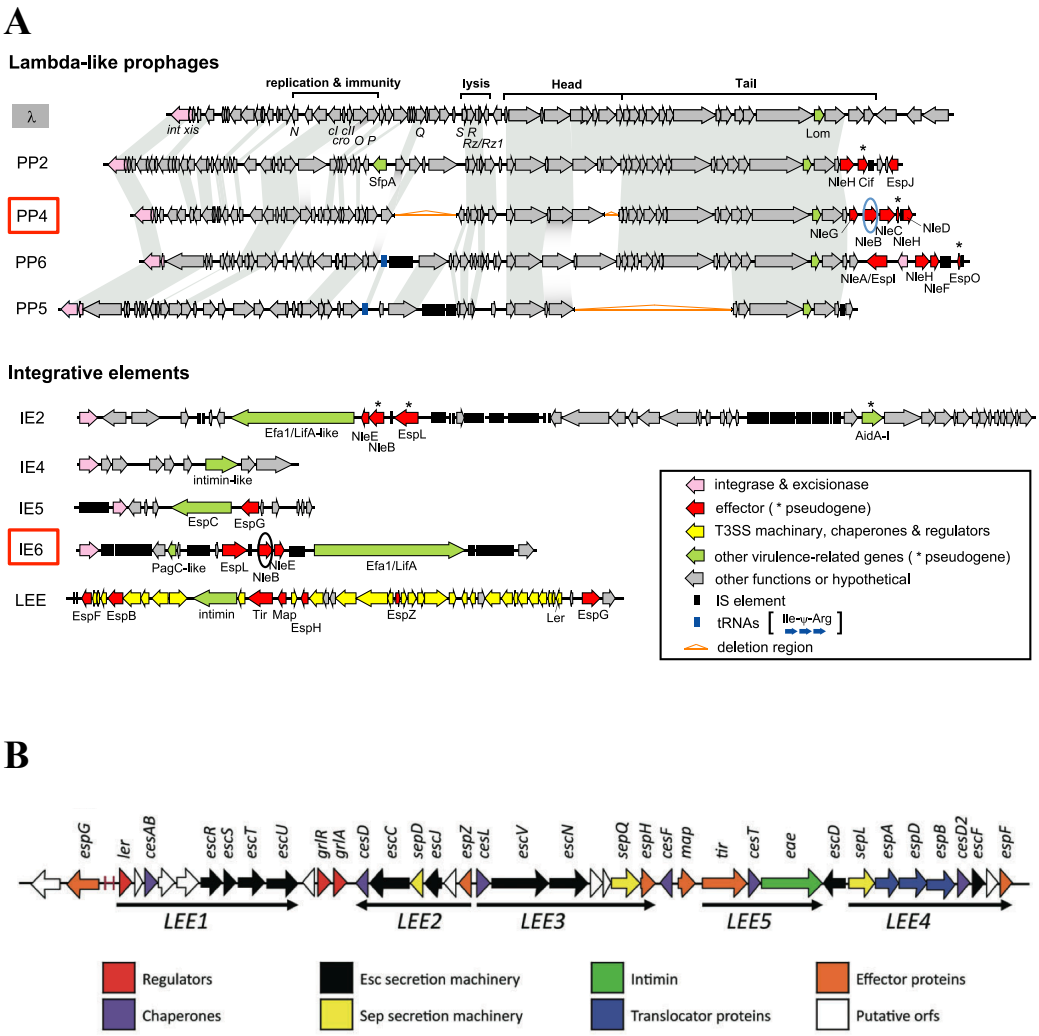

Figure 1.2. Distribution of mobile genetic elements of EPEC. (A) EPEC O127:H6 E2348/69 carries 4 lambda-like phages (PP2, 4, 5 and 6) and 5 integrative elements (IE2, 4, 5 and 6 and the LEE PAI). T3SS effectors are encoded on these genetic elements. Homologous genes in the lambda (accession no. NC_001416) and four PP genomes are indicated by grey shading. Note NleB1 is encoded on IE6 and NleB2 is encoded on PP4. Image adapted from (161). (B) Schematic diagram illustrating the genetic organisation of the EPEC E2348/69 LEE PAI. Image from (562).

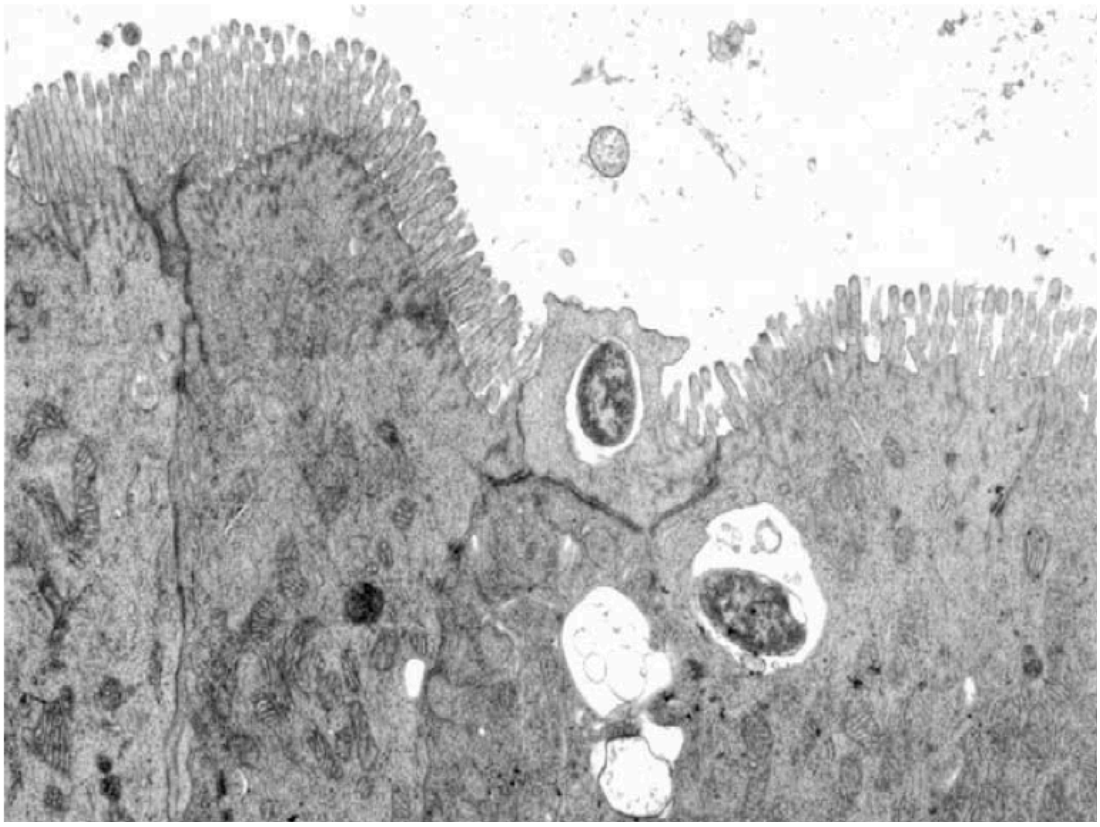

Figure 1.3. Electron micrograph showing invasion of enterocytes by *Salmonella* Typhimurium. *S.* Typhimurium invades intestinal epitheial cells in bovine ligated ileal loops. Membrane ruffles are seen at the apical surface. Image from (456).

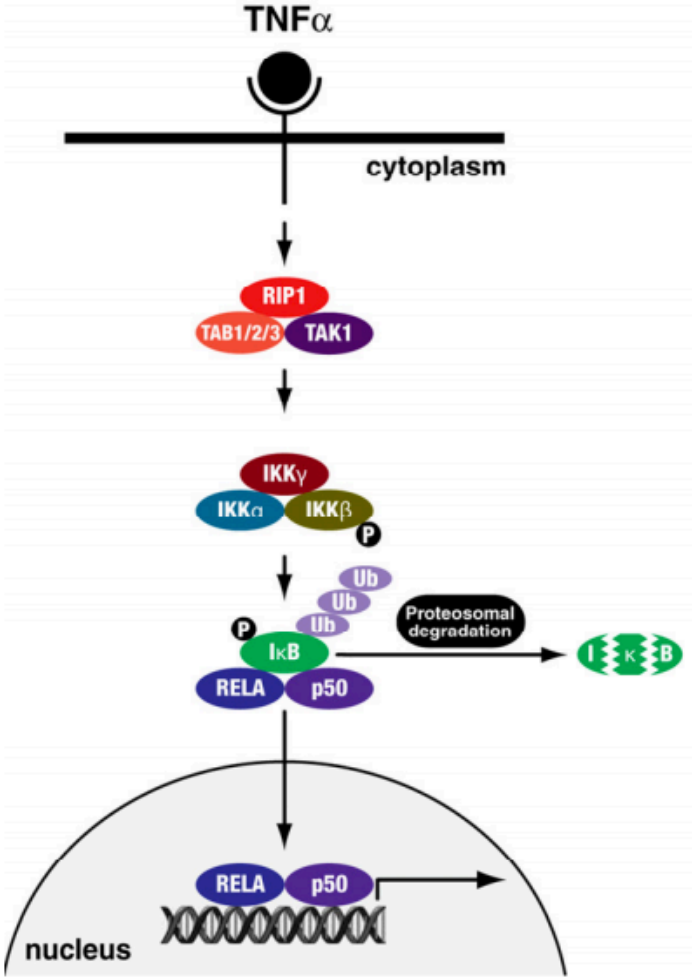

Figure 1.4. Schematic diagram of the canonical pathway of NF-κB activation. The canonical pathway of NF-κB activation is activated by the stimulation of cytokine receptors such as TNFR1. This triggers a signaling cascade, which converges to the activation of the IκB kinase (IKK) complex consisting of IKKα, IKKβ and IKKγ, and the phosphorylation and proteasomal degradation of IκB. This frees the NF-κB dimers which then translocate to the nucleus. Image from (563).

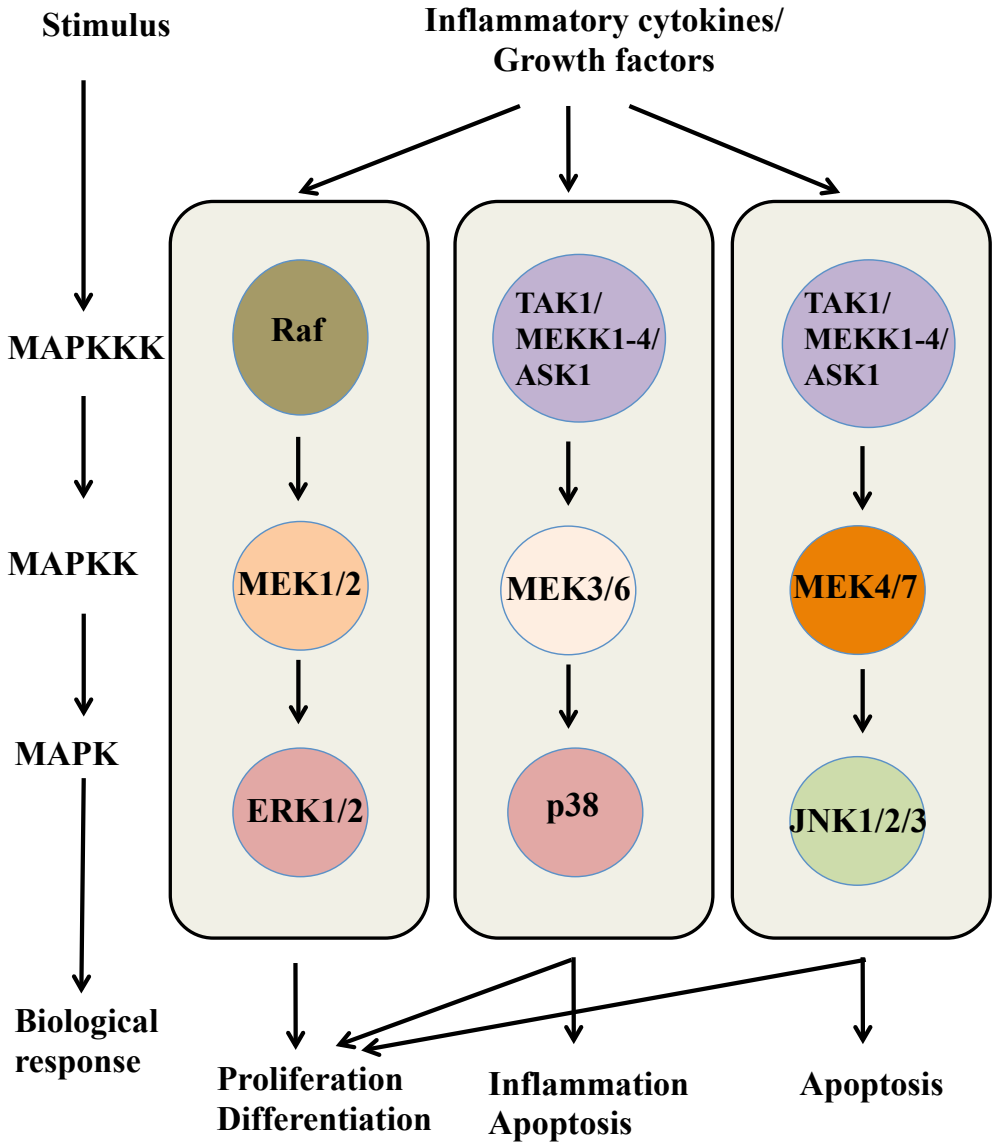

Figure 1.5. Schematic diagram of the major MAPK signaling pathways.
Mitogen-activated protein kinases (MAPKs) are serine/threonine kinases involved in many cellular processes including inflammation. Conventional MAPKS include ERK1/2 and p38 isoforms and are highlighted in pink. A broad range of extracellular stimuli activates the MAPKK kinases (MAPKKKs), which then phosphorylate and activate a downstream MAPK kinase (MAPKK). This in turn phosphorylates MAPKs. Image adapted from (564).

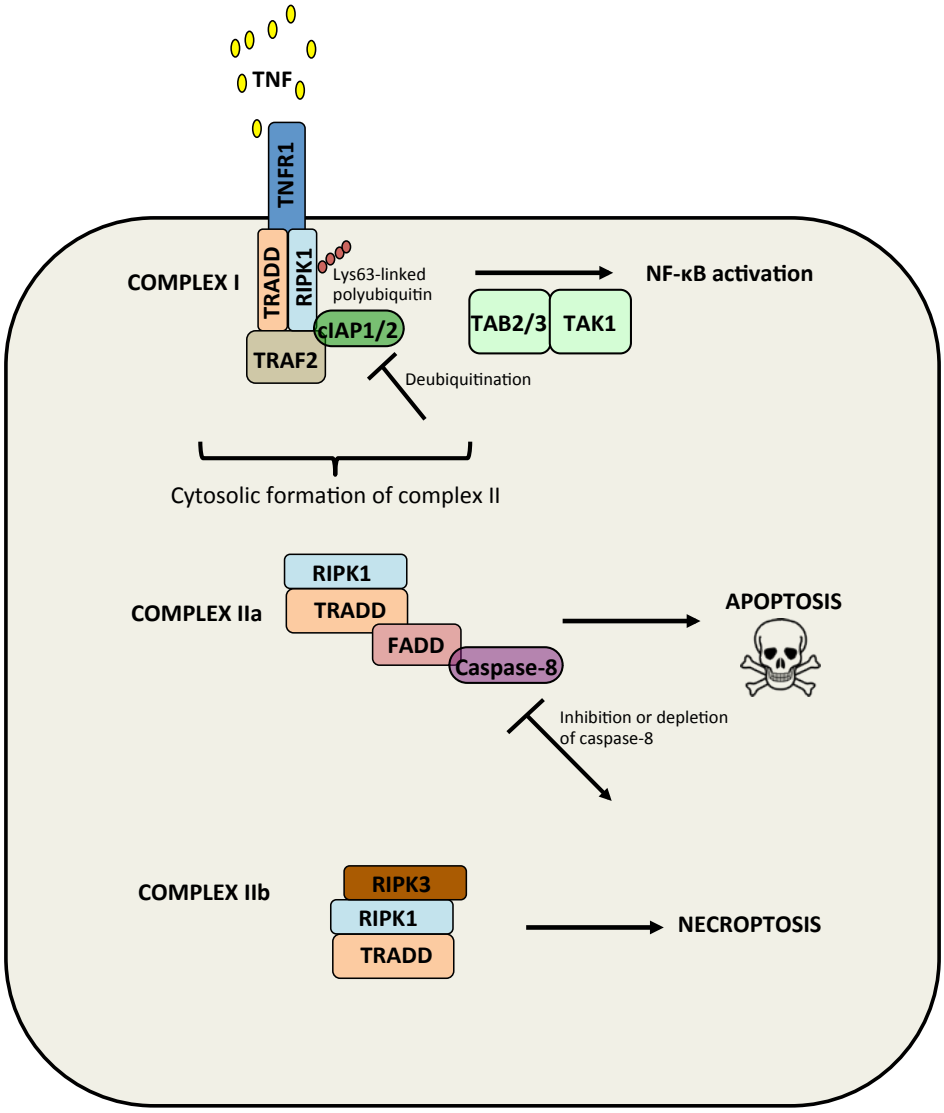

Figure 1.6. TNFR1 signaling pathways. Upon binding to TNF, TNFR1 recruits a membrane-bound complex called complex I. This complex consists of multiple adaptor proteins including TRADD, RIPK1, TRAF2 and cIAP1/2. In this complex, RIPK1 is polyubiquitinated and recruits TAK1 and TAB2/3. TAK1 activates the IKK complex resulting in NF-κB activation. When complex I is deubiquitinated by deubiquitinating enzymes, the receptor complex is internalised, leading to the formation of one of two cytosolic complexes called complex IIa and IIb. Complex IIa consists of TRADD, which recruits FADD and caspase-8 ultimately leading to host cell apoptosis. If caspase-8 is depleted or inhibited, RIPK1 and RIPK3 become engaged in the necroptotic pathway. Image adapted from (231, 565).

A

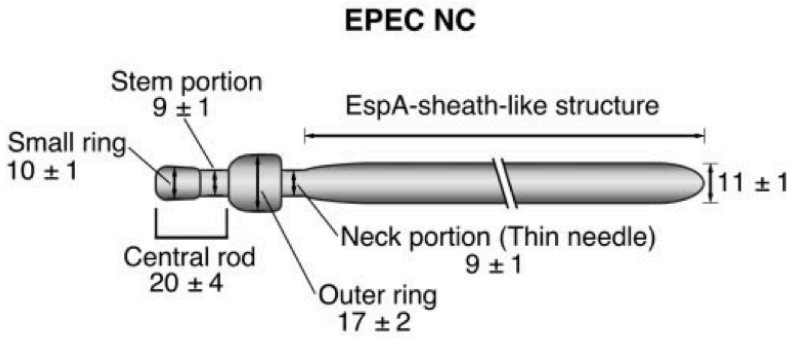

B

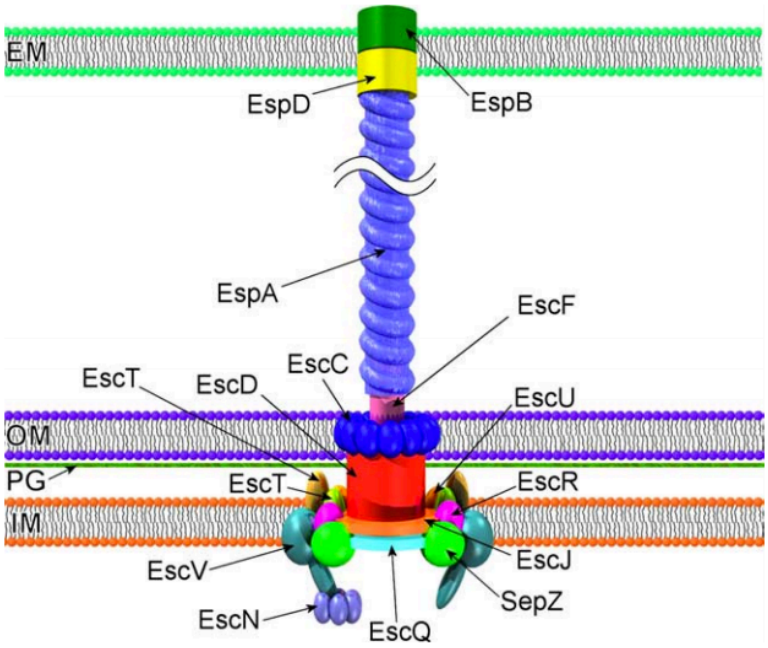

Figure 1.7. The EPEC T3SS. (A) Model of the EPEC NC core structure. The size of each structure is given in nanometers. Image from (566). (B) Schematic diagram of the T3SS encoded by the LEE PAI of EPEC. IM, inner membrane; PG, peptidoglycan layer; OM, outer membrane; EM, eukaryotic membrane. Note that the EspA pilus is a characteristic of the EPEC T3SS. Image from (567).

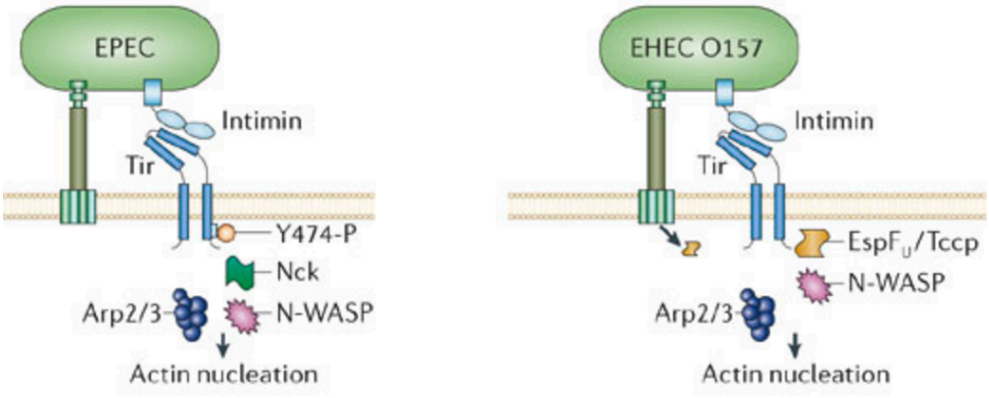

Figure 1.8. Schematic diagram of the intimate attachment induced by EPEC and EHEC. Tir-mediated actin recruitment differs in EPEC and EHEC. Tir is translocated via the T3SS and inserts itself in the host cell plasma membrane. The extracellular portion of Tir binds the bacterial outer membrane intimin. EPEC Tir phosphorylated at Y474 and recruits the host protein Nck which in turn recrutits N-WASP. EHEC Tir is not phosphorylated and recruits the translocated EHEC protein TccP. TccP associates with N-WASP and triggers actin assembly. Image from (568).

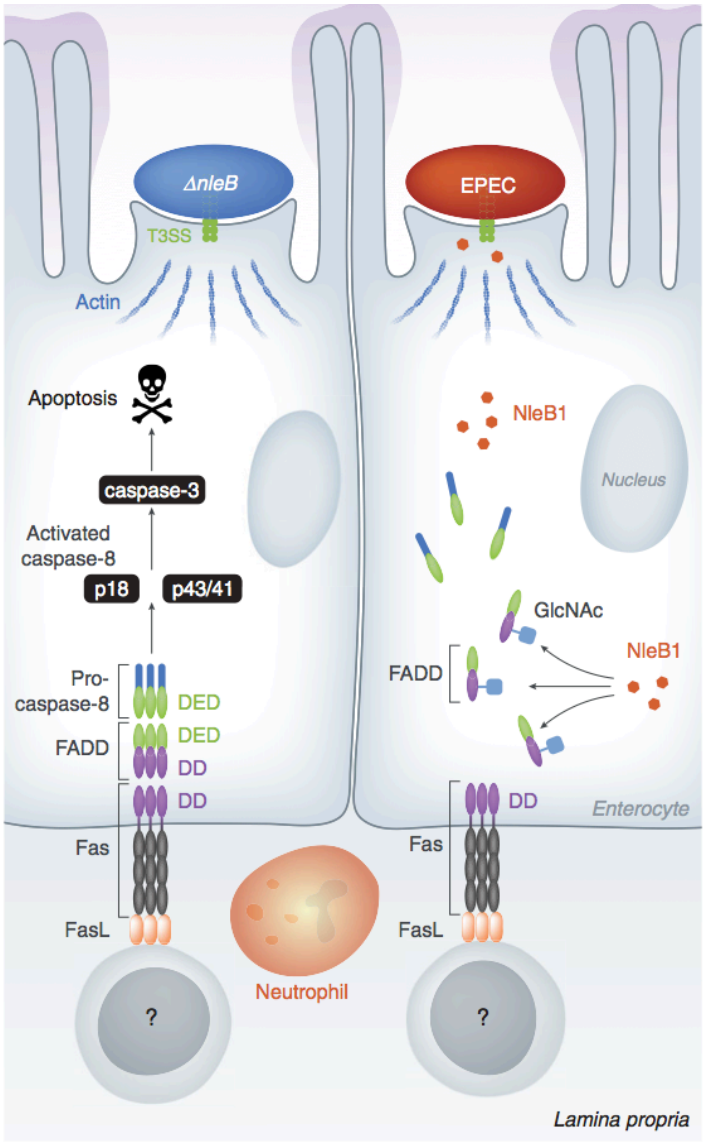

Figure 1.9. Schematic diagram showing inhibition of FasL-induced cell death in enterocytes during EPEC infection. Wild-type EPEC inhibits caspase-8 activation and apoptotic cell death using NleB1, which GlcNAcylates FADD (blue squares) and prevents formation of the DISC. EPEC lacking NleB1 (Δ*nleB1*) cannot inhibit FasL-driven apoptotic cell death. The specific source of FasL during EPEC infection has not yet been identified. Image from (561).

Chapter 2

Materials and methods

Chapter 2: Materials and methods

2.1 Bacterial strains, yeast strains, media and growth conditions

2.1.1 Bacterial strains, yeast strains and plasmids

The bacterial strains, yeast strains and plasmids used in this study are listed in Tables 2.1, 2.2 and 2.3 respectively.

2.1.2 Media

All bacterial and yeast media were purchased from Sigma-Aldrich (St Louis, USA), Oxoid Limited (Basingstoke, UK), Difco (Maryland, USA) or Amresco (Ohio, USA), unless otherwise stated and sterilised by autoclaving for 20 min at 121ºC. When solid media were required, liquid media were supplemented with 1.2 to 2.2 % (w/v) agar.

The following media were routinely used:

1. Luria-Bertani (LB) broth: 1% (w/v) tryptone, 0.5% (w/v) yeast extract, 171 mM NaCl, pH 7.2
2. SOB medium: 2% (w/v) tryptone, 0.5% (w/v) yeast extract, 10 mM NaCl, 2.5 mM KCl, 10 mM $MgCl_2$ and 10 mM $MgSO_4$
3. SOC medium: SOB supplemented with 20 mM glucose
4. Yeast extract peptone dextrose (YPD) medium: 1% (w/v) yeast extract, 2% (w/v) peptone, 2% (v/v) glucose
5. Yeast nitrogen minimal (YMM) medium or synthetic dextrose (SD) medium: 0.7% (w/v) YMM, 2% (v/v) glucose

2.1.3 Chemicals and reagents

All chemicals and reagents used in this study were of analytical grade. Chemicals and reagents were purchased from Sigma-Aldrich (St Louis, USA), Merck (Darmstadt, Germany) or Chem Supply (South Australia, Australia), unless otherwise stated. When required, antibiotics were added at the following concentrations: ampicillin (Amp; Astral Scientific, New South Wales, Australia), 100 μg/ml; kanamycin (Kan;

Amresco, Ohio, USA), 50 μg/ml or 100 μg/ml; nalidixic acid (Nal; Sigma-Aldrich), 50 μg/ml; chloramphenicol (Cm; Boehringer Mannheim, Germany), 10 μg/ml, 12.5 μg/ml or 25 μg/ml; streptomycin (Strep; Sigma-Aldrich), 50 μg/ml; tetracycline (Tet; Sigma-Aldrich), 12.5 μg/ml.

2.1.4 Culture conditions

2.1.4.1 Bacterial culture conditions

All *E. coli* and *C. rodentium* strains were grown at 37°C in LB broth with shaking at 180 rpm or in Dulbecco's modified Eagle's medium (DMEM) (Gibco, Life Technologies, NY, USA) without shaking. Antibiotics were added when necessary. For infection of HeLa cells, overnight cultures of EPEC grown in LB medium were subcultured 1:50 into DMEM and grown statically for 3-4 h at 37°C with 5% CO_2. The optical density (OD_{600}) of the bacterial cultures was measured to standardise the inoculum to an OD_{600} of 0.03 before infection. Cultures were induced with 1mM isopropyl-β-D-thiogalactopyranoside (IPTG; AppliChem, Darmstadt, Germany) for 30 min prior to infection when required.

All *Salmonella enterica* strains were grown at 37°C in LB broth supplemented with streptomycin with shaking at 180 rpm overnight. Additional antibiotics were added when required. For infection of HeLa cells or THP-1 cells, overnight cultures of *Salmonella enterica* grown in LB medium were subcultured 1:200 into fresh LB broth supplemented with streptomycin and grown statically for 20-21 h at 37°C with 5% CO_2. The OD_{600} of the bacterial cultures was measured to standardise the inoculum before infection at a multiplicity of infection (MOI) of 50. Cultures were induced with 1mM IPTG for 30 min prior to infection when necessary. Infected tissue cultures were centrifuged at 1,500 rpm at room temperature (RT) for 5 min to synchronise the infection.

2.1.4.2 Yeast growth conditions

Yeast strains were grown at 30°C in YPD medium or SD medium. SD medium was used as a basal medium to which supplements could be added when required, including the amino acids L-histidine (His), 20 μg/ml, L-methionine (Met), 20 μg/ml, L-tryptophan (Trp), 20 μg/ml, and L-leucine (Leu), 30 μg/ml, and the bases adenine (Ade), 24 μg/ml and uracil (Ura), 20 μg/ml. Kanamycin was added to a final concentration of 15 μg/ml. YPD medium was always used supplemented with adenine.

2.2 DNA isolation and purification

2.2.1 DNA purification

The Wizard® SV gel and PCR Clean-Up System (Promega Corporation, Wisconsin, USA.) was used to purify DNA from agarose gel or in solution. When DNA purification from agarose gel (Bioline, London, UK) was required, PCR products or restriction digests were run on agarose gel, excised in a minimal volume of agarose gel using a sterile scalpel blade and gel purified as per the manufacturer's instructions.

2.2.2 Genomic DNA extraction

Genomic DNA was extracted using the Quick-gDNA™ MiniPrep Kit (Zymo Research Corp., California, USA) according to the manufacturer's instructions. Prior to bacterial genomic DNA extraction, a loopful of freshly streaked bacterial cells was resuspended in 200 μl PBS and Proteinase K enzyme (New England Biolabs (NEB), Maryland, USA) was added to the resuspended cells at a final concentration of 1mg/ml. The mixture was then incubated at 37°C for 10 min.

2.2.3 Plasmid DNA extraction

Plasmid DNA was isolated using the QIAprep® Spin Miniprep kit (QIAGEN, California, USA) according to the manufacturer's instructions. When high concentrations of plasmids were required, plasmid DNA was isolated using the

NucleoBond®Xtra Midi kit (Machery-Nagel, Düren, Germany) using the manufacturer's instructions.

2.2.4 cDNA synthesis

RNA was extracted from HeLa cells and cDNA was generated by reverse transcription using the QuantiTect® Reverse Transcription kit (QIAGEN) as per the manufacturer's instructions.

2.2.5 Enzymatic manipulation of DNA

2.2.5.1 Restriction enzyme digestion

Restriction enzyme digests were performed using enzymes and buffers from Roche (Basel, Switzerland) and NEB (Maryland, USA) according to the manufacturer's instructions. Briefly, DNA digestion reactions routinely consisted of 1 to 1.5 µg of DNA, 5 to 10 Units (U) of restriction enzyme, and one tenth volume of 10 x restriction buffer made up to a final reaction volume of 20 to 50 µl with dH_2O. Reactions were generally incubated at the recommended temperature for up to 3 h.

2.2.5.2 DNA ligation

Ligation reactions were performed at an insert: vector molar ratio of 4:1 or 3:1 at 4°C or RT overnight. When DNA fragments needed to be ligated with the cloning vector pGEM®-T-Easy (Promega), the supplied reagents were used according to the manufacturer's instructions. For each ligation reaction, 50 ng of vector and the appropriate amount of insert were ligated with 1µl of T4 DNA ligase (NEB) and one tenth volume of 10 x reaction buffer (NEB) in a total volume of 10 or 20 µl.

2.2.6 Resolution and recovery of DNA fragments

Amplification or digestion products were run and analysed on 1%-2% (w/v) agarose gels stained with 1 x SYBR®Safe DNA Gel Stain (Invitrogen, California, USA) in TAE buffer (40 mM Tris, 0.114 % (v/v) glacial acetic acid, 1 mM EDTA (pH 8.3)). DNA was mixed with 6 x gel loading dye (NEB) prior to loading onto agarose gel.

The size of amplified or digested products was determined by comparison with 100 bp and 1kb DNA ladders (NEB). To visualise the DNA, the SYBR®Safe-stained gels were placed on a UV transilluminator (Syngene, Cambridge, UK) and digital images of gels were taken using the G:BOX HR Gel Documentation and Analysis System (Syngene, Cambridge, UK).

2.3 DNA transformation

2.3.1 Preparation of electrocompetent *E. coli* cells

Bacterial strains were cultured in 10 ml LB broth supplemented with antibiotics when required overnight at 37°C with shaking at 180 rpm. Overnight cultures were subinoculated 1:50 in 30 ml LB broth and grown at 37°C with shaking at 180 rpm to an OD_{600} of 0.8 to 1.0. The bacterial cells were incubated on ice for 30 min, pelleted at 4,000 rpm for 20 min at 4°C and resuspended in 0.4 volume ice-cold 10% glycerol (v/v). The bacterial cells were pelleted again and washed first in 0.2 volume of ice-cold 10% glycerol and then 0.1 volume of ice-cold 10% glycerol. The resulting pellet was resuspended in a final 0.01 volume of ice-cold 10% glycerol, frozen in 50 µl aliquots on dry ice and stored at -80°C until required.

2.3.2 Preparation of electrocompetent *Salmonella* cells

Bacterial strains were cultured in 10 ml LB broth supplemented with antibiotics when required overnight at 37°C with shaking at 180 rpm. Overnight cultures were subinoculated 1:100 in 200 ml SOB and grown at 37°C with shaking at 180 rpm to an OD_{600} of 0.8. The bacterial cells were incubated on ice for 15 min, pelleted at 6,000 rpm for 10 min at 4°C and resuspended in 0.5 volume ice-cold distilled water. The bacterial cells were pelleted again and washed in 0.02 volume of ic-cold 10% glycerol before centrifuging at 10,000 rpm for 10 min. The resulting pellet was resuspended in a final 0.005 volume of ice-cold 10% glycerol, frozen in 50 µl aliquots on dry ice and stored at -80°C until required.

2.3.3 Electroporation

Electroporation was performed by adding 50-100 ng of DNA to 50 µl electrocompetent cells. The mixture was transferred to a cold 0.1 cm gap electroporation cuvette (Cell Projects, Kent, UK) and then subjected to electroporation using a Micropulser electroporator (Bio-Rad Laboratories, Hercules, California, USA) with settings of 1.8 V, 25 µF capacitance, 200 Ohm resistance for about 4-6 ms. 250 µl or 1 ml of SOC was immediately added to the shocked cells which were then incubated for 1 hr at 37°C with shaking at 180 rpm. Three different volumes of the suspension (50 µl, 100 µl and the remaining culure pelleted and resuspended in 200 µl of fresh SOC media) were plated onto selective media and incubated at 37°C for 24 h to select for transformants.

2.3.4 Preparation of chemically competent cells

Bacterial strains were grown in 10 ml LB broth overnight at 37°C with shaking at 180 rpm, with the required antibiotic added when necessary. Overnight cultures were subinoculated 1:100 in 100 ml SOB and grown at 16°C with shaking at 200 rpm to an OD_{600} of 0.4 to 0.8. The bacterial cells were then harvested by centrifugation at 2,500 rpm for 15 min at 4°C, resuspended in 0.4 volume ice-cold transformation buffer (10 mM PIPES, 15 mM $CaCl_2$, 55mM MnCl2, 250 mM KCl, pH 6.7) and incubated on ice for 10 min. The bacterial cells were pelleted again and resuspended in 0.04 volume of ice-cold transformation buffer. DMSO (Sigma) was added to a final concentration of 7.5 % (v/v) and the cells were incubated on ice for 10 min. Competent cells were then frozen on ethanol dry ice bath and stored at -80°C in 50 µl aliquots until required.

2.3.5 Chemical transformation

Chemical transformation was performed by adding 100 ng of DNA to 50 µl of chemically competent cells. The mixture was incubated on ice for 30 to 60 min, then at 42°C for 90 s and on ice for 2 min. The chemical transformation reaction was added to 1 ml of SOC and incubated for 1 hr at 37°C with shaking. Aliquots of the

cells were plated onto selective media and incubated at 37°C overnight to select for transformants.

2.4 Oligonucleotides

Synthetic oligonucleotides used in sequencing and polymerase chain reactions reactions were ordered from Sigma-Aldrich (New South Wales, Australia). Oligonucleotide sequences are listed in Table 2.4.

2.5 Polymerase chain reaction (PCR)

PCR amplifications were generally performed using AmpliTaq Gold® DNA polymerase (Life Technologies) or GoTaq® DNA Polymerase (Promega) in a reaction volume of 50 µl. AmpliTaq Gold® DNA polymerase (Life Technologies) was used at a final concentration of 0.1 U/µl, with 0.7 mM of each dNTP, 0.2 µM of each primer, one tenth volume of 10 x PCR buffer, 2 mM $MgCl_2$ and 100 ng of template DNA. PCR amplifications were performed in a GS482 G-STORM thermal cycler (G-STORM, Somerset, UK). PCR conditions used, following a standard hot start of 95°C for 5 min, were 35 cycles of 95°C for 15 sec, 48-58°C for 15 sec (temperature dependent on the melting temperatures of the primers), and 72°C for 1-2 min (1 min per kb of PCR product), followed by one extension at 72°C for 7 min. GoTaq® Green Master Mix was used at a 1 x final concentration with 0.1 µM of each primer and 100 ng of template DNA. The PCR conditions involved denaturation at 95°C for 2 min, followed by 30 cycles of 30 sec at 95°C, 30 sec at 48-55°C (temperature dependent on the melting temperatures of the primers) and an extension at 72°C for 1 min per kb of PCR product.

2.6 Colony PCR

Colonies were picked using sterile toothpicks and each was used as template in a PCR reaction. The PCR reaction contained GoTaq® Green Master Mix at a 1 x final concentration and 0.1 µM of each primer in a total volume of 20 µl. The PCR conditions consisted of a denaturation step at 95°C for 2 min, followed by 30 cycles of 30 sec at 95°C, 30 sec at 48-55°C (temperature dependent on the melting

temperatures of the primers) and an extension at 72°C for 1 min per kb of PCR product.

2.7 DNA sequencing and analysis

Sequencing was performed using the ABI PRISM Big Dye Terminator v3.1 Cycle Sequencing kit. Capillary electrophoresis was performed by Micromon DNA Sequencing Facility (Monash University, Victoria, Australia) or by Applied Genetic Diagnostics (The University of Melbourne, Victoria, Australia). DNA sequence was analysed using Sequencher® version 5.0 sequence analysis software (Gene Codes Corporation, Ann Arbor, Michigan, USA) and BioEdit software (569).

2.8 Bioinformatics analysis

Amino acid sequences of the catalytic region of the glycosyltransferases Lgt1 from *Legionella pneumophila* (Lpl1319, accession number 2WZG_A, amino acids 209-260 and Lpg1368, accession number Q5ZVS2, amino acids 209-260), α-toxin from *Clostridium novyi* (accession number Q46149, amino acids 253-296), lethal toxin (LT) from *Clostridium sordellii* (accession number Q46342, amino acids 255-298), toxins A and B from *Clostridium difficile* (accession number CAC03681, amino acids 253-299 and accession number P18177, amino acids 255-298 respectively), PaTox from *Photorhabdus asymbiotica* (accession number CAQ84322, amino acids 2245-2290) and NleB1 from EPEC (accession number CAS10779, amino acids 176-230) were used to build an alignment using MUSCLE (Version 3.5 or 3.8.31) (570) through the Geneious tool (Version 8.1.4) (571).

Amino acid sequences of NleB1 homologues, NleB1 and NleB2 from EPEC O127:H6 strain E2348/69 (accession number CAS10779 and WP_000950813.1 respectively), NleB1 from EHEC O157:H7 strain Sakai or EDL933 (accession number WP_000953022.1), NleB1 from REPEC O15:H$^-$ strain 83/89 (accession number WP_000953025.1), NleB from *Citrobacter rodentium* ICC169 (accession number WP_012905389) and SseK1, SseK2 and SseK3 from *Salmonella enterica* serovar

Typhimurium strain SL1344 (accession number CBW20184, CBW18209 and CBW18025 respectively), were used to build an alignment using MUSCLE (Version 3.5 or 3.8.31) (570) through the Molecular Evolutionary Genetics Analysis 5 (MEGA 5) tool (572) or the Geneious tool (Version 8.1.4) (571). The MUSCLE aligned sequences were used to construct a Maximum Likelihood phylogenetic tree based on the JTT matrix-based model with 1000 bootstraps using MEGA 5 to infer homology between the amino acid sequences. The tree was edited using Dendroscope (573) and is drawn to scale with branch lengths measured in the number of substitutions per site, and bootstrap values indicated on the branches.

A set of protein sequences was curated based on the identification of NleB1 homologues from EPEC E2348/69, *C. rodentium* and *S.* Typhimurium SL1344. Sequences were identified using BLAST (574) against fully assembled *E. coli* genomes from PATRIC, draft *E. coli* assemblies and reference *Salmonella* genomes (575, 576). The nucleotide sequences were translated into amino acid sequences using EMBOSS (577) and the protein sequences were aligned with MUSCLE (570). The best fitting model JFF was determined using the Perl script Protein Model Selection for RAxML (578). Three pseudo-replicate RAxML analyses were run with 100 bootstraps each. The best scoring Maximum Likelihood tree was selected and midpoint rooted in Dendroscope (579). The accession numbers numbers used for phylogenetic analyses are provided in Supplementary Table 1 in the appendix section.

2.9 Construction of expression vectors

2.9.1 Construction of *nleB1* transposon mutants

Generation of a library of *nleB1* transposon mutants was carried out using the Mutation Generation System (MGS) F701 kit (Life Technologies) consisting of the purified enzyme MuA transposase and an artificial transposon carrying a chloramphenicol resistance marker, designated as entranceposon (M1-Cam^R). The transposon mutants were generated following the manufacturer's instructions in a

pEGFP-C2-NleB1 clone whereby EPEC E2348/69 *nleB1* (GenBank accession number FM180568.1) was cloned in between *Eco*RI and *Bam*HI restriction sites.

Briefly, the transposon insertion clones generated in the transposition reaction were digested with the restriction enzymes *Eco*RI and *Bam*HI to release the DNA of interest. This was then purified and ligated into the newly extracted cloning vector pEGFP-C2 digested with *Eco*RI and *Bam*HI. The newly ligated plasmids obtained were then digested with the restriction enzyme *Not*I to remove the body of the entranceposon. The *Not*I digested clones were then self-ligated, resulting in a 15 bp insertion in the *nleB1* gene. When the entranceposon insertion occurs in the coding region of the target gene *nleB1*, the 15 bp insertion is translated into five extra amino acids. The position of the pentapeptide insertion of each mutant was determined by sequencing with the primer pairs pEGFP-C2 F/NotI, NotI/pEGFP-C2 R and pEGFP-C2 F/R. Sequence alignment was carried out using the BioEdit software. Each mutant *nleB1* carrying the pentapeptide insertion was then digested with *Eco*RI and *Bam*HI from the pEGFP-C2 constructs, purified and ligated into the pTrc99A vector, digested with the same pair of restriction enzymes. The ligation reactions were individually transformed into XL-1 Blue cells and the plasmid extracts were further sequenced with the primer pair pTrc99A F/R.

2.9.2 Construction of *nleB1* site directed mutants

A library of site directed mutants of *nleB1* was obtained by using the QuikChange II Site-Directed Mutagenesis kit (Stratagene, California, USA) as per the manufacturer's instructions in a pEGFP-C2-NleB1 clone. Briefly, pEGFP-C2-NleB1 was used as template in the PCR reactions to generate the single and multiple site directed mutations in the NleB1 protein carrying an N-terminal GFP tag. The primer pairs P63 F/R, I64 F/R, L65 F/R, N66 F/R, K68A F/R, K81A F/R, D93A F/R, D121A F/R, D128A F/R, L157A F/R, Y219A F/R, Y234A F/R, P236A F/R, D237A F/R, G238A F/R, I239A F/R, H242A F/R, E253A F/R, N263A F/R, L267A F/R, A269E F/R, Y283A F/R, K292A F/R, PILN F/R, HKQ F/R, QES F/R, LGLL F/R, GSL F/R, DKL F/R, PDG F/R, PDG_{AKA} F/R, PDG_{AEA} F/R, PD_{AR} F/R, PDG_{SRS} F/R, PDG_{SES} F/R,

PD_{SE} F/R, SN F/R, LAGL F/R, KV F/R and KGI F/R were used to produce the mutations K68A, K81A, D93A, D121A, D128A, L157A, Y219A, Y234A, P236A, D237A, G238A, I239A, H242A, E253A, N263A, L267A, A269E, Y283A, K292A, PILN(63-66)AAAA, HKQ(140-142)AAA, QES(142-144)AAA, LGLL(155-158)AAAA, GSL(197-199)AAA, DKL(228-230)AAA, PDG(236-238)AAA, PDG(236-238)AKA, PDG(236-238)AEA, PD(236-237)AR, PDG(236-238)SRS, PDG(236-238)SES, PD(236-237)SE, SN(262-263)AA, LAGL(268-271)AEAA, KV(277-278)AA and KGI(289-291)AAA respectively . The PCR reactions were digested with *Dpn*I restriction enzyme at 37°C overnight to digest the parental template plasmid before subsequent transformation into XL-1 Blue cells. The transformation reactions were plated on LB agar (LA) supplemented with kanamycin and 3 colonies were selected per transformation for plasmid extraction and sequencing with pEGFP-C2 F/R. The constructs pTrc99A-$NleB1_{Y219A}$ and pTrc99A-$NleB1_{E253A}$ were obtained by digesting the corresponding pEGFP-C2 constructs with *Eco*RI and *Bam*HI and ligating into pTrc99A, predigested with the same pair of restriction enzymes.

2.9.3 Construction of vectors expressing *sseK2* and *sseK3* fused to an N-terminal enhanced green fluorescent protein (GFP) tag

The wild type *sseK2* and *sseK3* genes (Accession numbers CBW18209.1 and CBW18025.1 respectively) were amplified from *S.* Typhimurium SL1344 genomic DNA using the primer pairs GFP S2 F/R and GFP S3 F/R respectively and AmpliTaq Gold® DNA polymerase. The resultant PCR products of approximately 1 kb were purified and ligated into pGEM-T®-Easy vector at an insert:vector molar ratio of 3:1. The ligation reactions were transformed into XL-1 Blue cells and plated onto LA plates supplemented with ampicillin and X-gal at a final concentration of 80 µg/ml. For each transformation, 3 white colonies were chosen for growth in LB broths containing ampicillin and plasmid extractions were performed on the clones the following day. Following sequencing with the M13 F/R primers, the pGEM-T®-Easy constructs containing the correct *sseK2* and *sseK3* sequence were then digested with

*Eco*RI and *Sal*I restriction enzymes (NEB) to release the 1kb fragments which were gel purified. The resultant fragments were ligated into *Eco*RI and *Sal*I digested pEGFP-C2 at an insert:vector molar ratio of 3:1. The ligation reactions were then transformed into XL-1 Blue cells and colony PCR was performed using primers pEGFP-C2 F/R to select positive clones. The correct insert was confirmed by sequencing.

2.9.4 Construction of vectors expressing the putative catalytic mutant of *sseK1*, *sseK2* and *sseK3* fused to an N-terminal GFP tag

The pEGFP-C2-SseK1$_{DxD(229-231)AxA}$, pEGFP-C2-SseK2$_{DxD(239-241)AxA}$ and pEGFP-C2-SseK3$_{DxD(226-228)AxA}$ constructs were generated using the QuikChange II Site-Directed Mutagenesis kit (Stratagene) as per the manufacturer's instructions. Briefly, the above-mentioned constructs were generated using the primer pairs S1$_{AAA}$ F/R, S2$_{AAA}$ F/R and S3$_{AAA}$ F/R respectively and pEGFP-C2-SseK1, pEGFP-C2-SseK2 and pEGFP-C2-SseK3 as templates. Plasmids were digested with *Dpn*I restriction enzyme at 37°C overnight before subsequent transformation into XL-1 Blue cells. Transformants were selected on LA containing kanamycin. For each transformation, 3 transformants were selected for plasmid extraction and sequencing with the primer pair pEGFP-C2 F/R.

2.9.5 Construction of yeast expression plasmids for yeast two-hybrid screen

2.9.5.1 Construction of yeast bait plasmids

pGBKT7 was used as a bait plasmid in yeast studies. The bacterial gene *nleB2* from EPEC E2348/69 (Accession number FM180568.1 or CAS08589.1) was amplified from genomic DNA using the primer pair B2 F/R and AmpliTaq Gold® DNA polymerase. Similarly, *sseK2* and *sseK3* from *Salmonella* Typhimurium SL1344 were amplified using primer pairs S2 F/R and GFP S3 F/R respectively. The PCR products were ligated into the cloning vector pGEM-T®-Easy and the ligation reaction was transformed into XL-1 Blue cells. Transformants were then selected on LA containing ampicillin and X-gal. For each transformation, 3 white clones were selected and their

plasmids sequenced. The construct with the correct sequence was selected and digested with the appropriate restriction enzymes (*Eco*RI and *Bam*HI for *nleB2* and *sseK2, Eco*RI and *Sal*I for *sseK3*) to release the bacterial gene which was then ligated into pGBKT7 digested with the same set of restriction enzymes to create the plasmids pGBKT7-NleB2, pGBKT7-SseK2 and pGBKT7-SseK3. These plasmids were sequenced with the primer pair T7 F/pGBKT7 R to confirm ligation of the correct insert. pGBKT7-NleB1 was constructed by digesting pGBT9-NleB1, which carries *nleB1* flanked in between the restriction sites *Eco*RI and *Bam*HI, and ligating into pGBKT7 digested with *Eco*RI and *Bam*HI. Similarly, pGBKT7-SseK1 was generated by digesting pET28a-SseK1, which carries *sseK1* flanked by the sites *Eco*RI and *Sal*I, with *Eco*RI and *Sal*I and ligating into pGBKT7.

Bait vectors expressing EPEC NleB1 mutants ($NleB1_{Y219A}$, $NleB1_{E253A}$) fused to the GAL4 DNA binding domain were generated by using the Quick Change II Site-Directed Mutagenesis kit (Stratagene). pGBKT7-NleB1 was used as the template in the site-directed mutagenesis PCR reactions together with the primer pairs Y219A F/R and E253A F/R respectively.

2.9.5.2 Construction of yeast prey plasmids

pGADT7-AD was used as the prey plasmid in yeast studies. The primer pairs FADD DD F/R, TRADD DD F/R, RIPK1 DD F/R, Fas DD F/R, TNFR1 DD F/R and DR5 DD F/R were used to amplify the region encoding the death domain (DD) of FADD, TRADD, RIPK1, Fas, TNFR1 and DR5 respectively from HeLa cDNA. The primer pairs MyD88 F/R, IRAK1 F/R, IRAK4 F/R were used to amplify the region encoding the DD of MyD88, IRAK1 and IRAK4 respectively using the plasmids pFLAG-MyD88, pFLAG-IRAK1 and pFLAG-IRAK4 as templates. All the above PCR reactions were performed using AmpliTaq Gold® DNA polymerase and the resulting amplicons flanked by restriction sites: *Eco*RI-*dd FADD*-*Bam*HI (approximately 280 bp), *Eco*RI-*dd RIPK1*-*Sac*I (approximately 280 bp), *Eco*RI-*dd TRADD*-*Bam*HI (approximately 300 bp), *Eco*RI-*dd Fas*-*Sac*I (approximately 315 bp), *Nde*I-*dd*

*TNFR1-Bam*HI (approximately 270 bp), *Eco*RI-*dd DR5-Bam*H1 (approximately 315 bp), *Eco*RI-*dd MyD88-Bam*HI (approximately 260 bp), *Nde*I-*dd IRAK1-Eco*RI (approximately 280 bp) and *Eco*RI-*dd IRAK4-Bam*HI (approximately 320 bp) were purified, digested with the relevant pair of restriction enzymes and ligated into pGADT7-AD. The ligation reactions were transformed into XL-1 Blue cells and plated on LA containing ampicillin. The correct insert was verified by colony PCR and sequencing with the primer pair T7 F/pGADT7 R.

2.9.6 Construction of vectors expressing C-terminal TEM-1 fusions for β-lactamase translocation assays

The wild type EPEC E2348/69 *nleB1* gene was amplified with AmpliTaq Gold® DNA polymerase from genomic DNA using the primer pair B1 F/R, with B1 R designed without the *nleB1* stop codon to enable the C-terminal fusion to the TEM-1 protein. The PCR product was then purified and digested with *Kpn*I and *Eco*RI, before ligation into pCX340 digested with the same pair of restriction enzymes. The ligation reaction was then transformed into the Tet sensitive DH5α *E. coli* strain. Colonies were used as template with the primer pair pCX340 F/R in a colony PCR and positive clones were picked for plasmid extraction and sequencing with the same primer pair. The pCX340-NleB1 mutants were obtained by first amplifying mutated *nleB1* using the primer pair B1F/R and the constructs pEGFP-C2-NleB1$_{PILN(63-66)AAAA}$, pEGFP-C2-NleB1$_{Y219A,}$ pEGFP-C2-NleB1$_{PDG(236-238)AAA,}$ pEGFP-C2-NleB1$_{PDG(236-238)AKA}$, pEGFP-C2-NleB1$_{PDG(236-238)AEA}$, pEGFP-C2-NleB1$_{PD(236-237)AR}$, pEGFP-C2-NleB1$_{PDG(236-238)SRS}$, pEGFP-C2-NleB1$_{PDG(236-238)SES}$, pEGFP-C2-NleB1$_{PD(236-237)SE}$ or pEGFP-C2-NleB1$_{E253A}$ as template . The PCR products were purified, and digested with *Kpn*I and *Eco*RI, before ligation into pCX340 digested with the same pair of restriction enzymes. The correct insert was verified by colony PCR and sequencing.

2.9.7 Construction of expression vectors for protein purification

2.9.7.1 Construction of vectors expressing N-terminal glutathione-S-transferase (GST) tagged fusion proteins

Plasmids expressing the N-terminal GST-tagged NleB1 mutant proteins, GST-NleB1$_{PILN(63-66)AAAA}$, GST-NleB1$_{Y219A}$, GST-NleB1$_{PDG(236-238)AAA}$ and GST-NleB1$_{E253A}$, were constructed by amplifying the mutated *nleB1* genes with AmpliTaq Gold® DNA polymerase using the constructs pEGFP-C2-NleB1$_{PILN(63-66)AAAA}$, pEGFP-C2-NleB1$_{Y219A}$, pEGFP-C2-NleB1$_{PDG(236-238)}$ and pEGFP-C2-NleB1$_{E253A}$, respectively as templates and the primer pair pGEX-B1 F/R. Similarly, the construct pGEX-SseK3 was generated by amplifying the *sseK3* gene using pEGFP-C2-SseK3 as template and the primer pair pGEX S3 F/R. The amplicons of approximately 1 kb were digested with *Eco*RI and *Sal*I and ligated into pGEX-4T-1. The ligation reactions were transformed into XL-1 Blue cells and transformants were selected on LA containing ampicillin. Insertion of the correct insert into the vector pGEX-4T-1 was verified by colony PCR using the primer pair pGEX F/R and by sequencing.

2.9.7.2 Construction of vector expressing N-terminal His_6 tagged TRIM32

Mouse *TRIM32* (GenBank accession number) was amplified with AmpliTaq Gold® DNA polymerase using TRIM32 F/R primers and pEGFP-N1-TRIM32 as template. The PCR product was purified, digested with *Bam*HI and *Eco*RI and ligated into pET28a(+). The ligation reactions were transformed into XL-1 Blue cells and transformants were selected on LA containing kanamycin. Ligation of the correct insert into the vector pET28a(+) was verified by colony PCR using the primer pair T7 F/ R and by sequencing.

2.9.8 Construction of mammalian expression vectors expressing N-terminal FLAG tagged proteins.

Full length *CSN5* was amplified from HeLa cDNA using the primer pair CSN5 F/R and AmpliTaq Gold® DNA polymerase. The resultant PCR product of approximately 1 kb was gel purified and ligated into pGEM-T®-easy vector at an insert:vector molar

ratio of 3:1. The ligation reaction reaction was transformed into XL-1 Blue cells and plated onto LA supplemented with ampicillin and X-gal. Three individual white colonies were picked for plasmid extraction. The correct insert in the pGEM-T®-easy vector was verified by colony PCR and sequencing with M13F/R primers. The correct clone was digested with *Bgl*II and *Sal*I. The digested *CSN5* was purified and ligated into p3xFLAG-Myc-CMV-24.

Full length *TRIM32* was amplified using pEGFP-N1-TRIM32 as template and the primer pair TRIM32FLAG F/R. The PCR product of approximately 1kb was digested with *Eco*RI and *Bam*HI, purified and ligated into p3xFLAG-Myc-CMV-24 before transforming the reactions into XL-1 Blue cells. Colony PCR and sequencing were performed with the primer pair pFLAG F/R and primer TRIM32 seq F to ensure the correct insert has been ligated.

2.9.9 Construction of pACYC184 derivatives for use in mouse experiments

The wild type genes *nleB* from *C. rodentium* ICC169, *nleB1* and *nleB2* from EPEC E2348/69 and *nleB1* from EHEC O157:H7 Sakai were amplified with AmpliTaq Gold® DNA polymerase from genomic DNA using the primer pairs CR B F/R, EP B1 F/R, EP B2 F/R and EH B1 F/R, respectively. The PCR products of approximately 1 kb, which were flanked by the *Bam*HI and *Sal*I sites, were digested with the previously mentioned restriction enzymes and ligated behind the tetracycline promoter of the vector pACYC184, ensuring constitutive expression of the NleB proteins. In addition, to ensure similar translation levels of the NleB proteins, each forward primer contained a common ribosome binding site (RBS) sequence, AGGA, upstream of the ATG start codon, except the EP B2 F primer, which anneals upstream of the *nleB2* RBS sequence AGGA. The ligation reactions were transformed into XL-1 Blue cells and transformants were selected on LA containing chloramphenicol. Ligation of the correct insert into the vector pACYC184 was verified by colony PCR using the primer pair pACYC seq F/R and by sequencing.

2.10 Mammalian cell culture

2.10.1 Mammalian cells, media and maintenance

HeLa cells (human cervical cancer cells) and HEK293T cells (human embryonic kidney 293 cells expressing the SV40 large T-antigen) were maintained in DMEM, low glucose with GlutaMAX™ supplement and pyruvate (DMEM (1X) + GlutaMAX^{TM}-I) (Gibco, Life Technologies, NY, USA). THP-1 cells (human monocytic cells) were maintained in Roswell Park Memorial Institute (RPMI) 1640 medium with GlutaMAX™ supplement (RPMI + GlutaMAX^{TM}-I (1X)) (Gibco, Life Technologies). All tissue culture media were supplemented with 10% (v/v) heat-inactivated foetal bovine serum (FBS) (HyClone Laboratories, Thermo Fisher Scientific, Utah, USA). Cells were kept in a 37°C, 5%CO_2 incubator and passaged up to 40 times. Cells were split with 1ml 0.05% Trypsin-EDTA (1X) (Gibco, Life Technologies) per 75 cm^2 of tissue culture at a confluency of about 90% and resuspended with 10 volumes of the above tissue culture media supplemented with 10% FBS.

2.10.2 Transfection

HeLa cells or HEK293T cells were transfected using FuGENE®6 transfection reagent (Promega) as per the manufacturer's protocol. Briefly, cells were seeded one day prior to transfection for a confluency of about 80% the following day. FuGENE®6 transfection reagent was mixed with a reduced serum medium, Opti-MEM®I (1X) + GlutaMAX^{TM}-I (Gibco, Life Technologies) and incubated for 5 mins at RT before the addition of the DNA plasmid(s) of interest. A FuGENE®6:DNA ratio of 3:1 was used. The mixture was incubated at RT for 15-20 min and added to the cell culture for 16-24 h.

2.11 Dual luciferase reporter assay

To determine the effect of the NleB proteins of EPEC and the SseK effector proteins of *Salmonella* on the host NF-κB signalling pathway, a dual luciferase assay was performed. HeLa cells were seeded at a concentration of 2 x 10^5 cells/ml in 24 well plates 1 day before transfection and were 80-85 % confluent at the time of

transfection. 0.4 μg pEGFP-C2 or its derivatives, pEGFP-C2-NleB1 and its mutants, pEGFP-C2-NleB2, pEGFP-C2-NleE, pEGFP-C2-SseK1, pEGFP-C2-SseK2, pEGFP-C2-SseK3 and their putative catalytic mutants, were transfected along with 0.2 μg pNF-κB-Luc (Clontech, Palo Alto CA, USA) and 0.05 μg of the control pRL-TK (Promega, Madison WI, USA) in Opti-MEM medium (Invitrogen). Approximately 24 h after transfection, cells were either left unstimulated or stimulated with 20 ng/ml TNF (eBioscience, San Diego, USA) for about 16h. The cells were harvested and analysed by the dual luciferase reporter assay according to the manufacturer's instructions (Promega). Briefly, cells from each well were washed once with PBS and lysed in 100 μl of 1 x passive lysis buffer. The cell lysates were spun down at full speed for 2 mins and 20 μl of each centrifuged cell lysate were loaded in a 96 well plate. First, 50 μl of Luciferase Assay Reagent II (Promega) was added to the lysates for firefly luciferase activity measurement using a luminescence optic of the FluoStar Omega plate reader (BMG LABTECH), and then 50 μl of 1 x Stop & Glo Reagent (Promega) was added to the lysates to quench the firefly luciferase activity and activate the *Renilla* luciferase activity for measurement. The firefly luciferase activity of each sample was normalized to the *Renilla* luciferase activity.

2.12 β-lactamase translocation assay

The translocation of effector proteins from EPEC was measured by using translational fusions to TEM-1 β-lactamase (580). Translocation was detected in living host cells directly by using a fluorescent β-lactamase substrate CCF2/AM. 1 day before infection, HeLa cells were seeded in 96-well trays at a density of 2.5 x 10^4 cells per well. EPEC strains were cultured in 10 ml LB containing antibiotic as required, overnight at 37°C with shaking at 180 rpm. The bacterial cultures were subinoculated 1:75 in DMEM supplemented with the appropriate antibiotics and incubated at 37°C with 5% CO_2. 2.5 h later, the bacterial cultures were induced with IPTG for 30 min at a final concentration of 1 mM and the OD_{600} read. Cell monolayers were washed twice with PBS and infected with bacterial cultures at a starting OD_{600} of 0.03 for 2 h. The cells were then washed once with Hank's balanced salt solution (HBSS) (0.137

M NaCl, 5.4 mM KCl, 0.35 mM Na_2HPO_4, 5.6 mM glucose, 0.44 mM KH_2PO_4, 0.96 mM $CaCl_2$, 0.81 mM $MgSO_4$, 8.3 mM $NaHCO_3$) supplemented with 5 % HEPES buffer (0.3 M HEPES, 0.002 % (v/v) phenol red, pH 7.4) and the CCF2/AM dye (Beta-lactamase loading solutions, Life Technologies) was then loaded onto the cells for 1.5 h in the dark, before being replaced with HBSS containing 2.5 mM probenecid in 0.12 M Sodium dihydrogen orthophosphate pH 8.0. The blue emission fluorescence (450 nm) and green emission fluorescence (520 nm) were measured on a CLARIOstar Omega microplate reader (BMG Labtech), and the translocation signal was shown as the ratio between blue emission fluorescence and green emission fluorescence

2.13 *Salmonella* infection and IL-8 secretion

To determine if the SseK effectors have any effect on IL-8 secretion from host cells, HeLa cells and THP-1 cells were infected with wild type *S.* Typhimurium and its derivative mutants and stimulated with 20 ng/ml TNF and the cell supernatants were analysed for IL-8 secretion levels using the Quantikine Human IL-8 Immunoassay (R&D Systems, Minnesota, USA) according to the manufacturer's instructions. Briefly, HeLa cells were seeded at a concentration of 2 x 10^5 cells/ml 2 days before infection. THP-1 cells were seeded at a concentration of 8 x 10^5 cells/ml and differentiated with 0.05 μg/ml PMA 2 days before infection. 2 days prior to infection of the cells, 10 ml LB broths containing appropriate antibiotic selection were inoculated with *Salmonella* strains and grown with shaking overnight at 180 rpm at 37°C. The overnight cultures were then subinoculated 1:200 in fresh LB broths containing appropriate antibiotic selection and grown under static conditions for 20 h in a 37C, 5% CO2 incubator. The OD_{600} readings of the bacterial cultures were then measured and HeLa or THP-1 cells were infected at a multiplicity of infection (MOI) of 50. The 24 well plates were centrifuged at 1, 500 rpm for 5 mins to synchronise the infection and incubated for 1 h. The culture media was then replaced with media containing 100 μg/ml gentamycin (Pharmacia, Washington, USA) for 1 h and replaced with media containing 10 μg/ml gentamycin. Cells were then either left untreated or stimulated with 20 ng/ml TNF for 6 h and the cell culture supernatants

were collected and used to measure IL-8secretion using the Quantikine Human IL-8 Immunoassay (R&D Systems, MN) according to the manufacturer's instructions. Differences in IL-8 secretion were assessed for significance by one-way analysis of variance (ANOVA) with Tukey's Multiple Comparison post-test.

2.14 Protein analysis

2.14.1 Bolt® protein gel electrophoresis

When cell lysates were analysed, cells were lysed in cold 1 x RIPA lysis buffer (1 mM Tris-HCl pH 7.5, 15 mM NaCl, 0.5 mM EDTA, 0.01 % SDS, 0.1% Triton X-100, 0.1 % deoxycholate) containing 1 x protease inhibitor cocktail (cOmplete, Mini, EDTA free, Roche) on ice, spun down at 4 °C and the supernatants added to 1 x Bolt® LDS sample buffer (Life Technologies) and DTT (Astral Scientific) to a final concentration of 50 mM. Protein samples other than cell lysates were also mixed with LDS and DTT. Samples were heated at 70°C for 10 min, loaded onto Bolt® 4-12% Bis-Tris Plus gels (Life Technologies) or Bolt®10% Bis-Tris Plus gels (Life Technologies) along with SeeBlue® pre-stained protein standard (Life Technologies) and separated by electrophoresis using the XCell4 SureLock™ Midi-Cell system (Life Technologies) or the XCell SureLock™ Mini-Cell system (Life Technologies) and 1 x Bolt® MES SDS running buffer (Life Technologies) according to the manufacturer's instructions.

2.14.2 Protein visualisation

2.14.2.1 Colloidal Coomassie gel stain

Gels were rinsed in dH_2O for 10 min following electrophoresis and stained with colloidal Coomassie Blue protein stain (0.02% (w/v) Coomassie Brilliant Blue G-250, 5% (w/v) aluminium sulphate, 10% (v/v) ethanol, 2% (v/v) orthophosphoric acid) overnight. The gels were destained with Coomassie destain solution (10% (v/v) ethanol, 2% (v/v) orthophosphoric acid) for 1h and rinsed in dH_2O. Gel pictures were taken using an MFChemiBis imaging station (DNR Bio-Imaging Systems, Israel).

2.14.2.2 Immunoblotting

Proteins separated by electrophoresis were transferred from the Bolt® gels to nitrocellulose membranes using the iBlot2® gel transfer device (Life Technologies) and the iBlot2® nitrocellulose transfer stacks (Life Technologies) according to the manufacturer's instructions. The nitrocellulose membranes were blocked in 5% skim milk (w/v) in TBS (20 mM Tris, 50 mM NaCl, pH8.0) with 0.1% Tween 20 for 1 h before probing with the relevant primary antibodies and secondary antibodies when required. Antibody binding was visualised with an MFChemiBis imaging station and chemiluminescent substrates for horseradish peroxidase (HRP) (ECL western blotting reagents (GE Healthcare) or ECL Prime western blotting reagent (Amersham, USA)) as recommended by the manufacturer.

2.15 Detection of cleaved caspase-8 by immunoblot

For detection of cleaved caspase-8 during EPEC infection, HeLa cells were infected with various EPEC derivatives and then stimulated with FasL to induce host cell apoptosis by the extrinsic pathway before collection and analysis of cell lysates. Briefly, the day before tissue culture infection, HeLa cells were seeded at 2.5 x 10^5 cells/ml in 24 well plates (Greiner Bio One, Frickenhausen, Germany) and the various EPEC derivatives were cultured in 10 ml LB broths containing the required antibiotic overnight at 37°C with shaking at 180 rpm. The following day, the bacterial cultures were subinoculated 1:75 in DMEM supplemented with the appropriate antibiotics and incubated at 37°C with 5% CO_2 for 2.5 h before inducing NleB protein expression from the pTrc promoter with IPTG for another 30 min. HeLa cells were infected with the various EPEC strains for 2 h and treated with 100 μg/ml gentamycin with or without 20 ng/ml of Fcγ-FasL (Andreas Strasser, The Walter and Eliza Hall Institute for Medical Research, Victoria, Australia) for a further 2-3 h. HeLa cells were lysed and subjected to gel electrophoresis followed by transfer to nitrocellulose membranes. Membranes were incubated for at least 16h at 4°C with rabbit monoclonal anti-cleaved caspase-8 antibodies (Asp391) (18C8) (Cell Signaling Technology, USA) diluted 1:1000 in TBS with 5% skim milk and 0.1% Tween 20 (Chem-supply) or

mouse monoclonal anti-caspase-8 antibodies (1C12) (Cell Signaling Technology), which detects full length and cleaved caspase-8, diluted 1:1000 in TBS with 5% BSA (Sigma-Aldrich) and 0.1% Tween 20. Rabbit polyclonal anti-NleB1 antibodies (Hartland laboratory) diluted 1:200 in in TBS with 5% BSA and 0.1% Tween 20 and mouse monoclonal anti-β-actin antibodies (AC-15) (Sigma-Aldrich) diluted 1:5000 in TBS with 5% BSA and 0.1% Tween 20 were also used to probe the nitrocellulose membranes. Proteins were detected using anti-rabbit or mouse IgG horseradish peroxidase-conjugated secondary antibodies (Perkin-Elmer) and developed with ECL Prime Western blotting reagent (Amersham, USA). All secondary antibodies were diluted 1:3000 in TBS with 5% BSA and 0.1% Tween 20. Images were visualised using an MFChemiBis imaging station (DNR Bio-Imaging Systems).

The same technique was used to detect caspase-8 activation during *Salmonella* infection. Briefly, 2 days before infection, HeLa cells were seeded at a concentration of 2 x 10^5 cells/ml and *Salmonella* strains were grown in 10 ml LB broths containing appropriate antibiotic selection with shaking overnight at 180 rpm at 37°C. The following day, the overnight cultures were then subinoculated 1:200 in fresh LB broths containing appropriate antibiotic selection and grown under static conditions for 20 h in a 37°C, 5% CO2 incubator. The OD_{600} readings of the bacterial cultures were then measured and cells were infected at a MOI of 50. The 24 well plates were then centrifuged at 1, 500 rpm for 5 min to synchronise the infection and incubated for 1 h in a 37°C, 5% CO2 incubator. The culture media was then replaced with media containing 100 μg/ml gentamycin for 1 h and replaced with media containing 10 μg/ml gentamycin. Cells were then either left untreated or stimulated with 20 ng/ml Fcγ-FasL for 5-6 h and the cell lysates were collected and analysed for caspase-8 activation.

2.16 Immunoprecipitation

2.16.1 Immunoprecipitation by Anti-FLAG® M2 Magnetic Beads

HEK293T cells were seeded at approximately 5 x 10^5 cells/ml in 10 cm dishes (Corning) and were co-transfected with pEGFP-C2-NleB1 or its derivative site-directed mutants, pEGFP-C2-SseK1, pEGFP-C2-SseK2 or pEGFP-C2-SseK3 together with p3xFLAG vector containing the gene of interest. Immunoprecipitation with Anti-FLAG® M2 Magnetic Beads (Sigma-Aldrich) was performed as per the manufacturer's instructions. Briefly, 16-24 h after transfection, cells were washed twice with cold PBS and lysed in 600 µl cold RIPA lysis buffer containing 1 x protease inhibitor cocktail (cOmplete, Mini, EDTA free, Roche), 10 mM NaF, 2 mM Na_3VO_4 and 1 mM PMSF. Cell debris was pelleted and equal volume of supernatant was collected, 70 µl of which was kept as input protein. The remaining cell lysate was applied to equilibrated Anti-FLAG® M2 Magnetic beads and incubated on a rotating wheel at 4°C overnight. Beads were magnetically separated and washed 3 times with cold 1 x RIPA lysis buffer and the protein was eluted with 100 mg/ml FLAG peptide (Sigma-Aldrich). The beads were magnetically separated and the supernatants (IPs) along with the input samples were subjected to gel electrophoresis and transferred to nitrocellulose membranes. Membranes were probed with the following primary antibodies as necessary: mouse monoclonal anti-GFP (clones 7.1 and 13.1) (Roche), mouse monoclonal anti-GlcNAc (CTD 110.6) (Cell Signaling) or mouse monoclonal anti-β-actin (AC15) (Sigma) diluted 1:2000, 1:1000 and 1:5000 respectively in TBS with 5% BSA and 0.1% Tween 20. The immunoblots were then washed 3 times and probed with either HRP conjugated secondary goat anti-mouse antibodies (Bio-Rad) diluted 1:3000 in TBS with 5% BSA and 0.1% Tween 20 before developing with ECL western blotting detection reagents (GE Healthcare). Membranes probed with mouse anti-FLAG-HRP antibodies (Sigma) diluted 1:1000 were washed and developed. Antibody binding was visualised using an MFChemiBis imaging station (DNR Bio-Imaging Systems).

2.16.2 Immunoprecipitation by GFP-Trap®

HEK293T cells were seeded at approximately 5 x 10^5 cells/ml in 10 cm dishes (Corning) and were co-transfected with pEGFP-C2 empty vector or pEGFP-C2-SseK3 together with pcDNA-TRIM32 for 16-24 h. Following transfection, cells were lysed and immunoprecipitation was carried out according to instructions for immunoprecipitation of GFP-fusion proteins provided by the GFP-Trap®-M supplier (Chromotek, Germany).

2.17 Preparation of GST and His tagged proteins

Overnight cultures of BL21 (pGEX-4T-1), BL21 (pGEX-SseK3), BL21 (pGEX-NleB1), BL21 (pGEX-NleB1$_{PILN(63-66)AAAA}$), BL21 (pGEX-NleB1$_{Y219A}$), BL21 (pGEX-NleB1$_{PDG(236-238)AAA}$), BL21 (pGEX-NleB1$_{E253A}$), BL21 (pET-TRIM32) and BL21 (pET-FADD) grown in LB broth were diluted 1:100 in 200 ml of LB supplemented with either kanamycin (pET) or ampicillin (pGEX) with shaking to an optical density of 0.6 at 37°C. Bacterial cultures were incubated with 1mM IPTG and grown for a further 2 h and then pelleted by centrifugation. Bacterial cells were lysed using Avestin EmulsiFlex-C3 high pressure homogeniser. Proteins were purified by either nickel or glutathione affinity chromatography in accordance with the manufacturer's instructions (Novagen). Protein concentrations were determined using a bicinchoninic acid (BCA) kit (Thermo Scientific).

2.18 Incubation of GST and His tagged proteins

2 μg of purified recombinant proteins were incubated either alone or in combination at 37°C for 4 h in the presence of 1 mM UDP-GlcNAc (Sigma-Aldrich). Samples were subjected to gel electrophoresis and transferred to nitrocellulose membranes which were subsequently probed with the following primary antibodies: mouse monoclonal anti-GlcNAc (CTD 110.6) (Cell Signaling), which recognises *O*-linked and *N*-linked GlcNAc (581), rabbit polyclonal anti-GST (Cell Signaling), or mouse monoclonal anti-His (AD1.1.10) (AbD Serotech) diluted 1:1000, 1:1000 and 1:2000 respectively in TBS with 5% BSA and 0.1% Tween 20. The immunoblots were then

washed 3 times and probed with either HRP conjugated secondary goat anti-mouse antibodies (Perkin Elmer) or goat anti-rabbit antibodies (Perkin Elmer) diluted 1:3000 in TBS with 5% BSA and 0.1% Tween 20 before developing with ECL western blotting detection reagents (GE Healthcare). Images were visualised using an MFChemiBis imaging station (DNR Bio-Imaging Systems).

2.19 Preparation of bacterial whole cells to test protein expression

Bacterial strains were grown in LB broths containing antibiotics when necessary overnight at 37°C with shaking at 180 rpm. The following day, the bacterial cultures were subinoculated 1:75 in DMEM supplemented with the appropriate antibiotics and incubated at 37°C with 5% CO_2 for 2.5 h before inducing protein expression with IPTG for another 30 min. The OD_{600} readings were read. 1 ml of each culture was pelleted and the pellets were resuspended in PBS to an OD_{600} of 8.0. The whole cells were mixed with LDS and DTT and subjected to gel electrophoresis. The proteins were transferred onto a nitrocellulose membrane and probed with the appropriate antibodies.

2.20 Localisation of GFP-tagged NleB1 mutant proteins and SseK proteins by microscopy

To determine if the mutations in NleB1 affected the localisation of the NleB1 protein in tissue culture, HEK293T cells were seeded at 4 x 10^4 cells/ml on poly-L-lysine coated coverslips in 24 well plates and transfected the following day with constructs expressing GFP-tagged NleB1 and its mutants. Cells were fixed with 4% (w/v) paraformaldehyde (PFA) in PBS for 15 min at RT and stained with Hoechst diluted 1:2000 in 3% (w/v) BSA in PBS for 15 min. The coverslips were then mounted on glass slides using ProLong Gold anti-fade reagent (Invitrogen). The slides were visualized using a Zeiss confocal laser scanning microscope with diode laser lines at 405 nm and 488 nm and a 100x/EC Epiplan-Apochromat oil immersion objective.

To determine the localisation of the SseK proteins, HeLa cells were seeded at 8 x 10^4 cells/ml on coverslips in 24 well plates and transfected the following day with

constructs expressing the GFP-tagged SseK proteins. The HeLa cells were fixed with 4% (w/v) PFA in PBS for 15 min at RT and permeabilised with 0.2% (v/v) Triton X-100 (Sigma-Aldrich) in PBS for 3-4 min. Permeabilised cells were then washed with PBS and blocked with 3% (w/v) BSA in PBS for 30 min before being subjected to immunofluorescence staining with mouse anti-golgin 97 antibody (Invitrogen) diluted 1:200 in 3% (w/v) BSA in PBS for 1 h. The cells were washed with PBS and stained with anti-mouse antibodies conjugated to Alexa Fluor 568 (Life Technologies) diluted 1:1000 in 3% (w/v) BSA in PBS for 45 min. The cells were then washed and stained with DAPI diluted 1:20,000 in PBS for 5 min and the coverslips were mounted onto glass slides using ProLong Gold anti-fade reagent and examined by fluorescence microscopy using a Zeiss LSM700 inverted Axio Observer with LED laser lines at 405 nm, 488 nm and 555 nm and a 100x/EC Epiplan-Apochromat oil immersion objective.

2.21 Yeast studies

2.21.1 Yeast two-hybrid HeLa library screen

The BD Matchmaker normalised pretransformed HeLa cDNA library (Clontech, California, USA) was screened according to the manufacturer's protocols (Clontech PT3183-1 manual) to identify mammalian proteins interacting with NleB2, SseK1, SseK2 and SseK3. The yeast *Saccharomyces cerevisiae* strain AH109 clones expressing the bait proteins NleB2, SseK1, SseK2 and SseK3 were individually mated with the yeast *Saccharomyces cerevisiae* strain Y187 carrying the normalised HeLa cDNA library in the pGADT7-RecAB plasmid. The mating mixtures were plated onto quadruple drop-out (QDO or SD-Trp-Leu-Ade-His) plates to select for diploids expressing the reporter genes and incubated at 30°C and monitored for 2 to 3 weeks. Yeast colonies growing on the QDO plates during that time were then patched onto double drop-out (DDO or SD-Trp-Leu) then QDO plates to confirm a protein interaction. Colonies that were able to grow on both DDO and QDO plates were considered true positives whereas colonies that could only grow on DDO plates were deemed false positives. The pGADT7-Rec-cDNA plasmids were isolated from these

diploids with positive protein interactions using the Zymoprep™ Yeast Plasmid Miniprep I kit (Zymo Research Corp., CA, USA) and those plasmids were transformed into XL-1 Blue cells and plated onto LA supplemented with ampicillin. The pGADT7-Rec-cDNA plasmids were then extracted and sequenced using primer pGADT7 RecF/pGADT7 RecR to identify the cDNA inserts.

To reconfirm the protein interaction, the bait and newly extracted prey plasmids were both transformed into the yeast strain PJ69-4A, which has the same growth limitations as strain AH109. Transformants were selected on DDO plates and then streaked out on DDO and QDO plates to verify protein interaction. Negative control strains were also made with the bait plasmid transformed together with an empty prey plasmid and vice versa to show that the bait protein was not directly interacting with the activation domain and that the prey protein was not directly interacting with the binding domain.

2.21.2 Yeast transformation

Yeast strains AH109 and PJ69-4A were transformed or co-transformed with plasmids using the lithium acetate method (582) and transformants were plated out on appropriate selective yeast plates. Briefly, yeast strains AH109 or PJ69-4A was streaked on YPD plates supplemented with adenine and incubated at 30°C for 3 days. Two or three pink colonies from the streak plates were then used to inoculate a 10 ml YPD broth supplemented with adenine and grown at 30°C overnight at 200 rpm. The overnight culture was subinoculated into fresh YPD broth containing adenine at a starting OD_{600} of 0.20 and grown at 30°C to an OD_{600} of 0.6-0.8. The yeast culture was then centrifuged at 4,000 rpm for 7 min and the pellet was resuspended in distilled water before being spun down again. The yeast pellet was then resuspended in 100 mM lithium acetate and centrifuged. The lithium acetate was removed and the cells were resuspended in 400 mM lithium acetate, vortexed and centrifuged. The lithium acetate was removed from the yeast pellet and polyethylene glycol (PEG 3350;Sigma-Aldrich) was added, followed by 1 M lithium acetate, herring sperm DNA (ssDNA) at a final concentration of 2 mg/ml, water and the plasmid DNA of interest before vortexing. The mixture was then incubated 30°C for 30 mins and heat shocked at

42°C for 20 mins before being spun down. The transformation mixture was then removed and the pellet was resuspended in distilled water and plated on selective yeast plates which were incubated at 30°C for 3 days.

2.21.3 Preparation of protein extracts from yeast

Proteins were extracted from yeast using a published protocol which involves alkali treatment of yeast cells (583). The yeast strain of interest was grown in selective liquid culure overnight and was standardised to an OD_{600} of 2.5. The yeast culture was then centrifuged at 4,000 rpm. The yeast pellet was resuspended in water and 0.2 M NaOH was added. The mixture was then incubated for 5 min at room temperature, pelleted, resuspended in 2 x SDS sample reducing buffer (130 mM Tris, 140 mM SDS, 20% (v/v) glycerol, 30 μM bromophenol blue, 5% (v/v) 2-mercaptoethanol, pH 6.8), boiled for 3 mins and pelleted again. The supernatant containing the protein extracts was collected for analysis by western blot.

2.22 Mouse experiments

2.22.1 C57BL/6 mice

5 to 8 week old female, specific pathogen-free (SPF) C57BL/6 mice were housed in groups of five or less in individually ventilated cages with free access to food and water and maintained in the Department of Microbiology and Immunology BioResource Facility, Peter Doherty Institute for Infection and Immunity, University of Melbourne, Victoria. Mice were handled in a Biohazard Class II cabinet.

2.22.2 Single infection

Bacterial strains were cultured in 10 ml LB broths containing antibiotics as required overnight at 37°C with shaking. The following day, bacterial cells were harvested by centrifugation at 3,220 x g for 10 min at RT and the supernatant discarded. The bacterial cell pellet was then resuspended in a 0.1 volume PBS. Unanaesthetised mice were each given 200 μl of a bacterial suspension containing approximately 2 x 10^9 CFU in PBS by oral gavage using a 20-gauge intubation needle (Cole-Palmer, Vernon

Hills, IL, USA). 5 to 8 mice were used per group. Mice were weighed every 2 days after inoculation and monitored.

2.22.3 Bacterial counts

The viable count of the bacterial inoculum was determined retrospectively by serial dilution and plating onto LB agar containing the appropriate antibiotics. For the single-strain infection experiments, faecal samples were collected aseptically from each mouse on various days for 14 days after inoculation and emulsified in PBS at a final concentration of 100 mg/ml. The number of viable bacteria per gram of faeces was determined by plating serial dilutions of the samples onto antibiotic selective media. The limit of detection was 400 CFU/g faeces.

Table 2.1. Bacterial strains used in this study

Strains	Relevant characteristics	Reference
E. coli		
DH5α	laboratory strain K-12 *endA1 hsdR17* (r_k^- m_k^+) *supE44 thi-1 recA1 gyrA* (Nal^R) *relA* Δ(*lacIZYA-argF*)U169 deo*R* (Φ80*d*lacΔ[*lacZ*]M15)	(584)
XL-1 Blue	Host strain *recA1 endA1 gyrA96 thi-1 hsdR17 supE44 relA1 lac[F'proAB lacIqZΔM15 Tn10* (Tet^R)]	Stratagene
BL21 C41 (DE3)	F^- *ompT hsdS*$_B$ (r_B^- m_B^-) *gal dcm* λ (DE3) [*lacI lacUV5*-T7 gene 1 *ind1 sam7 nin5*])	Novagen
EPEC E2348/69	Wild type EPEC strain O127:H6	(28)
EPEC Δ*nleB1*	E2348/69 Δ*nleB1*::Cm (Cm^R)	(401)
EPEC Δ*escN*	E2348/69 Δ*escN*::Kan (Kan^R)	(374)
C. rodentium		
ICC169	Spontaneous Nal^R derivative of wild type *C. rodentium* biotype 4280	(167)
CR Δ*nleB*	ICC169 Δ*nleB*::Kan (Nal^r, Kan^r)	(401)
***S.* Typhimurium**		
SL1344	Wild type *S. enterica* serovar Typhimurium strain SL1344	Nathaniel Brown
Δ*invA*	SL1344 SPI-1 T3SS mutant	Richard Strugnell
Δ*ssaR*	SL1344 SPI-2 T3SS mutant	Richard Strugnell
Δ*sseK1*	SL1344 Δ*sseK1*	(560)

Δ*sseK2*	SL1344 Δ*sseK2*	(560)
Δ*sseK3*	SL1344 Δ*sseK3*	(559)
Δ*sseK1*/2/3	SL1344 Δ*sseK1*Δ*sseK2*Δ*sseK3*	(559)

Table 2.2. Yeast strains used in this study

Strains	**Relevant characteristics**	**Reference**
S.cerevisiae		
PJ69-4A	*MATa, trp1-901, leu2-3,112,ura3-52 his3-200,gal4*Δ*, gal80*Δ*,LYS2::GAL1-HIS3, GAL2-ADE2, met2::GAL7-lacZ*	Clontech
AH109	*MATa, trp1-901, leu2-3, 112, ura3-52, his3-200, gal4*Δ, *gal80*Δ, *LYS2::GAL1*$_{UAS}$*-GAL1*$_{TATA}$*-HIS3, GAL2*$_{UAS}$*-GAL2*$_{TATA}$*-ADE2, URA3::MEL1*$_{UAS}$*-MEL1*$_{TATA}$*-lacZ*	Clontech
Y187	*MATa*, *ura3-52*, *his3-200*, *ade2-101*, *trp1-901*, *leu2-3, 112*, *gal4*Δ, *met–*, *gal80Δ*, *MEL1*, *URA3*::*GAL1*$_{UAS}$ *- GAL1*$_{TATA}$*-lacZ*	Clontech

Table 2.3. Plasmids used in this study

Plasmids	Relevant characteristics	Reference
pGEM®-T-Easy	High copy number cloning vector, Amp^R	Promega
pET28a(+)	Low copy number bacterial expression vector carrying an N-terminal His_6 tag, Kan^R	Novagen
pET28a-FADD	Full length FADD in pET28a(+), Kan^R	(401)
pET 28a-TRIM32	Full length TRIM32 in pET28a(+), Kan^R	This study
pET28a-SseK1	*sseK1* from *S.* Typhimurium SL1344 in pET28a(+), Kan^R	Michelle Kelly
pGEX-4T-1	Low copy number N-terminal glutathione-S-transferase fusion vector, Amp^R	GE Healthcare
pGEX-NleB1	*nleB1* from EPEC E2348/69 in pGEX-4T-1, Amp^R	(401)
pGEX-NleB1$_{PILN(63-66)AAAA}$	*nleB1* from EPEC E2348/69 in pGEX-4T-1 with $PILN_{(63-66)}$ motif mutated to AAAA, Amp^R	This study
pGEX-NleB1$_{Y219A}$	*nleB1* from EPEC E2348/69 in pGEX-4T-1 with amino acid Y_{219} mutated to A, Amp^R	This study
pGEX-NleB1$_{PDG(236-238)AAA}$	*nleB1* from EPEC E2348/69 in pGEX-4T-1 with $PDG_{(236-238)}$ motif mutated to AAA, Amp^R	This study
pGEX-NleB1$_{E253A}$	*nleB1* from EPEC E2348/69 in pGEX-4T-1 with amino acid E_{253} mutated to A, Amp^R	This study
pGEX-SseK3	*sseK3* from *S.* Typhimurium SL1344 in pGEX-4T-1, Amp^R	This study
pTrc99A	Low copy bacterial expression vector with inducible *lacI* promoter, Amp^R	Pharmacia Biotech
pTrc99A-NleB1	*nleB1* from EPEC E2348/69 in pTrc99A, Amp^R	(377)
pTrc99A-NleB1$_{DxD(221-223)AxA}$	*nleB1* from EPEC E2348/69 in pTrc99A with $DxD_{(221-223)}$ catalytic motif mutated to AxA, Amp^R	(401)

pTrc99A-NleB1$_{Y219A}$	*nleB1* from EPEC E2348/69 in pTrc99A with amino acid Y_{219} mutated to A, Amp^R	This study
pTrc99A-NleB1$_{E253A}$	*nleB1* from EPEC E2348/69 in pTrc99A with amino acid E_{253} mutated to A, Amp^R	This study
pGADT7-AD	High copy number yeast expression vector carrying a GAL4 activation domain, Amp^R (bacterial selection), Leu (selectable marker in yeast)	Clontech
pGADT7-DD FADD	Death domain of FADD in pGADT7-AD, Amp^R, Leu	This study
pGADT7-DD TRADD	Death domain of TRADD in pGADT7-AD, Amp^R, Leu	This study
pGADT7-DD RIPK1	Death domain of RIPK1 in pGADT7-AD, Amp^R, Leu	This study
pGADT7-DD MyD88	Death domain of MyD88 in pGADT7-AD, Amp^R, Leu	This study
pGADT7-DD IRAK1	Death domain of IRAK1 in pGADT7-AD, Amp^R, Leu	This study
pGADT7-DD IRAK4	Death domain of IRAK4 in pGADT7-AD, Amp^R, Leu	This study
pGADT7-DD Fas	Death domain of Fas in pGADT7-AD, Amp^R, Leu	This study
pGADT7-DD TNFR1	Death domain of TNFR1 in pGADT7-AD, Amp^R, Leu	This study
pGADT7-DD DR5	Death domain of DR5 in pGADT7-AD, Amp^R, Leu	This study
pGADT7-TRIM32	Mouse TRIM32 in pGADT7-AD, Amp^R, Leu	This study
pGBT9-NleB1	*nleB1* from EPEC E2348/69 flanked by *Eco*RI and *Bam*HI sites rom EPEC E2348/69 in pGBT9 yeast bait vector	Michelle Kelly
pGBKT7	High copy number yeast expression vector	Clontech

	carrying a GAL4 DNA binding domain, Kan^R (bacterial selection), Trp (selectable marker in yeast)	
pGBKT7-NleB1	*nleB1* from EPEC E2348/69 in pGBKT7, Kan^R, Trp	This study
pGBKT7-NleB1$_{Y219A}$	*nleB1* from EPEC E2348/69 in pGBKT7 with amino acid Y_{219} mutated to A, Kan^R, Trp	This study
pGBKT7-NleB1$_{E253A}$	*nleB1* from EPEC E2348/69 in pGBKT7 with amino acid E_{253} mutated to A, Kan^R, Trp	This study
pGBKT7-NleB2	*nle2* from EPEC E2348/69 in pGBKT7, Kan^R, Trp	This study
pGBKT7-SseK1	*sseK1* from *S.* Typhymurium SL1344 in pGBKT7, Kan^R, Trp	This study
pGBKT7-SseK2	*sseK2* from *S.* Typhymurium SL1344 in pGBKT7, Kan^R, Trp	This study
pGBKT7-SseK3	*sseK3* from *S.* Typhymurium SL1344 in pGBKT7, Kan^R, Trp	This study
pcDNA-TRIM32	Full length TRIM32 with N-terminal Myc epitope tag in pCDNA3.1 (+), Amp^R	Rohan Teasdale
p3xFLAG-Myc-CMV-24	Shuttle vector for *E. coli* and mammalian cells carrying an N-terminal 3 X FLAG peptide, Amp^R	Sigma-Aldrich
pFLAG-CSN5	Full length CSN5 in p3xFLAG-Myc-CMV-24, Amp^R	This study
pFLAG-TRIM32	Full length TRIM32 in p3xFLAG-Myc-CMV-24, Amp^R	This study
pFLAG-FADD	Full length FADD in p3xFLAG-Myc-CMV-24, Amp^R	Ashley Mansell
pFLAG-MyD88	Full length MyD88 in p3xFLAG-Myc-CMV-24, Amp^R	Ashley Mansell

pFLAG-IRAK1	Full length IRAK1in p3xFLAG-Myc-CMV-24, Amp^R	Ashley Mansell
pFLAG- IRAK4	Full length IRAK4in p3xFLAG-Myc-CMV-24, Amp^R	Ashley Mansell
pCX340	Cloning vector used to construct C-terminal TEM-1 β-lactamase fusions, Tet^R	(580)
pTEM-NleB1	*nleB1* from EPEC E2348/69 in pCX340, Tet^R	This study
pTEM-NleB1$_{PILN(63-66)AAAA}$	*nleB1* from EPEC E2348/69 in pCX340 with $PILN_{(63-66)}$ motif mutated to AAAA , Tet^R	This study
pTEM-NleB1$_{Y219A}$	*nleB1* from EPEC E2348/69 in pCX340 with amino acid Y_{219} mutated to A , Tet^R	This study
pTEM-NleB1$_{PDG(236-238)AAA}$	*nleB1* from EPEC E2348/69 in pCX340 with $PDG_{(236-238)}$ motif mutated to AAA , Tet^R	This study
pTEM-NleB1$_{PDG(236-238)AKA}$	*nleB1* from EPEC E2348/69 in pCX340 with $PDG_{(236-238)}$ motif mutated to AKA , Tet^R	This study
pTEM-NleB1$_{PDG(236-238)AEA}$	*nleB1* from EPEC E2348/69 in pCX340 with $PDG_{(236-238)}$ motif mutated to AEA , Tet^R	This study
pTEM-NleB1$_{PDG(236-238)SRS}$	*nleB1* from EPEC E2348/69 in pCX340 with $PDG_{(236-238)}$ motif mutated to SRS , Tet^R	This study
pTEM-NleB1$_{PDG(236-238)SES}$	*nleB1* from EPEC E2348/69 in pCX340 with $PDG_{(236-238)}$ motif mutated to SES , Tet^R	This study
pTEM-NleB1$_{E253A}$	*nleB1* from EPEC E2348/69 in pCX340 with amino acid E_{253} mutated to A , Tet^R	This study
pEGFP-N1-TRIM32	Full length TRIM32 in pEGFP-N1 vector, Kan^R	Rohan Teasdale
pEGFP-C2	Expression vector carrying EGFP to N-terminus of partner protein, Kan^R	Clontech
pEGFP-C2-NleE	*nleE* from EPEC E2348/69 in pEGFP-C2, Kan^R	(377)
pEGFP-C2-NleB1	*nleB1* from EPEC E2348/69 in pEGFP-C2, Kan^R	(401)

pEGFP-C2-NleB1$_{P63A}$	*nleB1* from EPEC E2348/69 in pEGFP-C2 with amino acid P_{63} mutated to A, Kan^R	This study
pEGFP-C2-NleB1$_{I64A}$	*nleB1* from EPEC E2348/69 in pEGFP-C2 with amino acid I_{64} mutated to A, Kan^R	This study
pEGFP-C2-NleB1$_{L65A}$	*nleB1* from EPEC E2348/69 in pEGFP-C2 with amino acid L_{65} mutated to A, Kan^R	This study
pEGFP-C2-NleB1$_{N66A}$	*nleB1* from EPEC E2348/69 in pEGFP-C2 with amino acid N_{66} mutated to A, Kan^R	This study
pEGFP-C2-NleB1$_{K68A}$	*nleB1* from EPEC E2348/69 in pEGFP-C2 with amino acid K_{68} mutated to A, Kan^R	This study
pEGFP-C2-NleB1$_{K81A}$	*nleB1* from EPEC E2348/69 in pEGFP-C2 with amino acid K_{81} mutated to A, Kan^R	This study
pEGFP-C2-NleB1$_{D93A}$	*nleB1* from EPEC E2348/69 in pEGFP-C2 with amino acid D_{93} mutated to A, Kan^R	This study
pEGFP-C2-NleB1$_{D121A}$	*nleB1* from EPEC E2348/69 in pEGFP-C2 with amino acid D_{121} mutated to A, Kan^R	This study
pEGFP-C2-NleB1$_{D128A}$	*nleB1* from EPEC E2348/69 in pEGFP-C2 with amino acid D_{128} mutated to A, Kan^R	This study
pEGFP-C2-NleB1$_{L157A}$	*nleB1* from EPEC E2348/69 in pEGFP-C2 with amino acid L_{157} mutated to A, Kan^R	This study
pEGFP-C2-NleB1$_{Y219A}$	*nleB1* from EPEC E2348/69 in pEGFP-C2 with amino acid Y_{219} mutated to A, Kan^R	This study
pEGFP-C2-NleB1$_{Y234A}$	*nleB1* from EPEC E2348/69 in pEGFP-C2 with amino acid Y_{234} mutated to A, Kan^R	This study
pEGFP-C2-NleB1$_{P236A}$	*nleB1* from EPEC E2348/69 in pEGFP-C2 with amino acid P_{236} mutated to A, Kan^R	This study
pEGFP-C2-NleB1$_{D237A}$	*nleB1* from EPEC E2348/69 in pEGFP-C2 with amino acid D_{237} mutated to A, Kan^R	This study
pEGFP-C2-NleB1$_{G238A}$	*nleB1* from EPEC E2348/69 in pEGFP-C2 with amino acid G_{238} mutated to A, Kan^R	This study

pEGFP-C2-NleB1$_{I239A}$	*nleB1* from EPEC E2348/69 in pEGFP-C2 with amino acid I_{239} mutated to A, Kan^R	This study
pEGFP-C2-NleB1$_{H242A}$	*nleB1* from EPEC E2348/69 in pEGFP-C2 with amino acid H_{242} mutated to A, Kan^R	This study
pEGFP-C2-NleB1$_{E253A}$	*nleB1* from EPEC E2348/69 in pEGFP-C2 with amino acid E_{253} mutated to A, Kan^R	This study
pEGFP-C2-NleB1$_{N263A}$	*nleB1* from EPEC E2348/69 in pEGFP-C2 with amino acid N_{263} mutated to A, Kan^R	This study
pEGFP-C2-NleB1$_{L267A}$	*nleB1* from EPEC E2348/69 in pEGFP-C2 with amino acid L_{267} mutated to A, Kan^R	This study
pEGFP-C2-NleB1$_{A269A}$	*nleB1* from EPEC E2348/69 in pEGFP-C2 with amino acid A_{269} mutated to E, Kan^R	This study
pEGFP-C2-NleB1$_{Y283A}$	*nleB1* from EPEC E2348/69 in pEGFP-C2 with amino acid Y_{238} mutated to A, Kan^R	This study
pEGFP-C2-NleB1$_{K292A}$	*nleB1* from EPEC E2348/69 in pEGFP-C2 with amino acid K_{292} mutated to A, Kan^R	This study
pEGFP-C2-NleB1$_{PILN(63-66)AAAA}$	*nleB1* from EPEC E2348/69 in pEGFP-C2 with $PILN_{(63-66)}$ motif mutated to AAAA, Kan^R	This study
pEGFP-C2-NleB1$_{HKQ(140-142)AAA}$	*nleB1* from EPEC E2348/69 in pEGFP-C2 with $HKQ_{(140-142)}$ motif mutated to AAA, Kan^R	This study
pEGFP-C2-NleB1$_{QES(142-144)AAA}$	*nleB1* from EPEC E2348/69 in pEGFP-C2 with $QES_{(142-144)}$ motif mutated to AAA, Kan^R	This study
pEGFP-C2-NleB1$_{LGLL(155-158)AAAA}$	*nleB1* from EPEC E2348/69 in pEGFP-C2 with $LGLL_{(155-158)}$ motif mutated to AAAA, Kan^R	This study
pEGFP-C2-NleB1$_{GSL(197-199)AAA}$	*nleB1* from EPEC E2348/69 in pEGFP-C2 with $GSL_{(197-199)}$ motif mutated to AAA, Kan^R	This study
pEGFP-C2-NleB1$_{DxD(221-223)AxA}$	*nleB1* from EPEC E2348/69 in pEGFP-C2 with $DxD_{(221-223)}$ catalytic motif mutated to AAA, Kan^R	(401)
pEGFP-C2-	*nleB1* from EPEC E2348/69 in pEGFP-C2 with	This study

NleB1$_{DKL(228-230)AAA}$	DKL$_{(228-230)}$ motif mutated to AAA, Kan^R	
pEGFP-C2-NleB1$_{PDG(236-238)AAA}$	*nleB1* from EPEC E2348/69 in pEGFP-C2 with PDG$_{(236-238)}$ motif mutated to AAA, Kan^R	This study
pEGFP-C2-NleB1$_{SN(262-263)AA}$	*nleB1* from EPEC E2348/69 in pEGFP-C2 with SN$_{(262-263)}$ motif mutated to AA, Kan^R	This study
pEGFP-C2-NleB1$_{LAGL(268-271)AEAA}$	*nleB1* from EPEC E2348/69 in pEGFP-C2 with LAGL$_{(268-271)}$ motif mutated to AEAA, Kan^R	This study
pEGFP-C2-NleB1$_{KV(277-278)AA}$	*nleB1* from EPEC E2348/69 in pEGFP-C2 with KV$_{(277-278)}$ motif mutated to AA, Kan^R	This study
pEGFP-C2-NleB1$_{KGI(289-291)AAA}$	*nleB1* from EPEC E2348/69 in pEGFP-C2 with KGI$_{(289-291)}$ motif mutated to AAA, Kan^R	This study
pEGFP-C2-NleB2	*nleB2* from EPEC E2348/69 in pEGFP-C2, Kan^R	(401)
pEGFP-C2-NleB2$_{DxD(221-223)AAA}$	*nleB1* from EPEC E2348/69 in pEGFP-C2 with DxD$_{(221-223)}$ putative catalytic motif mutated to AAA, Kan^R	Jaclyn Pearson
pEGFP-C2-SseK1	*sseK1* from *S*. Typhymurium SL1344 in pEGFP-C2, Kan^R	Michelle Kelly
pEGFP-C2-SseK1$_{DxD(229-231)AxA}$	*sseK1* from *S*. Typhymurium SL1344 in pEGFP-C2 with DxD$_{(229-231)}$ putative catalytic motif mutated to AAA, Kan^R	This study
pEGFP-C2-SseK2	*sseK2* from *S*. Typhymurium SL1344 in pEGFP-C2, Kan^R	This study
pEGFP-C2-SseK2$_{DxD(239-241)AxA}$	*sseK2* from *S*. Typhymurium SL1344 in pEGFP-C2 with DxD$_{(239-241)}$ putative catalytic motif mutated to AAA, Kan^R	This study
pEGFP-C2-SseK3	*sseK3* from *S*. Typhymurium SL1344 in pEGFP-C2, Kan^R	This study
pEGFP-C2-sseK3$_{DxD(226-228)AxA}$	*sseK3* from *S*. Typhymurium SL1344 in pEGFP-C2 with DxD$_{(226-228)}$ putative catalytic motif mutated to AAA, Kan^R	This study

pRL-TK	Renilla luciferase vector, Amp^R	Promega
pNF-κB-Luc	Vector for measuring NF-κB dependent luciferase expression, Amp^R	Clontech
pACYC184	Medium copy number cloning vector, Cm^R, Tet^R	NEB
pACYC184-$NleB_{CR}$	*nleB* from *C. rodentium* ICC169 in pACYC184, Cm^R	This study
pACYC184-$NleB_{Y219ACR}$	*nleB* from *C. rodentium* ICC169 in pACYC184 with amino acid Y_{219} mutated to A, Cm^R	This study
pACYC184-$NleB_{E253ACR}$	*nleB* from *C. rodentium* ICC169 in pACYC184 with amino acid E_{253} mutated to A, Cm^R	This study
pACYC184-$NleB1_{EPEC}$	*nleB1* from EPEC E2348/69 in pACYC184, Cm^R	This study
pACYC184-$NleB2_{EPEC}$	*nleB2* from EPEC E2348/69 in pACYC184, Cm^R	This study
pACYC184-$NleB1_{EHEC}$	*nleB1* from EHEC O157:H7 Sakai in pACYC184, Cm^R	This study

Table 2.4. List of primers used in this study

Name	Primer sequences 5'-3'
pEGFP-C2 F	AACACCCCCATCGGCG
pEGFP-C2 R	GTAACCATTATAAGCTGC
NotI	TGCGGCCGCA
pTrc99A F	CGGTTCTGGCAAATATTC
pTrc99A R	GCAGTTCCCTACTCTCGC
P63A F	GCGATACGAAAAAGGAGAAGTAGCAATATTGAATACCAA AGAACATCCG
P63A R	CGGATGTTCTTTGGTATTCAATATTGCTACTTCTCCTTTTTC GTATCGC
I64A F	GCGATACGAAAAAGGAGAAGTACCAGCATTGAATACCAA AGAACATCCG
I64A R	CGGATGTTCTTTGGTATTCAATATTGCTACTTCTCCTTTTTC GTATCGC
L65A F	GCGATACGAAAAAGGAGAAGTACCAATAGCGAATACCAA AGAACATCCGTATTTG
L65A R	CAAATACGGATGTTCTTTGGTATTCGCTATTGGTACTTCTC CTTTTTCGTATCGC
N66A F	GATACGAAAAAGGAGAAGTACCAATATTGGCTACCAAAG AACATCCGTATTTGAGC
N66A R	GCTCAAATACGGATGTTCTTTGGTAGCCAATATTGGTACTT CTCCTTTTTCGTATC
K68A F	GAAGTACCAATATTGAATACCGCAGAACATCCGTATTTGA GC
K68A R	GCTCAAATACGGATGTTCTGCGGTATTCAATATTGGTACTT C
K81A F	GAGCAATATTATAAATGCTGCAGCAATAGAAAATGAGCGT ATAATCGG
K81A R	CCGATTATACGCTCATTTTCTATTGCTGCAGCATTTATAAT ATTGCTC
D93A F	GTATAATCGGTGTGCTGGTAGCTGGAAATTTTACTTATGA ACAAAAAAAG
D93A R	CTTTTTTTGTTCATAAGTAAAATTTCCAGCTACCAGCACAC CGATTATAC
D121A F	CAAAATATAAAAATAATCTACCGAGCAGCTGTGGATTTCA GCATGTATG
D121A R	CATACATGCTGAAATCCACAGCTGCTCGGTAGATTATTTTT ATATTTTG
D128A F	CAGATGTGGATTTCAGCATGTATGCTAAAAAACTATCTGA TATTTAC
D128A R	GTAAATATCAGATAGTTTTTTAGCATACATGCTGAAATCC ACATCTG

L157A F	GAGGGATAATTATCTGTTAGGCGCATTAAGAGAAGAGTTAAAAAATATCC
L157A R	GGATATTTTTTAACTCTTCTCTTAATGCGCCTAACAGATAATTATCCCTC
Y219A F	CGCCCTGTAGCGGATGTATAGCTCTTGATGCCGACATGATTATTAC
Y219A R	GTAATAATCATGTCGGCATCAAGAGCTATACATCCGCTACAGGGCG
Y234A F	CCGATAAATTAGGAGTCCTGGCTGCTCCTGATGGTATCGCTGTG
Y234A R	CACAGCGATACCATCAGGAGCAGCCAGGACTCCTAATTTATCGG
P236A F	GGAGTCCTGTATGCTGCTGATGGTATCGCTGTGC
P236A R	GCACAGCGATACCATCAGCAGCATACAGGACTCC
D237A F	GGAGTCCTGTATGCTCCTGCTGGTATCGCTGTGCATGTAG
D237A R	CTACATGCACAGCGATACCAGCAGGAGCATACAGGACTCC
G238A F	GGAGTCCTGTATGCTCCTGATGCTATCGCTGTGCATGTAG
G238A R	CTACATGCACAGCGATAGCATCAGGAGCATACAGGACTCC
I239A F	GGAGTCCTGTATGCTCCTGATGGTGCCGCTGTGCATGTAG
I239A R	CTACATGCACAGCGGCACCATCAGGAGCATACAGGACTCC
H242A F	CTCCTGATGGTATCGCTGTGGCTGTAGATTGTAATGATGAG
H242A R	CTCATCATTACAATCTACAGCCACAGCGATACCATCAGGAG
E253A F	GTGGATTGTAATGATAATAGAAAAAGTCTTGCAAATGGTGCAATAGTTGTCAATC
E253A R	GATTGACAACTATTGCACCATTTGCAAGACTTTTTCTATTATCATTACAATCCAC
N263A F	GTCAATCGTAGTGCTCATCCAGCATTACTTGCAGGCCTCGATATTATG
N263A R	CATAATATCGAGGCCTGCAAGTAATGCTGGATGAGCACTACGATTGAC
L267A F	GTAATCATCCAGCAGCACTTGCAGGCCTCGATATTATGAAGAG
L267A R	CTCTTCATAATATCGAGGCCTGCAAGTGCTGCTGGATGATTAC
A269E F	GTAATCATCCAGCATTACTTGAAGGCCTCGATATTATGAAGAG
A269E R	CTCTTCATAATATCGAGGCCTTCAAGTAATGCTGGATGATTAC
Y283A F	GTAAAGTTGACGCTCATCCAGCTTATGATGGTCTAGGAAAGGG
Y283A R	CCCTTTCCTAGACCATCATAAGCTGGATGAGCGTCAACTTTAC
K292A F	GATGGTCTAGGAAAGGGTATCGCGCGGCATTTTAACTATT

	CATCG
K292A R	CGATGAATAGTTAAAATGCCGCGCGATACCCTTTCCTAGA CCATC
PILN F	GCGATACGAAAAAGGAGAAGTAGCAGCAGCGGCTACCAA AGAACATCCGTATTTG
PILN R	CAAATACGGATGTTCTTTGGTAGCCGCTGCTGCTACTTCTC CTTTTTCGTATCGC
HKQ F	CTGATATTTACCTTGAAAATATCGCTGCAGCAGAATCATA CCCTGCCAGTGAGAGGG
HKQ R	CCCTCTCACTGGCAGGGTATGATTCTGCTGCAGCGATATTT TCAAGGTAAATATCAG
QES F	CCTTGAAAATATCCATAAAGCAGCAGCATACCCTGCCAGT GAGAGGG
QES R	CCCTCTCACTGGCAGGGTATGCTGCTGCTTTATGGATATTT TCAAGG
LGLL F	CAGTGAGAGGGATAATTATCTGGCAGCCGCAGCAAGAGA AGAGTTAAAAAATATCCCAGAAGG
LGLL R	CCTTCTGGGATATTTTTTAACTCTTCTCTTGCTGCGGCTGC CAGATAATTATCCCTCTCACTG
GSL F	GGCCATATTGAAGGCTGCAGCTGCGTTTACAGAGACGGGA AAAACTGG
GSL R	CCAGTTTTTCCCGTCTCTGTAAACGCAGCTGCAGCCTTCAA TATGGCC
DKL F	GCCGACATGATTATTACCGCTGCAGCAGGAGTCCTGTATG CTCCTG
DKL R	CAGGAGCATACAGGACTCCTGCTGCAGCGGTAATAATCAT GTCGGC
PDG F	GATAAATTAGGAGTCCTGTATGCTGCTGCTGCTATCGCTGT GCATGTAGATTG
PDG R	CAATCTACATGCACAGCGATAGCAGCAGCAGCATACAGG ACTCCTAATTTATC
PDG_{AKA} F	CGATAAATTAGGAGTCCTGTATGCTGCTAAGGCTATCGCT GTGCATGTAGATTG
PDG_{AKA} R	CAATCTACATGCACAGCGATAGCCTTAGCAGCATACAGGA CTCCTAATTTATCG
PDG_{AEA} F	CGATAAATTAGGAGTCCTGTATGCTGCTGAGGCTATCGCT GTGCATGTAGATTG
PDG_{AEA} R	CAATCTACATGCACAGCGATAGCCTCAGCAGCATACAGGA CTCCTAATTTATCG
PD_{AR} F	CGATAAATTAGGAGTCCTGTATGCTGCTAGGGGTATCGCT GTGCATGTAGATTG
PD_{AR} R	CAATCTACATGCACAGCGATACCCCTAGCAGCATACAGGA CTCCTAATTTATCG
PDG_{SRS} F	CCGATAAATTAGGAGTCCTGTATGCTAGTAGGAGTATCGC TGTGCATGTAGATTGTAATGATGAG

PDG_{SRS} R	CTCATCATTACAATCTACATGCACAGCGATACTCCTACTAGCATACAGGACTCCTAATTTATCGG
PDG_{SES} F	CGATAAATTAGGAGTCCTGTATGCTAGTGAGAGTATCGCTGTGCATGTAGATTG
PDG_{SES} R	CAATCTACATGCACAGCGATACTCTCACTAGCATACAGGACTCCTAATTTATCG
PD_{SE} F	CGATAAATTAGGAGTCCTGTATGCTAGTGAGGGTATCGCTGTGCATGTAGATTG
PD_{SE} R	CAATCTACATGCACAGCGATACCCTCACTAGCATACAGGACTCCTAATTTATCG
SN F	GGTGCGATAGTTGTCAATCGTGCTGCTCATCCAGCATTACTTGC
SN R	GCAAGTAATGCTGGATGAGCAGCACGATTGACAACTATCGCACC
LAGL F	GTCAATCGTAGTAATCATCCAGCATTAGCTGAAGCCGCCGATATTATGAAGAGTAAAGTTGACGC
LAGL R	GCGTCAACTTTACTCTTCATAATATCGGCGGCTTCAGCTAATGCTGGATGATTACTACGATTGAC
KV F	GGCCTCGATATTATGAAGAGTGCAGCTGACGCTCATCCATATTATG
KV R	CATAATATGGATGAGCGTCAGCTGCACTCTTCATAATATCGAGGCC
KGI F	CATCCATATTATGATGGTCTAGGAGCGGCTGCCAAGCGGCATTTTAACTATTCATCG
KGI R	CGATGAATAGTTAAAATGCCGCTTGGCAGCCGCTCCTAGACCATCATAATATGGATG
GFP S2 F	GAATTCATGGCACGTTTTAATGCCG
GFP S2 R	GTCGACTTACCTCCAAGAACTGGCAG
GFP S3 F	GAATTCATGTTTTCTCGAGTCAGAGG
GFP S3 R	GTCGACTTATCTCCAGGAGCTGATAG
$S1_{AAA}$ F	GGTGTATATATCTTGCTGCTGCTATGATTATCACGGAAAAACTGG
$S1_{AAA}$ R	CCAGTTTTTCCGTGATAATCATAGCAGCAGCAAGATATATACACC
$S2_{AAA}$ F	GTGGGTGCATATATCTTGCTGCAGCTATGTTACTTACTGATAAAC
$S2_{AAA}$ R	GTTTATCAGTAAGTAACATAGCTGCAGCAAGATATATGCACCCAC
$S3_{AAA}$ F	CTGGAGGTGGCTGCATATATCTTGCTGCTGCTATGTTACTTACAG
$S3_{AAA}$ R	CTGTAAGTAACATAGCAGCAGCAAGATATATGCAGCCACCTCCAG
B1 F	CC GGT ACC ATGTTATCTTCATTAAATGTCC
B1 R	C GGA ATT CCC CCATGAACTGCTGGTATAC
pCX340 F	AAGGCGCACTCCCGTTC

pCX340 R	GTCATTCTGAGAATAGTG
pGEX F	CGTATTGAAGCTATCCCACAA
pGEX R	GGGAGCTGCATGTGTCAGAG
pGEX B1 F	CGCGAATTCATGTTATCTTCATTAAATGTCCTTC
pGEX B1 R	CGCGTCGACTTACCATGAACTGCTGGTATAC
pGEX S3 F	CGCGAATTCATGTTTTCTCGAGTCAGAGGTTTTC
pGEX S3 R	CGCGTCGACTTATCTCCAGGAGCTGATAGTCAAACTGC
B2 F	CGGAATTCATGCTTTCACCGATAAGGACAACTTTC
B2 R	CGGGATCCTTACCATGAACTGCATGTATACTGAC
S2 F	CGGAATTCATGGCACGTTTTAATGCCG
S2 R	CGGGATCCTTACCTCCAAGAACTGGC
T7 F	AATACGACTCACTATAGG
T7 R	GCTAGTTATTGCTCAGCGG
pGBKT7 R	CGTTTTAAAACCTAAGAGTC
pGADT7 R	GGTGCACGATGCACAG
pGADT7 RecF	CTATTCGATGATGAAGATACCCCACC
pGADT7 RecR	AGATGGTGCACGATGCACAGTTG
FADD DD F	CGCGAATTCATGCTGTGTGCAGCATTTAACGTCATATG
FADD DD R	CGCGGATCCTTACTGCTGAACCTCTTGTACCAGG
TRADD DD F	CGCGAATTCATGAGCCTGAAGGACCAACAGACG
TRADD DD R	CGCGGATCCCTACAGGCCCAGCAAGTCCTC
RIPK1 DD F	CGCGAATTCATGACGGATAAACACCTGGACCC
RIPK1 DD R	CGCGAGCTCTTAGACGTAAATCAAGCTGCTCAG
Fas DD F	CGCGAATTCAATTTATCTGATGTTGACTTGAGTAAATATAC
Fas DD R	CGCGAATTCATGAATTTATCTGATGTTGACTTGAG
TNFR1 DD F	CGCCATATGATGACGCTGTACGCCGTGGTGG
TNFR1 DD R	CGCGGATCCTCACTCGATGTCCTCCAGGCAGC
DR5 DD F	CGCGAATTCATGGATCCCACTGAGACTCTGAGAC
DR5 DD R	CGCGGATCCTTAGAACTTTCCAGAGCTCAACAAGTG
MyD88 DD F	CGCGAATTCATGGTGCGGCGCCGCCTGTC
MyD88 DD R	CGCGGATCCTCATCCCAGCTCCAGCAGCACG
IRAK1 DD F	CGCCATATGATGCACTTCTTGTACGAGGTGCCG
IRAK1 DD R	CGCGAATTCTCATGTGATGATGTCCCGCGCAC
IRAK4 DD F	CGCGAATTCATGACATATGTGCGCTGCCTCAATG
IRAK4 DD R	CGCGGATCCTTAGGGAACAGCATCTGGGAGC
TRIM32 F	CGCGGATCCATGGCTGCGGCTGCAG
TRIM32 R	CGCGAATTCTTAAGGGGTGGAATATCTTCTCAG
TRIM32FLAG F	CGCGAATTCAATGGCTGCGGCTGCAG
TRIM32FLAG R	CGCGGATCCTTAAGGGGTGGAATATCTTCTCAG
TRIM32 seq F	CCACACAGTGGCCATCC
CSN5 F	GAAGATCTGATGGCGGCGTCCGGGAG
CSN5 R	CGCGTCGACTTAAGAGATGTTAATTTGATTAAACAGTTTA TCC
p3xFLAG F	AATGTCGTAATAACCCCGCCCCGTTGACGC
p3xFLAG R	TATTAGGACAAGGCTGGTGGGCAC

M13 F	TGTAAAACGACGGGCCAGT
M13 R	TCACACAGGAAACAGCTATGA
CR B F	CGGGATCCGGATAAACAGGACGACGAATGTTATCTCCATT AAATGTTCTTCAATTTAATTTC
CR B R	CGGTCGACTTACCATGAACTGTTGGTATACATACTGG
EP B1 F	CGGGATCCGGATAAACAGGACGACGAATGTTATCTTCATT AAATGTCCTTCAATCCAGC
EP B1 R	CGGTCGACTTACCATGAACTGCTGGTATACATACTGG
EP B2 F	CGGGATCCGAGTTAGTTGTGAAGAAAATATGG
EP B2 R	CGGTCGACTTACCATGAACTGCATGTATACTGAC
EH B1 F	CGGGATCCGGATAAACAGGACGACGAATGTTATCTTCATT AAATGTCCTTCAATCCAGC
EH B1 R	CGGTCGACTTACCATGAACTGCAGGTATACATACTGGTAT TC
pACYC seq F	GTACTGCCGGGCCTCTTG
pACYC seq R	GAAGGCTTGAGCGAGGGCG

Chapter 3
Investigating functional regions and/or binding domains of the glycosyltransferase NleB1 from EPEC

Chapter 3. Investigating functional regions and/or binding domains of the glycosyltransferase NleB1 from EPEC

3.1 Introduction

EPEC is a diarrhoeal pathogen of children that utilises a type III secretion system (T3SS) to inject virulence effector proteins directly into enterocytes during infection. Numerous non-LEE encoded effectors that disrupt host cell signalling have been characterised in recent years (360). For example, NleB1 is a unique glycosyltransferase effector that disrupts death receptor signalling in host cells (401, 441, 561).

Glycosyltransferases are enzymes that catalyse the transfer of a sugar moiety from an activated sugar donor substrate containing a phosphate leaving group to a specific acceptor substrate that can either be a protein, a lipid, a polysaccharide or a nucleic acid, forming a glycosidic bond (585, 586). The sugar unit is usually activated in the form of nucleoside diphosphate sugars such as uridine diphosphate-glucose (UDP-Glc), uridine diphosphate-galactose (UDP-Gal), uridine diphosphate-*N*-acetyl glucosamine (UDP-GlcNAc), uridine diphosphate-*N*-acetyl galactosamine (UDP-GalNAc), guanosine diphosphate-mannose (GDP-Man) and guanosine diphosphate-fucose (GDP-Fuc) (586). However, mononucleoside phosphates such as cytidine 5'monophospho-*N*-acetylneuraminic acid (CMP-NeuAc) and lipid phosphates such as dolichol phosphate oligosaccharides are also used as sugar donors (586). Although the sugar is most commonly transferred to a hydroxyl substituent of the acceptor, giving rise to the formation of an *O*-linked glycosidic linkage, it can also be transferred to an amide group resulting in the formation of an *N*-linked glycosidic bond (586). Glycosyl transfer to proteins usually occurs to the oxygen nucleophile of the hydroxyl group of serine or threonine side chains or to the nitrogen nucleophile of the amide group of an asparagine side chain (587-592).

Unlike classic *O*-linked protein glycosylation, *O*-GlcNAc modification involves attachment of a single GlcNAc moiety to the hydroxyl group of serine or threonine residues and is not elongated (Figure 3.1A) (592, 593). *N*-linked glycosylation usually occurs at an asparagine residue within a consensus asparagine-X-serine/threonine (NX(S/T)) sequon on the acceptor protein substrate, where X is any amino acid residue except proline (594). Classical *N*-linked glycosylation requires the assembly of an oligosaccharide chain on a lipid carrier and its *en bloc* transfer from the cytoplasm across the ER membrane in eukaryotes or plasma membrane in prokaryotes by an oligosacccharyl transferase (OST) (595, 596). However, a non-classical *N*-linked glycosylation of asparagine residues in an NX(S/T) motif by a bacterial cytoplasmic glycosyltransferase has recently been discovered (597-599).

The presence of glycosyltransferases in both eukaryotes and prokaryotes has revealed that in spite of significant differences at the amino acid sequence level, these enzymes show structural similarity (586). They are all globular proteins with either a GT-A or a GT-B fold type. The GT-A fold consists of an α/β/α sandwich, which is reminiscent of two β/α/β Rossmann domains, typical of nucleotide binding domains, closely abutting to form a continuous central β sheet (Figure 3.1B) (586). Enzymes possessing a GT-A fold generally have a signature aspartate-x-aspartate (DxD) motif, which participates in a divalent metal cation and/or sugar donor binding, essential for the catalytic reaction (600, 601). However, the DxD motif is by no means invariant and some glycosyltransferases of the GT-A fold lacking this motif have been identified (602). Whenever present, this motif is located in a short loop connecting one β strand to a smaller β strand (603). Glycosyltransferases of the GT-A fold have two distinct domains; the N-terminal domain generally recognises the sugar nucleotide and the C-terminal domain contains the acceptor substrate-binding site (603, 604). The GT-B fold also consists of two β/α/β Rossmann domains. However, in the GT-B fold, the two Rossmann domains do not associate tightly with each other and rather face each other, with the active site lying in the resulting cleft (Figure 3.1B) (586). Unlike enzymes of the GT-A fold, enzymes of the GT-B fold have their

sugar donor-binding site in the C-terminal domain and their acceptor substrate-binding site in their N-terminal region (603, 604).

Generally, glycosyltransferases are specific for both the sugar donor substrate and the acceptor substrate (604). Although homology modelling has been useful to infer substrate docking sites, the solved crystal structures of numerous glycosyltransferases of either the GT-A or the GT-B fold along with mutagenesis experiments have enabled the identification of particular residues involved in either the sugar substrate binding or acceptor substrate binding. For example, aspartate-286 (D286) and D288 of the DxD motif and tryptophan-102 (W102) of *Clostridium difficile* toxin B, a glucosyltransferase that has been extensively characterised, were shown to be necessary for Mn^{2+} and UDP-binding respectively (605, 606), whereas arginine-455 (R455), D461, lysine-463 (K463) and glutamate-472 (E472) were important for enzyme-protein substrate recognition (607).

Unlike typical *O*-linked *N*-acetylglucosamine (*O*-GlcNAc) transferases which transfer a GlcNAc moeity in *O*-glycosidic linkages to serines or threonines of their targets, NleB1 catalyses the addition of a single GlcNAc moiety in an *N*-glycosidic linkage to arginine-117 (R117) of the Fas associated death domain protein, FADD (401). This modification prevents the interaction between FADD and Fas and subsequent assembly of the canonical death inducing signalling complex (DISC), thereby inhibiting FasL-induced cell death. Since the discovery of this unusual glycosylation reaction, another example of arginine glycosylation has been identified in which the bacterial glycosyltransferase, EarP, rhamnosylates translation elongation factor P to activate its function (608).

Apart from the DxD catalytic motif of NleB1, little is known about other functional sites in the protein and the regions required for substrate binding and specificity. Unlike the human *O*-GlcNAc transferase (OGT) that possesses N-terminal tetratricopeptide repeats (TPRs) necessary for substrate binding, NleB1 appears to

lack such a motif (609-611). In this chapter, we aimed to map residues of NleB1 that are potentially important for the function of the enzyme and/or binding of the substrates. Here a library of 22 random transposon-based, in-frame, linker insertion mutants of NleB1 were tested during EPEC infection of HeLa cells for their ability to block caspase-8 activation in response to FasL. Immunoblot analysis of caspase-8 cleavage products showed that 14 mutant derivatives of NleB1 no longer inhibited caspase-8 activation, including the catalytic DxD mutant. Regions of interest around the linker insertion sites were examined further with multiple or single amino acid substitutions. Co-immunoprecipitation studies of 34 site-directed mutants showed that the NleB1 derivatives with the mutations E253A, Y219A and PILN(63-66)AAAA bound but did not GlcNAcylate FADD. A further mutant derivative, PDG(236-238)AAA, did not bind or GlcNAcylate FADD.

3.2 Results

3.2.1 Generation of an in-frame, 5 amino acid residue insertion library of NleB1 from EPEC

In order to gain insight into the functional and/or binding regions of the unique GlcNAc transferase enzyme NleB1, a plasmid encoding NleB1 (pEGFP-C2-NleB1) was mutated using the bacteriophage MuA transposase (Figure 3.2). Artificial transposons carrying a chloramphenicol resistance marker gene, designated as entranceposons (M1-Cam^R) were randomly inserted into the target plasmid *in vitro*. Following transformation of the transposition reaction in *E. coli* XL-1 Blue, the transformants were plated on LA containing kanamycin and chloramphenicol to select for pEGFP-C2-NleB1 constructs carrying M1-Cam^R and pooled for plasmid extraction.

To ensure the generation of mutations only in the *nleB1* gene and not in the vector backbone, plasmids were digested with *Eco*RI and *Bam*HI to release *nleB1* containing the entranceposon. The DNA of interest of approximately 2 kb was separated by agarose gel electrophoresis, purified and ligated in newly extracted pEGFP-C2 vector. The ligation reaction was transformed in *E. coli* and selected on LA plates containing kanamycin and chloramphenicol. The plasmids obtained after pooling were digested with *Not*I and closed by self-ligation to remove the body of the entranceposon, resulting in a 15 bp in frame insertion in the *nleB1* gene. The ligation was again transformed in *E. coli* but this time plated on LA containing kanamycin only. Colony PCR was performed to map the 15 bp insertion in individual clones. The 15 bp insertion is translated into 5 variable extra amino acids (Table 3.1). The exact position of the pentapeptide insertion of each mutant was determined by sequencing. A total of 27 transposon mutants of NleB1 was obtained, two of which (NleB1$_{Tn262}$) both contained the pentapeptide insertion at the same position, between amino acids 261 and 262 of NleB1, although the pentapeptide sequence differed (Figure 3.3, Table 3.1). Derivatives of *nleB1* carrying the 15 bp insertions were cloned into pTrc99A (Figure 3.4) in order to test the library of mutants during EPEC infection.

3.2.2 Screening of transposon mutants of NleB1 for loss of function

As mentioned previously, NleB1 inhibits FasL-induced formation of the DISC and subsequent caspase-8 activation and apoptotic cell death during EPEC infection. Therefore, transposon insertion mutants of NleB1 were screened for their ability to inhibit caspase-8 activation during EPEC infection. HeLa cells were infected with various EPEC derivatives including wild type EPEC E2348/69, Δ*nleB1* carrying pTrc99A and Δ*nleB1* complemented with wild type *nleB1* or an *nleB1* insertion mutant derivative encoded on pTrc99A. Caspase-8 activation was then induced by treatment with FasL.

All 27 *nleB1* mutants were tested for their ability to block caspase-8 activation except 5, which likely carried an insertion into the N-terminal translocation signal of NleB1 (Table 3.2, Figure 3.5) (612-615). Caspase-8 activation was assessed by immunoblot using an antibody that recognises only cleaved (activated) caspase-8. As expected, complementation of Δ*nleB1* with wild type *nleB1* resulted in inhibition of caspase-8 activation to a similar level as that observed in cells infected with wild type EPEC E2348/69 (Figure 3.5) (401). Of the 22 insertion mutants tested, 14 no longer inhibited caspase-8 cleavage, including $nleB1_{Tn221}$ carrying an insertion in the catalytic DxD region (residues 221-223) (Figure 3.5, Table 3.2). In addition, both $nleB1_{Tn262}$ mutants appeared equally unable to inhibit caspase-8 activation, irrespective of the pentapeptide sequence introduced between amino acids 261 and 262.

3.2.3 Generation of a library of site-directed mutants of NleB1 from EPEC

To further examine potential functional regions of NleB1 that were identified by screening the transposon mutants of NleB1 for loss of function, a total of 34 amino acid substitutions around the transposon-based linker insertion sites were constructed using the QuikChange II Site-Directed Mutagenesis kit, 23 of which were single amino acid substitutions and 11 were multiple site-directed mutants (Figure 3.6, Table 3.3). Ten of the 34 (9 single and 1 multiple) amino acid substitutions were created in

the N-terminus of NleB1 as this region was not examined in the caspase-8 screening assay which required translocation of NleB1 and hence the N-terminal translocation signal. Multiple residues around the transposon insertion sites were mutated in an attempt to subsequently validate or narrow down potential functional regions of NleB1. Glu^{253} to Ala (E253A) was also chosen as previous work showed that this mutation impaired the ability of NleB1 to inhibit NF-κB activation upon TNF stimulation (441).

3.2.4 Screening of site-directed mutants of NleB1 for loss of function

NleB1-mediated inhibition of FasL-induced caspase-8 activation and the subsequent apoptotic cell death relies on its glycosyltransferase activity. NleB1 binds to and modifies FADD by adding a single GlcNAc moiety at arginine-117 (R117), preventing the Fas-FADD interaction and DISC assembly. Therefore, site-directed mutants were then tested for their ability to GlcNAcylate FADD. HEK293T cells were co-transfected with plasmids expressing derivatives of GFP-tagged NleB1 and FLAG-FADD before FLAG-FADD was immunoprecipitated from the cell lysates. The immunoprecipitates (IPs) were then examined for GlcNAcylation of FADD using an antibody to GlcNAc and for binding by co-immunoprecipitation of GFP-tagged NleB1 derivatives (Figure 3.7, Table 3.3) using anti-GFP antibodies. We reasoned that mutants that have lost their enzymatic activity would still activate caspase-8 via FADD and would not inhibit host apoptotic cell death.

The catalytic mutant $NleB1_{DxD(221\text{-}223)AxA}$ which was also included in the screening assay as a control was unable to GlcNAcylate FADD although it could still bind to FADD (Figure 3.7C). One multiple site-directed mutant, $NleB1_{PILN(63\text{-}66)AAAA}$, and two single site-directed mutants of NleB1, $NleB1_{Y219A}$ and $NleB1_{E253A}$, were also unable to GlcNAcylate FADD (Figure 3.7A, C-D, Table 3.3). Additionally, one multiple site-directed mutant, $NleB1_{PDG(236\text{-}238)AAA}$, showed reduced ability to GlcNAcylate FADD (Figure 3.7A,C, Table 3.3). The loss of function mutants, $NleB1_{PILN(63\text{-}66)AAAA}$, $NleB1_{Y219A}$ and $NleB1_{E253A}$ still bound to FADD whereas $NleB1_{PDG(236\text{-}238)AAA}$ did not

interact with FADD (Figure 3.7 A, C, Table 3.3). NleB1 carrrying the mutations D93A, L157A, GSL(197-199)AAA, G238A, I239A, L267A, Y283A and K292A bound weakly to FADD (Figure 3.7, Table 3.3) whereas NleB1 with mutations D128A, LGLL(155-158)AAAA, DKL(228-230)AAA, LAGL(268-271)AEAA and KGI(289-291)AAA did not appear to bind FADD (Figure 3.7, Table 3.3). Interestingly, all these mutants still mediated FADD GlcNAcylation suggesting that NleB1-subsrate interactions need not be stable and long lasting for GlcNAcylation to occur (Figure 3.7, Table 3.3)

3.2.5 A subset of NleB1 mutants are unable to GlcNAcylate FADD *in vitro*

NleB1 has been shown to directly GlcNAcylate FADD in the presence of the sugar donor, UDP-GlcNAc *in vitro*. To confirm the loss of function of 4 NleB1 mutants ($NleB1_{PILN(63\text{-}66)AAAA}$, $NleB1_{Y219A}$, $NleB1_{PDG(236\text{-}238)AAA}$ and $NleB1_{E253A}$), recombinant NleB1 proteins with an N-terminal GST tag and recombinant FADD with an N-terminal His_6 tag were purified and incubated either alone or together in the presence of UDP-GlcNAc. The NleB1 mutants, with the exception of $NleB1_{E253A}$, were not highly soluble. This was shown by the low detection level of GST-tagged NleB1 mutant proteins slightly below the 62 kDa marker in the soluble and elution fractions following protein purification compared to the more intense band of the same size observed in the insoluble fractions by western blot (Figure 3.8). Given this, the amount of each recombinant protein was standardised prior to the incubation period. Proteins were examined for GlcNAcylation using anti-GlcNAc antibodies. Whereas incubation of GST-NleB1 and His_6-FADD with UDP-GlcNAc led to FADD GlcNAcylation (Figure 3.9), this was not observed when any of GST-$NleB1_{PILN(63\text{-}66)AAAA}$, GST-$NleB1_{PDG(236\text{-}238)AAA}$, GST-$NleB1_{Y219A}$ or GST-$NleB1_{E253A}$ were used (Figure 3.9). Furthermore, no GlcNAcylation was observed when GST, GST-NleB1 or its derivative site-directed mutants and His-FADD were individually incubated with UDP-GlcNAc (Figure 3.9).

3.2.6 Amino acid substitutions PILN(63-66)AAAA, Y219A, PDG(236-238)AAA and E253A did not affect cellular localisation of NleB1

Since the mutant proteins purified were not highly soluble, we decided to test if the mutations affected the folding of the NleB1 mutant proteins and changed the cytosolic localisation of NleB1 in transfected cells. However, GFP-tagged NleB1 as well as GFP-tagged NleB1 mutants all showed diffuse cytosolic staining in HEK293T transfected cells by immunofluorescence microscopy (Figure 3.10). None of the proteins formed aggregates or exhibited abnormal subcellular staining.

3.3 Discussion

Initial studies suggested NleB1 adopts a GT-A fold based on results obtained from HHPred/HHSearch protein structure and function prediction tools (442, 616, 617). The prediction software revealed that the central part of NleB1 bears significant similarity to the GT8 family of glycosyltransferases, which include the eukaryotic glycogenins, and identified a DxD motif, which is a characteristic feature of GT-A glycosyltransferases. The host protein glyceraldehyde 3-phosphate dehydrogenase (GAPDH) was initially proposed as the target of NleB1 binding and *O*-GlcNAc modification (442). It was suggested that this modification by NleB1 inhibited activation of TNF receptor-associated factor 2 (TRAF2) and downstream NF-κB signalling (442).

More recently, Li *et al.* showed that when GAPDH and NleB1 were ectopically co-expressed in HEK293T cells, and GAPDH was co-immunoprecipitated from the cell lysates, no GlcNAcylation of the latter was observed by anti-*O*-GlcNAc antibody blotting (441). In addition, they showed that GAPDH was not modified by NleB1 purified from bacteria using a ^{3}H-UDP-GlcNAc labelling assay and using mass spectrometry showed that GAPDH co-expressed with NleB1 or *C. rodentium* NleB in HEK293T cells was not modified (441). Instead, NleB1 was found to add a GlcNAc moiety to a conserved arginine, R117 of FADD and R235 of TRADD, in an *N*-linked glycosidic linkage, thereby blocking FasL, TRAIL and TNF-induced apoptotic cell death (401, 441). The identification of the addition of a single *N*-linked GlcNAc moiety to a conserved arginine in a number of DD proteins and its effect on death signalling pathways were novel discoveries in the field of glycobiology.

Other than the DxD$^{221\text{-}223}$ motif and E253 (441), specific amino acid residues and regions of NleB that participated in this unusual biochemical activity were unknown. To identify additional functional regions of NleB1, a library of insertion mutants of NleB1 was screened for the ability to inhibit caspase-8 activation during EPEC infection of HeLa cells. Of the 22 insertion mutants tested, 14 no longer inhibited

FasL-induced caspase-8 cleavage. Regions around these pentapeptide insertions were investigated further by site-directed mutagenesis. However, few of these amino acid substitutions resulted in loss of function. The disparity in the high number of insertion mutants that lost their ability to inhibit FasL-induced caspase-8 cleavage during EPEC infection versus the smaller number of site-directed mutants that lost enzymatic activity may reflect the greater structural changes introduced by the pentapeptide insertion and/or the limitation of using caspase-8 cleavage during infection as a screen, which relied on efficient translocation of the NleB1 insertion mutants by the EPEC T3SS. Even though NleB1 can glycosylate the DD of both FADD and TRADD in this study, the effect of NleB1 mutants on the Fas signaling pathway was investigated due to the importance of this pathway in controlling infection with A/E pathogens (401).

Co-immunoprecipitation experiments with ectopically expressed GFP-NleB1 mutants and FLAG-FADD and incubation of recombinant GST-NleB1 mutant proteins and His_6-FADD in the presence of UDP-GlcNAc revealed that 4 mutant derivatives ($NleB1_{PILN(63-66)AAAA}$, $NleB1_{PDG(236-238)AAA}$, $NleB1_{Y219A}$ and $NleB1_{E253A}$) were unable to GlcNAcylate FADD. FADD was also not modified with GlcNAc in the presence of the catalytic triad mutant $NleB1_{DxD(221-223)AxA}$. This is consistent with previous studies that showed that the DxD triad is essential for the catalytic activity of the enzyme. However, this mutation did not prevent binding of the NleB1 mutant with FADD, indicating that this region is not important for interaction with the acceptor substrate FADD. In fact the DxD motif is only known to coordinate divalent ions and/or a portion of the UDP-sugar donor substrate (600, 601). Three of the total 34 site-directed mutants tested ($NleB1_{PILN(63-66)AAAA}$, $NleB1_{Y219A}$, $NleB1_{E253A}$) also bound FADD while lacking GlcNAcylation activity, indicating that the regions mutated could contribute to the function of the enzyme rather than to substrate recognition. Interestingly when the individual amino acid residues (residues 63-66) of the PILN motif and the downstream lysine residue (K68) were mutated to alanines, none of the individual mutations prevented FADD GlcNAcylation and these single site-directed

mutants still bound FADD. This suggested that all 4 PILN residues together are essential for the enzymatic activity of NleB1.

It is generally assumed that the reaction catalysed by glycosyltransferases follows a sequential ordered mechanism whereby the metal ion and the sugar nucleotide bind first resulting in a conformational change that creates the acceptor substrate binding site (604, 618-623). The crystal structures of several glycosyltransferases of either the GT-A or GT-B fold reveal that at least one flexible loop region located near the sugar donor binding site has a crucial role in the catalytic reaction. For example, both the mammalian glycosyltransferase β4Gal-T1 and the bacterial *N. meningitidis* enzyme LgtC have 2 flexible loops which act as a lid covering the bound sugar substrate (624-626), exposing a binding site for the acceptor substrate. Detailed structural analysis of NleB1 will help to define the role of $PILN^{63-66}$ in any conformational shift upon UDP-GlcNAc binding whereas $PDG^{236-238}$ may be important for acceptor substrate binding since mutating this region inhibited both FADD modification and binding. Interestingly, a number of NleB1 amino acid substitutions that led to weak or no binding to FADD still showed efficient GlcNAcylation. One possible explanation for this is that the mutations affected the substrate binding stability and activity kinetics so that a transient interaction was sufficient for GlcNAcylation to occur.

To determine if the 4 mutations ($NleB1_{PILN(63-66)AAAA}$, $NleB1_{PDG(236-238)AAA}$, $NleB1_{Y219A}$ and $NleB1_{E253A}$) that abrogated FADD GlcNAcylation *in vitro* affect the folding and therefore potentially the localisation of NleB1, these 4 NleB1 mutants with an N-terminal GFP tag were expressed in HEK293T cells. All 4 mutants were localised in the cytosol as is the case with GFP-tagged wild type NleB1, suggesting that the mutations do not severely affect the folding of the NleB1 mutants and do not change their subcellular localisation.

In summary, while we identified a number of regions of NleB1 that appeared to be essential for enzymatic function, namely residues 63-66, 219, 236-238 and 253, these

regions will need to be investigated further to confirm their importance in NleB1 function and virulence during infection.

A

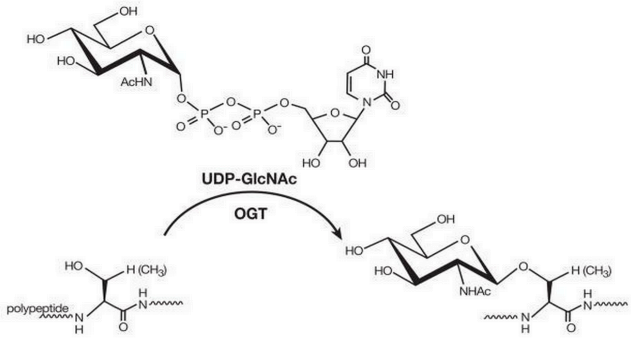

B

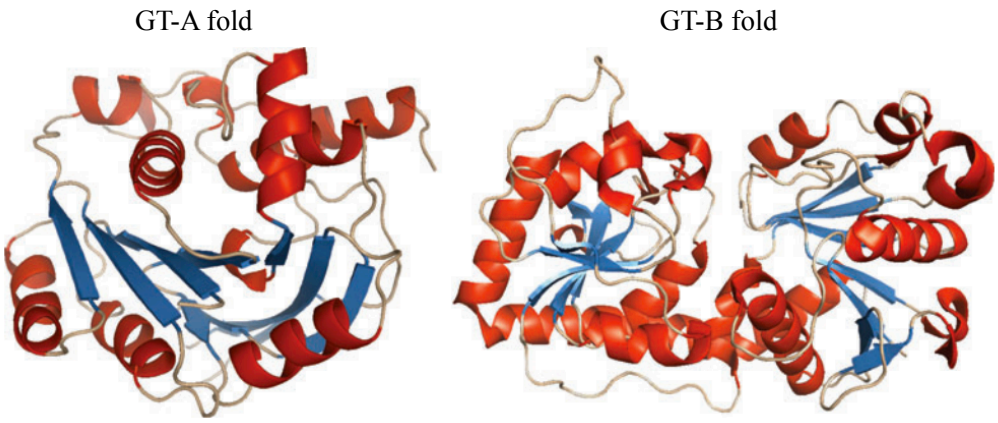

Figure 3.1. Schematic diagram of the *O*-GlcNAc modification catalysed by an *O*-GlcNAc transferase (OGT) and overall structural folds of GT-A and GT-B glycosyltransferases. (A) In an *O*-GlcNAc modification, a single GlcNAc moiety is transferred from UDP-GlcNAc to the oxygen nucleophile from the hydroxyl group of a peptide acceptor. Image adapted from (627). (B) The GT-A fold is represented by the enzyme SpsA from *Bacillus subtilus,* Protein Data Bank (PDB) 1qgq and the GT-B fold is represented by the bacteriophage T4 β-glucosyltransferase, PDB 1jg7. Image from (586).

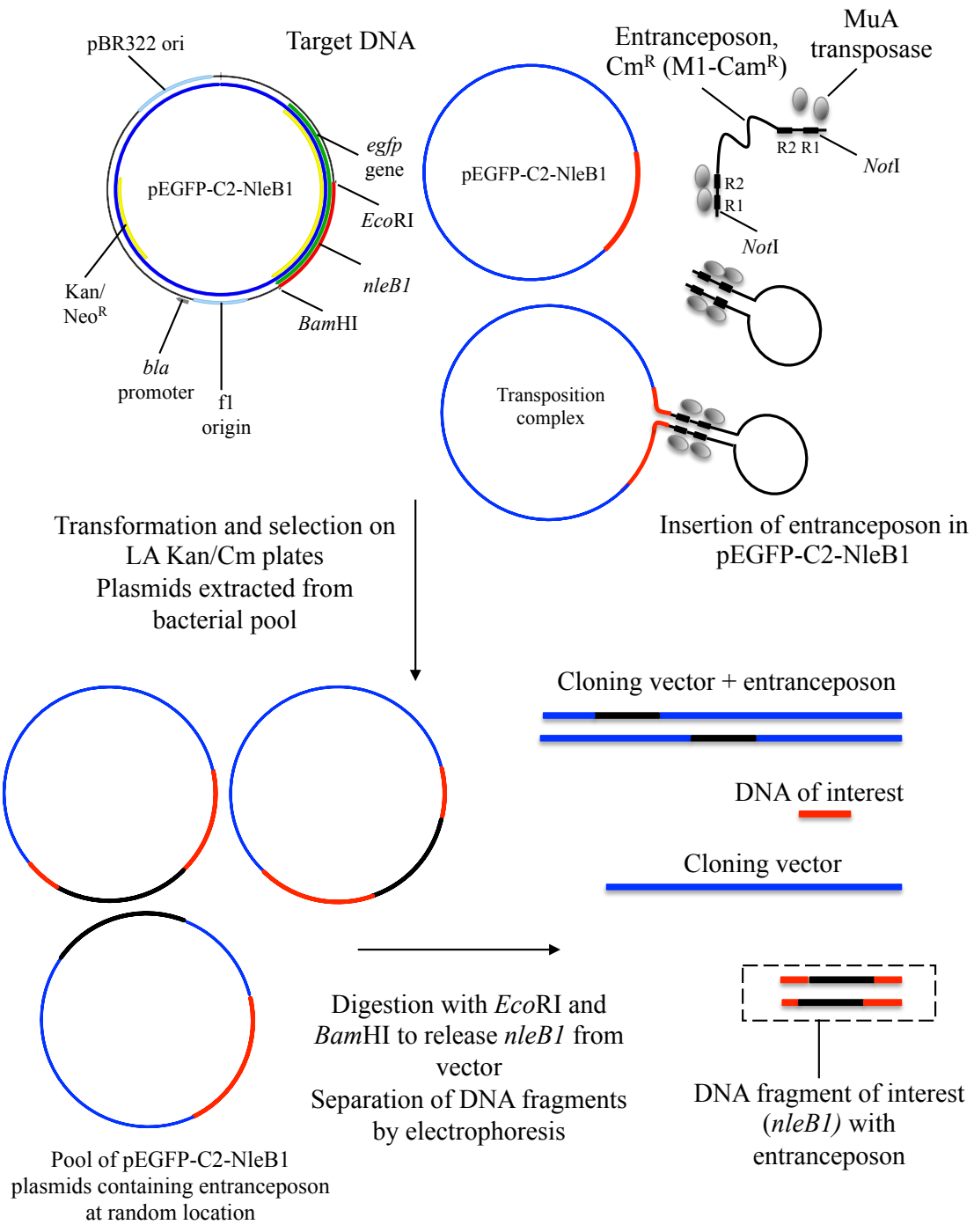
pBR322 ori
Target DNA
pEGFP-C2-NleB1
egfp gene
EcoRI
nleB1
BamHI
Kan/ Neo^R
bla promoter
f1 origin
pEGFP-C2-NleB1
Entranceposon, Cm^R (M1-Cam^R)
MuA transposase
R2 R1
NotI
R2
R1
NotI
Transposition complex
Insertion of entranceposon in pEGFP-C2-NleB1
Transformation and selection on LA Kan/Cm plates
Plasmids extracted from bacterial pool
Cloning vector + entranceposon
DNA of interest
Cloning vector
Digestion with EcoRI and BamHI to release nleB1 from vector
Separation of DNA fragments by electrophoresis
DNA fragment of interest (nleB1) with entranceposon
Pool of pEGFP-C2-NleB1 plasmids containing entranceposon at random location

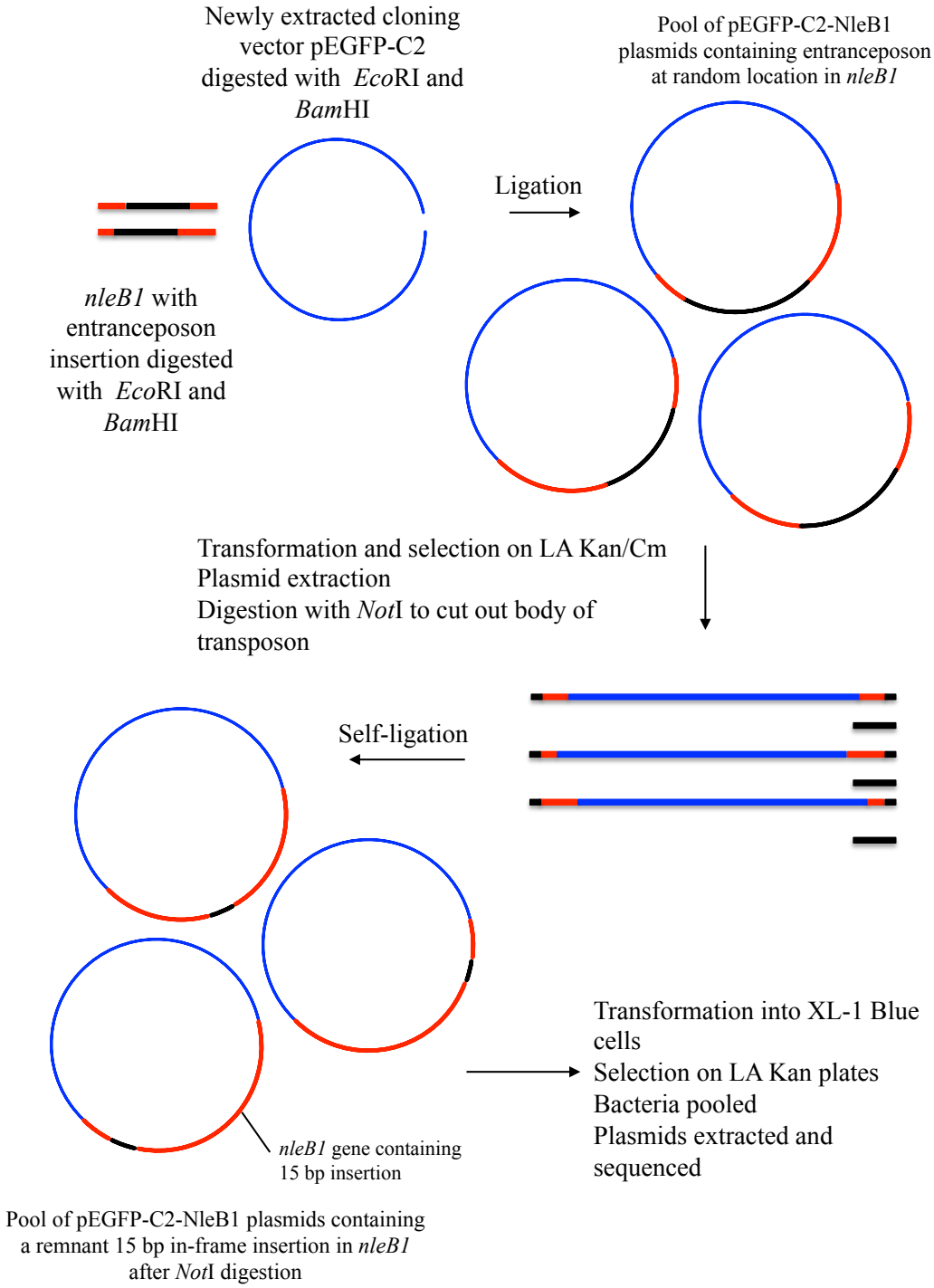

Figure 3.2. Schematic diagram of the construction of NleB1 transposon mutants. The random transposon-based, in-frame, linker insertion mutants of NleB1 were generated using the bacteriophage MuA transposase. Diagram adapted from the Thermo Scientific Mutation Generation System Kit, F-701, Manual.

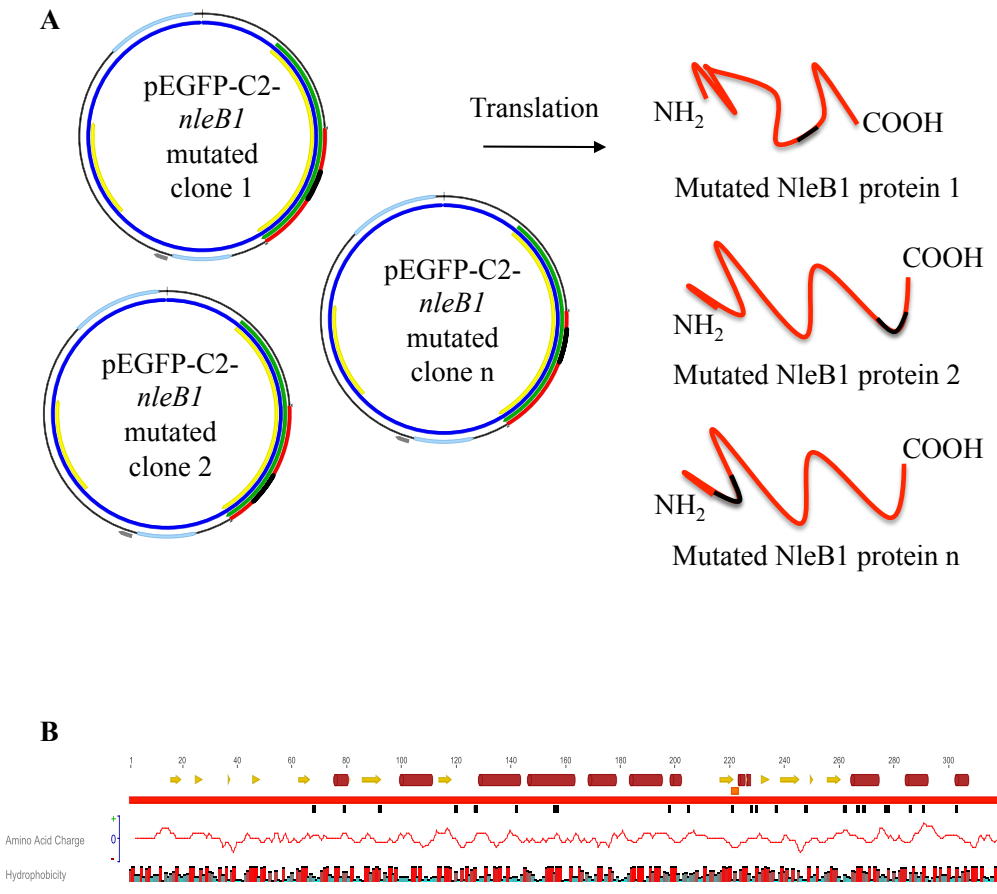

Figure 3.3. Schematic diagram mapping the transposon insertion sites in NleB1. (A) The mutated *nleB1* genes code for mutant NleB1 proteins with the pentapeptide inserted in different positions. (B) NleB1 is depicted as the continuous red arrow. The catalytic DxD region is represented as an orange box. Transposon insertion sites are represented as black boxes. The secondary structure of NleB1 was predicted by Jnet (628). Yellow arrows represent β sheets and dark red cylinders represent α helices. The amino acid polarity graph is plotted by the EMBOSS (577) charge tool through Geneious (571) and the hydrophobicity of each residue is shown below the NleB1 protein. Amino acid residues are coloured from red through to blue according to the hydrophobicity value, where red is the most hydrophobic and blue is the most hydrophilic.

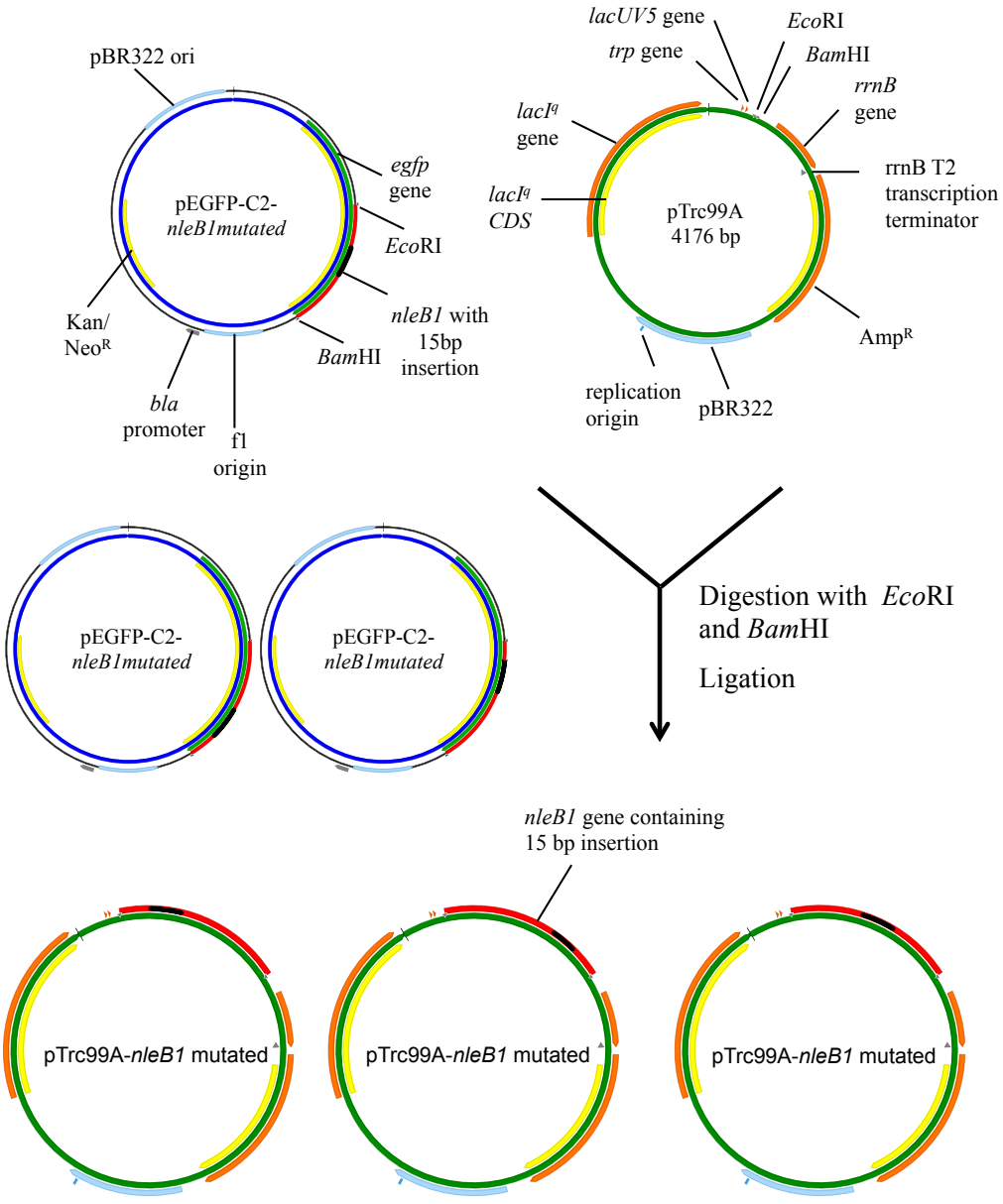

Figure 3.4. Schematic diagram of the generation of *nleB1* transposon mutants in the pTrc99A vector. The library of *nleB1* mutants constructed using the MuA transposase was digested from the pEGFP-C2 constructs and ligated into the pTrc99A vector backbone.

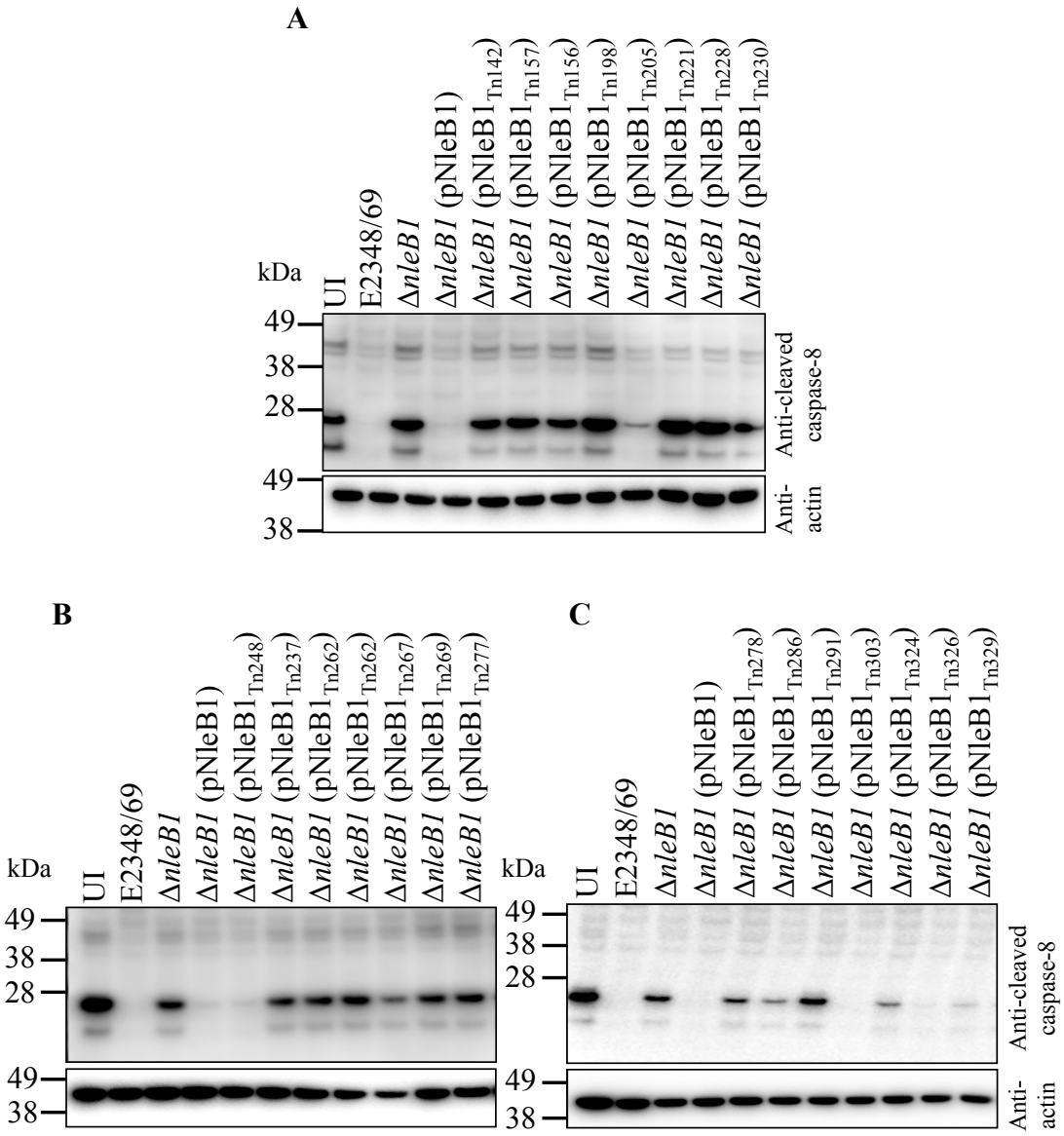

Figure 3.5. Screening of NleB1 transposon mutants for their ability to inhibit FasL-induced cell death during EPEC infection. (A-C) Immunoblots showing cleaved caspase-8 in HeLa cells infected with EPEC E2348/69 derivatives carrying the different NleB1 mutants in the pTrc99A vector backbone and stimulated with FasL. Cells were harvested for immunoblotting and cleaved caspase-8 was detected with anti-cleaved caspase-8 antibodies. Antibodies to β-actin were used as a loading control. Representative immunoblot from at least three independent experiments. UI; uninfected.

A

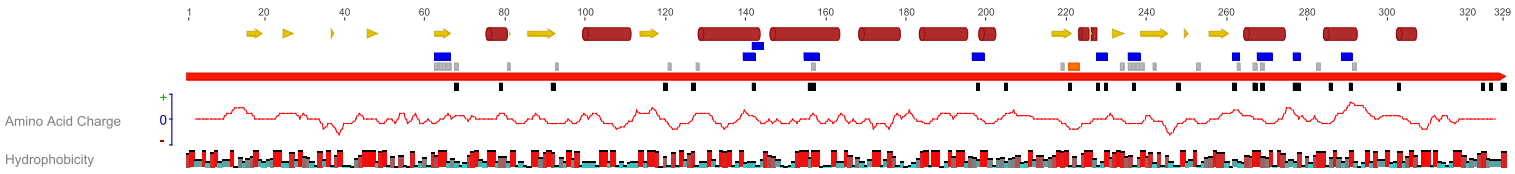
Amino Acid Charge
Hydrophobicity

B

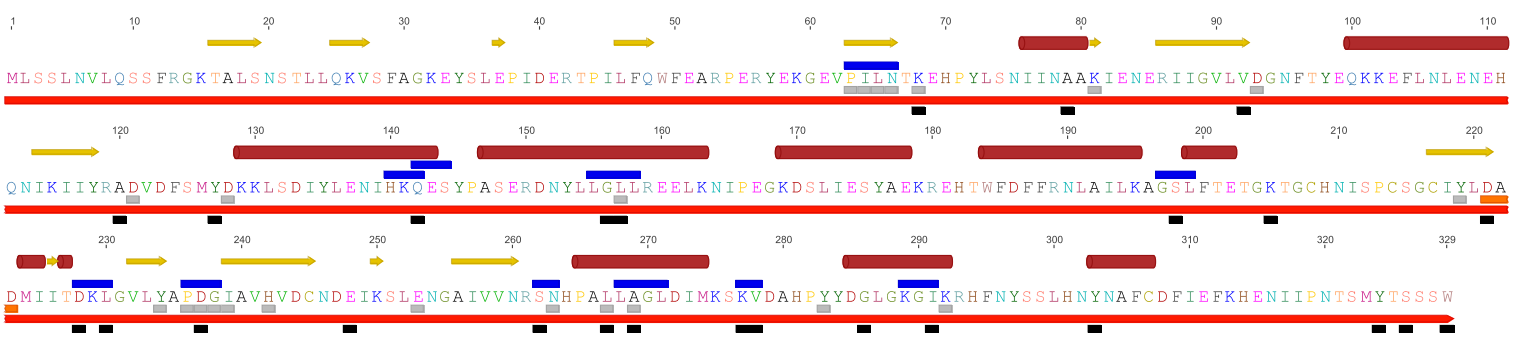
MLSSLNVLQSSFRGKTALSNSTLLQKVSFAGKEYSLEPIDERTPILFQWFEARPERYEKGEVPILNTKEHPYLSNIINAAKIENERIIGVLVDGNFTYEQKKEFLNLENEH
QNIKIIYRADVDFSMYDKKLSDIYLENIHKQESYPASERDNYLLGLLREELKNIPEGKDSLIESYAEKREHTWFDFFRNLAILKAGSLFTETGKTGCHNISPCSGCIYLDA
DMIITDKLGVLYAPDGIAVHVDCNDEIKSLENGAIVVNRSNHPALLAGLDIMKSKVDAHPYYDGLGKGIKRHFNYSSLHNYNAFCDFIEFKHENIIPNTSMYTSSSW

Figure 3.6. Schematic diagram showing the single site-directed mutants, multiple site-directed mutants and transposon mutants. (A) NleB1 protein is depicted as the continuous red arrow. The catalytic DxD region is represented as an orange box. Transposon insertion sites are represented as black boxes and single and multiple site-directed mutations are represented by grey and blue boxes respectively. The secondary structure of NleB1 was predicted by Jnet (628). Yellow arrows represent β sheets and dark red cylinders represent α helices. The amino acid polarity graph is plotted by the EMBOSS (577) charge tool through Geneious (571) and the hydrophobicity of each residue is shown below the NleB1 protein. Amino acid residues are coloured from red through to blue according to the hydrophobicity value, where red is the most hydrophobic and blue is the most hydrophilic. (B) Same as in (A) except that the NleB1 amino acid sequence is shown above the red arrow.

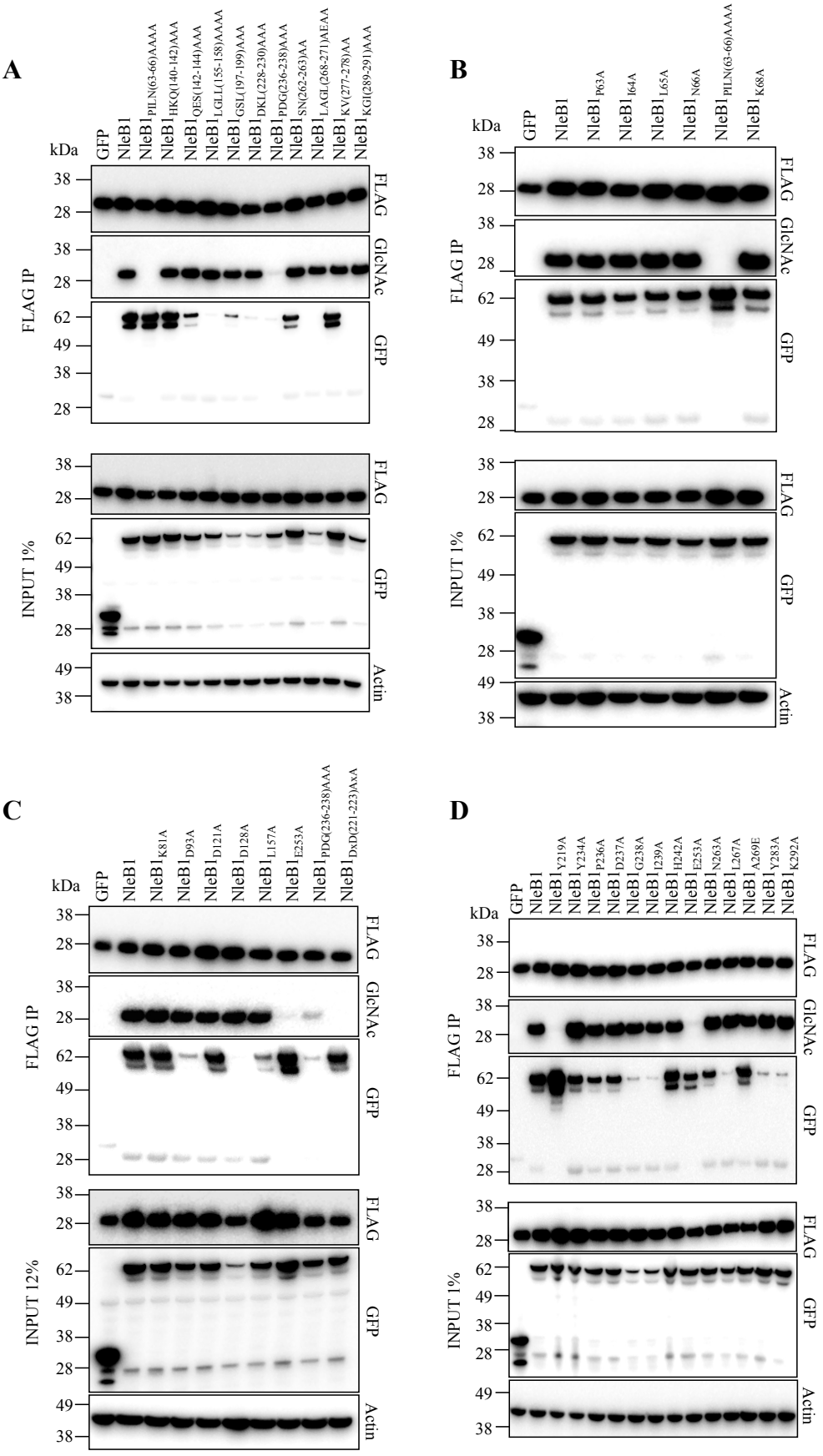
A
B
C
D
kDa
GFP
NleB1
FLAG IP
INPUT 1%
INPUT 12%
FLAG
GlcNAc
GFP
Actin

Figure 3.7. Screen of site-directed mutants of NleB1 for their ability to GlcNAcylate and bind FADD. (A-D) Immunoblots of inputs and immunoprecipitates (IPs) of anti-FLAG immunoprecipitations performed on lysates of HEK293T cells co-transfected with pFLAG-FADD and pEGFP-C2-NleB1 (GFP-NleB1) or the pEGFP-C2 constructs encoding the site directed mutants of NleB1. The FLAG-FADD IPs were tested for GlcNAcylation by immunoblotting with anti-GlcNAc antibodies. GFP-NleB1 and the mutants were tested for immunoprecipitation with FLAG-FADD by immunoblotting of the IPs with anti-GFP antibodies. Antibodies to β-actin were used as a loading control. Representative immunoblot from at least three independent experiments.

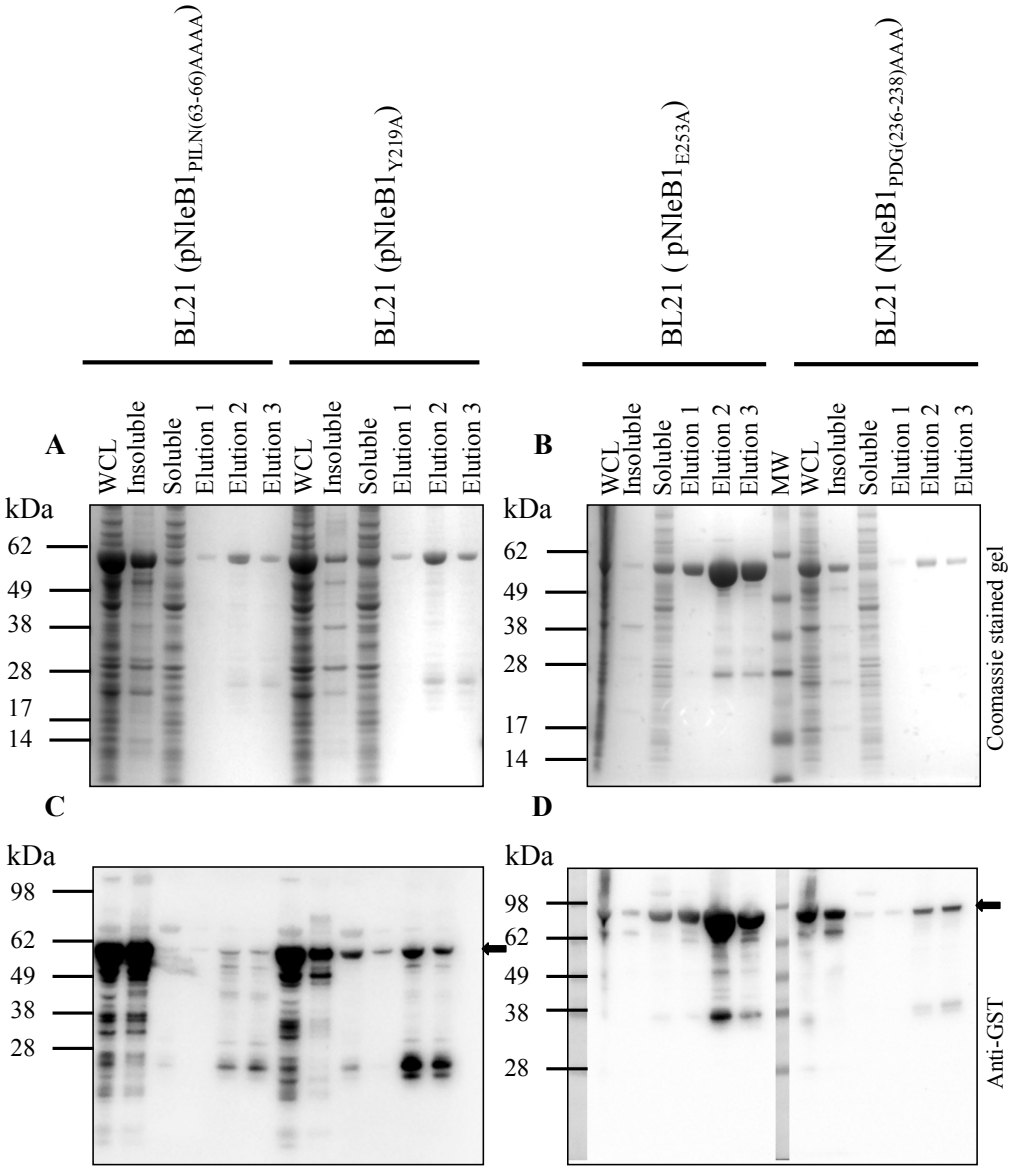

Figure 3.8. Purification of GST-NleB1 mutants. (A-B) Coomassie stained gels of whole cell lysates (WCL), soluble and insoluble fractions and elutions from bacterial cultures. (C-D) Immunoblots showing purified GST-NleB1 mutants. WCLs, soluble and insoluble fractions and elutions were separated by gel electrophoresis and transferred to immunoblots which were probed with anti-GST antibody. Arrow indicates position of GST-NleB1 mutants. Bands of lower molecular weight are possibly degradation products of GST-NleB1 mutants.

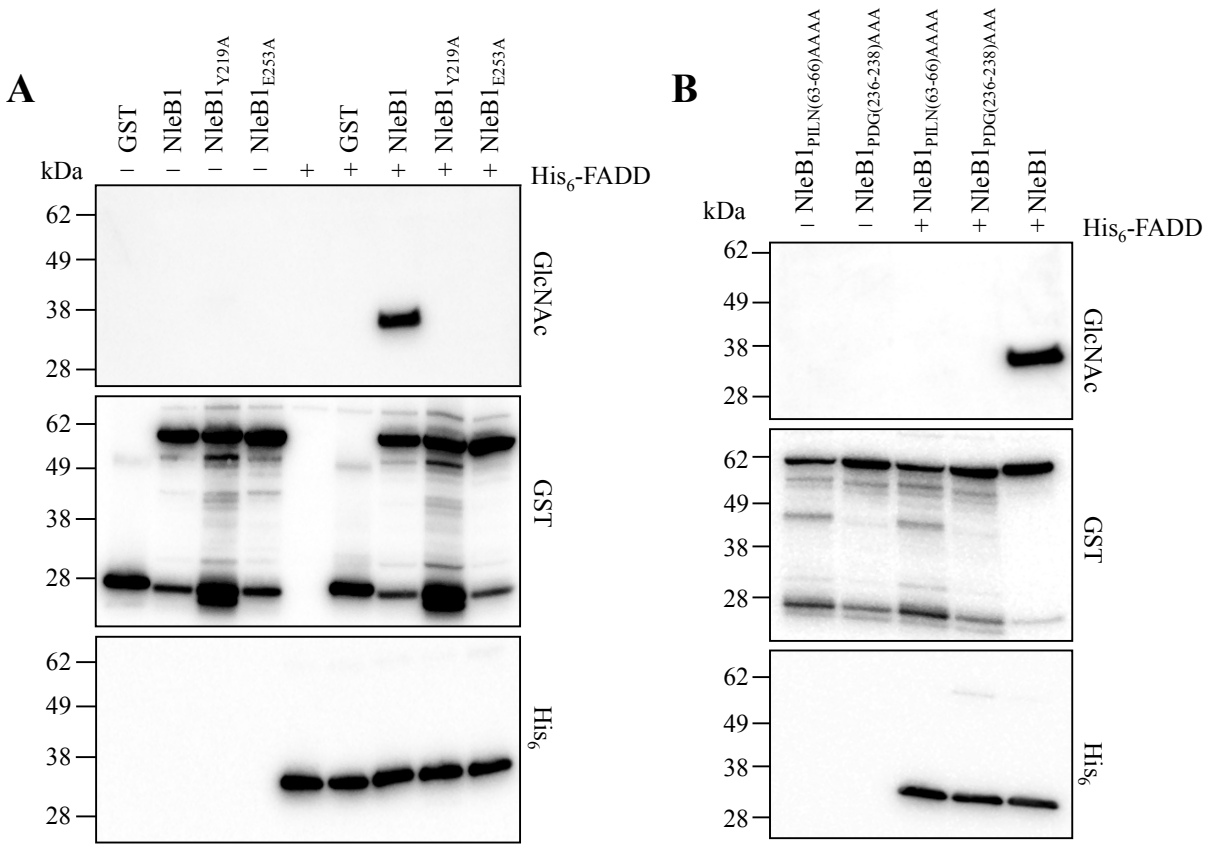

Figure 3.9. Enzymatic activity of NleB1 mutants. (A-B) Immunoblots of recombinant protein incubations from *in vitro* assay for NleB1-mediated GlcNAc modification of FADD. Recombinant GST-NleB1 or mutants and His-FADD were incubated alone or together in the presence of 1 mM UDP-GlcNAc. GlcNAcylation of FADD was tested by immunoblotting with anti-GlcNAc antibodies and the presence of the GST and His fusion proteins was detected by immunoblotting with anti-GST and anti-His antibodies. Representative immunoblot from at least three independent experiments.

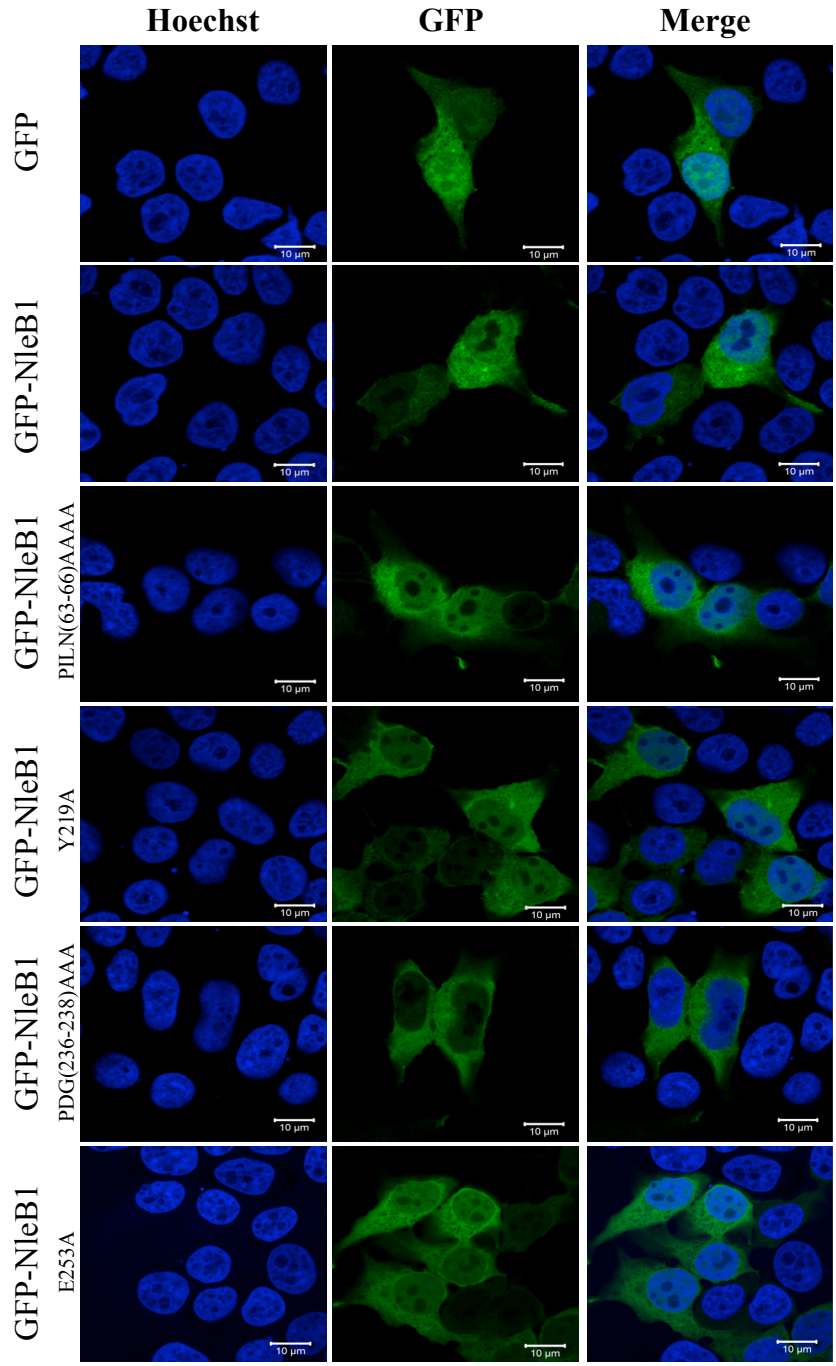

Figure 3.10. Cellular localisation of NleB1 mutants. GFP-NleB1 and its derivative mutants, which inhibit FADD GlcNAcylation, were ectopically expressed and localised uniformly in the cytoplasm of HEK293T cells. Scale bar, 10 µm.

Table 3.1. List of NleB1 transposon-based mutants with the linker pentapeptide sequence shown

NleB1 mutant	Pentapeptide insertion sequence
$NleB1_{Tn68}$	NAAAT
$NleB1_{Tn79}$	AAAAN
$NleB1_{Tn92}$	VAAAL
$NleB1_{Tn120}$	AAAAR
$NleB1_{Tn127}$	YAAAM
$NleB1_{Tn142}$	CGRNK
$NleB1_{Tn156}$	GAAAL
$NleB1_{Tn157}$	CGRIG
$NleB1_{Tn198}$	CGRTG
$NleB1_{Tn205}$	CGRTG
$NleB1_{Tn221}$	DAAAL
$NleB1_{Tn228}$	DAAAT
$NleB1_{Tn230}$	CGRNK
$NleB1_{Tn237}$	DAAAP
$NleB1_{Tn248}$	CGRND
$NleB1_{Tn262}$	MRPHR
$NleB1_{Tn262}$	SAAAR
$NleB1_{Tn267}$	CGRTA
$NleB1_{Tn269}$	AAAAL
$NleB1_{Tn277}$	CGRKS
$NleB1_{Tn278}$	CGRSK
$NleB1_{Tn286}$	CGRND
$NleB1_{Tn291}$	IAAAG
$NleB1_{Tn303}$	CGRNN
$NleB1_{Tn324}$	CGRSM
$NleB1_{Tn326}$	SAAAT
$NleB1_{Tn329}$	LRPHS

Tn: transposon insertion site

Table 3.2. List of EPEC derivatives and their effect on caspase-8 activation during EPEC infection

EPEC strain	Pentapeptide insertion sequence	Caspase-8 activation[a]
WT	–	–
Δ*nleB1*	–	+++
Δ*nleB1* + pNleB1	–	–
Δ*nleB1* + pNleB1$_{Tn68}$	NAAAT	NT
Δ*nleB1* + pNleB1$_{Tn79}$	AAAAN	NT
Δ*nleB1* + pNleB1$_{Tn92}$	VAAAL	NT
Δ*nleB1* + pNleB1$_{Tn120}$	AAAAR	NT
Δ*nleB1* + pNleB1$_{Tn127}$	YAAAM	NT
Δ*nleB1* + pNleB1$_{Tn142}$	CGRNK	+++
Δ*nleB1* + pNleB1$_{Tn156}$	GAAAL	+++
Δ*nleB1* + pNleB1$_{Tn157}$	CGRIG	+++
Δ*nleB1* + pNleB1$_{Tn198}$	CGRTG	+++
Δ*nleB1* + pNleB1$_{Tn205}$	CGRTG	+
Δ*nleB1* + pNleB1$_{Tn221}$	DAAAL	+++
Δ*nleB1* + pNleB1$_{Tn228}$	DAAAT	+++
Δ*nleB1* + pNleB1$_{Tn230}$	CGRNK	+++
Δ*nleB1* + pNleB1$_{Tn237}$	DAAAP	+++
Δ*nleB1* + pNleB1$_{Tn248}$	CGRND	–
Δ*nleB1* + pNleB1$_{Tn262}$	MRPHR	+++
Δ*nleB1* + pNleB1$_{Tn262}$	SAAAR	+++
Δ*nleB1* + pNleB1$_{Tn267}$	CGRTA	+
Δ*nleB1* + pNleB1$_{Tn269}$	AAAAL	+++
Δ*nleB1* + pNleB1$_{Tn277}$	CGRKS	+++
Δ*nleB1* + pNleB1$_{Tn278}$	CGRSK	++
Δ*nleB1* + pNleB1$_{Tn286}$	CGRND	+
Δ*nleB1* + pNleB1$_{Tn291}$	IAAAG	+++
Δ*nleB1* + pNleB1$_{Tn303}$	CGRNN	–
Δ*nleB1* + pNleB1$_{Tn324}$	CGRSM	+
Δ*nleB1* + pNleB1$_{Tn326}$	SAAAT	–
Δ*nleB1* + pNleB1$_{Tn329}$	LRPHS	+

[a]HeLa cell lysates were examined for caspase-8 activation levels after EPEC infection and FasL stimulation; +, ++ and +++ indicate the increasing levels of caspase-8 cleavage with three + signs indicating comparable levels of caspase-8 cleavage as in uninfected HeLa cells stimulated with FasL, – indicates the absence of caspase-8 cleavage similar to what is observed in the presence of functional NleB1, Tn; transposon insertion at given position, NT; not tested

Table 3.3. Site-directed mutants of NleB1 and their effect on FADD GlcNAcylation and binding

NleB1 single site-directed mutants	Ability to GlcNAcylate FADD[a]	Binding to FADD[b]
P63A	+++	+++
I64A	+++	+++
L65A	+++	+++
N66A	+++	+++
K68A	+++	+++
K81A	+++	+++
D93A	+++	+
D121A	+++	+++
D128A	+++	−
L157A	+++	+
Y219A	−	+++
Y234A	+++	+++
P236A	+++	+++
D237A	+++	+++
G238A	+++	+
I239A	+++	+
H242A	+++	+++
E253A	−	+++
N263A	+++	+++
L267A	+++	+
A269E	+++	+++
Y283A	+++	+
K292A	+++	+
NleB1 multiple site-directed mutants	**Ability to GlcNAcylate FADD[a]**	**Binding to FADD[b]**
PILN (63-66) AAAA	−	+++
HKQ (140-142) AAA	+++	+++
QES (142-144) AAA	+++	++
LGLL (155-158) AAAA	+++	−
GSL (197-199) AAA	+++	+
DKL (228-230) AAA	+++	−
PDG (236-238) AAA	+	−
SN (262-263) AA	+++	++
LAGL (268-271) AEAA	+++	−
KV (277-278) AA	+++	+++
DAD(221-223)AAA	−	+++
KGI (289-291) AAA	+++	−

[a,b] +, ++ and +++ indicate the increasing level of FADD GlcNAcylation or binding, with +++ reflecting the level of FADD GlcNAcylation or binding observed in the presence of wild type NleB1, − is indicative of an absence of FADD GlcNAcylation or binding

Chapter 4
Functional impact of selected NleB1 mutations during infection

Chapter 4. Functional impact of selected NleB1 mutations during infection

4.1 Introduction

Glycosyltransferases catalyse the transfer of carbohydrate moieties to various targets including proteins. These carbohydrate components have diverse roles ranging from cell adhesion (629-631), cell to cell interactions (632) and signalling (633-636) to host-pathogen interactions (300, 637). Cytosolic glycosylation is also a vital molecular mechanism by which various bacterial toxins and effector proteins subvert eukaryotic host cell function (638). Two major groups of bacterial proteins possessing glycosyltransferase activity have been described (638). One group comprises the clostridial cytotoxins produced by *Clostridium difficile*, *Clostridium novyi* and *Clostridium sordellii*. The other group consists of the glycosyltransferases produced by *Legionella pneumophila*.

The genus *Clostridium* consists of Gram-positive rod-shaped anaerobic bacteria. *C. difficile* toxins A and B, *C. novyi* α-toxin and *C. sordellii* lethal toxin (LT) are released by the clostridia into the environment and taken up by endocytosis into eukaryotic target cells where they modify small GTPases of the Rho and Ras subfamilies by mono-*O*-glucosylation at specific threonine residues (639-643). However, instead of using UDP-Glc as the sugar donor substrate, *C. novyi* α-toxin modifies its target by the addition of a GlcNAc moiety (644).

Clostridium difficile was first identified as an emerging pathogen causing antibiotic-associated diarrhoeal diseases in 1978 (645, 646). Since then, its major virulence factors toxins A and B have been studied intensively. The glucosylation of GTPases of the Rho subfamily such as Rho, Rac and Cdc42 by toxins A and B is generally accepted as being central to the action of these toxins (647). Rho GTPases control a panoply of cellular functions such as the organisation of the actin cytoskeleton and the integrity of the intestinal epithelial barrier (643). Addition of a glucose moiety using UDP-Glc to Rho GTPases by toxins A and B locks those proteins into an inactive state, inhibiting downstream signalling pathways. This is thought to result in the

disruption of the cell cytoskeleton leading to apoptotic cell death and fluid accumulation in and damage to the large intestine (643). Earlier studies involving the intragastric administration of hamsters with purified toxin preparations had led to the hypothesis that toxin A was the major virulence determinant of *C. difficile* (648). Hamsters that were administered toxin A displayed fluid accumulation, inflammation and death of intestinal tissues whereas those given toxin B did not display any disease symptoms unless the intestine was damaged or co-administered with sublethal concentrations of toxin A, suggesting that both toxins act synergistically (648). Interestingly, more recently, Lyras *et al.* showed that toxin B is the main virulence factor of *C. difficile* by infection of hamsters with isogenic mutants of toxin A (Δ*tcdA*) or toxin B (Δ*tcdB*) (649). The majority of hamsters infected with the Δ*tcdA* mutant died whereas the majority of those infected with the Δ*tcdB* mutant did not. Subsequent analysis of the hamsters infected with the Δ*tcdB* mutant that did not die showed that the isogenic Δ*tcdB* mutants reverted to wild type in those animals. While this study showed that toxin B is more important for virulence *in vivo*, the fact that purified toxin A was able to induce the classical symptoms of disease in hamsters cannot be disregarded and could be explained by the amount of toxins administered intragastrically as opposed to the lower amount naturally produced during infection by the *C. difficile* strain used in the experiments by Lyras *et al.* (649-651). Overall, these studies highlighted the importance of the glucosyltransferases toxins A and B in their contribution to virulence in animals.

On the other hand, the LT from *C. sordellii* and the α-toxin from *C. novyii*, appear to be involved in gas gangrene (652). LT modifies Rac and Cdc42 but not Rho from the Rho GTPase subfamily as well as Ras, Ral and Rap from the Ras GTPase subfamily using UDP-Glc as the sugar donor (653-655). For example, mono-*O*-glucosylation of HA-tagged Ras by LT at threonine-35 (Thr^{35}) locks Ras in the inactive GDP-bound form, inhibiting its binding to the Raf kinase and blocking the Ras downstream signalling (656). *C. novyii* α-toxin was found to selectively use UDP-GlcNAc as the

sugar donor and to transfer the GlcNAc moiety to Thr^{37} of Rho or Thr^{35} of Rac and Cdc42 (644).

Members of the genus *Legionella* are fastidious Gram-negative rod-shaped bacteria that can reside in a phagosome within host cells such as alveolar macrophages. The bacteria remain independent of the classical endolysosomal pathway using a type IV secretion system (T4SS) (657, 658) to release effector proteins into host cells that interfere with cellular functions (659, 660). Amongst the *Legionella* effectors released are the glucosyltransferases Lgt1, Lgt2 and Lgt3, which have been shown to be highly effective virulence factors (661-664). The species *Legionella pneumophila* is the major cause of a severe pneumonia in humans, called Legionnaire's disease. While *L. pneumophila* strain Philadelphia-1 possesses all three Lgt enzymes, other strains possess only Lgt1 and Lgt3 (661, 663). Additionally, Lgt1 and Lgt2 are produced predominantly in the stationary phase of *in vitro* bacterial growth as well as during replication within the natural amoeba host *Acanthamoeba castellanii*, when the bacteria become remarkably virulent (663). This is in contrast to Lgt3, which is produced in the lag phase prior to the start of intracellular bacterial replication (663). However, all three glycosyltransferases transfer glucose from UDP-Glc to serine-53 (S53) of mammalian elongation factor 1A (eEF1A) (663). eEF1A plays a vital role in ribosome-dependent protein synthesis (665) by assisting recruitment of aminoacylated tRNA to the A-site of mRNA-charged ribosomes (666). eEF1A also aids folding of newly synthesised proteins and the proteasomal degradation of misfolded proteins (667, 668) as well as apoptosis (669, 670). The addition of glucose to S35 of eEF1A inhibits protein synthesis, demonstrated by both *in vitro* transcription/translation studies and ^{35}S-methionine incorporation assays in mammalian cells grown in methionine-free medium in the presence of the Lgt enzymes (662, 663). The inhibition of protein synthesis leads to host cell death. Furthermore, several residues of the Lgt enzymes involved in the binding of the UDP-Glc sugar donor and the eEF1A acceptor substrate were identified and found to have a role in virulence in microinjection studies (664). HeLa cells microinjected with wild type Lgt1 displayed

morphological traits of apoptosis whereas those microinjected with the GST control or a catalytically inactive DxD Lgt1 mutant did not (664). However, it is still not clear why *L. pneumophila* injects three proteins with similar enzymatic function and localisation into host cells.

The two aforementioned groups of bacterial glycosyltransferases modify mammalian proteins inside host cells and block cell signaling pathways or the protein machinery. Bacterial glycosyltransferases that catalyse the addition of a carbohydrate moiety to targets other than proteins have also been studied. For example, the galactosyltransferase LgtC from *Neisseria meningitidis* catalyses the transfer of galactose from UDP-Gal to a terminal lactose of its lipooligosaccharide structure (626).

While the previous chapter has enabled the mapping of potential functional regions of NleB1, the experiments performed to identify these regions were mostly performed by ectopic expression of NleB1 and its mutants. This chapter aims to determine if the NleB1 mutants of interest from chapter 3 were translocated by the T3SS machinery of EPEC into mammalian cells when expressed in EPEC and if they maintained their function during EPEC infection. Additionally, the role of these mutations *in vivo* is addressed in this chapter, using the *Citrobacter rodentium* mouse model of A/E pathogen infection.

4.2 Results

4.2.1 NleB1 and NleB1 mutants are expressed in EPEC

When ectopically expressed in mammalian cells, the site-directed mutants $NleB1_{PILN(63-66)AAAA}$, $NleB1_{Y219A}$, $NleB1_{PDG(236-238)AAA}$ and $NleB1_{E253A}$, were unable to catalyse the GlcNAcylation of FADD *in vitro*. To study the effect of these mutations on NleB1 function during EPEC infection, we first decided to test the expression of NleB1 and the NleB1 mutants fused to a C-terminal β-lactamase TEM-1 reporter in EPEC and their translocation in EPEC infected HeLa cells. EPEC has 2 homologues of NleB termed NleB1 and NleB2 (161). NleB1 and NleB2 share 84% similarity and 61% identity. While only NleB1 has been shown to be involved in the inhibition of host cell apoptosis, both NleB1 and NleB2 are known T3SS effectors (381, 671, 672) and will be used as controls in subsequent translocation assays.

A translational fusion of NleB1 to the β-lactamase TEM-1 was generated using the vector pCX340 and introduced in wild type EPEC E2348/69, the isogenic Δ*nleB1* derivative and the T3SS mutant, Δ*escN*. Expression of NleB1 was detected by immunoblot using anti-β-lactamase TEM-1 and anti-NleB1 antibodies. The NleB1-TEM-1 fusion was predicted to be approximately 62 kDa in size. A band slightly above 28 kDa, corresponding to β-lactamase TEM-1 only, was observed with bacterial cell pellets from cultures of Δ*nleB1*, Δ*escN* and wild type EPEC E2348/69 carrying pCX340 on the immunoblots probed with anti-β-lactamase (Figure 4.1A-B). However, no endogenous NleB1 was observed from cultures of Δ*escN* and wild type EPEC E2348/69 carrying pCX340 on the immunoblot probed with anti-NleB1 (Figure 4.1A-B), presumably due to the *in vitro* culture conditions used. On the immunoblots probed with anti-β-lactamase TEM-1 antibodies as well as those probed with the anti-NleB1 antibodies, three distinct bands ranging from approximately just above 49 and 62 kDa were observed from cultures of Δ*nleB1*, Δ*escN* and wild type EPEC carrying pTEM-NleB1, indicating the presence of the NleB1 β-lactamase TEM-1 fusion protein as well as possible degradation products of NleB1-TEM-1 in all 3 EPEC strains (Figure 4.1A-B).

Similarly, translational fusions of NleB2 and NleB1 mutant derivatives were generated using pCX340. The expression of the NleB2 protein in wild type EPEC E2348/69 and the T3SS mutant, Δ*escN*, as well as expression of the NleB1 mutant proteins from bacterial cultures of Δ*nleB1* and Δ*escN* carrying the pTEM constructs were tested by immunoblotting of the bacterial cell pellets with anti-β-lactamase TEM-1 and anti-NleB1 antibodies. When overexpressed from the pTEM contructs, NleB2 was detected in both wild type and Δ*escN* on the immunoblot probed with anti-β-lactamase TEM-1 antibodies (Figure 4.1B). However, the NleB2 β-lactamase TEM-1 fusion could not be recognised efficiently with the anti-NleB1 antibodies. Additionally, all 4 NleB1 mutant proteins were expressed in the Δ*nleB1* strain overexpressing the NleB1 fusion proteins as shown in Figure 4.1 C and D.

4.2.2 NleB1$_{Y219A}$ and NleB1$_{E253A}$ are translocated into HeLa cells by EPEC

Since E2348/69 Δ*nleB1* complemented with wild type *nleB1* or its derivative mutants will be used during *in vitro* infection to test for NleB1 mutants that have lost the ability to inhibit caspase-8 activation, the translocation of NleB1 was first checked and compared in both wild type EPEC and Δ*nleB1* expressing NleB1-TEM-1. Translocation was detected in living host cells by first infecting HeLa cells with EPEC derivatives expressing the NleB1-TEM-1 fusion proteins. HeLa cells were then loaded with the CCF2/AM fluorescent substrate containing 2 fluorophores, coumarin and fluorescein. In the absence of β-lactamase TEM-1, the substrate remains intact and the excitation of the coumarin results in fluorescence energy transfer to the fluorescein moiety and the emission of green light at 520 nm. However, when TEM-1 β-lactamase is present, the CCF2/AM substrate is cleaved separating the fluorophores, thereby disrupting the energy transfer and resulting in a blue fluorescence at 450 nm. Therefore, translocation was detected in HeLa cells by measuring the blue/green (450 nm/520 nm) emission ratio as described previously (673).

A low blue to green emission ratio was observed in cells infected with Δ*nleB1* carrying the empty pCX340 vector as well as in cells infected with wild type EPEC

carrying the same vector (Figure 4.2A), indicating that the β-lactamase TEM-1 on its own is not translocated in HeLa cells. A similar emission ratio was seen in cells infected with Δ*escN* expressing only the β-lactamase TEM-1 (Figure 4.2A). However, the emission ratio increased significantly when the cells were infected with either wild type EPEC E2348/69 or Δ*nleB1* expressing the NleB1-TEM-1 fusion, indicating that NleB1 was efficiently translocated by both EPEC strains (Figure 4.2A). In contrast, no increase in the emission ratio was observed for the NleB1 fusion expressed in Δ*escN*, confirming that the translocation of NleB1 was dependent on a functional T3SS (Figure 4.2A). A significantly higher emission ratio was observed when cells were infected with wild type EPEC expressing NleB2-TEM1 compared to the ratio seen in cells infected with Δ*escN* expressing the same fusion protein (Figure 4.2B), confirming previous reports that NleB2 is translocated via the T3SS (672).

Translocation of the NleB1 mutants by E2348/69 Δ*nleB1* into infected HeLa cells was also tested. No significant difference in the emission ratio was observed in cells infected with Δ*nleB1* expressing NleB1$_{PDG(236\text{-}238))AAA}$-TEM-1 compared to the ratio seen in cells infected with Δ*escN* expressing NleB1$_{PDG(236\text{-}238))AAA}$-TEM-1 or in cells infected with Δ*nleB1* carrying the empty pCX340 vector (Figure 4.3), suggesting that this NleB1 mutant was not translocated in HeLa cells. Similar results were observed for the NleB1$_{PILN(63\text{-}66)AAAA}$-TEM-1 (Figure 4.3), suggesting that it was also not translocated in HeLa cells. The emission ratio was significantly higher in cells infected with Δ*nleB1* expressing the NleB1$_{Y219A}$-TEM-1 compared to the ratio in cells infected with Δ*nleB1* expressing TEM-1 only or in cells infected with Δ*escN* expressing the NleB1$_{Y219A}$-TEM-1 (Figure 4.3). This confirmed that NleB1$_{Y219A}$ was translocated by the T3SS. The same observation was seen for the NleB1$_{E253A}$ mutant (Figure 4.3), indicating that this mutant was also translocated via the T3SS.

4.2.3 Mutations at positions 236-238 in NleB1 inhibit translocation into HeLa cells

NleB1$_{PDG(236-238)AAA}$ was not translocated in HeLa cells. Therefore, we hypothesised that mutation of the amino acids proline-236 (P236), aspartate-237 (D237) and glycine-238 (G238) to alanine, which has a non polar side chain rendered NleB1 more hydrophobic and thus led to the formation of improperly folded proteins. This may result in the inhibition of NleB1 translocation by the T3SS of EPEC, which generally accepts unfolded proteins (674, 675). The amino acids proline (P), asparate (D) or glycine (G) at positions 236-238 were therefore mutated to different combinations of amino acids, including amino acids which have electrically charged side chains such as glutamate (E), lysine (K), arginine (R) and amino acids with polar side chains such as serine (S) in an attempt to make the protein more soluble.

The following NleB1 mutants, NleB1$_{PDG(236-238)AEA}$, NleB1$_{PDG(236-238)AKA}$, NleB1$_{PD(236-237)AR}$, NleB1$_{PDG(236-238)SRS}$, NleB1$_{PDG(236-238)SES}$, NleB1$_{PD(236-237)SE}$, were obtained by site-directed mutagenesis and tested for their ability to GlcNAcylate FADD. GFP-NleB1 and the derivative mutants were ectopically expressed individually in HEK293T cells along with FLAG-FADD and the cells were lysed. Immunoprecipitated FLAG-FADD was examined for GlcNAcylation and binding to the GFP-tagged NleB1 mutants by immunoblot using anti-GlcNAc and anti-GFP antibodies respectively. FLAG-FADD was GlcNAcylated in the presence of GFP-NleB1 (Figure 4.4). A similar level of FADD GlcNAcylation was observed in the presence of GFP-NleB1$_{PD(236-237)AR}$ and GFP-NleB1$_{PD(236-237)SE}$ and a reduced level of FADD GlcNAcylation was observed in the presence of GFP-NleB1$_{PDG(236-237)AEA}$ and GFP-NleB1$_{PDG(236-238)SES}$ (Figure 4.4). No GlcNAcylation of FLAG-FADD was observed when co-expressed with GFP-NleB1$_{PDG(236-238)AKA}$, GFP-NleB1$_{PDG(236-238)SRS}$ and GFP-NleB1$_{PDG(236-238)SES}$ (Figure 4.4).

Since we were interested in NleB1 loss of function mutants, we tested the expression of NleB1$_{PDG(236-238)AEA}$, NleB1$_{PDG(236-238)AKA}$, NleB1$_{PDG(236-238)SRS}$ and NleB1$_{PDG(236-}$

$_{238)SES}$ in EPEC and their translocation in HeLa cells. All 4 NleB1 mutants fused to β-lactamase TEM-1 were expressed in both Δ*nleB1* (Figure 4.5A-B) and Δ*escN* (data not shown). However, when the mutants were tested in the β-lactamase translocation assay, there was no significant difference in the blue to green emission ratio observed in cells infected with Δ*nleB1* expressing the mutant NleB1-TEM-1 fusions compared to Δ*escN* expressing the mutant NleB1 fusions (Figure 4.5C). There was also no significant difference compared to Δ*nleB1* expressing TEM-1 only (Figure 4.5C). This suggested that none of the new mutants were translocated in HeLa cells. In summary, only mutations Y219A and E253A abrogated the function of NleB1 while still allowing NleB1 translocation in host cells (Table 4.1).

4.2.4 Conservation of tyrosine-219 (Y219) in glycosyltransferases from *Clostridium*, *Legionella* and *Photorhabdus* species

Although NleB1 shares little homology with proteins of known function at the primary amino acid sequence, NleB1 was first proposed to be a glycosyltransferase by *in silico* fold recognition (442). Here we compared the NleB1 amino acid sequence with empirically established three-dimensional structures using FUGUE (676). FUGUE identified NleB1 as an unambiguous structural homologue of the *Photorhabdus asymbiotica* protein toxin (PaTox) (FUGUE Z-score of 4.43, 95% confidence). In addition to causing disease in insects, *P. asymbiotica* is an emerging human pathogen (677). PaTox was recently identified as a glycosyltransferase targeting eukaryotic Rho GTPases, thereby inhibiting Rho activation and causing host cell death (678). When the region around the catalytic site of PaTox was compared to that of glycosylating toxins from *Clostridium* species and *L. pneumophila*, several residues around the DxD triad were conserved (678). Hence we compared the catalytic region of NleB1 to that of PaTox, *L. pneumophila* glucosyltransferase 1 (Lgt1), α-toxin of *Clostridium novyi*, LT of *Clostridium sordellii* and toxins A and B of *Clostridium difficile* using the MUSCLE alignment tool (570). This showed a number of conserved amino acids including the DxD motif and the tyrosine residue

equivalent to Y219 of NleB1, suggesting the importance of Y219 in the enzymatic function of NleB1 (Figure 4.6).

4.2.5 Testing NleB1 mutants for FADD, TRADD and RIPK1 death domain (DD) binding by a yeast two-hybrid system

In an initial yeast two-hybrid screen (Y2HS) to identify host cell binding partners of NleB1, the DD-containing proteins FADD and RIPK1 were identified several times. Transformation into a different yeast strain, PJ69-4A, confirmed the interactions and in addition revealed that the DD of FADD and RIPK1 were essential for mediating the interaction with NleB1 (401). Further studies using co-immunoprecipitation confirmed the above interactions as well as the interaction of NleB1 with the DD of TRADD (401, 441). Therefore, we tested the interaction between $NleB1_{Y219A}$ and $NleB1_{E253A}$ and the DD of FADD, TRADD and RIPK1 using the yeast two-hybrid system. *Saccharomyces cerevisiae* strain PJ69-4A is auxotrophic for two nitrogenous bases, adenine and uracil, and 4 amino acids, histidine, leucine, methionine and tryptophan, which are all required for growth on SD plates. The bait and prey plasmids used (pGBKT7 and pGADT7-AD respectively) provide the genes necessary for tryptophan and leucine synthesis respectively. Therefore, addition of the supplements may be omitted when selecting for yeast colonies harbouring one (SD-trp or SD-leu) or both (double drop-out (DDO); SD-trp-leu) of those plasmids. Cloning of genes into the bait plasmid creates a GAL4 DNA binding domain fusion whereas cloning of genes into the prey plasmid creates a GAL4 activation domain fusion. After transformation of the yeast strain PJ69-4A, if a protein interaction occurs between the bait and the prey proteins, the binding domain and the activation domain are brought into close proximity to each other, enabling the activation of four reporter genes, *ADE2*, *HIS3*, *MEL1* and *LacZ*, and growth on quadruple drop-out media (QDO; SD-trp-leu-ade-his). Therefore, yeast colonies which grow on QDO should contain both the bait and prey plasmids whereby there is an interaction between the bait and prey proteins.

The yeast transformation studies confirmed that the DD of FADD, TRADD and RIPK1 are sufficient for binding to NleB1 (Figure 4.7). Furthermore, although $NleB1_{Y219A}$ and $NleB1_{E253A}$ can each still bind to the DD of FADD and RIPK1 as shown by growth of the co-transformed yeast on the QDO plates, they cannot bind to the DD of TRADD (Figure 4.7), suggesting that the residues Y219 and E253A may confer some substrate specificity to the acceptor substrate TRADD. The binding of these 2 NleB1 mutants to the DD of FADD in yeast is consistent with the FLAG IP results (Figure 3.7 from chapter 3). Plasmids expressing NleB1 and its mutants fused to the GAL4-DNA binding domain were each transformed with the empty prey plasmid pGADT7-AD and the yeast plated onto DDO and QDO as controls. Absence of growth on the QDO plates indicates that there is no interaction between NleB1 or the NleB1 mutants with the GAL4-activation domain (Figure 4.7). Additionally, there was no interaction between the GAL4-DNA binding domain and the DD of FADD, TRADD or RIPK1 as shown by absence of growth for yeast co-transformed with the empty bait vector pGBKT7 and prey vectors expressing the DDs (Figure 4.7). Autoactivation by the DDs was also tested by transforming yeast with the prey plasmids and selecting on SD-Leu, triple drop out (TDO or SD-Trp-Leu-His) and QDO. Absence of growth on TDO and QDO (Figure 4.8) shows that the DDs do not autoactivate the reporter genes.

4.2.6 $NleB1_{Y219A}$ and $NleB1_{E253A}$ do not inhibit TNF-induced NF-κB activation to the same extent as NleB1

Previous studies have shown that NleB1 inhibits TNF-induced NF_KB activation (377). However, while NleB1 blocks TNF-induced NF-κB activation, it does not inhibit IL-8 secretion during EPEC infection (401), suggesting that NleB1 prevents NF-κB activation as a consequence of binding to DD proteins such as RIPK1 and TRADD which form part of the TNF signaling pathway. To determine if the single mutations Y219A and E253A affected the ability of NleB1 to block NF-κB activation, a dual luciferase reporter assay was performed in HeLa cells transfected with plasmids

expressing GFP, GFP-NleB1 or GFP-NleB1 mutants together with pNF$_K$B-luc and pRL-TK and stimulated with TNF.

When GFP only was expressed in cells stimulated with TNF, a high luciferase activity was observed, indicating NF-κB activation (Figure 4.9). On the other hand, when GFP-NleB1 was expressed in cells stimulated with TNF, a significant decrease in luciferase activity was noted, indicating that NleB1 inhibits activation of the NF-κB reporter (Figure 4.9A-B). In the presence of GFP-NleB1$_{Y219A}$ or GFP-NleB1$_{E253A}$ and following TNF stimulation, the luciferase activity was significantly reduced when compared to stimulated cells expressing GFP only, although the reduction in luciferase activity was not as marked as in the presence of wild type NleB1 (Figure 4.9A). Furthermore, when the luciferase activity of stimulated cells expressing the NleB1 mutants was individually compared to that of stimulated cells expressing wild type NleB1, a significant difference was observed (Figure 4.9). This indicates that the mutations Y219A and E253A impair the inhibitory activity of NleB1 in TNF-induced NF-κB activation. Other single site directed mutants of NleB1 such as NleB1$_{K81A}$, NleB1$_{D93A}$, NleB1$_{D121A,}$ NleB1$_{D128A}$ and NleB1$_{L157A}$ inhibited NF-κB activation to the same extent as wild type NleB1 following TNF stimulation (Figure 4.9B).

4.2.7 NleB1$_{Y219A}$ and NleB1$_{E253A}$ cannot inhibit caspase-8 activation during EPEC infection

To determine if NleB1$_{Y219A}$ or NleB1$_{E253A}$ delivered by the T3SS blocked caspase-8 cleavage in response to FasL stimulation, HeLa cells were infected with wild type EPEC E2348/69, Δ*nleB1* or Δ*nleB1* complemented with *nleB1*, *nleB1$_{Y219A}$* or *nleB1$_{E253A}$*. As shown previously, wild type EPEC E2348/69 prevented caspase-8 cleavage compared to the Δ*nleB1* mutant (Figure 4.10) (401) whereas complementation of Δ*nleB1* with native *nleB1* restored inhibition of caspase-8 cleavage. None of NleB1$_{DxD(221-223)AxA}$, NleB1$_{Y219A}$ or NleB1$_{E253A}$ were able to inhibit caspase-8 cleavage. The expression of wild type NleB1 or its mutants from the complementation pTrc99A vector was verified by immunoblotting using anti-NleB1

antibodies on cell pellets from IPTG induced bacterial cultures used to infect the HeLa cells (data not shown).

4.2.8 Amino acid residues Y219 and E253A in NleB are crucial for bacterial colonisation and virulence *in vivo*

Infection of mice with the EPEC-like mouse pathogen, *C. rodentium*, is widely used as a small animal model of EPEC infection. NleB from *C. rodentium* is needed for full colonisation of mice (381), and NleB from *C. rodentium* has been shown to to inhibit TNF-induced NF-κB activation to a similar extent as EPEC NleB1 and to GlcNAcylate several death domain proteins including FADD, TRADD and RIPK1 (441). Since the amino acid residues Y219 and E253 are conserved in *C. rodentium* NleB, we investigated whether $NleB_{Y219A}$ and $NleB_{E253A}$ could complement the function of NleB *in vivo*. Wild type C57BL/6 mice were inoculated orally with one of wild type *C. rodentium* carrying pACYC184, the isogenic Δ*nleB* mutant carrying pACYC184 or Δ*nleB* carrying pACYC184 encoding wild type *C. rodentium nleB,* $nleB_{Y219A}$ or $nleB_{E253A}$. Faecal samples were collected on days 2, 7, 10, 12 and 14 and the number of viable bacteria (CFU) per gram of faeces was determined. No differences in *C. rodentium* faecal CFU were observed between the 5 groups of mice on day 2 following infection (Figure 5A). However, on days 7, 10 and 12 colonisation by the Δ*nleB* carrying pACYC184 was significantly lower than wild type *C. rodentium* carrying pACYC184 or Δ*nleB* complemented with wild type *nleB* (Figure 4.11A). This is consistent with previous findings showing that NleB is required for virulence in mice (381, 401). Neither $nleB_{Y219A}$ nor $nleB_{E253A}$ were able to restore colonisation to Δ*nleB* indicating that these amino acids were essential for the virulence function of NleB *in vivo* (Figure 4.11A).

To ensure that the lower levels of colonisation of Δ*nleB* carrying pACYC184 encoding $nleB_{Y219A}$ or $nleB_{E253A}$ were not due to Δ*nleB* losing the complementation vectors, faecal samples were collected from each group and plated on Luria agar containing nalidixic acid and chloramphenicol (Nal/Cm) (selecting for *C. rodentium*

and pACYC184) or Nal only (selecting for *C. rodentium*) on day 10 after infection. No differences were observed in the number of faecal CFU from each group indicating that carriage of the pACYC184 plasmid derivatives was stable (Figure 4.11B).

While the faecal samples were collected on days 2, 7, 10, 12 and 14, mice were weighed every second day. During the course of the experiment, the mice did not lose more than 5% of their initial body weight and the weight change gradually increased (Figure 4.11C).

4.2.9 Testing the ability of EPEC NleB1, EPEC NleB2 and EHEC NleB1 to complement *C. rodentium* Δ*nleB* colonisation in mice

While NleB2 was not found to contribute to the inhibition of host cell death (401), its role in virulence has not been determined to date. *C. rodentium* has only one copy of NleB, which shares higher amino acid identity to NleB1 from EPEC (441). This has made it difficult to determine the role of NleB2 *in vivo*. *C. rodentium* NleB, EPEC NleB1 and NleB2 and EHEC NleB1 share a minimum percentage identity of 60% and a maximum percentage identity of 98% among each other, the highest percentage identity being shared between EPEC NleB1 and EHEC NleB1. To investigate the ability of NleB homologues from A/E pathogens to complement the *C. rodentium* Δ*nleB* mutant, the genes encoding these homologues were expressed under the control of the constitutive Tet promoter of pACYC184 behind a common ribosome binding site in the *C. rodentium* Δ*nleB* isogenic mutant.

Wild type C57BL/6 mice were orally inoculated with one of wild type *C. rodentium* carrying pACYC184, the isogenic Δ*nleB* mutant carrying pACYC184, Δ*nleB* mutant carrying pACYC84 encoding wild type *C. rodentium nleB* ($nleB_{CR}$,), EPEC E2348/69 *nleB1* ($nleB1_{EPEC}$), EPEC E2348/69 *nleB2* ($nleB2_{EPEC}$) or EHEC EDL933 *nleB1* ($nleB1_{EHEC}$). Faecal samples were collected on days 2, 6, 8, 10, 12 and 14 and the number of viable bacteria per gram of faeces was determined. No significant

differences in the viable counts were observed amongst the 6 groups of mice during the early stage of infection (day 2) (Figure 4.12A), indicating that the 6 strains were equally able to colonise the intestine of mice on day 2 post infection. However, on days 6, 8, 10, 12 and 14 following oral gavage, colonisation by *C. rodentium* Δ*nleB* carrying pACYC184 was significantly lower than wild type *C. rodentium* carrying pACYC184 or Δ*nleB* complemented with *C. rodentium nleB* (Figure 4.12A). This confirmed that *C. rodentium* NleB is essential for colonisation of the gut and virulence in mice. However, there was a significant difference in faecal CFU between each of the groups of mice infected with the *C. rodentium* Δ*nleB* expressing the NleB homologues and the group of mice infected with wild type *C. rodentium*. During the course of the experiment, the mice did not lose more than 5% of their initial body weight and steadily gained weight (Figure 4.12B). This indicated that none of NleB1 and NleB2 from EPEC or NleB1 from EHEC O157:H7 could complement the *C. rodentium* Δ*nleB* mutant.

4.3 Discussion

EPEC uses the T3SS effector NleB1 to inhibit extrinsic death receptor signalling and subsequent host cell apoptosis both *in vitro* and *in vivo* (401, 441). FADD GlcNAcylation, which is required for the inhibition of apoptosis, was abrogated in the presence of $NleB1_{PILN(63\text{-}66)AAAA}$, $NleB1_{Y219A}$ and $NleB1_{E253A}$ or significantly reduced in the presence of $NleB1_{PDG(236\text{-}238)AAA}$ *in vitro*. The work in this chapter focused on the contribution of selected regions of NleB1 to its enzymatic activity during EPEC infection *in vitro* and *C. rodentium* virulence *in vivo*. First, we sought to test the expression of these NleB1 mutants in EPEC, their translocation via the T3SS and whether they lost the ability to inhibit host cell apoptosis during EPEC infection.

The expression of selected NleB1 mutants from the previous chapter and their translocation in HeLa cells by Δ*nleB1* were tested. While all 4 mutants were expressed in EPEC, only $NleB1_{Y219A}$ and $NleB1_{E253A}$ were translocated by the T3SS. A possible reason for $NleB1_{PILN(63\text{-}66)AAAA}$ not being translocated by the T3SS is that the 4 mutated residues found within the first 100 amino acids at the N-terminus of the protein were vital for the secretion of NleB1 by the T3SS. While T3SS effectors do not have a consensus secretion signal sequence, the first 15-20 amino acids in the N-terminus are known to be required for secretion (612, 613) and a downstream region of 50-100 amino acids is responsible for binding to chaperones prior to translocation (614, 615, 679-683). Numerous studies have suggested that T3SS effectors require a chaperone to guide them to the T3SS machinery in an unfolded state (674, 675).

The absence of translocation of $NleB1_{PDG(236\text{-}238)AAA}$ via the T3SS is less likely to be due to the residues $PDG^{236\text{-}238}$ being involved in the T3SS chaperone binding region. It is possible that the mutation of these residues to alanine affects the folding and solubility of the protein, preventing it from being maintained in an unfolded state prior to secretion via the T3SS. In fact, recombinant GST-$NleB1_{PILN(63\text{-}66)AAAA}$ and GST-$NleB1_{PDG(236\text{-}238)AAA}$ were mostly observed in the insoluble fractions rather than in purified elutions. When the $PDG^{236\text{-}238}$ motif was mutated to new combinations of

amino acids with diverse chemical properties, namely like or unlike chemical properties, the resulting NleB1 mutants, $NleB1_{PDG(236-238)AKA}$, $NleB1_{PDG(236-238)SRS}$ and $NleB1_{PDG(236-238)SES}$ were unable to GlcNAcylate FADD and $NleB1_{PDG(236-238)AEA}$ showed only slight GlcNAcylation of FADD *in vitro*. All 4 NleB1 mutants were expressed in the Δ*nleB1* and Δ*escN* EPEC strains although none were translocated in HeLa cells, further highlighting importance of the $PDG^{236-238}$ region integrity in secretion by the T3SS.

In light of the β-lactamase translocation assay results, only two of the four selected NleB1 mutant proteins ($NleB1_{Y219A}$ and $NleB1_{E253A}$) were chosen for further investigation due to the fact that they were translocated during EPEC infection and that the mutations inhibit the enzymatic activity of NleB1 *in vitro*. Interestingly Y219 was conserved in the glycosyltransferases from *Clostridium* and *Legionella* and in the recently characterised PaTox glycosyltransferase from *Photorhabdus asymbiotica*. Furthermore, this conserved tyrosine residue (Y284) in *C. difficile* toxin B, located just upstream of the DxD motif, is necessary for glycosyltransferase activity (607). The crystal structure of the catalytic region of *C. difficile* toxin B combined with mutagenesis and enzyme kinetics studies have revealed that mutation of Y284 to alanine significantly reduced the enzymatic activity of toxin B and inhibited its cytotoxic effect (605, 607). However, it was also shown that the strong reduction in enzyme activity of the Y284A toxin B mutant could not be explained by an impaired sugar donor substrate interaction via the 2'-hydroxyl group of the ribose moiety of the sugar donor. The infeasibility of this hypothesis was demonstrated by measuring the distance between the hydroxyl group of Y284 and that of the ribose as well as kinetic assay results (607). It has been postulated that Y284A could potentially have a vital role in the positioning of D286 of the DxD motif for its interaction with the metal cation, Mn^{2+}, required for the catalytic reaction to occur (607). Despite Y284A of toxin B not interacting with the sugar donor, it remains a possibility that Y219 in NleB1 could interact with the UDP-GlcNAc by hydrophobic π-stacking interactions as is the case with numerous aromatic side chain-containing amino acids (606, 678,

684). However, Y219 in NleB1 could also interact with UDP-GlcNAc via hydrogen bonds as the equivalent tyrosine of *C. difficile* toxin A (Y283) is positioned in close proximity to two carbonyls of the ribose ring and a water molecule (685, 686).

The crystal structure of NleB1 with UDP-GlcNAc will help elucidate the role of Y219 in binding the donor sugar. Alternatively, a UDP-GlcNAc hydrolysis assay could also be performed to determine if Y219 binds the sugar donor. Glycosyltransferases usually hydrolyse the sugar donor in the absence of the acceptor substrate (621, 687-691). Provided NleB1 hydrolyses UDP-GlcNAc in the absence of FADD, NleB1 and $NleB1_{Y219A}$ could be tested for their ability to bind and hydrolyse UDP-GlcNAc. A UDP-GlcNAc binding assay could also be developed perhaps using isothermal titration calorimetry (ITC). ITC has been used successfully in characterising the binding affinity of ligands for proteins (692-694). UDP-GlcNAc could be titrated into a sample cell containing NleB1 or $NleB1_{Y219A}$ and the heat change during the titrations would be recorded and compared.

Translocated $NleB1_{Y219A}$ and $NleB1_{E253A}$ were unable to inhibit caspase-8 activation, further validating the *in vitro* GlcNAcylation results in chapter 3. Additionally, *C. rodentium* strains expressing $NleB_{Y219A}$ and $NleB_{E253A}$ showed significantly reduced intestinal colonisation compared to *C. rodentium* expressing wild type NleB.

Previously, both *C. rodentium* NleB and EPEC NleB1 were shown to complement *C. rodentium* Δ*nleB* colonisation to wild type levels in mice (441). Therefore, we extended this complementation study to NleB1 and NleB2 of EPEC and NleB1 of EHEC. However, in this study, only *C. rodentium* NleB was able to restore intestinal bacterial colonisation to a similar level to wild type *C. rodentium*. One possible explanation to account for the lack of the complementation ability by EPEC NleB1, unlike what was previously observed by Li *et al.*, is that full length EPEC *nleB1* was constitutively expressed in our complementation studies. Importantly, a chimeric version of EPEC NleB1 constructed by fusing 42 residues of the N-terminal end of *C.*

rodentium NleB to EPEC NleB1 behind the promoter of *C. rodentium* NleB was used by Li *et al.* (441). This suggests that *C. rodentium* could not secrete EPEC NleB1 via the T3SS, highlighting the complexity and fidelity of the T3SS signal sequence to its translocation machinery. The same reasoning could apply to the lack of the complementation ability of EPEC NleB2 or EHEC NleB1. Chimeric versions of EPEC NleB1 and its homologous proteins should be constructed and tested in mice to verify whether they can restore intestinal colonisation in this model.

In this chapter, we showed that mutation of the 4 selected NleB1 regions, PILN(63-66), PDG(236-238), Y219, E253 impaired NleB1 enzymatic activity *in vitro*. However only 2 were translocated via the T3SS during EPEC infection. These 2 mutations in NleB1, Y219A and E253A, abrogated NleB1 inhibition of caspase-8 activation *in vitro*, a step downstream of FADD GlcNAcylation. Furthermore, *C. rodentium* expressing $NleB_{Y219A}$ and $NleB_{E253A}$, were attenuated for virulence *in vivo*, confirming the importance of the GlcNAc transferase activity of NleB in intestinal colonisation and virulence in mice.

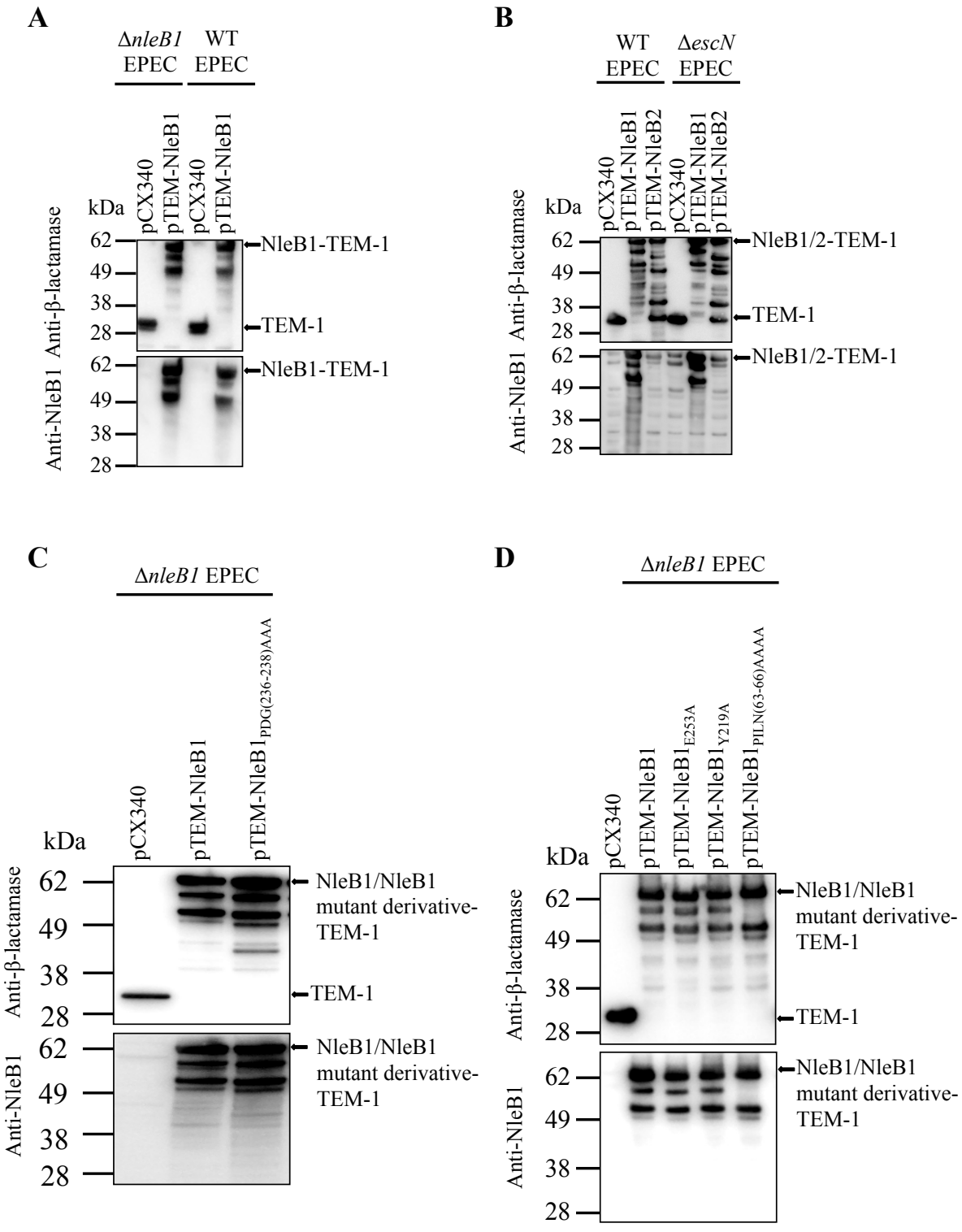
A
ΔnleB1 EPEC
WT EPEC
pCX340
pTEM-NleB1
pCX340
pTEM-NleB1
kDa
62
49
38
28
Anti-β-lactamase
NleB1-TEM-1
TEM-1
Anti-NleB1
62
49
38
28
NleB1-TEM-1
B
WT EPEC
ΔescN EPEC
pCX340
pTEM-NleB1
pTEM-NleB2
pCX340
pTEM-NleB1
pTEM-NleB2
kDa
62
49
38
28
Anti-β-lactamase
NleB1/2-TEM-1
TEM-1
Anti-NleB1
62
49
38
28
NleB1/2-TEM-1
C
ΔnleB1 EPEC
pCX340
pTEM-NleB1
pTEM-NleB1PDG(236-238)AAA
kDa
62
49
38
28
Anti-β-lactamase
NleB1/NleB1 mutant derivative-TEM-1
TEM-1
Anti-NleB1
62
49
38
28
NleB1/NleB1 mutant derivative-TEM-1
D
ΔnleB1 EPEC
pCX340
pTEM-NleB1
pTEM-NleB1E253A
pTEM-NleB1Y219A
pTEM-NleB1PILN(63-66)AAAA
kDa
62
49
38
28
Anti-β-lactamase
NleB1/NleB1 mutant derivative-TEM-1
TEM-1
Anti-NleB1
62
49
38
28
NleB1/NleB1 mutant derivative-TEM-1

Figure 4.1. Expression of NleB1 or mutant derivatives and NleB2 TEM-1 fusions in EPEC E2348/69. (A-B) Analysis of whole cell lysates reveals comparable expression levels of the NleB1-TEM-1 fusion in wild type EPEC E2348/69 and its derivative Δ*nleB1* and Δ*escN* strains and NleB2-TEM-1 fusion in EPEC E2348/69 and its derivative Δ*escN* strain. (C-D) NleB1 mutants fused to TEM-1 are expressed in the Δ*nleB1* EPEC strain. Representative immunoblot of three independent experiments.

A

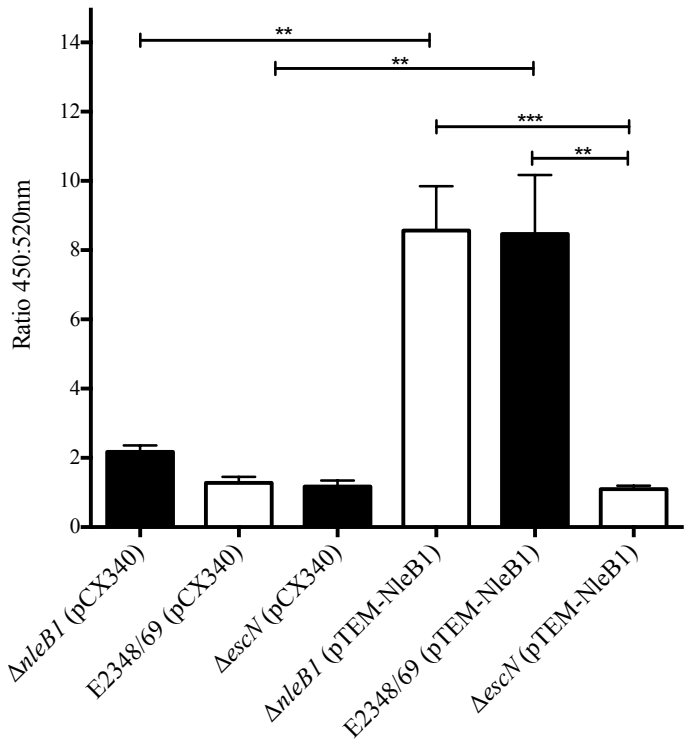
**
**
***
**
Ratio 450:520nm
0
2
4
6
8
10
12
14
ΔnleB1 (pCX340)
E2348/69 (pCX340)
ΔescN (pCX340)
ΔnleB1 (pTEM-NleB1)
E2348/69 (pTEM-NleB1)
ΔescN (pTEM-NleB1)

B

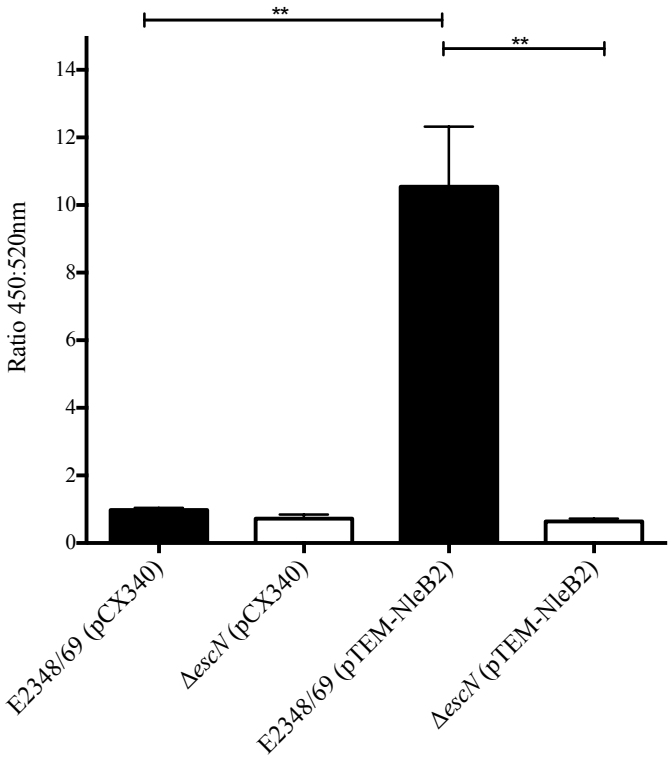
**
**
Ratio 450:520nm
0
2
4
6
8
10
12
14
E2348/69 (pCX340)
ΔescN (pCX340)
E2348/69 (pTEM-NleB2)
ΔescN (pTEM-NleB2)

Figure 4.2. Translocation of NleB1 and NleB2 derivatives by EPEC. (A) Blue/green fluorescence ratio for NleB1-TEM-1 translocation by EPEC E2348/69 and its derivative Δ*nleB1* strain. Cells were infected with EPEC derivatives for 2 h. Results are the mean ± SEM of at least three independent experiments carried out in triplicate. ***Significant difference (*p<0.01, p<0.001, p<0.0001), one way ANOVA with Tukey's multiple comparisons test) (B) Blue/green fluorescence ratio for NleB2-TEM-1 translocation by EPEC E2348/69. Cells were infected with EPEC derivatives for 2 h. Results are the mean ± SEM of at least two independent experiments carried out in triplicate. ***Significant difference (*p<0.01, p<0.001, p<0.0001), one way ANOVA with Tukey's multiple comparisons test)

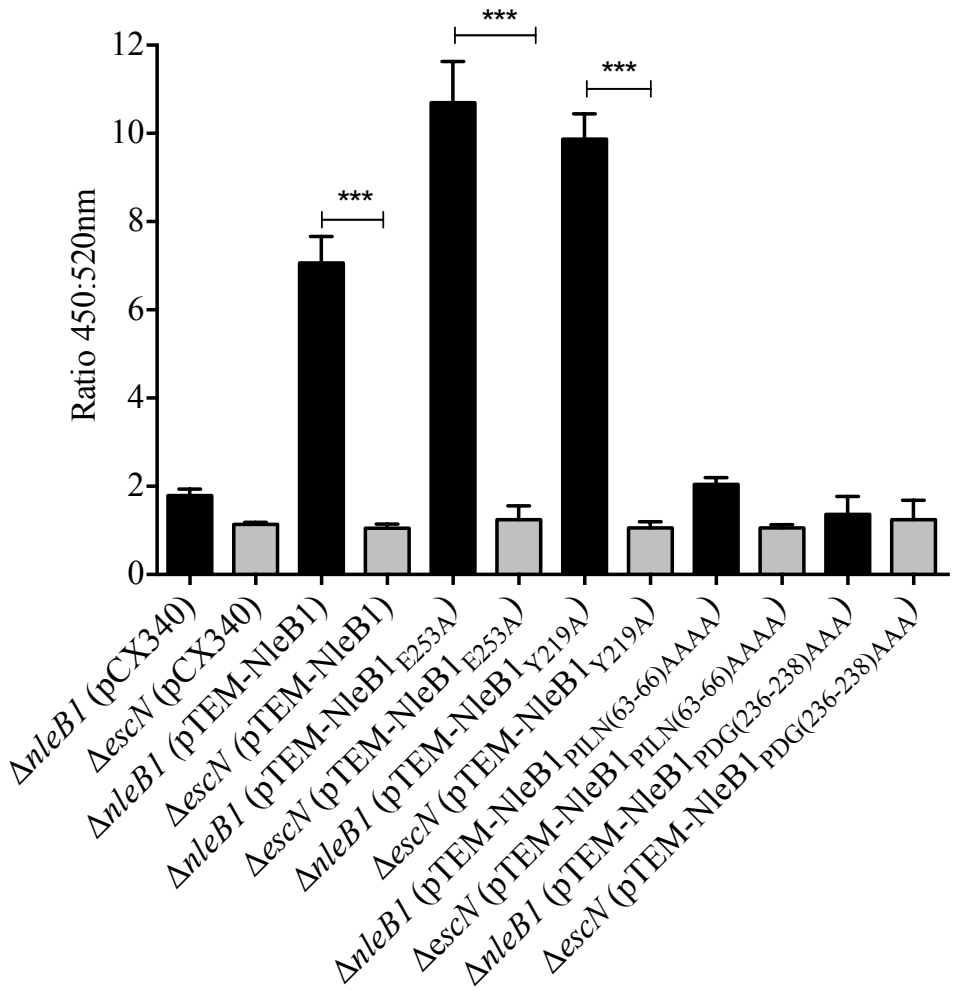

Figure 4.3 Translocation of NleB1 mutants from EPEC. $NleB1_{Y219A}$ and $NleB1_{E253A}$, but not $NleB1_{PILN(63-66)AAAA}$-TEM-1 and $NleB1_{PDG(236-238)AAA}$-TEM-1 fusions, were translocated from the EPEC Δ*nleB1* isogenic mutant. HeLa cells were infected with EPEC derivatives for 2 h. Results are the mean ± SEM of three independent experiments carried out in triplicate. ***Significant difference (*p<0.01, **p<0.001, ***p<0.0001), one way ANOVA with Tukey's multiple comparisons test)

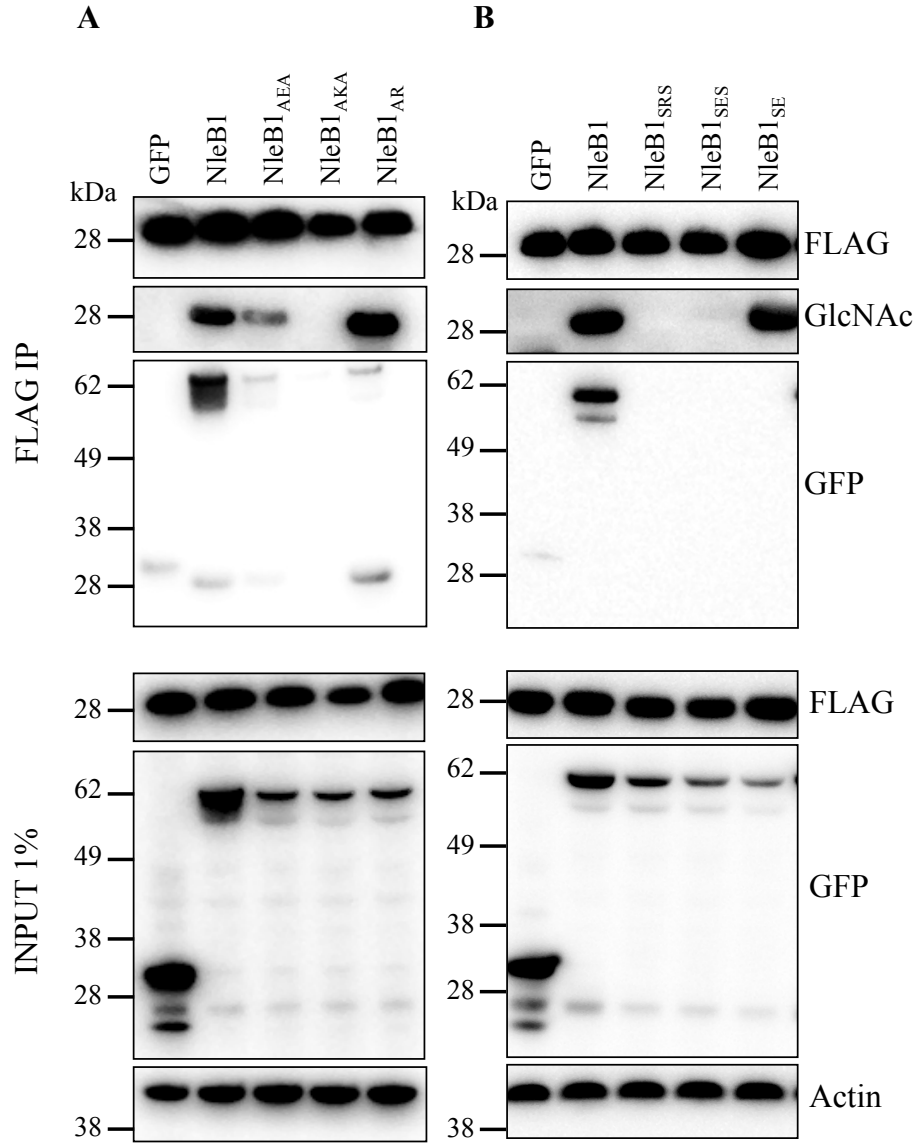

Figure 4.4. Investigation of the effect of NleB1 proteins with mutations at residues 236-238 on the GlcNAcylation of and binding to FADD. (A-B) Immunoblots of inputs and immunoprecipitates (IP) of anti-FLAG immunoprecipitations performed on lysates of HEK293T cells co-transfected with pFLAG-FADD and pEGFP-C2 or pEGFP-C2-NleB1 or pEGFP-C2-NleB1 mutants (mutations of $PDG^{236-238}$ to AKA, AEA, SRS, SES or $PD^{236-237}$ to AR or SE). Antibodies to β-actin were used as a loading control. Representative immunoblot from at least three independent experiments.

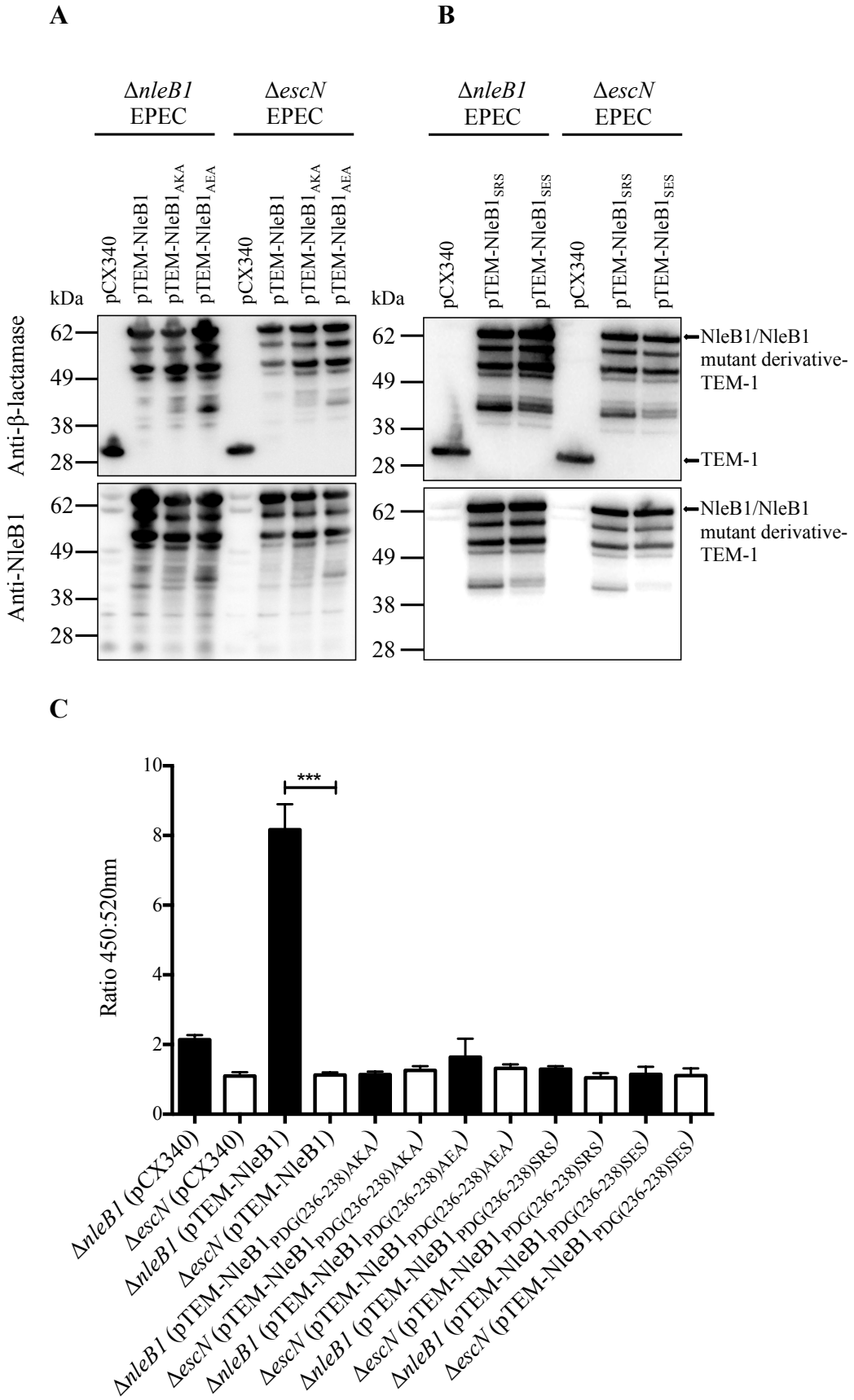
A
B
ΔnleB1 EPEC
ΔescN EPEC
pCX340
pTEM-NleB1
pTEM-NleB1AKA
pTEM-NleB1AEA
pTEM-NleB1SRS
pTEM-NleB1SES
kDa
62
49
38
28
Anti-β-lactamase
Anti-NleB1
NleB1/NleB1 mutant derivative-TEM-1
TEM-1
C
Ratio 450:520nm
***
ΔnleB1 (pCX340)
ΔescN (pCX340)
ΔnleB1 (pTEM-NleB1)
ΔescN (pTEM-NleB1)
ΔnleB1 (pTEM-NleB1PDG(236-238)AKA)
ΔescN (pTEM-NleB1PDG(236-238)AKA)
ΔnleB1 (pTEM-NleB1PDG(236-238)AEA)
ΔescN (pTEM-NleB1PDG(236-238)AEA)
ΔnleB1 (pTEM-NleB1PDG(236-238)SRS)
ΔescN (pTEM-NleB1PDG(236-238)SRS)
ΔnleB1 (pTEM-NleB1PDG(236-238)SES)
ΔescN (pTEM-NleB1PDG(236-238)SES)

Figure 4.5. Expression and translocation of NleB1 mutants with mutations at residues 236-238 from EPEC. (A-B) Expression of NleB1$_{PDG(236-238)AKA}$, NleB1$_{PDG(236-238)AEA}$, NleB1$_{PDG(236-238)SRS}$ and NleB1$_{PDG(236-238)SES}$-TEM-1 fusions in the Δ*nleB1* and Δ*escN* EPEC strains. Representative immunoblot from at least three independent experiments. (C) NleB1$_{PDG(236-238)AKA}$, NleB1$_{PDG(236-238)AEA}$, NleB1$_{PDG(236-238)SRS}$ and NleB1$_{PDG(236-238)SES}$ are not translocated from the Δ*nleB1* EPEC strain. HeLa cells were infected with EPEC derivatives for 2 h. Results are the mean ± SEM of three independent experiments carried out in triplicate. ***Significant difference (*p<0.01, **p<0.001, ***p<0.0001), one way ANOVA with Tukey's multiple comparisons test)

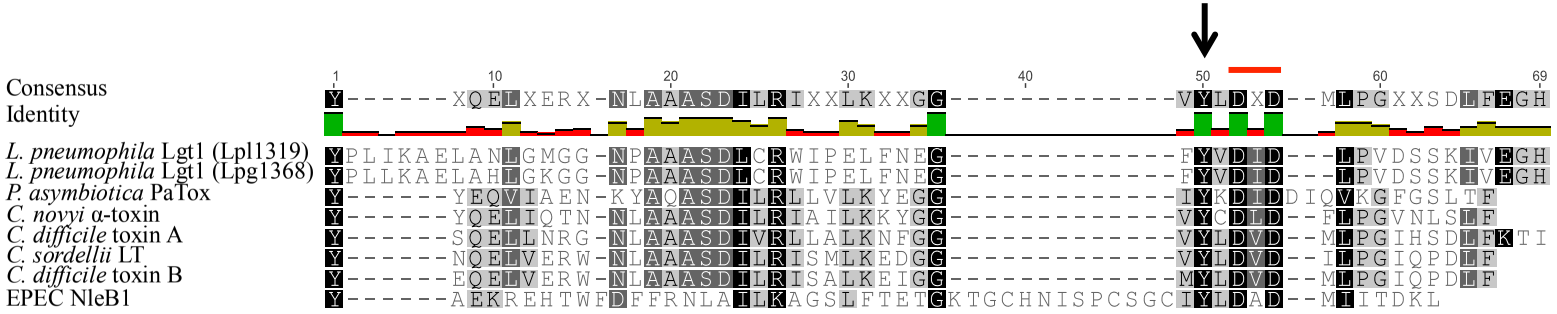
Consensus
Identity
L. pneumophila Lgt1 (Lpl1319)
L. pneumophila Lgt1 (Lpg1368)
P. asymbiotica PaTox
C. novyi α-toxin
C. difficile toxin A
C. sordellii LT
C. difficile toxin B
EPEC NleB1

Figure 4.6. Sequence similarity of NleB1 central portion with the catalytic region of glycosyltransferases from *Clostridium*, *Legionella* and *Photorhabdus* species. Amino acid sequence multiple alignment of the region surrounding the DxD motif (marked with a red line) of EPEC E2348/69 NleB1 (residues 176-236, accession number CAS10779) with different bacterial glycosyltransferases including *Legionella pneumophila* Lgt1 (Lpl1319) (residues 209-260, accession number 2WZG), *Legionella pneumophila* Lgt1 (Lpg1368) (residues 209-260, accession number Q5ZVS2), *Photorhabdus asymbiotica* PaTox (residues 2245-2290, accession number CAQ84322), *Clostridium novyi* α toxin (residues 253-296, accession number Q46149), *Clostridium sordellii* LT (residues 255-298, accession number Q46342), *Clostridium difficile* toxin A (residues 253-299, accession number CAC03681) and *Clostridium difficile* toxin B (residues 255-298, accession number P18177) was generated using MUSCLE (570) through the Geneious tool (571). Tyrosine-219 in EPEC NleB1 is conserved in the other glycosyltransferases and is shown with a black arrow. The weighted shading of highlights indicates the percentage similarity of aligned residues with darker colours indicating the highest conservation. The identity across all sequences for every residue is displayed above the aligned sequences. Green means that the residue at the given position is the same across all sequences. Yellow is for less than complete identity and red refers to very low identity for the given position. '-' indicates gaps inserted by Geneious based on the Blosum62 substitution matrix to generate the alignment.

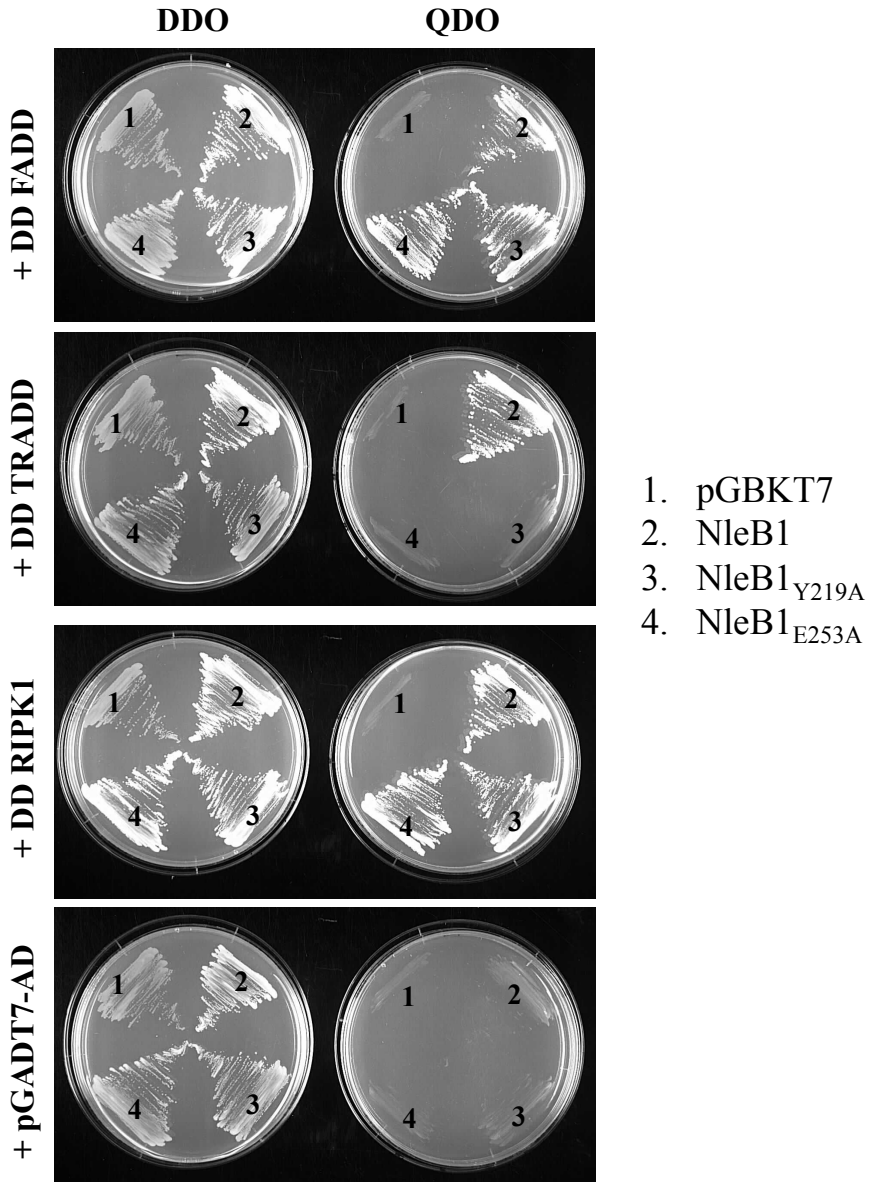

Figure 4.7. NleB1$_{Y219A}$ and NleB1$_{E253A}$ mutants bind to FADD and RIPK1 but not to TRADD. The yeast strain PJ69-4A was transformed with the indicated plasmid combinations (bait plus prey) to test the interaction of NleB1 mutants with the DDs of FADD, TRADD and RIPK1. Yeast strains were grown on DDO (SD-Trp-Leu) and QDO (SD-Trp-Leu-Ade-His) media. Growth on the DDO medium is indicative of a successful transformation with both bait and prey plasmids. Growth on the QDO medium indicates that the bait and prey proteins interact in yeast.

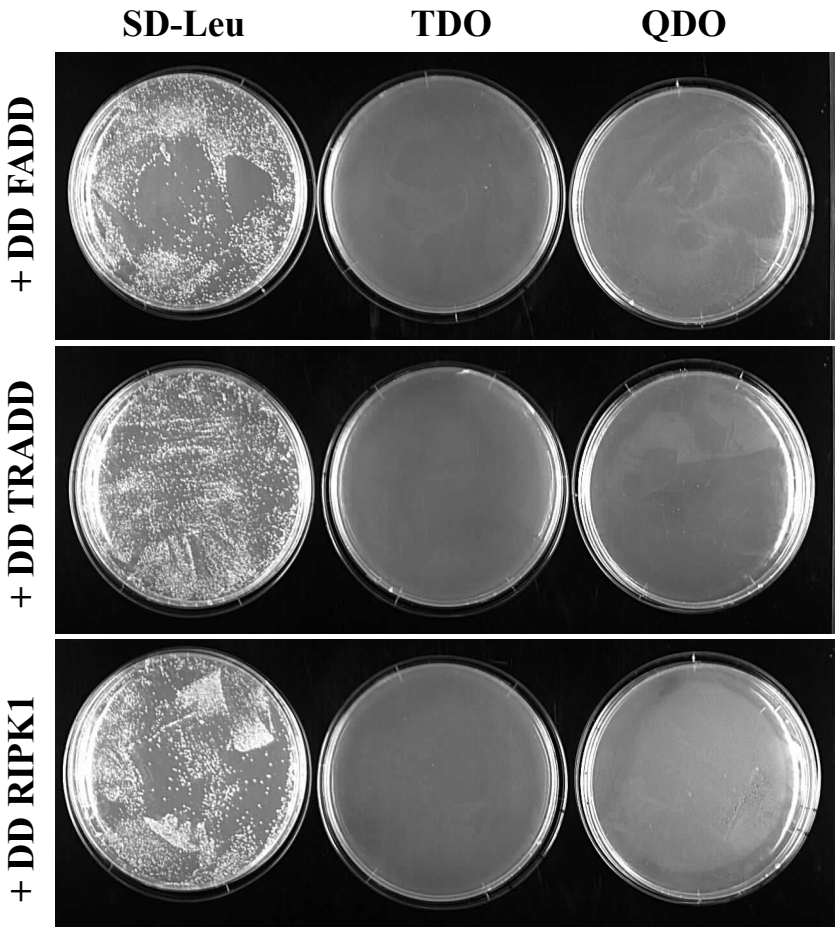

Figure 4.8 DD of FADD, TRADD and RIPK1 do not autoactivate reporter genes in Y2H system. The yeast strain PJ69-4A was transformed with the prey plasmids expressing the DD of FADD, TRADD and RIPK1 and plated on SD-Leu, TDO (medium stringency, SD-Trp-Leu-His) and QDO (highest stringency, SD-Trp-Leu-Ade-His) media to test if the prey proteins auto-activate reporter genes. Growth on SD-Leu indicates a successful transformation with the prey plasmid. Absence of growth on the TDO and QDO medium indicates that the prey proteins do not autoactivate reporter genes in yeast.

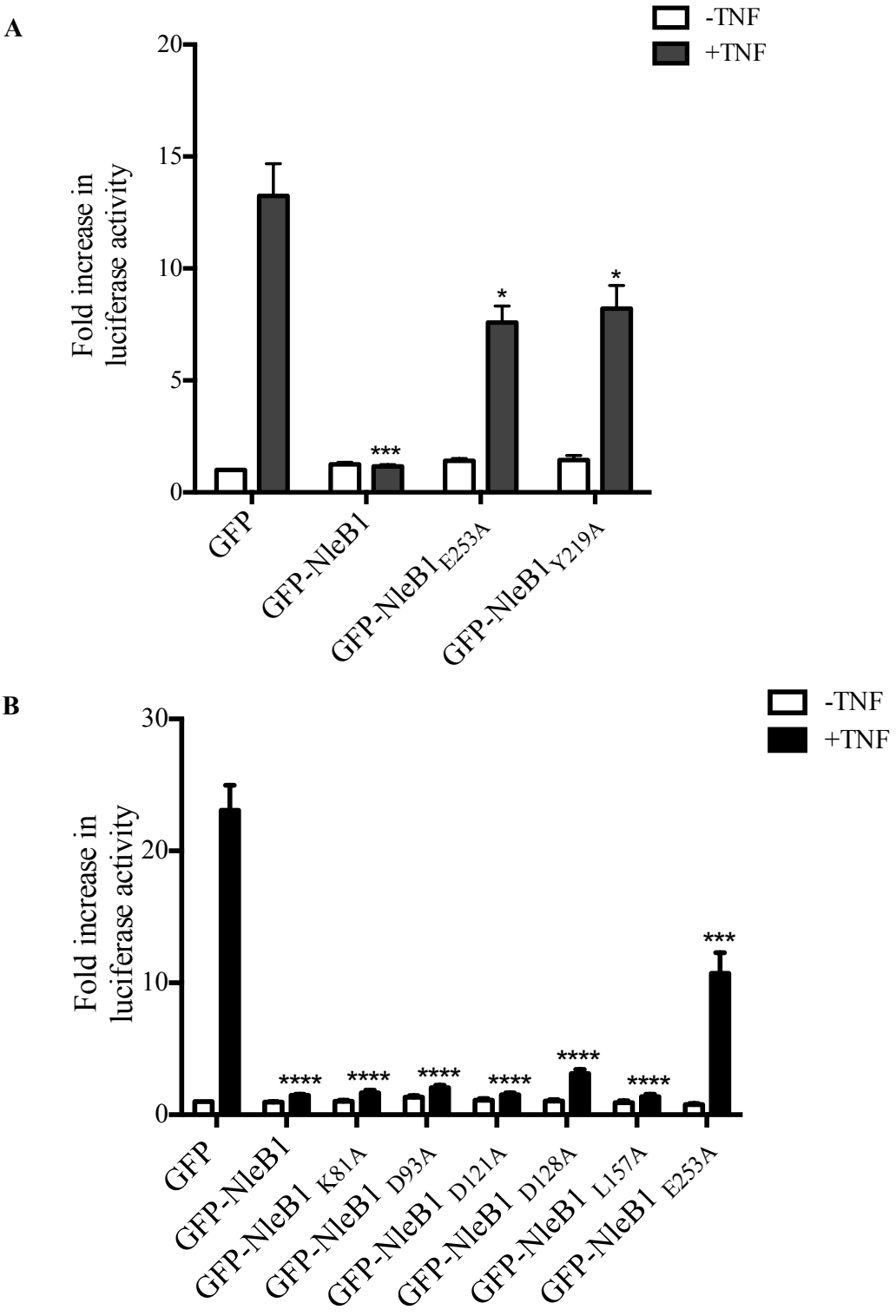
A
-TNF
+TNF
Fold increase in luciferase activity
20
15
10
5
0
***
*
*
GFP
GFP-NleB1
GFP-NleB1E253A
GFP-NleB1Y219A
B
-TNF
+TNF
Fold increase in luciferase activity
30
20
10
0
****
****
****
****
****
****
***
GFP
GFP-NleB1
GFP-NleB1 K81A
GFP-NleB1 D93A
GFP-NleB1 D121A
GFP-NleB1 D128A
GFP-NleB1 L157A
GFP-NleB1 E253A

Figure 4.9. Effect of NleB1 mutants on TNF-induced NF-κB luciferase reporter activation. (A-B) A total of 7 NleB1 variants including $NleB1_{Y219A}$ and $NleB1_{E253A}$ were expressed ectopically in HEK293T cells. Cells were stimulated with TNF and NF-κB activation measured as a fold change normalised to *Renilla* luciferase. Results are the mean ± SEM of three independent experiments carried out in duplicate. ***Significantly different to pEGFP-C2 transfected cells stimulated with TNF. (*$p<0.05$, **$p<0.001$, ***$p<0.0001$), one way ANOVA with Tukey's multiple comparisons test)

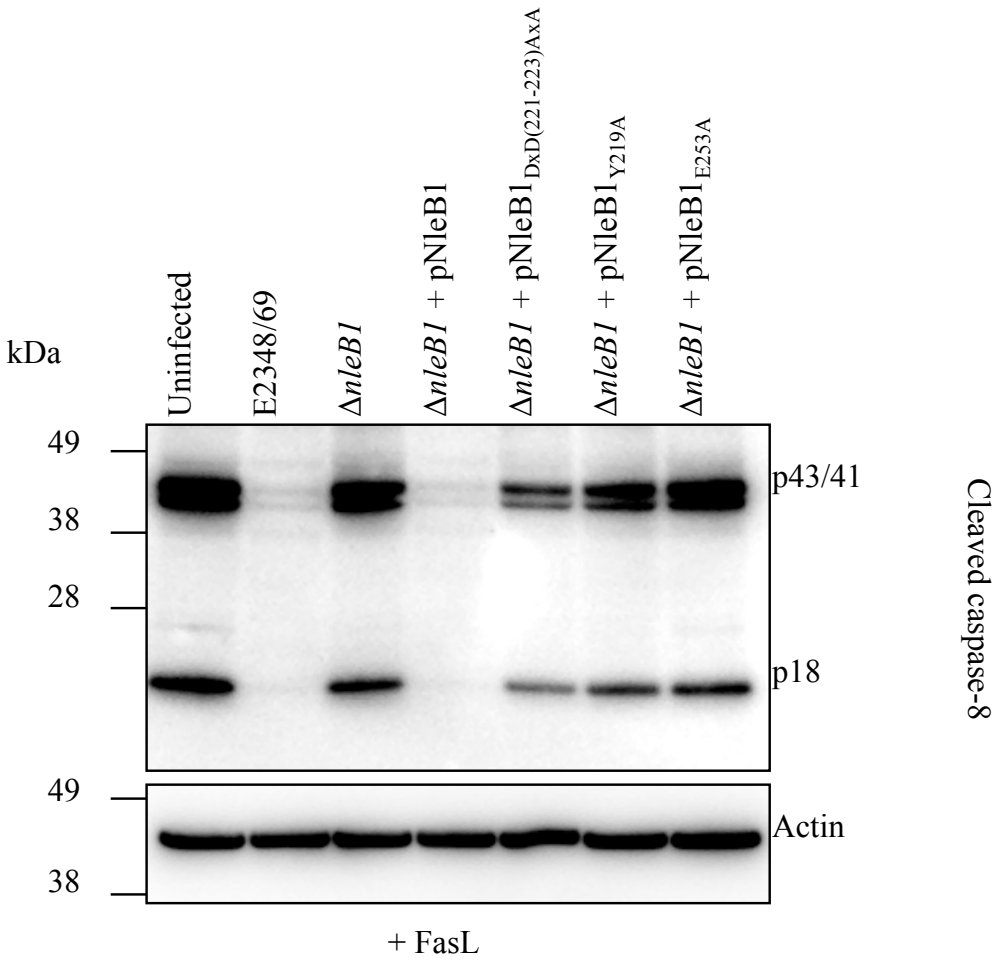

Figure 4.10. Effect of mutations Y219A and E253A on ability of NleB1 to inhibit caspase-8 activation. Immunoblot showing cleaved caspase-8 in HeLa cells infected with EPEC derivatives expressing the different NleB1 mutants ($NleB1_{DxD(221-223)AxA}$, $NleB1_{Y219A}$, $NleB1_{E253A}$) from the pTrc99A vector backbone and stimulated with FasL. Cells were harvested for immunoblotting and cleaved caspase-8 was detected with anti-cleaved caspase-8 antibodies. Antibodies to β-actin were used as a loading control. Representative immunoblot from at least three independent experiments.

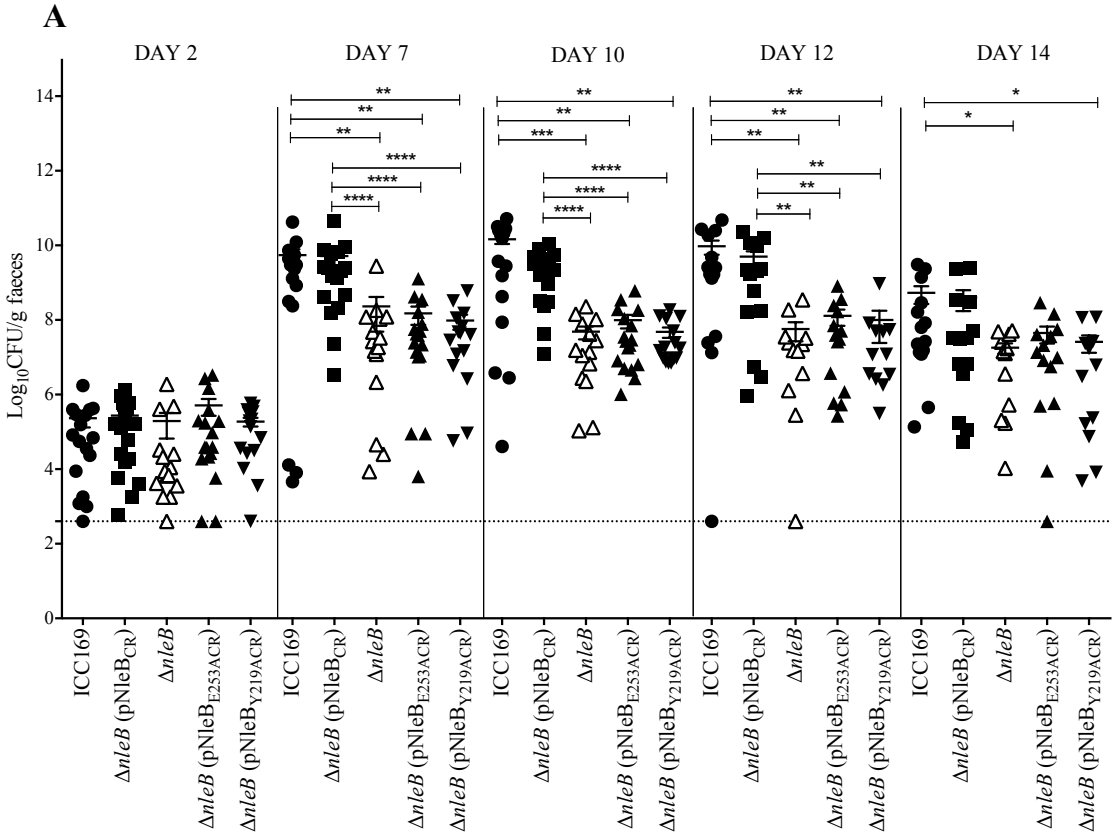
A
DAY 2
DAY 7
DAY 10
DAY 12
DAY 14
Log10CFU/g faeces
0
2
4
6
8
10
12
14
ICC169
ΔnleB (pNleBCR)
ΔnleB
ΔnleB (pNleBE253ACR)
ΔnleB (pNleBY219ACR)

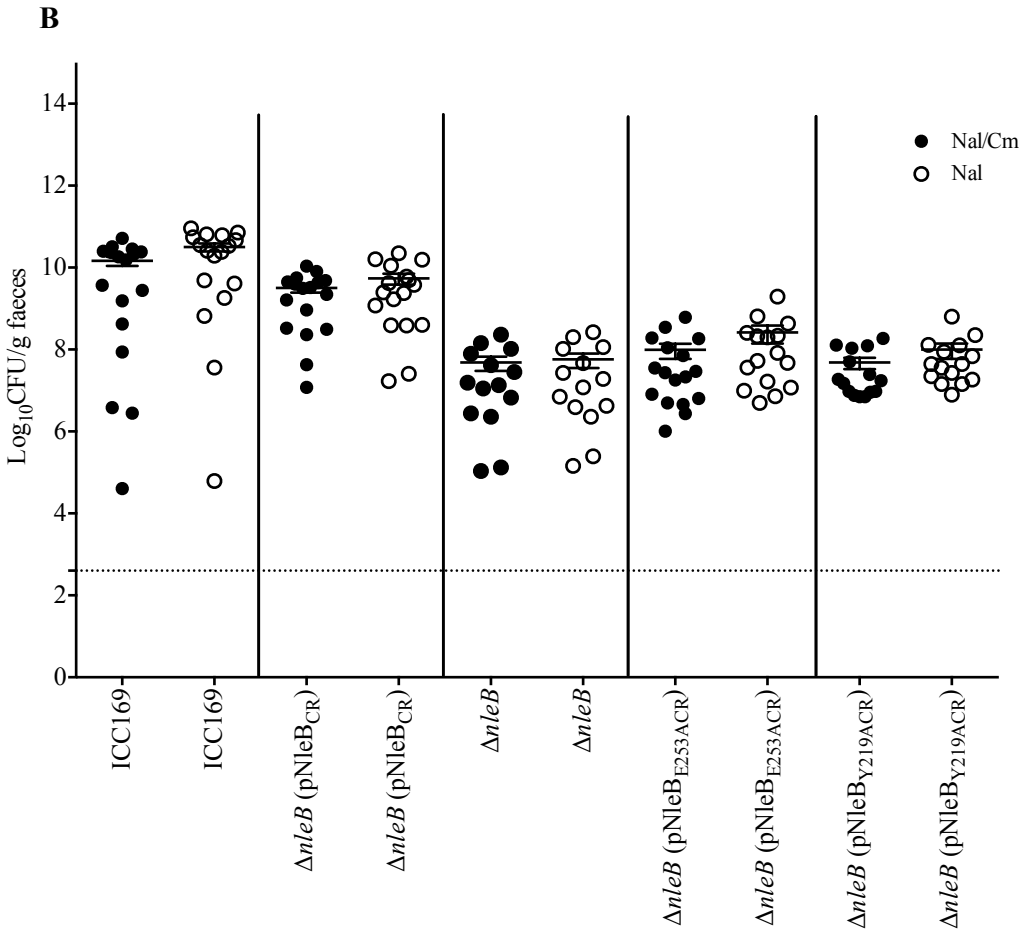
B
Log10CFU/g faeces
14
12
10
8
6
4
2
0
Nal/Cm
Nal
ICC169
ICC169
ΔnleB (pNleBCR)
ΔnleB (pNleBCR)
ΔnleB
ΔnleB
ΔnleB (pNleBE253ACR)
ΔnleB (pNleBE253ACR)
ΔnleB (pNleBY219ACR)
ΔnleB (pNleBY219ACR)

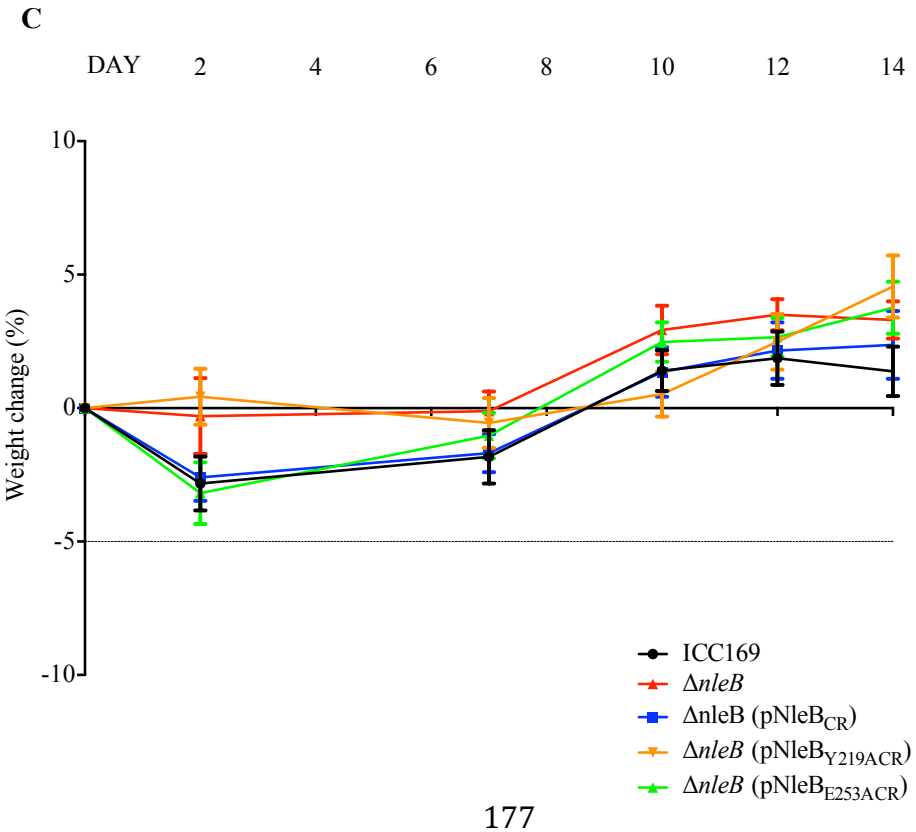
C
DAY 2 4 6 8 10 12 14
Weight change (%)
10
5
0
-5
-10
ICC169
ΔnleB
ΔnleB (pNleBCR)
ΔnleB (pNleBY219ACR)
ΔnleB (pNleBE253ACR)

Figure 4.11. Residues Y219 and E253 are important for virulence of NleB1 *in vivo*. (A) Colonisation of C57BL/6 mice with indicated *C. rodentium* derivatives. Each data point represents $\log_{10}$ CFU per g faeces per individual animal on days 2,7, 10, 12 and 14 after infection. Mean ± SEM are indicated, dotted line represents the detection limit. ***Significant difference Mann-Whitney U-test (*p<0.05, **p<0.01, ***p<0.001, ****p<0.0001). (B) Comparison of viable counts of *C. rodentium* derivatives from faecal samples collected on day 10 post infection on LA Nal and Cm and LA Nal.

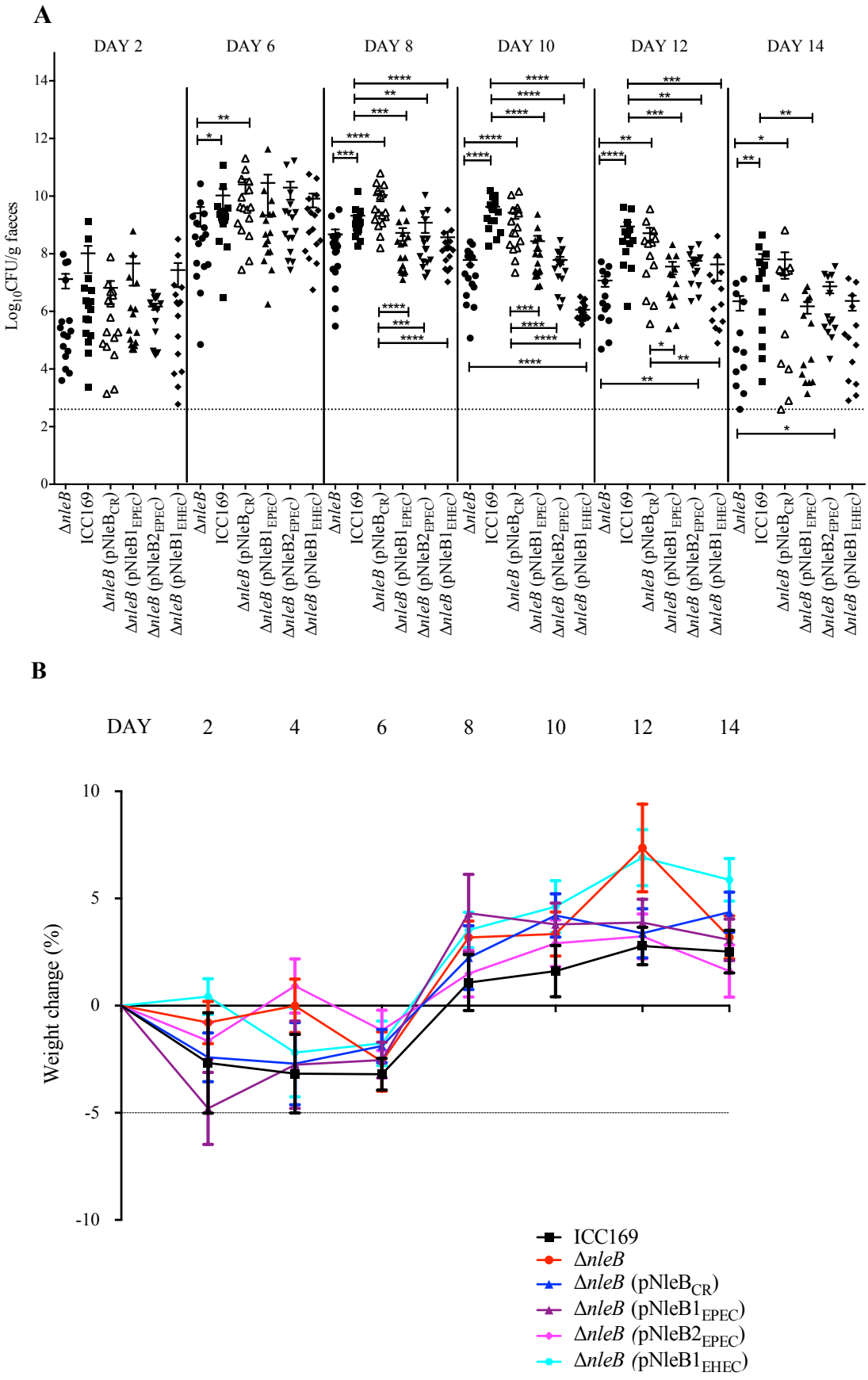
A
DAY 2
DAY 6
DAY 8
DAY 10
DAY 12
DAY 14
Log10CFU/g faeces
ΔnleB
ICC169
ΔnleB (pNleBCR)
ΔnleB (pNleB1EPEC)
ΔnleB (pNleB2EPEC)
ΔnleB (pNleB1EHEC)
B
DAY 2 4 6 8 10 12 14
Weight change (%)
ICC169
ΔnleB
ΔnleB (pNleBCR)
ΔnleB (pNleB1EPEC)
ΔnleB (pNleB2EPEC)
ΔnleB (pNleB1EHEC)

Figure 4.12. Complementation of *C. rodentium* Δ*nleB* derivative with NleB homologues from A/E pathogens. (A) Colonisation of C57BL/6 mice with indicated *C. rodentium* derivatives. Each data point represents $\log_{10}$ CFU per g faeces per individual animal on days 2, 4, 6, 8, 10, 12 and 14 after infection. Mean ± SEM are indicated, dotted line represents the detection limit. ***Significant difference Mann-Whitney U-test (*p<0.05, **p<0.01, ***p<0.001, ****p<0.0001). (B) % weight change of C57BL/6 mice infected with *C. rodentium* derivatives over course of experiment. No weight loss greater than 5% was observed. $NleB1_{EPEC}$; NleB1 from EPEC E2348/69, $NleB2_{EPEC}$; NleB2 from EPEC E2348/69 and $NleB1_{EHEC}$; NleB1 from EHEC O157:H7 strain EDL933.

Table 4.1. Summary of NleB1 mutants of interest

NleB1 multiple site-directed mutants	Ability to GlcNAcylate FADD[a]	Binding to FADD[b]	Translocation by EPEC[c]
No mutation	+++	+++	+
PILN (63-66) AAAA	−	+++	−
Y219A	**−**	**+++**	**+**
PDG (236-238) AAA	+	+	−
E253A	**−**	**+++**	**+**

[a, b] +++ is indicative of the level of FADD GlcNAcylation and binding observed in the presence of wild type NleB1, − is indicative of an absence of FADD GlcNAcylation and binding

[c] + is indicative of translocation by EPEC, − is indicative of no translocation by EPEC

Chapter 5

Preliminary investigation of NleB2 from EPEC and SseK1, 2 and 3 from *Salmonella*

Chapter 5. Preliminary investigation of NleB2 from EPEC and SseK1, SseK2 and SseK3 from *Salmonella*

5.1 Introduction

NleB1 from EPEC but not NleB2 inhibits host cell apoptosis (401). The binding partners of NleB1 from EPEC have been identified and the mechanism of action of NleB1 and its contribution to virulence *in vitro* and *in vivo* have been thoroughly investigated (401, 441). Close homologues of NleB1 exist in EPEC, other A/E pathogens as well as in *Salmonella* species where they are termed *Salmonella* secreted effectors K1, K2 and K3 (SseK1, SseK2 and SseK3) (401, 441, 559, 560).

SseK1 and SseK2 were first proposed as T3SS effectors based on homology to *C. rodentium* NleB, which is a known T3SS effector (560). SseK1 and SseK2 are encoded on distinct pathogenicity islets in the bacterial chromosome (560). A third homologous protein termed SseK3 encoded within the phage ST64B lysogen was subsequently discovered while comparing the genomes of *Salmonella* Typhimurium SL1344 and LT2 (559). While SseK1 and SseK2 are present in most available *Salmonella* genome sequences, SseK3 has a limited distribution in these genome sequences, consistent with it being encoded on an active phage lysogen (559). The phage ST64B is present in *S*. Typhimurium strain SL1344 (695) but not in the LT2 strain (696). *Salmonella* Typhimurium strain SL1344 is more virulent than LT2 in BALB/c mice due to an *rpoS* mutation in LT2 (697). The function of the SseK effectors has not been deciphered to date and consequently, the significance of the translocation of these three NleB homologous proteins by *Salmonella* is not clear.

Many known *Salmonella* effectors are present as multiple, functionally non-redundant homologues. For example, the homologues SopD and SopD2 share 63% similarity and 43% identity (698). The high degree of amino acid conservation between these two proteins is spread along their entire length although more significantly at the N-terminus and at the C-terminus, the latter of which contains a putative coiled-coil

domain (699). In spite of the strong homology between the two proteins, SopD has a cytoplasmic localisation in both transfected and infected cells whereas SopD2 localises to late endocytic compartments in transfected cells and to the SCV in infected cells (699), suggesting different functions for the proteins. While both SopD and SopD2 are essential for *Salmonella* pathogenesis in the mouse model of systemic infection (698), only SopD2 contributes to Sif formation in infected epithelial cells (698) and binds to the host GTPase Rab7 to block delivery of endocytic contents to lysosomes (700). In addition, SopE and SopE2 share 69% identity (488, 489, 701). Although both function as guanine nucleotide exchange factors (GEFs) for host cellular RhoGTPases, SopE can activate the RhoGTPases Cdc42 and Rac1 whereas SopE2 has been found to activate only Cdc42 (702). Each RhoGTPase can activate specific signalling cascades and cellular functions (703, 704). Therefore, by selectively targeting different RhoGTPases, SopE and SopE2 manipulate particular cellular functions (702).

In spite of the sparse distribution of bacteriophage ST64B in *Salmonella* genomes, the potential role of SseK3 in virulence should not be disregarded. SopE and GogB are examples of phage-encoded effectors that contribute to *Salmonella* virulence (521, 705). The *sopE* gene is encoded within a temperate bacteriophage, which is only present in a few *Salmonella* strains including *S.* Typhimurium SL1344 (705, 706). Despite its limited distribution, the carriage of *sopE* enhances *Salmonella* virulence; SopE-expressing strains have been linked with severe epidemics (706) and disruption of the *sopE* gene in *S.* Typhimurium SL1344 resulted in a two-fold reduction in the invasiveness of tissue culture cells compared to the wild type strain (489). The distribution of *sopE* shows that some virulence effector proteins may be passed on by horizontal gene transfer at an appreciable frequency. As previously mentioned, GogB is encoded within the bacteriophage Gifsy-1 (521) and inhibits NF-κB activation and inflammation by manipulating the host ubiquitination system (522).

All three SseK effectors are expressed under SPI-2 inducing conditions and translocated via the SPI-2 T3SS into eukaryotic cells (559, 560). Interestingly, although SseK2 appeared to be translocated at a lower level than SseK1 and at a later stage following *Salmonella* infection (560), SseK1 can be a substrate of both the SPI-1 and SPI-2 T3SSs *in vitro* (560). Although SseK3 translocation can be detected when infected host cells are fractionated, its translocation via the SPI-2 T3SS could not be confirmed given that SseK3 expression was not detected in HeLa cells infected with the SPI-2 mutant (Δ*ssaR*) (559).

Many SPI-2 effectors localise with membrane compartments within the host cell such as the SCV or Sifs (707-709). While SseK1 is distributed uniformly in the host cell cytosol (by cell fractionation and immunoblotting experiments as well as by immunofluorescence (560)), SseK3 was observed in both membrane and cytosolic fractions of wild type *Salmonella* infected cells (559), suggesting a different cellular localisation and hence possibly function of the SseK effectors. Initial work on SseK1 and SseK2 did not find a prominent role in virulence, either in terms of intracellular replication, Sif formation or in BALB/c mice following intraperitoneal infection with Δ*sseK1*, Δ*sseK2* or Δ*sseK12 S*. Typhimurium SL1344 derivatives (560). To address the possibility of functional redundancy by SseK3, a triple *sseK* mutant (Δ*sseK123*) was constructed and tested. No difference was observed in terms of intracellular bacterial replication, although SseK1 and SseK2 had a minor role in virulence, demonstrated by a lower competitive index compared to wild type *S*. Typhimurium SL1344 during infection of 129 SvJ mice (559).

In view of the homology amongst the NleB and SseK effectors, we hypothesised that the SseK effectors may also bind DD-containing proteins and inhibit death receptor signalling. In this study, we aimed to identify the potential binding partners of the SseK effectors and to infer their role in *Salmonella* virulence. Additionally, since the binding partner and function of NleB2 from EPEC had not been determined, we also aimed to investigate the potential target(s) of NleB2.

5.2 Results

5.2.1 NleB homologues in *Salmonella* termed SseK1, SseK2 and SseK3 share high percentage similarity and identity with NleB1 of EPEC

SseK1, SseK2 and SseK3 from *Salmonella* are close homologues of NleB1 from EPEC. The amino acid sequence of the NleB1 homologues in EPEC E2348/69, other A/E pathogens such as REPEC E22, EHEC O157:H7 Sakai and *C. rodentium* ICC169 and in the facultative intracellular gastrointestinal pathogen *S.* Typhimurium SL1344 were aligned (Figure 5.1A) and the alignment was used to construct a Maximum Likelihood phylogenetic tree to infer relatedness between the amino acid sequences. The amino acid conservation was spread relatively evenly across the whole length of the proteins except at the N-terminal region, suggesting that the entire protein sequence was involved in function rather than a particular domain(s) (Figure 5.1B).

NleB1 and NleB2 from EPEC and the SseK effectors from *Salmonella enterica* serovar Typhimurium SL1344 share between 76-92% similarity and 48-75% amino acid identity with each other (Table 5.1). EPEC, EHEC and REPEC NleB1 are nearly identical and each share 89% amino acid identity with *C. rodentium* NleB and 61, 62 and 61% amino acid identity respectively with the more divergent effector NleB2 from EPEC. Since the divergence of *nleB1/nleB* and *nleB2*, the latter has accumulated more non-synonymous mutations as reflected by the lower percentage of amino acid identities between NleB2 and each of the SseK effectors (Table 5.1) and the length of the branches separating NleB2 from the SseK effectors (Figure 5.2). SseK2 and SseK3 are more closely related to each other than to SseK1, sharing 92% similarity and 75% amino acid identity compared to 84-85% similarity and 61-62% identity with SseK1 (Figure 5.1B and Table 5.1). A more extensive search of NleB1 homologues from EPEC, EHEC, *C. rodentium* and *Salmonella* Typhimurium was performed using BLAST (574) and the amino acid sequences were aligned (572). The alignment was used to construct a Randomized Axelerated Maximum Likelihood (RAxML) (578) phylogenetic tree to infer homology between the sequences. Even though the NleB and SseK proteins clearly comprise a family, sequence and

phylogenetic analyses show that the SseK proteins from *Salmonella* form their own group/clade separate from the NleB proteins (Figure 5.2).

5.2.2 Subcellular localisation of SseK1, SseK2 and SseK3

Since protein localisation is often tightly linked with function, the subcellular distribution of the SseK effectors was investigated. It was previously stated that SseK1 localises to the host cell cytosol (560), which is unusual as SPI-2 effectors usually associate with membrane components within the host cell. In contrast, SseK3 was recently found to localise with p230, a trans-golgi network marker, but not with early endosome and lysosome markers upon ectopic expression in tissue culture (710). This is consistent with SseK3 in the membrane fraction of *Salmonella* infected cells. Here, we tested the localisation of the SseK effectors by ectopic expression in HeLa cells. Vectors expressing GFP-tagged SseK1, SseK2 and SseK3 were individually transfected into HeLa cells and GFP fusion proteins were visualised by fluorescence microscopy. GFP-SseK1 was observed uniformly throughout the host cell cytosol, similar to the GFP control (Figure 5.3). This is consistent with the previously mentioned fractionation and immunofluorescence microscopy experiments. Interestingly, GFP-SseK2 and GFP-SseK3 appeared to co-localise with the Golgi bodies within HeLa cells.

5.2.3 SseK3 binds to TRIM32 *in vitro*

Work in our collaborator's laboratory (Teasdale laboratory, Institute for Molecular Bioscience, The University of Queensland) identified the Tripartite Motif 32 (TRIM32) protein, which is a known E3 ubiquitin ligase (711, 712), as a potential binding partner of SseK3 by immunoprecipitation and mass spectrometry (710). GFP-SseK3 was expressed ectopically in HEK293 cells and immunoprecipitated using GFP-nanotrap agarose beads. The immunoprecipitate was separated by gel electrophoresis and stained with colloidal Coomassie Blue. Bands from the immunoprecipitate sample were excised, digested with trypsin and identified by HPLC-ESI-MS/MS. 18 unique peptides of TRIM32 were identified from the GFP-

SseK3 immunoprecipitated sample that were absent from samples of untransfected HEK293 cells or cells expressing GFP only (710).

To verify the binding of SseK3 to TRIM32, GFP-SseK3 and myc-TRIM32 were ectopically expressed in HEK293T cells and GFP-SseK3 was immunoprecipitated with GFP-Trap and examined for binding to myc-TRIM32 using anti-myc antibodies. A band of about 72 kDa, corresponding to myc-TRIM32, was immunoprecipitated with GFP-SseK3 but not with GFP alone (Figure 5.4). The interaction between SseK3 and TRIM32 was shown to be specific given that endogenous TRIM32 was not observed in pull downs with GFP-SseK1 or GFP-SseK2 (710).

Binding was further verified by a reciprocal immunoprecipitation study. GFP, GFP-SseK1, GFP-SseK2 and GFP-SseK3 were each ectopically expressed with FLAG-TRIM32 in HEK293T cells and FLAG-TRIM32 was immunoprecipitated from the cell lysates. HEK293T cells expressing GFP-NleB1 and FLAG-FADD were used as a positive binding control. As expected, GFP-NleB1 immunoprecipitated with FLAG-FADD (Figure 5.5). In addition, a band of about 62 kDa in the FLAG IP from cells expressing GFP-SseK3 and FLAG-TRIM32 was detected with anti-GFP antibodies indicating that GFP-SseK3 immunoprecipitated with FLAG-TRIM32 (Figure 5.5). The presence of faint bands of about 30 kDa and 62 kDa on the anti-GFP immunoblot, corresponding to GFP and GFP-SseK1 or GFP-SseK2 respectively, (Figure 5.5) suggested that GFP may bind to the FLAG tag or to the anti-Flag beads. As expected, FLAG-FADD was GlcNAcylated in the presence of NleB1 (Figure 5.5). The presence of a faint band of approximately 62 kDa was observed in the FLAG-TRIM32 immunoprecipitate sample from cells expressing GFP-SseK3 and FLAG-TRIM32 using anti-GlcNAc antibodies (Figure 5.5). This raised the possibility that SseK3 could GlcNAcylate TRIM32.

5.2.4 SseK3 does not GlcNAcylate TRIM32 *in vitro*

To determine if SseK3 GlcNAcylates TRIM32, recombinant GST-SseK3 and His-TRIM32 were purified and incubated alone or together in the presence of UDP-

GlcNAc. GST-NleB1 and His-FADD were incubated in the presence of UDP-GlcNAc as a control for the *in vitro* GlcNAcylation assay. As expected His-FADD was GlcNAcylated in the presence of GST-NleB1 but His-TRIM32 was not modified with GlcNAc in the presence of GST-SseK3 (Figure 5.6).

5.2.5 The SseK effectors do not bind to the DD of FADD, TRADD and RIPK1

NleB1 binds the DD of FADD, TRADD and RIPK1. In view of the homology amongst the NleB and SseK effectors, we hypothesized that the SseK effectors may also bind and modify these DD proteins. To investigate these protein interactions, bait plasmids expressing NleB1, NleB2 or SseK1, 2 or 3 and prey plasmids expressing the DDs of FADD, TRADD or RIPK1 were co-transformed in the yeast strain PJ69-4A and plated onto selective media, namely DDO and QDO. Yeast growth on the DDO medium indicated that the yeast strain PJ69-4A was successfully transformed with the bait and prey plasmids as indicated (Figure 5.7A).

PJ69-4A co-transformed with pGBKT7-NleB1 and one of the pGADT7-AD constructs expressing the DD of FADD, TRADD or RIPK1 grew on the QDO medium, confirming the interaction of NleB1 with the DD of FADD, TRADD and RIPK1. In contrast, PJ69-4A co-transformed with bait plasmids expressing the SseK effectors and prey plasmids expressing the DDs were unable to grow on the QDO medium. This indicated that unlike NleB1, the SseK effectors do not bind to the DDs of FADD, TRADD and RIPK1 in yeast. Interestingly, NleB2 bound to the DD of RIPK1 but not to the DD of FADD or TRADD in yeast (Figure 5.7A). Furthermore, none of the NleB or SseK effectors bound to the GAL4 activation domain expressed by pGADT7-AD, indicating that the positive interactions observed in our yeast studies were not a consequence of the bait proteins binding non-specifically to the activation domain from the prey plasmid.

5.2.6 Investigating the binding of SseK1, SseK2 and SseK3 to the DD of MyD88, IRAK1, IRAK4, Fas, TNFR1 and DR5

NleB1 binds to and GlcNAcylates the DD of FADD and TRADD at a conserved arginine residue (401, 441). This arginine residue is found in the DD of RIPK1, TNFR1, Fas and DR5. Li *et al.* showed by mass spectrometry that NleB1 modifies the DD of RIPK1 and TNFR1 and to a lesser extent the DD of Fas following ectopic expression in HEK293T cells (441). DDs lacking the conserved arginine such as that of MyD88 and IRAK1 were not GlcNAcylated by NleB1 (441). Here, we investigated binding of the NleB/SseK effectors to the DD of MyD88, IRAK1 and IRAK4, which lack the conserved arginine, and to the DD of the death receptors Fas, TNFR1 and DR5, which contain the conserved arginine. None of the NleB/SseK effectors bound to the DD of MyD88, IRAK1, IRAK4, Fas and DR5 in yeast (Figure 5.8). Interestingly, NleB1 and NleB2 from EPEC and SseK3 from *S.* Typhimurium appeared to bind to the DD of TNFR1 (Figure 5.8).

5.2.7 SseK3 binds to and GlcNAcylates the DD of TNFR1 *in vitro*

To confirm the interaction between SseK3 and the DD of TNFR1, GFP or GFP-SseK3 along with FLAG-DD of TNFR1 were ectopically expressed in HEK293T cells and the DD of TNFR1 was immunoprecipitated from the cell lysates. A faint band of about 62 kDa was observed on the immunoblot of the immunoprecipitates probed with anti-GFP antibodies, indicating that GFP-SseK3 was pulled down with the DD of TNFR1 (Figure 5.9). This validated the results obtained from the yeast co-transformation experiment. We hypothesised that SseK3 binds and GlcNAcylates the DD of TNFR1, given that it is a homologue of NleB1, which possesses GlcNAc transferase activity. Therefore, the immunoprecipitated DD of TNFR1 was tested for GlcNAcylation. A band of about 14 kDa was observed on the immunoblot of the immunoprecipitates probed with anti-GlcNAc antibodies, indicating that the DD of TNFR1 was GlcNAcylated in the presence of GFP-SseK3 (Figure 5.9). No GlcNAcylation of the DD of TNFR1 was observed in the presence of GFP alone or in

the presence of the GFP-tagged putative catalytic mutant of SseK3, GFP-SseK3$_{DxD(226-228)AxA}$ (Figure 5.9). In addition, a band above the 62 kDa marker was observed in the FLAG immunoprecipitate from HEK293T cells expressing GFP-SseK3 and FLAG-DD of TNFR1 on the immunoblot probed with anti-GlcNAc antibodies (Figure 5.9). It is possible that this band represents a multimer of FLAG-DD of TNFR1 or FLAG-DD of TNFR1 interacting with endogenous TNFR1.

5.2.8 SseK1 and SseK3 inhibit TNF-induced NF-κB activity

Stimulation of TNFR1 can lead to NF-κB activation and the induction of inflammation. Since SseK3 appeared to bind to the DD of TNFR1, the effect of the SseK effectors, particularly SseK3, on NF-κB activation following TNF stimulation was investigated using a dual luciferase reporter assay. The EPEC effector NleE, a potent inhibitor of NF-κB activation and inflammation, was included in the dual luciferase assay as a control. TNF-induced HeLa cells expressing GFP only displayed a high luciferase activity indicative of a high level of NF-κB activation (Figure 5.10A). This level of NF-κB activation was significantly reduced in the presence of GFP-NleE and GFP-NleB1 from EPEC and GFP-SseK1 and GFP-SseK3 from *S.* Typhimurium after TNF stimulation (Figure 5.10A). However, no significant reduction in NF-κB activation was observed in the presence of NleB2 from EPEC or SseK2 from *S.* Typhimurium following TNF stimulation (Figure 5.10A).

To determine if the DxD motif of the NleB homologues was essential for the NF-κB inhibitory activity, the DxD mutants of the NleB homologues were included in the dual luciferase reporter assays. While NleB1, SseK1 and SseK3 were able to inhibit TNF-induced NF-κB activation, mutation of the DxD motif relieved this inhibitory activity of the proteins (Figure 5.10B).

5.2.9 Secretion of the pro-inflammatory cytokine IL-8 during *Salmonella* infection

The end point of NF-κB activation is transcription of pro-inflammatory cytokines such as IL-8 and the induction of inflammation. Given that SseK1 and SseK3 inhibited TNF-induced NF-κB activation in the dual luciferase assay, this suggested that SseK1 and SseK3 may inhibit NF-κB-dependent *IL-8* gene expression. The effect of the SseK effectors on IL-8 secretion was therefore investigated during *Salmonella* infection.

To test this, we examined production of the NF-κB dependent pro-inflammatory cytokine IL-8 from *S.* Typhimurium infected HeLa cells, which were either unstimulated or stimulated with TNF. As shown in Figure 5.11A, HeLa cells infected with wild type *S.* Typhimurium, the SPI-2 mutant, Δ*ssaR*, and the *sseK* deletion mutants, Δ*sseK1,* Δ*sseK2,* Δ*sseK3,* Δ*sseK1/2/3* secreted similar levels of IL-8 secretion. However, IL-8 secretion was significantly reduced in cells infected with the SPI-1 mutant, Δ*invA*, to a similar level as in uninfected and unstimulated cells (Figure 5.11A). In contrast, when uninfected cells were stimulated with TNF, IL-8 secretion was increased significantly (Figure 5.11A). A high IL-8 secretion level was also observed when cells were infected with the SPI-1 mutant and stimulated with TNF (Figure 5.11A). A significant decrease in IL-8 production was observed in cells infected with wild type *S.* Typhimurium and stimulated with TNF (Figure 5.11A). Interestingly, no significant increase in IL-8 secretion was observed when cells were infected with any of the *sseK* deletion mutants or the SPI-2 mutant and stimulated with TNF, suggesting that none of the SseK effectors had a role in the inhibition of IL-8 secretion during *Salmonella* infection (Figure 5.11A).

Since macrophages are a common niche for *Salmonella* infection, THP-1 cells were also infected with the *S.* Typhimurium derivatives and left untreated or stimulated with TNF. The cell supernatants were analysed for IL-8 secretion level. The overall level of IL-8 secretion from THP-1 cells was higher than that observed from HeLa

cells, which is in accordance with the role of macrophages in the production of pro-inflammatory cytokines (713, 714). No inhibition of IL-8 secretion was observed by wild type *S.* Typhimurium following infection of THP-1 cells (Figure 5.11B), and neither did the SseK effectors inhibit IL-8 secretion during infection of THP-1 cells (Figure 5.11B).

5.2.10 Investigation of the potential binding partners of NleB2, SseK1, SseK2 and SseK3 by yeast two-hybrid screening

Since the SseK effectors did not appear to bind to DD-containing proteins, apart from SseK3 which bound the DD of TNFR1 in yeast and in co-immunoprecipitation experiments, we searched for novel host cell binding partners. Yeast two-hybrid screens using SseK1, SseK2 and SseK3 as bait proteins and a normalised HeLa cell cDNA library as the prey were performed to identify potential human binding partners. A yeast two-hybrid screen using NleB2 from EPEC as the bait was also performed in an attempt to identify binding partners, which could help decipher the as yet unknown function of NleB2 from EPEC.

Prior to performing the yeast mating, the yeast strain AH109 was individually transformed with each of the pGBKT7 constructs expressing NleB2, SseK1, SseK2 or SseK3. pGBKT7 encodes the gene for tryptophan synthesis. The transformants were plated on SD-Trp, TDO and QDO plates. Growth of the transformants on SD-Trp but not on TDO or QDO media indicates a successful transformation and that the bait proteins NleB2, SseK1, SseK2 and SseK3 did not autoactivate yeast reporter genes (Figure 5.12A).

Furthermore, the expression of the bait proteins was tested in yeast using an alkaline treatment for protein extraction from the AH109 strains harbouring the bait plasmids. The protein extracts were subjected to gel electrophoresis and immunoblotting with anti-myc antibodies, given that the bait proteins, in addition to being fused with a GAL4 DNA binding domain, were also expressed as a fusion to a c-Myc epitope tag.

Each of the bait proteins was expressed in yeast as shown by the presence of a band of approximately 58 kDa on the immunoblot probed with anti-myc antibodies (Figure 5.12B). However, of the bait proteins tested, SseK2 appeared to be the most efficiently expressed in yeast (Figure 5.12B).

The above results enabled execution of the next step of the yeast screening experiment. The HeLa cell cDNA pretransformed yeast strain Y187 was mixed with each of the yeast strains AH109 harbouring the bait proteins and grown overnight before plating on the highest stringency selective media, QDO. Colonies that grew on QDO were patched onto DDO and QDO plates to eliminate false positives. Plasmids were extracted from those colonies that grew on both selective media and transformed into *E. coli* XL-1 Blue cells prior to plating on LA supplemented with ampicillin to select for the pGADT7-RecAB constructs containing the cDNA prey library. The prey constructs were extracted and identified by sequencing. The presence of an open reading frame fused to the GAL4-AD sequence was verified and the sequence was compared to a non-redundant protein database using blastx. The potential binding partners of each bait protein are shown in Tables 5.2-5.3. COP9 signalosome subunit 5 (CSN5), also known as Jun activation domain-binding protein 1 (JAB1), was recovered multiple times in the yeast two-hybrid screens.

5.2.11 Validation of targets from yeast two-hybrid screens

Interaction of the bait proteins with CSN5 required validation. Interestingly, it was previously found that CSN5 is often a false positive from yeast two-hybrid screens as it was shown to interact with the binding domain of GAL4 alone (715)**.** Therefore, the binding of SseK3 and other homologues to CSN5 was verified by co-immunoprecipitation experiments. HEK293T cells were transfected with either pEGFP-C2 and pFLAG-CSN5 or with a pEGFP-C2 construct expressing NleB1, NleB2, SseK1, SseK2 or SseK3 together with pFLAG-CSN5. The cells were lysed and FLAG-CSN5 was immunoprecipitated. The immunoprecipitate samples were examined for GlcNAcylation and binding to the GFP-tagged NleB1 homologues with

anti-GlcNAc and anti-GFP antibodies respectively. GFP and GFP-NleB1 homologues (GFP-NleB1, GFP-NleB2, GFP-SseK1, GFP-SseK2 and GFP-SseK3) all bound to FLAG-CSN5 (Figure 5.13), suggesting that CSN5 binds to the GFP tag. This suggests that CSN5 is promiscuous for binding and that the interaction between each of the NleB and SseK effectors to CSN5 is a false positive arising from CSN5 binding non-specifically to the tag of the effectors.

The binding of SseK2 to FAPP1-associated protein 1 (FASP1), also known as MIS18 kinetochore protein A, was verified by co-transforming the bait plasmid pGBKT7-SseK2 and the prey plasmid encoding FASP1 (pGADT7-RecAB-FASP1), which was recovered from the yeast two-hybrid screen, into the yeast strain PJ69-4A and plating on both DDO and QDO media. Yeast co-transformed with the bait and prey plasmids expressing SseK2 and FASP1 respectively grew on the QDO medium, indicating that the two proteins bind to each other in yeast (Figure 5.14A). This binding of FASP1 to SseK2 was specific since no binding of SseK1 and SseK3 to CSN5 was observed (Figure 5.14A). Furthermore, FASP1 did not interact with the binding domain of GAL4 alone since yeast co-transformed with empty pGBKT7 and the prey plasmid expressing FASP1 failed to grow on QDO medium (Figure 5.14A). Additionally, the ability of FASP1 to autoactivate reporter genes to enable growth on QDO was verified; yeast transformed with the prey plasmid expressing FASP1 alone grew on SD-Leu but not on the TDO and QDO plates (Figure 5.14B). This confirmed that FASP1 did not autoactivate the yeast reporter genes.

5.3 Discussion

Since the identification of the SseK effectors, several studies have investigated their contribution to *Salmonella* virulence. However, these studies have yielded conflicting results. While Kujat Choy *et al*. found no role for SseK1 and SseK2 in the susceptible BALB/c mouse model (560), Brown *et al*. found a role in virulence for SseK1 and or SseK2 in orally gavaged 129 SvJ mice as a Δ*sseK12* double mutant was outcompeted by wild type *S*. Typhimurium strain SL1344 (559). A more recent study investigating the role of 48 *Salmonella* effectors in murine pathogenesis showed that none of the Δ*sseK* single mutants (Δ*sseK1*, Δ*sseK2*, Δ*sseK3*) were attenuated in competition experiments with wild type SL1344 in 129 SvJ mice by intraperitoneal injection (716). The discrepancy in the results of these *in vivo* studies could be due to a number of factors including the mouse strain used, the mode of infection as well as the *Salmonella* derivatives used. For example, infection of susceptible mouse strains containing mutations in Nramp1 such as C57BL/6 and BALB/c mice (717, 718), lacks sensitivity as only *Salmonella* strains bearing mutations in major virulence factors targeting the innate immune system are identified, whereas strains bearing mutations in minor virulence factors or virulence factors required for persistence in the host are not picked up.

Additionally, intracellular replication studies have reported conflicting results, whereby the Δ*sseK123* triple mutant was either fully virulent during *Salmonella* infection (559) or displayed reduced replication compared to wild type *Salmonella* (719). Altogether, these findings were inconclusive and the host targets and function of the SseK effectors remained to be determined. Phylogenetic analyses showed that the SseK effectors form a distinct subset from the other NleB1 homologues in A/E pathogens, suggesting that the SseK effectors could have different functions to NleB1. Although the SseK effectors form a clade, they would not be expected to have exactly the same function given that the distance between SseK1 and SseK2/3 is roughly equivalent to that between the NleB1 and NleB2 sub-clades. Additionally, the tree topology suggests that SseK2 and SseK3 but not SseK1 would be more likely to have

a conserved function and further examination of the differences between SseK2 and SseK3 may shed light on the binding observed between SseK3 and TRIM32. Furthermore, the Golgi association of SseK2 and SseK3 in transfected HeLa cells compared to the cytosolic localisation of SseK1 further suggests different functions within the SseK family members. Interestingly, despite localising to the Golgi bodies, SseK2 or SseK3 do not have a predicted transmembrane region.

TRIM32, an E3-ubiquitin ligase, was identified as a potential binding partner of SseK3 by co-immunoprecipitation and mass spectrometry (710). While this interaction was confirmed *in vitro*, the biological significance of this binding was not ascertained. TRIM32 ubiquitinates many mammalian proteins including actin (712), PIASγ (711), X-linked inhibitor of apoptosis (XIAP) (720), c-Myc (721) and the transcription factor p73 (722) and viral proteins such as human immunodeficiency virus (HIV)-1 Tat (723) and influenza A virus PB1 (724). TRIM32 possesses an N-terminal RING domain, which is crucial for the binding of E2-conjugating enzymes (725) as well as six repeats of the NHL motif in the C-terminus that is thought to mediate protein-protein interactions (726). A potential role for TRIM32 in innate immunity and apoptosis has been suggested although the exact mechanism of action has not yet been elucidated. Mouse TRIM32 is expressed at a high level in a mouse skin carcinogenesis model and in mouse skin tumours induced *in vivo* by UVB irradiation (727). Furthermore, TRIM32 expression protects keratinocytes from apoptosis induced by UVB and TNF treatment both *in vitro* and *in vivo* (727). TRIM32 may inhibit apoptosis, at least in keratinocytes, by binding to and ubiquitinating PIASγ, a member of STAT-interacting proteins involved in the regulation of several transcription factors including STATs and NF-κB (728), leading to its proteasomal degradation (727). The depletion of PIASγ is thought to promote survival through stimulation of NF-κB transcriptional activity. Recently, TRIM32 was shown to inhibit apoptosis by promoting the ubiquitination and proteasomal degradation of the tumour suppressor p53 (729).

TRIM32 has previously been shown to possess all the hallmarks of E3-ubiquitin ligases, including self-ubiquitination and ubiquitination of target proteins (727). Interestingly, the interaction between SseK3 and TRIM32 did not affect the auto-ubiquitination of TRIM32 and SseK3 was not ubiquitinated by TRIM32 (710). We showed here that SseK3 did not GlcNAcylate TRIM32 despite binding it. However, it is possible that the level of GlcNAcylation on TRIM32 was below detection level by immunoblotting with anti-GlcNAc antibodies, in which case, radioactive labeling experiments with UPD-^{14}C GlcNAc could be a more sensistive way of detecting TRIM32 modification.

None of the SseK effectors bound the DD of FADD, TRADD or RIPK1, which are targets of NleB1, according to a yeast two-hybrid based system. Although these initial yeast results suggested that the SseK effectors did not interfere with the host death receptor signalling pathway, they were in contrast to a previous study by Li *et al*., whereby SseK1 was found to GlcNAcylate TRADD *in vitro* (441). Therefore, the binding of the SseK effectors to other DDs was also tested in yeast and this showed that while the SseK effectors did not bind to the DD of MyD88, IRAK1, IRAK4, DR5 and Fas, SseK3 bound the DD of TNFR1. NleB1 was unable to bind to the DD of Fas in our yeast studies. We hypothesised that the lower efficiency of Fas GlcNAcylation by overexpressed NleB1 in *in vitro* studies by Li *et al*. could be due to a weaker interaction between NleB1 and Fas. NleB2 also bound to the DD of RIPK1 and TNFR1 in yeast. The binding of NleB2 to the DD of RIPK1 is consistent with results from previous pull-down experiments performed in our laboratory (Jaclyn Pearson, PhD Thesis). Ectopically expressed GFP-NleB2 was immunoprecipitated with FLAG-RIPK1 by GFP pull down from HEK293T cell lysates although the binding between GFP-NleB2 and FLAG-RIPK1 appeared to be weaker than that between GFP-NleB1 and FLAG-RIPK1 (Jaclyn Pearson, PhD Thesis).

The interaction between SseK3 and the DD of TNFR1 was confirmed by a co-immunoprecipitation experiment. Additionally GFP-SseK3 appeared to GlcNAcylate

the DD of TNFR1. This finding could be confirmed by mass spectrometry. Additionally, the pull down experiment could be performed on HEK293T cells that have been transfected with FLAG-DD TNFR1 prior to infection with *S*. Typhimurium expressing a tagged version of SseK3, such as HA-tagged SseK3, or its putative catalytic mutant. SseK3 delivered by *Salmonella* during a more natural infection condition could substantially support the finding and ease concerns that the result is due to overexpression of SseK3 in the cell. The binding and modification of the DD of TNFR1 by SseK3 suggested the effector may block TNF signaling.

Stimulation of TNFR1 by TNF can result in inflammation (730). Therefore, the effects of SseK3 on the host transcription factor NF-κB and the pro-inflammatory cytokine IL-8 were investigated. While ectopically expressed GFP-SseK3 inhibited TNF-induced NF-κB activity in the NF-κB-dependent dual luciferase assay, none of the SseK effectors appeared to have a role in the inhibition of IL-8 production during *Salmonella* infection. This could be due to other effectors with anti-inflammatory properties being secreted by the *Salmonella* derivatives into the host cells such as AvrA and SspH1 (531, 553-556). It would be interesting to construct a triple *sseK* mutant in a *Salmonella* derivative lacking the major anti-inflammatory effectors or to construct and complement a *Salmonella* derivative lacking all T3SS effectors for use in tissue culture infections and IL-8 assays.

As it stands, it is unclear what the functional consequences are of either the SseK3-DD TNFR1 or SseK3-TRIM32 binding. It has been suggested that the SseK3-TRIM32 interaction may help promote SseK3 localisation to the Golgi rather than reflect an inhibition of TRIM32 function (710). TNFR1 is not Golgi located and so this strong localisation of SseK3 to the Golgi is not consistent with the DD of TNFR1 being the true target. FASP1 was found to be a putative target of SseK2 from the yeast two-hybrid screen and although preliminary yeast studies found that the binding between FASP1 and SseK2 was non-overlapping with the other SseK effectors, little is known about this mammalian protein other than its contribution to centromere

function during mitosis (731). More work is evidently required to characterise NleB2 from EPEC and SseK1-3 from *Salmonella* and to validate their host targets during infection.

A

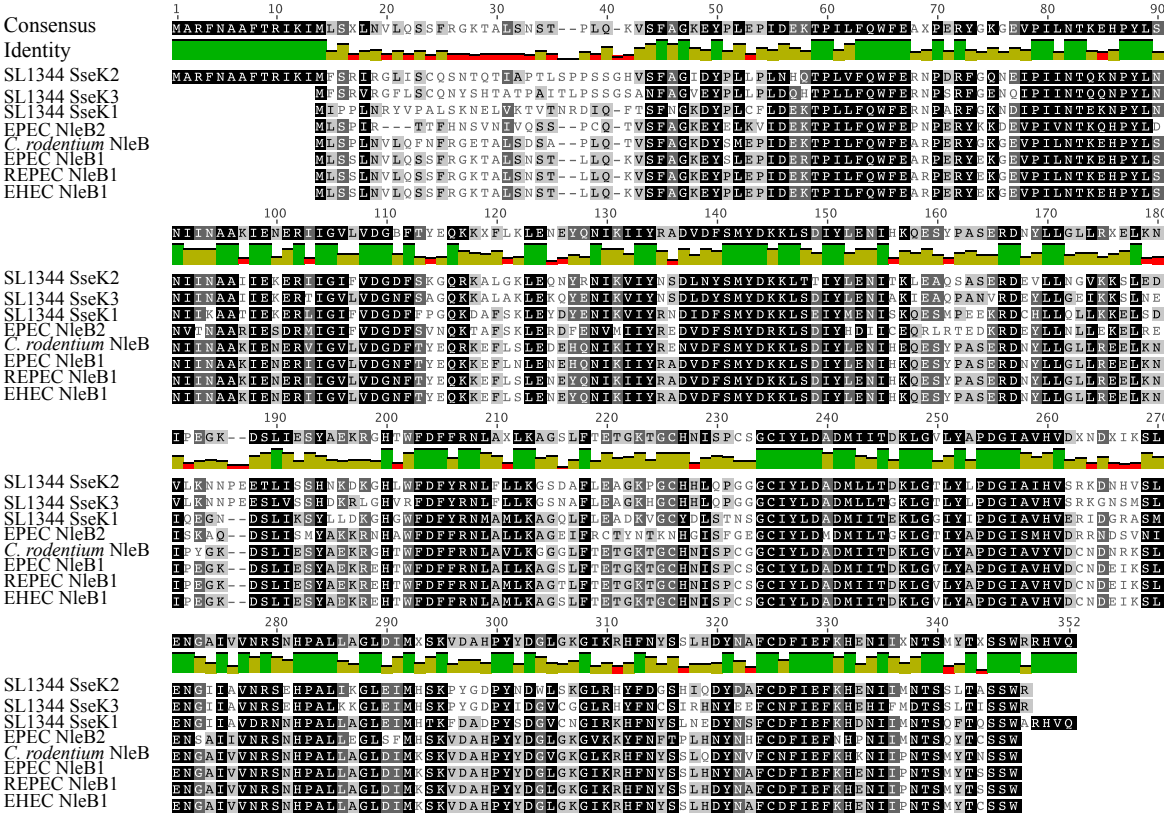
Consensus
Identity
SL1344 SseK2
SL1344 SseK3
SL1344 SseK1
EPEC NleB2
C. rodentium NleB
EPEC NleB1
REPEC NleB1
EHEC NleB1

B

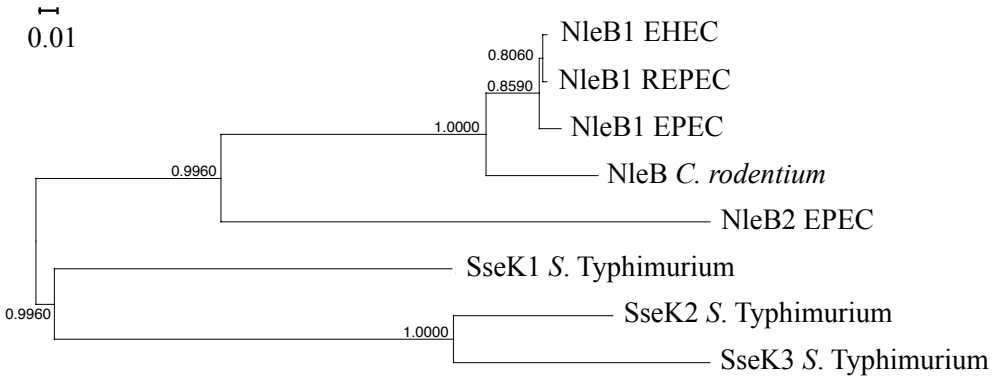
0.01
NleB1 EHEC
NleB1 REPEC
NleB1 EPEC
NleB C. rodentium
NleB2 EPEC
SseK1 S. Typhimurium
SseK2 S. Typhimurium
SseK3 S. Typhimurium
0.8060
0.8590
1.0000
0.9960
0.9960
1.0000

Figure 5.1. Analysis of NleB1 homologues from EPEC, EHEC, *C. rodentium* and *Salmonella* (A) Alignment of NleB1 homologues from EPEC, EHEC, *C. rodentium* and *Salmonella*. Eight amino acid sequences annotated as NleB1 and NleB2 EPEC (O127:H6, strain E2348/69), NleB1 EHEC (O157:H7 strain Sakai or EDL933), NleB1 REPEC (015:H⁻ strain 83/89), NleB *C. rodentium* (ICC169) and SseK1, SseK2 and SseK3 *Salmonella* Typhimurium (SL1344) with accession numbers; CAS10779, WP_000950813.1, WP_000953022.1, WP_000953025.1, WP_012905389, CBW20184, CBW18209 and CBW18025 respectively were aligned using MUSCLE (570) through the Geneious tool (571). (B) Phylogenetic analysis of NleB1 homologous proteins from EPEC, EHEC, *C. rodentium* and *Salmonella*. The alignment was used to construct a Maximum Likelihood phylogenetic tree (based on the JTT matrix-based model with 1000 bootstraps) using MEGA5 (572) to infer homology between the amino acid sequences. The tree was edited using Dendroscope (579) and is drawn to scale with branch lengths measured in the number of substitutions per site, and bootstrap values indicated on the branches.

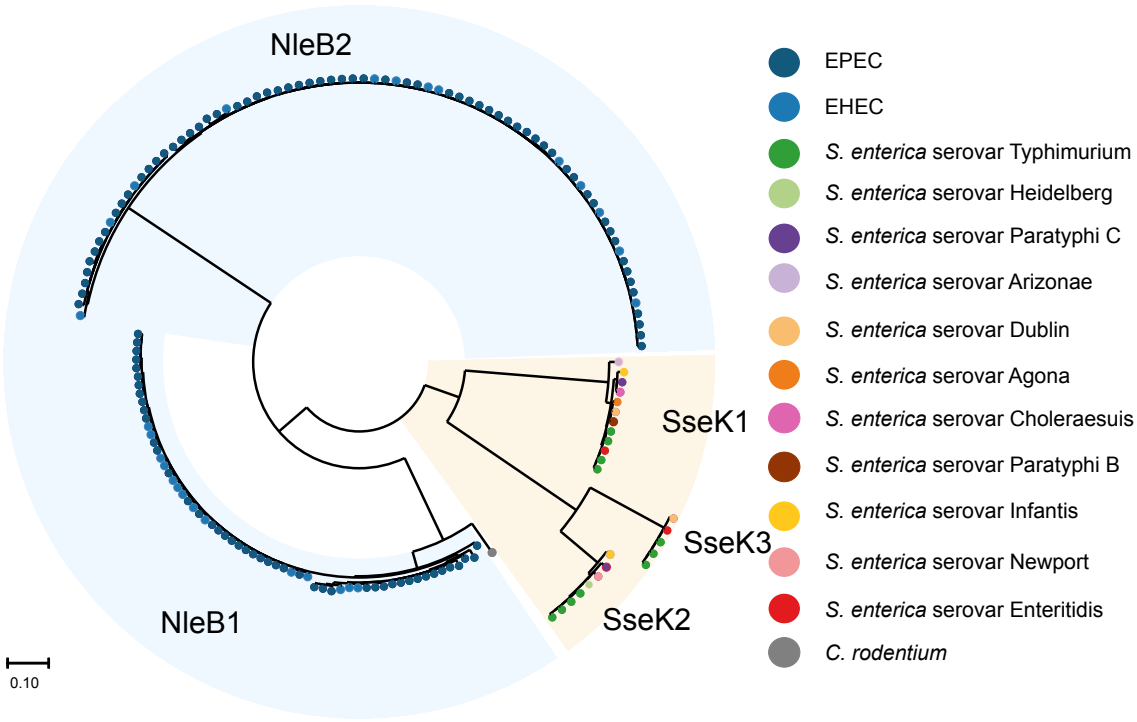

Figure 5.2. Distribution of NleB1 homologues in A/E pathogens and *Salmonella* species. Phylogenetic analysis of NleB1 homologues from EPEC, EHEC, *C. rodentium* and *Salmonella* species was computed using RAxML based on the JFF matrix-based model and was constructed using MEGA5 (572). Background colouring highlights the different genera while the tips are coloured by species or pathotype (i.e., *Salmonella* serovars). Each tip is representative of an NleB1 homologue from different isolates, i.e., there are four SseK1 homologues from four different strains of *S.* Typhimurium.

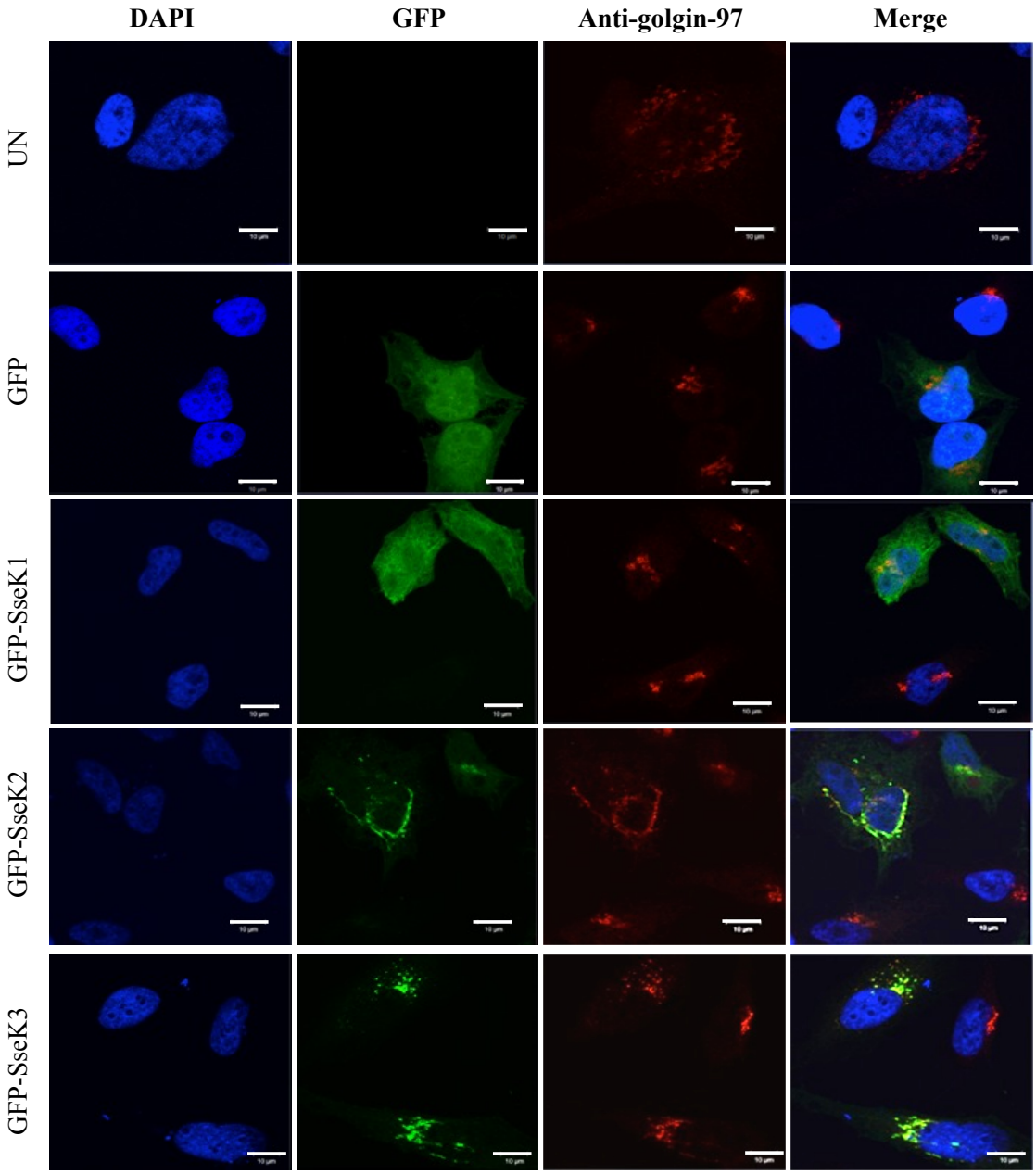

Figure 5.3. Subcellular localisation of GFP-SseK1, GFP-SseK2 and GFP-SseK3. GFP-SseK1, GFP-SseK2 and GFP-SseK3 were expressed ectopically in HeLa cells. GFP-SseK1 was uniformly distributed in the cytosol while GFP-SseK2 and GFP-SseK3 co-localised with the Golgi bodies in transfected HeLa cells. Scale bar, 10 μm. UN, untransfected HeLa cells, GFP, HeLa cells transfected with pEGFP-C2 vector.

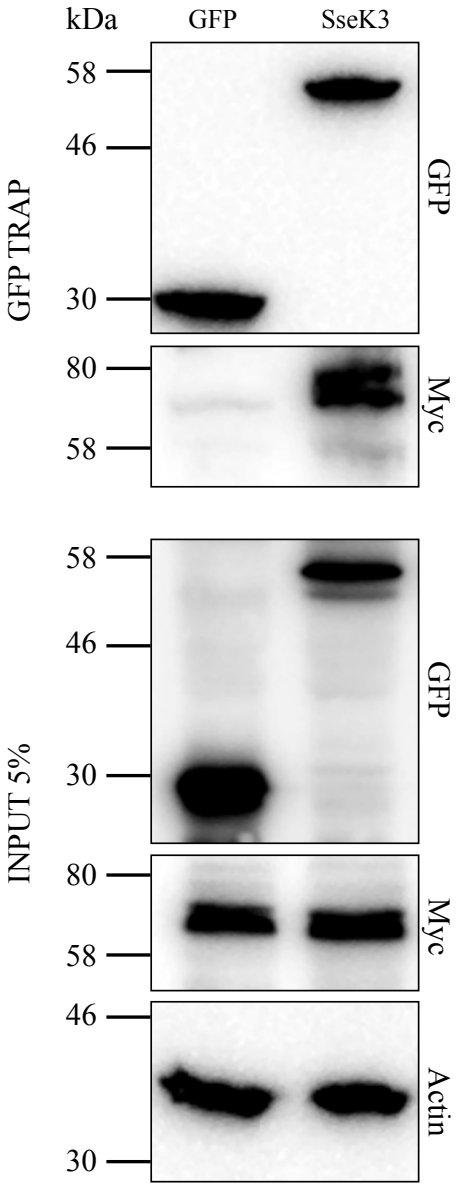

Figure 5.4. SseK3 binds to TRIM32 *in vitro*. Immunoblots of inputs and immunoprecipitates (IPs) of GFP Trap immunoprecipitations performed on lysates of HEK293T cells co-transfected with pcDNA-TRIM32 and pEGFP-C2 (GFP) or pEGFP-C2-SseK3 (GFP-SseK3). Myc-TRIM32 was tested for immunoprecipitation with GFP and GFP-SseK3 by immunoblotting of the GFP Trap IPs with anti-Myc antibodies. Antibodies to β-actin were used as a loading control. Representative immunoblot from two independent experiments.

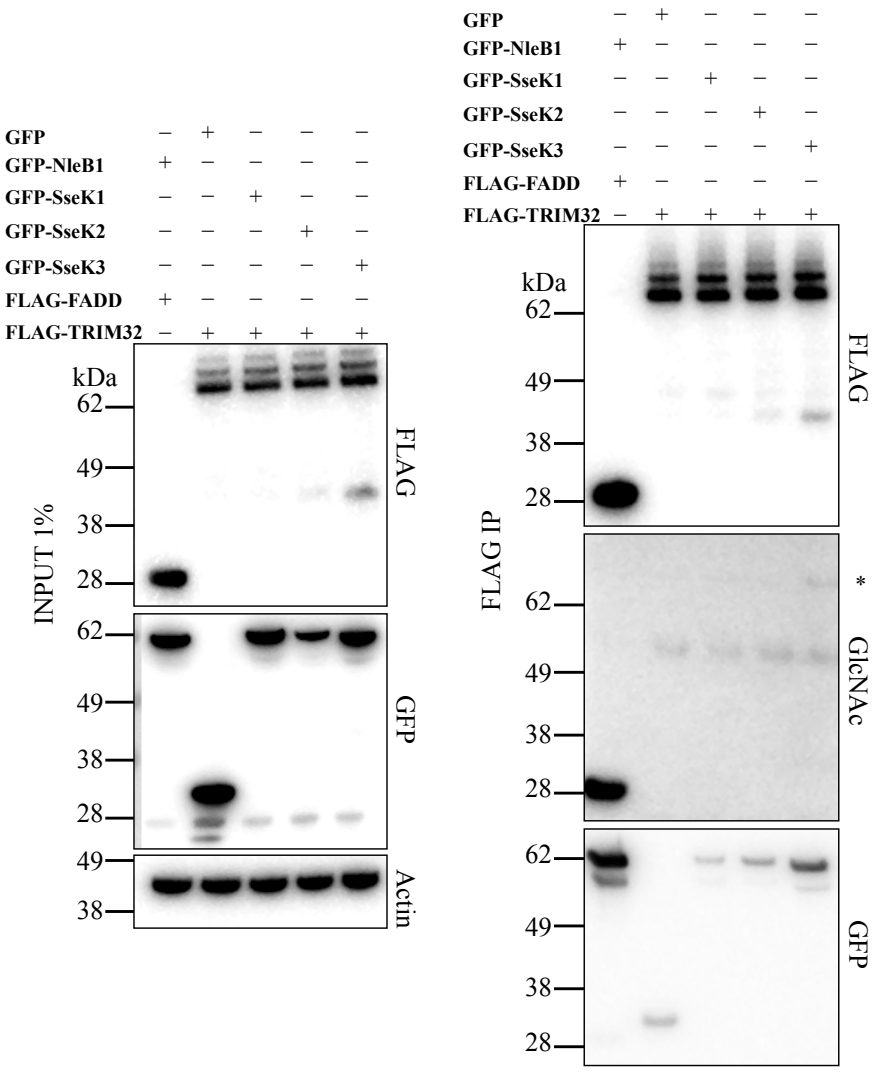

Figure 5.5. Reciprocal immunoprecipitation validates binding of SseK3 to TRIM32 *in vitro*. Immunoblots of inputs and immunoprecipitates (IPs) of anti-FLAG immunoprecipitations performed on lysates of HEK293T cells co-transfected with pFLAG-TRIM32 and pEGFP-C2 (GFP), pEGFP-C2-SseK1 (GFP-SseK1), pEGFP-C2-SseK2 (GFP-SseK2) or pEGFP-C2-SseK3 (GFP-SseK3). The FLAG-TRIM32 IPs were tested for GlcNAcylation by immunoblotting with anti-GlcNAc antibodies. A faint band (asterisk) corresponding to FLAG-TRIM32 is observed in the anti-GlcNAc immunoblot in the presence of GFP-SseK3. GFP, GFP-SseK1, GFP-SseK2 and GFP-SseK3 were tested for immunoprecipitation with FLAG-TRIM32 by immunoblotting of the IPs with anti-GFP antibodies. Antibodies to β-actin were used as a loading control. Representative immunoblot from at least three independent experiments.

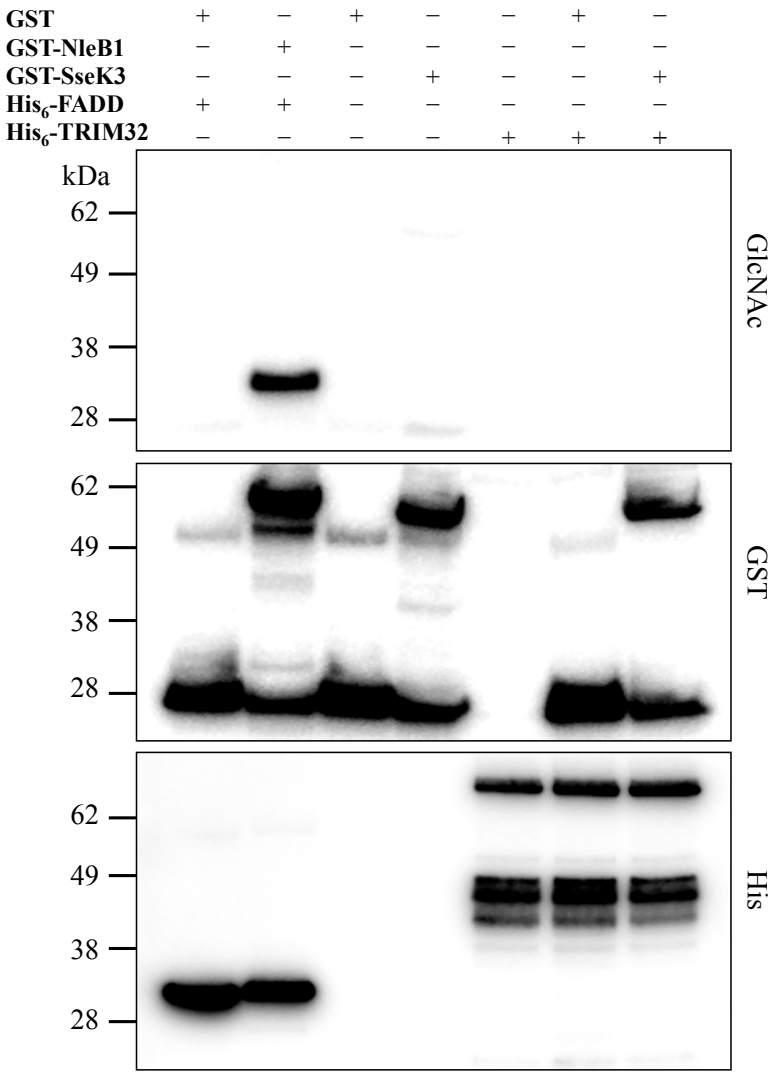

Figure 5.6. SseK3 does not GlcNAcylate TRIM32 *in vitro*. Immunoblots of recombinant protein incubations from i*n vitro* assay for SseK3-mediated GlcNAc modification of TRIM32. Recombinant GST-SseK3 and His-TRIM32 were incubated alone or together in the presence of 1 mM UDP-GlcNAc. GlcNAcylation of TRIM32 was tested by immunoblotting with anti-GlcNAc antibodies and the presence of the GST and His fusion proteins was detected by immunoblotting with anti-GST and anti-His antibodies. Representative immunoblot from at least three independent experiments. The incubation of GST-NleB1 and His-FADD was used as a control.

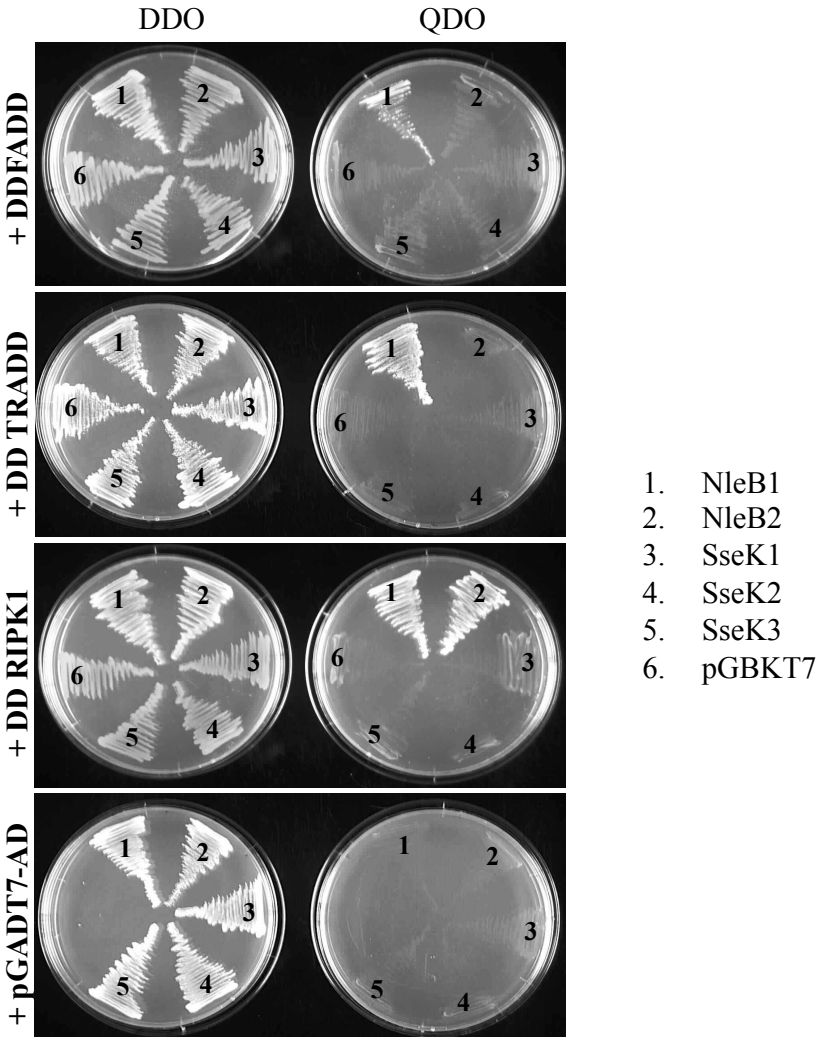

Figure 5.7. SseK1, SseK2 and SseK3 do not bind to the DD of FADD, TRADD and RIPK1. The yeast strain PJ69-4A was transformed with the indicated plasmid combinations (bait plus prey) to assay the interaction of the SseK effectors with the DDs of FADD, TRADD and RIPK1. Growth on the DDO medium is indicative of a successful transformation of bait and prey plasmids. Growth on the QDO medium indicates an interaction between bait and prey proteins.

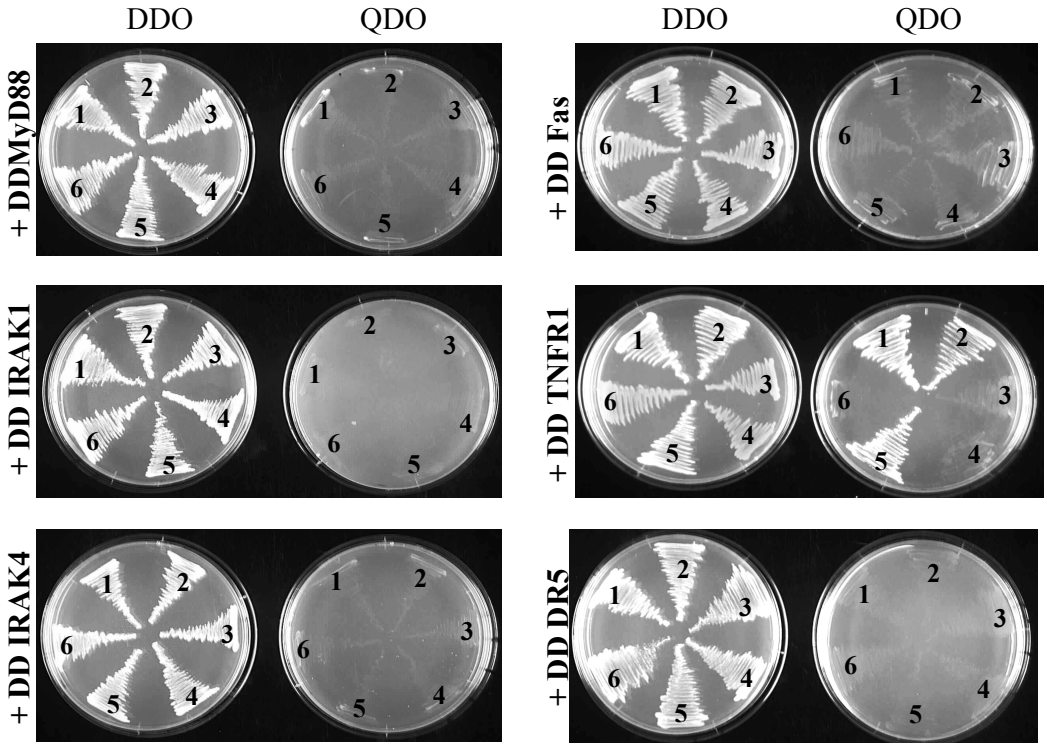

1. NleB1
2. NleB2
3. SseK1
4. SseK2
5. SseK3
6. pGBKT7

Figure 5.8. Investigation of the interaction between each of the SseK effectors and the DDs of MyD88, IRAK1, IRAK4, Fas, TNFR1 or DR5. The yeast strain PJ69-4A was transformed with the indicated plasmid combinations (bait plus prey) to assay the interaction of the SseK effectors with the DDs of MyD88, IRAK1, IRAK4 which lack the conserved arginine, and the DDs of the DRs Fas, TNFR1 and DR5. Yeast strains were grown on the selective media, DDO and QDO media. Growth on the DDO medium is indicative of a successful transformation of bait and prey plasmids. Growth on the QDO medium indicates an interaction between bait and prey proteins.

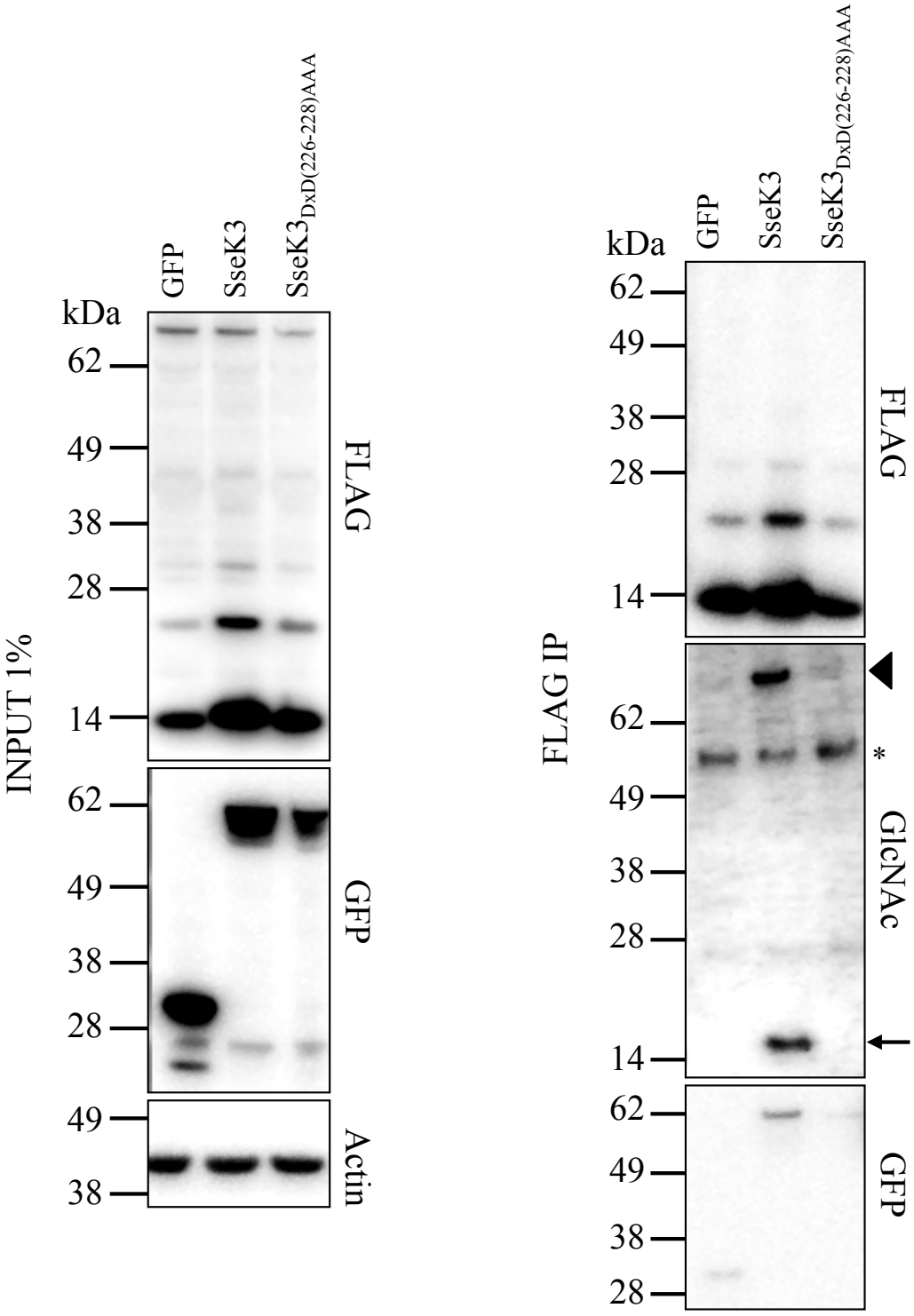
INPUT 1%
GFP
SseK3
SseK3DxD(226-228)AAA
kDa
62
49
38
28
14
FLAG
GFP
Actin
FLAG IP
GlcNAc
*

Figure 5.9. SseK3 binds and GlcNAcylates the DD of TNFR1. Immunoblots of inputs and immunoprecipitates (IPS) of anti-FLAG immunoprecipitations performed on lysates of HEK293T cells co-transfected with pFLAG-DD TNFR1 and pEGFP-C2, pEGFP-C2-SseK3 (GFP-SseK3) or pEGFP-C2-SseK3$_{DxD(226-228)AAA}$ (putative catalytic mutant GFP-SseK3$_{DxD(226-228)AAA}$). The FLAG-DD TNFR1 IPs were tested for GlcNAcylation by immunoblotting with anti-GlcNAc antibodies. GFP, GFP-SseK3 and GFP-SseK3$_{DxD(226-228)AAA}$ were tested for immunoprecipitation with FLAG-DD TNFR1 by immunoblotting of the IPs with anti-GFP antibodies. Antibodies to β-actin were used as a loading control. Representative immunoblot from at least three independent experiments. Asterisk denotes non-specific bands. Arrow indicates GlcNAcylated DD of TNFR1 and arrowhead possibly indicates GlcNAcylated multimers of DD of TNFR1.

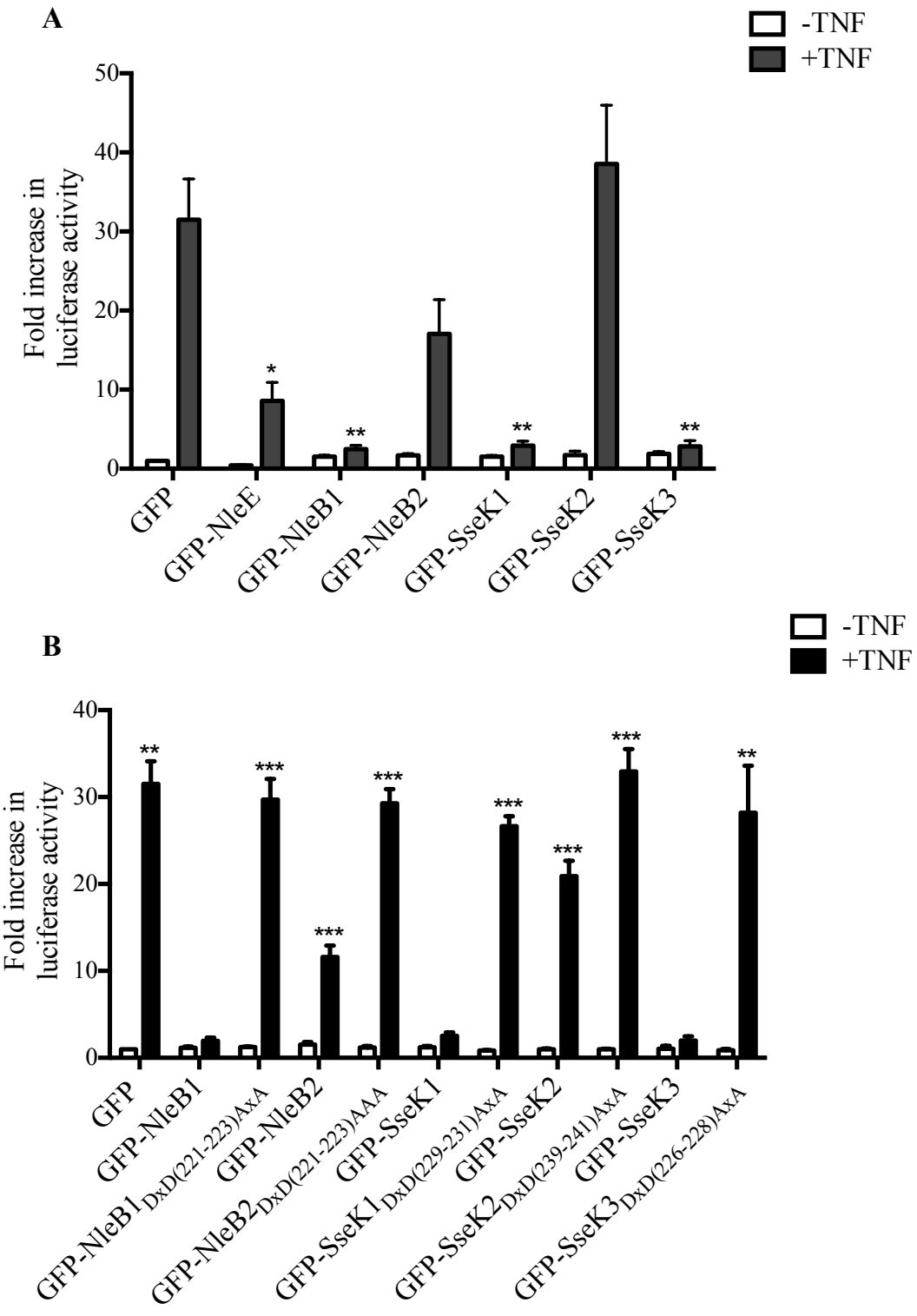
A
-TNF
+TNF
Fold increase in luciferase activity
50
40
30
20
10
0
*
**
**
**
GFP
GFP-NleE
GFP-NleB1
GFP-NleB2
GFP-SseK1
GFP-SseK2
GFP-SseK3
B
-TNF
+TNF
Fold increase in luciferase activity
40
30
20
10
0
**
***
***
***
***
***
***
**
GFP
GFP-NleB1
GFP-NleB1DxD(221-223)AxA
GFP-NleB2
GFP-NleB2DxD(221-223)AAA
GFP-SseK1
GFP-SseK1DxD(229-231)AxA
GFP-SseK2
GFP-SseK2DxD(239-241)AxA
GFP-SseK3
GFP-SseK3DxD(226-228)AxA

Figure 5.10. Effect of SseK1, SseK2, SseK3 and the putative catalytic mutants on NF-κB activation in response to TNF stimulation. (A) Fold increase in NF-κB dependent luciferase activity in HeLa cells transfected with pEGFP-C2 (GFP), pEGFP-C2-NleE (GFP-NleE), pEGFP-C2-NleB1 (GFP-NleB1), pEGFP-C2-NleB2 (GFP-NleB2), pEGFP-C2-SseK1 (GFP-SseK1), pEGFP-C2-SseK2 (GFP-SseK2) or pEGFP-C2-SseK3 (GFP-SseK3) and left unstimulated or stimulated with TNF for 16 h where indicated. Results are the mean ± SEM of three independent experiments carried out in duplicate. *** Significant difference (*p<0.05, **p<0.01, ***p<0.001, ****p<0.0001), one way ANOVA with Tukey's multiple comparisons test. (B) Fold increase in NF-κB dependent luciferase activity in HeLa cells transfected with pEGFP-C2 (GFP), pEGFP-C2-NleB1 (GFP-NleB1), pEGFP-C2-NleB2 (GFP-NleB2), pEGFP-C2-SseK1 (GFP-SseK1), pEGFP-C2-SseK2 (GFP-SseK2), pEGFP-C2-SseK3 (GFP-SseK3) or the constructs expressing the putative catalytic mutants and left unstimulated or stimulated with TNF for 16 h where indicated. Results are the mean ± SEM of three independent experiments carried out in duplicate. *** Significant difference (*p<0.05, **p<0.01, ***p<0.001, ****p<0.0001), one way ANOVA with Tukey's multiple comparisons test.

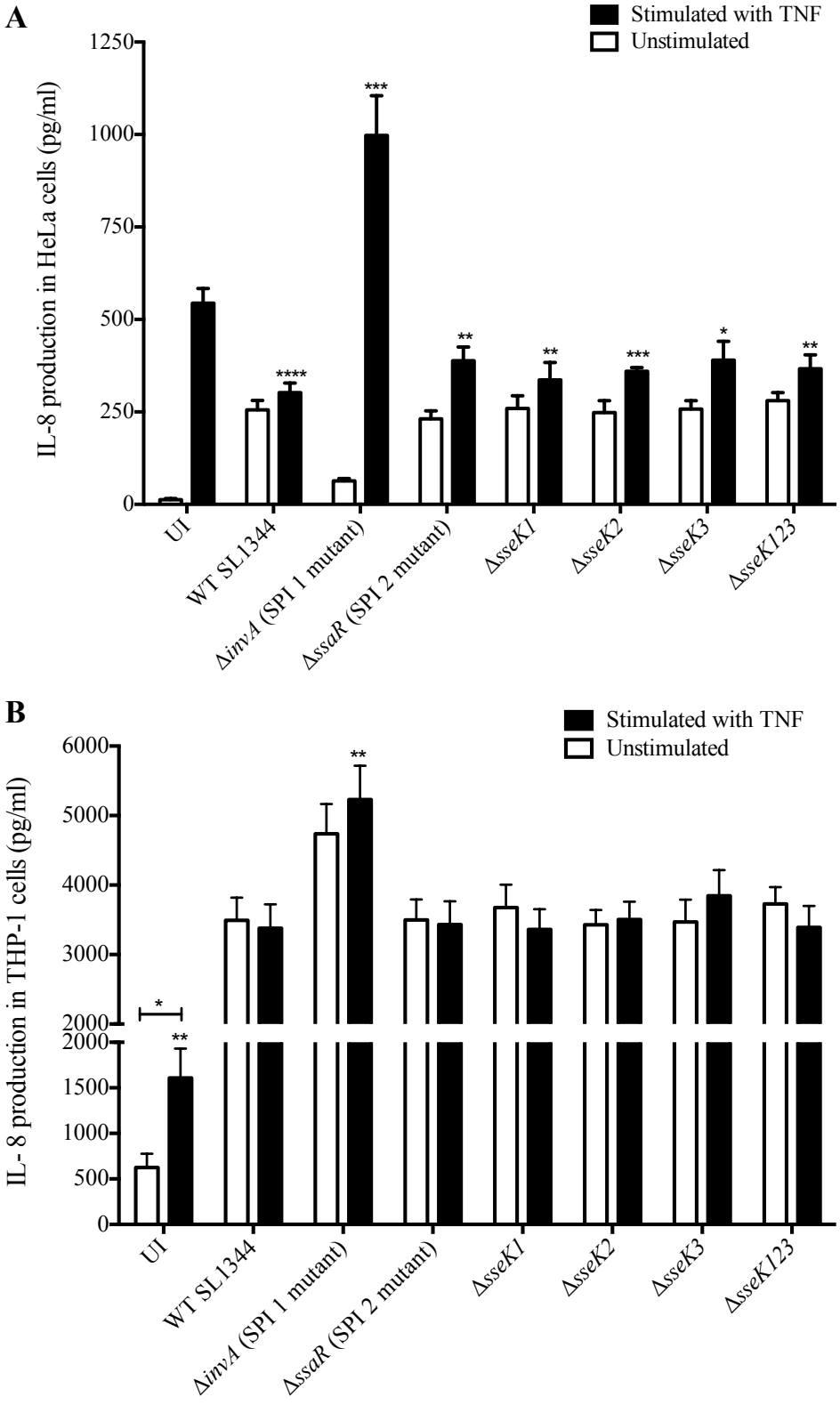
A
Stimulated with TNF
Unstimulated
IL-8 production in HeLa cells (pg/ml)
1250
1000
750
500
250
0
***
****
**
**
***
*
**
UI
WT SL1344
ΔinvA (SPI 1 mutant)
ΔssaR (SPI 2 mutant)
ΔsseK1
ΔsseK2
ΔsseK3
ΔsseK123
B
Stimulated with TNF
Unstimulated
IL- 8 production in THP-1 cells (pg/ml)
6000
5000
4000
3000
2000
2000
1500
1000
500
0
**
*
**
UI
WT SL1344
ΔinvA (SPI 1 mutant)
ΔssaR (SPI 2 mutant)
ΔsseK1
ΔsseK2
ΔsseK3
ΔsseK123

Figure 5.11. Effect of SseK1, SseK2 and SseK3 on TNF-induced IL-8 secretion from infected HeLa and THP-1 cells. (A) HeLa cells were infected with derivatives of *S.* Typhimurium SL1344 for 2 h and left unstimulated (white bars) or stimulated with TNF (black bars) for 6 h. Results are the mean ± SEM of at least three independent experiments carried out in duplicate. *** Significant difference (*p<0.05, **p<0.01, ***p<0.001), one way ANOVA with Tukey's multiple comparisons test. (B) THP-1 cells were infected with derivatives of *S.* Typhimurium SL1344 for 2 h and left unstimulated (white bars) or stimulated with TNF (black bars) for 6 h. Results are the mean ± SEM of at least three independent experiments carried out in duplicate. *** Significant difference (*p<0.05, **p<0.01, ***p<0.001), one way ANOVA with Tukey's multiple comparisons test.

A

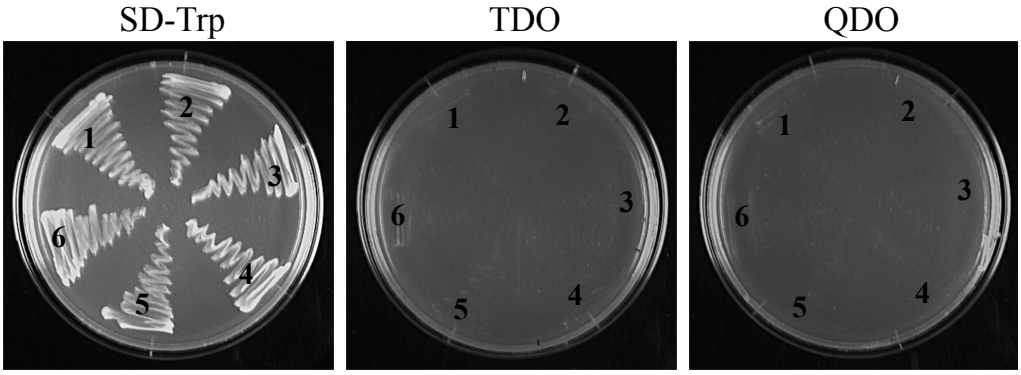

1. AH109 (pGBKT7)
2. AH109 (pGBKT7-NleB1)
3. AH109 (pGBKT7-NleB2)
4. AH109 (pGBKT7-SseK1)
5. AH109 (pGBKT7-SseK2)
6. AH109 (pGBKT7-SseK3)

B

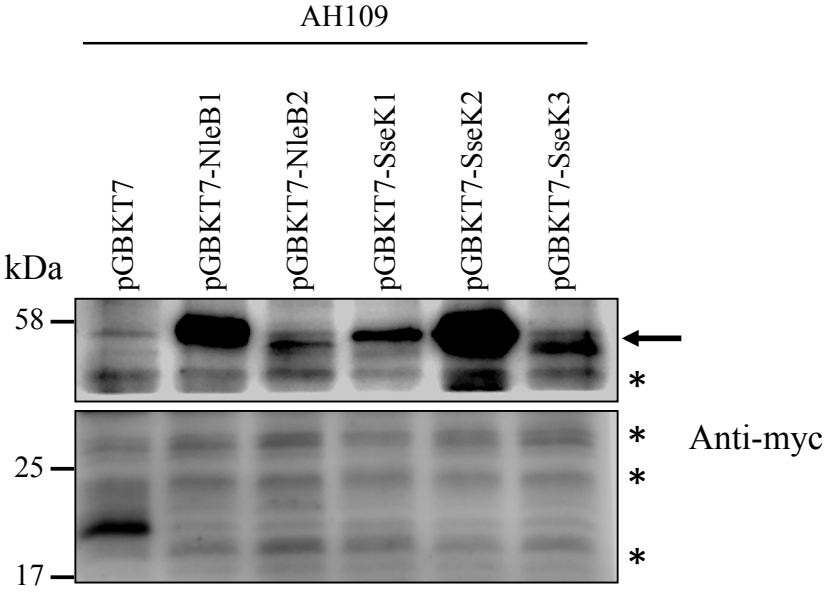

Figure 5.12 Expression of bait proteins NleB2, SseK1, SseK2 and SseK3 in yeast. (A) The yeast strain AH109 was transformed individually with each of the bait constructs pGFBKT7-NleB1, pGBKT7-NleB2, pGBKT7-SseK1, pGBKT7-SseK2 and pGBKT7-SseK3 and the transformants were plated on the selective media SD-Trp, TDO (medium stringency media, SD-Trp-Leu-His) and QDO (highest stringency, SD-Trp-Leu-Ade-His). Growth on the SD-Trp medium indicates a successful transformation with the bait plasmid. Absence of growth on the TDO and QDO plates is indicative of no autoactivation of reporter genes by the bait protein. (B) Proteins were extracted from the transformed yeast and subjected to gel electrophoresis and immunoblotting. The expression of the fusion bait proteins (indicated by an arrow) was determined using anti-myc antibodies. Representative immunoblot from at least two independent experiments. Asterisk denotes non-specific bands.

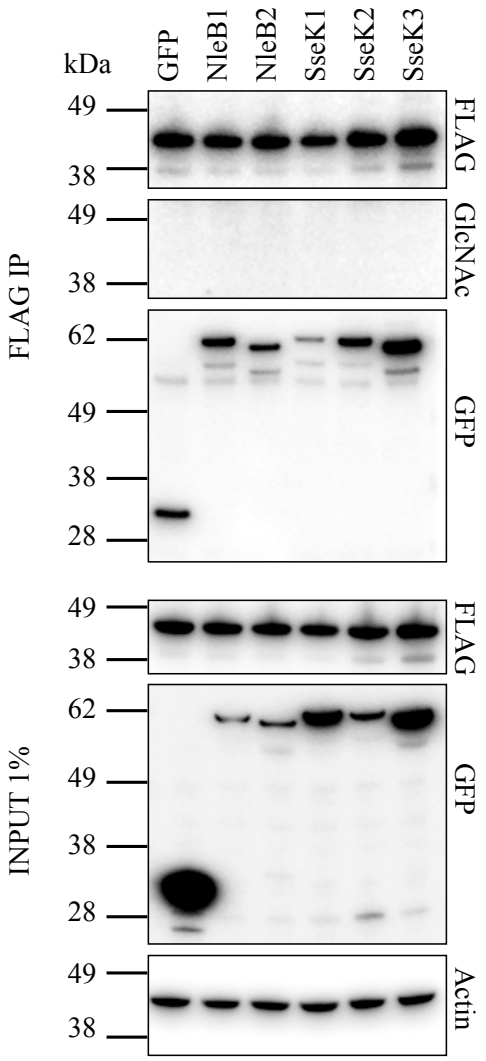

Figure 5.13. Testing the interaction between the NleB/SseK effectors and CSN5 by co-immunoprecipitation. Immunoblots of inputs and immunoprecipitates (IPs) of anti-FLAG immunoprecipitations performed on lysates of HEK293T cells co-transfected with pFLAG-CSN5 and pEGFP-C2 (GFP), pEGFP-C2-NleB1 (GFP-NleB1), pEGFP-C2-NleB2 (GFP-NleB2), pEGFP-C2-SseK1 (GFP-SseK1), pEGFP-C2-SseK2 (GFP-SseK2) or pEGFP-C2-SseK3 (GFP-SseK3). The FLAG-CSN5 IPs were tested for GlcNAcylation by immunoblotting with anti-GlcNAc antibodies. GFP, GFP-NleB1, GFP-NleB2, GFP-SseK1, GFP-SseK2 and GFP-SseK3 were tested for immunoprecipitation with FLAG-CSN5 by immunoblotting of the IPs with anti-GFP antibodies. Antibodies to β-actin were used as a loading control. Representative immunoblot from at least three independent experiments.

A

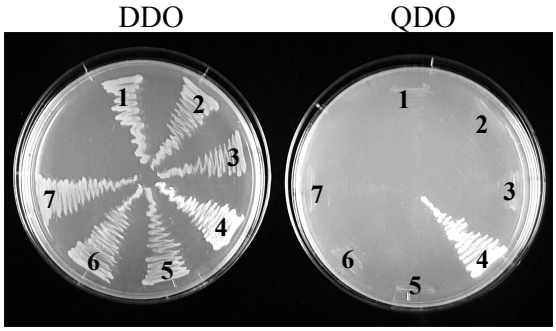

1. SseK1 + pGADT7-AD
2. SseK1 + FASP1
3. SseK2 + pGADT7-AD
4. SseK2 + FASP1
5. SseK3 + pGADT7-AD
6. SseK3 + FASP1
7. pGBKT7 + FASP1

B

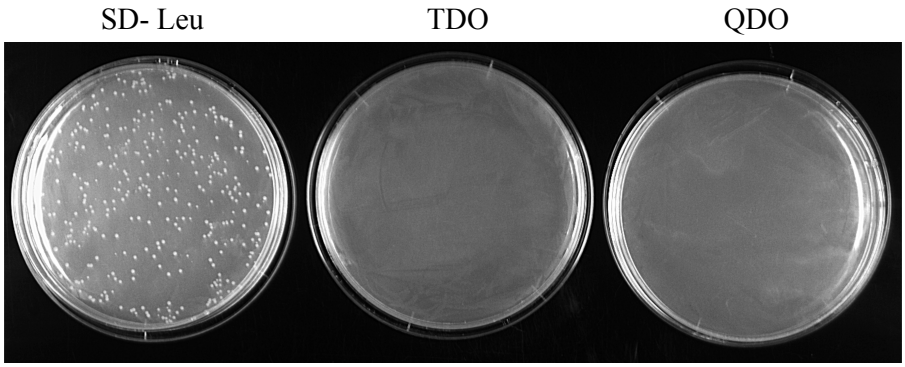

Figure 5.14. The binding of SseK2 to FASP1 in yeast is non-overlapping with SseK1 or SseK2. (A) The yeast strain PJ69-4A was transformed with the bait constructs pGBKT7-SseK1, pGBKT7-SseK2 or pGBKT7-SseK3 and the prey plasmid expressing FASP1. The transformants were plated on the selective media DDO (SD-Trp-Leu) and QDO (SD-trp-Leu-Ade-His). Growth on the DDO medium indicates a successful transformation with both bait and prey constructs. Growth on the QDO medium indicates the presence of an interaction between the bait and prey proteins. (B) FASP1 expression in yeast does not autoactivate reporter genes in yeast. The yeast strain PJ69-4A was transformed with the prey plasmid expressing FASP1. The transformants were plated on the selective media SD-Leu, TDO (medium stringency media, SD-Trp-Leu-His) and QDO (highest stringency, SD-Trp-Leu-Ade-His). Growth on the SD-Leu medium indicates a successful transformation. Absence of growth on the TDO and QDO plates is indicative of no autoactivation of reporter genes by the bait protein.

Table 5.1 Comparison between the NleB/SseK effectors

Comparison between effectors	% identity	% similarity
NleB1 *versus* NleB2	61.2	84.3
NleB1 *versus* SseK1	61.8	84.3
NleB1 *versus* SseK2	57.3	83.1
NleB1 *versus* SseK3	57.8	80.4
NleB2 *versus* SseK1	55.7	80.9
NleB2 *versus* SseK2	48.2	76.6
NleB2 *versus* SseK3	49.5	78.1
SseK1 *versus* SseK2	61.8	85.2
SseK1 *versus* SseK3	60.5	83.9
SseK2 *versus* SseK3	75.2	91.6

Table 5.2 List of potential binding partners of NleB2

NleB2 binding protein	GenBank accession number	Total amino acids	Amino acids in Y2HS clone	Number of times uncovered
Phosphoglucomutase-1 isoform 3	NP_001166290.1	365	264-365, 271-365, 273-365	5
COP9 signalosome complex subunit 5	NP_006828.2	334	35-200, 35-334	5
COP9 signalosome complex subunit 5 variant	BAD92371.1	276	17-150, 17-153	2
40 S ribosomal protein S20 isoform 2	NP_001014.1	119	42-119	1
Cysteine and histidine-rich domain-containing protein 1 isoform X2	XP_011541050.1	218	15-218	1
Na+/K+ transporting ATPase beta 3 polypeptide	AAX55913.1	137	50-137	1
Niemann-Pick disease, type C2, isoform CRA_b	EAW81178.1	199	32-199	1
Dynein, cytoplasmic 1, heavy chain 1, isoform CRA_a	EAW81759.1	4583	4436-4583	1

Table 5.3 List of potential binding partners of SseK1

SseK1 binding protein	GenBank accession number	Total amino acids	Amino acids in Y2HS clone	Number of times uncovered
COP9 signalosome complex subunit 5	NP_006828.2	334	10-309	2
SNARE-associated protein Snapin	NP_036569.1	136	38-136, 45-136	2
Tapasin isoform 3 precursor	NP_757346.2	361	231-257	1
Glutamine-rich protein 1	NP_060200.2	776	693-776	1
Protein TALPID isoform 1	NP_001231118.1	1644	1382-1644	1
DNA-(apurinic or apyrimidinic site) lyase 2 isoform 2	NP_001258677.1	347	47-283	1
Filamin-B isoform 4	NP_001157791.1	2578	1546-1802	1

Table 5.4 List of potential binding partners of SseK2

SseK2 binding protein	GenBank accession number	Total amino acids	Amino acids in Y2HS clone	Number of times uncovered
Protein Mis18-alpha	NP_061817.1	233	128-233	1

Table 5.5 List of potential binding partners of SseK3

SseK3 binding protein	GenBank accession number	Total amino acids	Amino acids in Y2HS clone	Number of times uncovered
Hypothetical protein	CAE45949.1	714	1-13, 1-14	11
COP9 signalosome complex subunit 5 variant	BAD92371.1	276	17-130, 17-249, 93-210, 110-229, 113-233	5
COP9 signalosome complex subunit 5	NP_006828.2	334	24-334, 49-238, 49-280, 49-334	4
Isopentenyl-diphosphate Delta-isomerase 1 isoform X1	XP_005252502.1	228	49-228, 50-228	3
ZBED5 protein	AAH47754.1	495	68-317, 68-325, 68-335,	4
Na^+/K^+ transporting, beta 3 polypeptide	AAX55913.1	137	2-137, 69-137	2
Na^+/K^+ transporting, beta 3 polypeptide	AAX55911.1	119	1-119	1
Na^+/K^+ transporting, beta 3 polypeptide	EAW78989.1	198	78-198	1
Chain B, crystal structure of human	4FJV_B	86	1-13	2

otubain 2 and ubiquitin complex				
MAGE-D2	AAG38603.1	135	65-97	2
Peptidyl-prolyl cis-trans isomerase FKBP3 isoform X1	XP_011534867.1	191	74-187, 74-191	2
SNARE-associated protein Snapin	NP_036569.1	136	45-136	1
Cytoskeleton associated protein 5 (CKAP5)	AAH35554	953	292-566	1
Phosphoglucomutase-1	NP_001166290.1	365	271-365	1
Pyruvate dehydrogenase protein X component, mitochondrial isoform X1	XP_011518692.1	441	63-292	1
Brain mitochondrial carrier protein 1 isoform 2 precursor	NP_001269125.1	322	23-135	1
Ins P4-binding protein	CAA61580.1	834	694-715	1
Electroneutral sodium bicarbonate exchanger 1 isoform X5	XP_006719763.1	800	748-800	1
Calsyntenin-1 isoform 2 precursor	NP_055759.3	971	285-329	1

Extracellular protein	AAA65590.1	387	302-355	1
Unnamed protein product	BAH14414.1	247	105-247	1
Alpha-5 type IV collagen	AAA99480.1	1604	1477-1604	1
Dynactin 2 (p50), isoform CRA_a	EAW97027.1	138	112-138	1
Ribosome-releasing factor 2, mitochondrial isoform 2	NP_733792.1	732	544-732	1

Chapter 6

Perspectives

Chapter 6. Perspectives

Enteric bacterial pathogens such as EPEC, EHEC and *Salmonella* have evolved by the acquisition of a formidable array of virulence determinants that enable them to colonise the intestinal tract. The exposure of intestinal cells to EPEC-derived PAMPs, intimate attachment of the bacteria as well as the activity of effector proteins such as Map, EspF, Cif and EspH all stimulate intrinsic apoptotic pathways and stress responses that are countered by effectors such as NleD, NleF, EspZ and EspO. The action of these cell death-suppressing effectors promotes survival of the infected cell, thereby prolonging EPEC adherence to the intestinal mucosa. In addition, EPEC has evolved specific mechanisms to inhibit death receptor-mediated inflammation and apoptosis in response to immune system surveillance and host death ligand-mediated elimination of infected cells. Importantly, the GlcNAc transferase activity of NleB1 and its role in the inhibition of extrinsic apoptotic cell death revealed a previously unappreciated role for Fas signalling in fighting gut infection and exemplifies how EPEC has adapted to avoid the intestinal innate immune response.

Renewed interest in the contribution of protein glycosylation to bacterial pathogenesis has recently highlighted a class of soluble bacterial *N*-linked asparagine glycosyltransferases (NGTs) (732, 733). Furthermore, glycoproteins from pathogenic bacteria such as *Haemophilus influenzae* (597, 734), *Actinobacillus pleuropneumoniae* (733), *Pseudomonas aeruginosa* (735, 736), *Neisseria meningitidis* (737) and *Campylobacter jejuni* (738) also highlight the importance of bacterial glycosylation. The uniqueness of NleB1 as a glycosyltransferase lies in its ability to catalyse arginine *N*-GlcNAcylation given that arginine is an unconventional glycosyl acceptor site. Arginine residues are commonly subjected to post-translational modifications such as methylation (739-741) or deimination (citrullination) of their guanidine side chains (742) by methyl transferases or deiminases. So far, other than NleB1-mediated arginine glycosylation of DD proteins, only two modifications involving an arginine have been documented; the identification of the sweet corn

amylogenin which self-β glucosylates on an arginine residue in 1995 (743) and the more recent arginine rhamnosylation of the translation elongation factor (EF-P) in bacteria (608).

In this study, we aimed to investigate the functional regions as well as the potential substrate docking sites of NleB1 in order to gain a better understanding of this unusual glycosyltransferase. The residues Y219 and E253 were found to be critical for the catalytic activity of NleB1 *in vitro* and *in vivo* but not for the binding of NleB1 to FADD. It is possible that Y219 of NleB1 could interact with UDP-GlcNAc given that the conserved tyrosines of *C. difficile* toxin A (Y283) and *C. difficile* toxin B (Y284A) are positioned in close proximity to the ribose ring of UDP-Glc (607, 685, 686). Although E253 is highly conserved among the NleB/SseK effectors, it is not found in other glycosyltransferases and may be involved in the unusual ability of NleB1 to glycosylate arginine. However, in the absence of empirical structural information, the function of E253 in NleB1 enzymatic activity is unknown.

How NleB1 catalyses this unique glycosylation reaction is not understood. Two mechanisms of action have been proposed for both GT-A and GT-B glycosyltransferases (inverting or retaining) based on the anomeric carbon configuraton of the donor sugar substrate (586). The inverting mechanism is expected to follow a single S_N-2 like nucleophilic substitution reaction whereby an amino acid side chain within the enzyme serves as a base catalyst that deprotonates the incoming nucleophile of the acceptor substrate (586). Aspartate (D), glutamate (E) or His (H) residues are popular candidates for the catalytic base which can be located within or outside the DxD motif (744). It has been suggested that H498 is more likely to be the catalytic base in human OGT which is an inverting GT-B enzyme (687) while H558 (745) or a tyrosine (Y) residue (746) have been suggested in the bacterial homologues. In contrast, the mechanism of retaining glycosyltransferases is still being debated (586). A double-displacement mechanism involving a covalently bound glycosyl-enzyme intermediate has been suggested (586). This model demands the

existence of an appropriately positioned nucleophile in the enzyme active site. Following the first nucleophilic substitution on the sugar donor, the diphosphate leaving group is thought to assume the role of base catalyst, activating the incoming acceptor substrate for the second nucleophilic attack. Although the feasibility of this model of action has long been questioned due to the absence of a reported catalytic nucleophile or catalytically competent covalent intermediate (586), the recent detection of covalent glycosyl-enzyme intermediates for GalNAc-transferase GTA and Gal-transferase GTB has alleviated doubts on the double-displacement mechanism (747).

The possibility of either residue (Y219 or E253) functioning as catalytic base in the case of an inverting mechanism or as a nucleophile in the case of a retaining mechanism has not been investigated. While the mechanism of action of NleB1 could first be addressed by determining the type of glycosidic linkage (α or β) between the GlcNAc moiety and the DD of FADD, TRADD or RIPK1 by combining ^{1}H-NMR spectroscopy and mass spectrometry, a more pressing question is how a conserved arginine within the DDs can be deprotonated given that it is a very poor nucleophile. Interestingly, several mechanistic models for *N*-glycosylation by OST have been proposed given that the amide group of asparagine is a rather poor nucleophile. Amides are planar structures and the nitrogen lone pair is delocalised with the π-system of the carbonyl group (748). While it was initially believed that the amide group required activation by the enzyme possibly by an amide-imidol tautomerisation event (749), the crystal structure of *Campylobacter lari* OST PglB has disproved this tautomerisation hypothesis for OST and proposed a model whereby the amide is twisted (C-N bond twisting) (750). However, the latter mechanism was deemed to be unlikely in the case of *N*-glycosylation by the *N*-glycosyltransferase of *Actinobacillus pleuropneumoniae* HMWC1 (732). Tautomerism of guanidines has been reported and can be studied by ^{15}N-NMR (751). Therefore, this questions the possibility of NleB1 activating the guanidine group of arginine by a tautomerisation event. The crystal structure of NleB1 in complex with and without UDP-GlcNAc will help provide

insights into mechanism of action of this unique enzyme and shed light on this unusual post translational modification.

Upon mutation of the amino acids $PDG^{236-238}$, the resulting NleB1 mutant was unable to bind and GlcNAcylate FADD *in vitro*. Other than this region, no other residue or stretch of residues essential for enzyme-acceptor substrate binding was uncovered in this study. It is possible that the mutation of multiple sites is required to abrogate binding to the substrate FADD rather than the mutation of a single site. The crystal structure of NleB1 will help to ascertain the contribution of the amino acids $PDG^{236-238}$ in acceptor substrate binding. However, this motif is also conserved in the SseK effectors. Therefore, this questions the likelihood for the role of the PDG motif in substrate recognition given that the SseK effectors do not appear to share the same binding partners as NleB1. Alternatively, NleB1 substrate recognition may occur via peptide conformation recognition. Recently, crystal structures of human OGT in complex with substrate peptides have shown that the substrates bind the active site in an extended fashion (687, 752-754). This suggests that the enzyme may recognise a conserved extended peptide conformation or 'molecular mimicry' surrounding the O-GlcNAc site irrespective of amino acid sequence, rather than relying merely on TPR motifs, which are not always present in bacterial homologues of OGTs (755).

Mutation of the residues $PILN^{63-66}$ to alanines did not prevent the binding of NleB1 to FADD despite inhibiting glycosyltransferase activity. This mutant was also not translocated by the T3SS during EPEC infection. Therefore, the residues 63-66 of NleB1 were hypothesised to be important for translocation and perhaps chaperone binding. This could be addressed by comparing the translocation of $NleB1_{PILN(63-66)AAAA}$ from wild type EPEC and a Δ*cesT* strain, given that CesT is a chaperone for Tir and other non-LEE encoded effectors (756).

The presence of NleB1 homologues in *Salmonella* suggests that arginine GlcNAcylation may not be exclusive to EPEC. The presence of the DxD motif and

conserved equivalent Y219 and E253 residues leads us to speculate that NleB2 from EPEC and the SseK effectors from *Salmonella* could also possess glycosyltransferase activity whose donor and acceptor substrates differ to those of NleB1. Additionally, the Golgi localisation of SseK2 and SseK3 is reminiscent of the Golgi localisation of mammalian glycosyltransferases (757). To investigate the glycosyltransferase activity of these homologues, mammalian intestinal or macrophage cell lysates could be incubated with purified NleB2, SseK1, SseK2 or SseK3 and radiolabeled UDP sugar donors. The incubated lysates can be subjected to SDS-PAGE and autoradiography. Alternatively, recent success in generating an antibody that can efficiently recognise arginine *N*-GlcNAcylation (758) could be helpful in addressing this question as well as in building up a compendium of possible host arginine-GlcNAcylated targets. On the other hand, it remains a possibility that the SseK effectors have the same target as NleB1 but in different mammalian species. For example, while theres is no clear evidence for a major role of SseK1 in virulence in mice, a screen of random insertion mutants of *S*. Typhimurium using transposon-directed insertion site-sequencing (TraDIS) revealed the importance of SseK1 in the colonisation of chickens, pigs and cattle (759). Therefore, cell lines from different mammalian species could be used while investigating the glycosyltransferase activity of these homologues *in vitro*.

Li *et al*. found that NleB1 inhibited an alternative form of cell death following TNFR1 stimulation called necroptosis (441). Stimulation of TNFR1 can lead to necroptosis upon inhibition of caspase-8 activation (231). The adaptor protein RIPK1 binds RIPK3 leading to the phosphorylation of MLKL by activated RIPK3. Phosphorylated oligomers of MLKL translocate to the plasma membrane leading to necroptosis (760). Interestingly, unpublished work in our laboratory has shown that another EPEC effector, EspL, inhibits host cell death by necroptosis upon stimulation of the TNFR1 (Pearson *et al*., 2015, submitted). MDF cells which express both RIPK1 and RIPK3 were protected from necroptosis upon stimulaton of the TNFR1 by TNF, the caspase inhibitor z-VAD and the SMAC-mimetic IAP antagonist compound A, in the presence of EspL. This was shown to be due to the cleavage of RIPK1 and

RIPK3 in a conserved region called the receptor-interacting protein (RIP) homotypic interaction motifs (RHIM), which was mediated by the cysteine protease activity of EspL. Interestingly, EspL is encoded upstream of NleB1 and NleE on the integrative element IE6 of the EPEC genome. Thus, EPEC has gained the ability to control inflammatory, apoptotic and necroptotic signaling by acquiring a single genetic locus encoding the T3SS effectors EspL, NleB1 and NleE.

The acquisition of these three effectors together was observed in typical EPEC, EHEC (761) as well as some atypical EPEC strains in a recent study (762). Atypical EPEC causes mild but prolonged diarrhoea in patients in industrialised and developing countries (147-150). It has been reported that aEPEC may decrease apoptosis of intestinal epithelial cells (763) possibly due to the lack of Bfp (764). It is likely that the carriage of EspL, NleB and NleE homologues in aEPEC helps modulate the innate immune system of the host to prolong its colonisation. In view of the growing focus on and the shift to therapeutics that target bacterial factors essential for infection and colonisation instead of those that target *in vitro* viability similar to conventional antibiotics, NleB, EspL and NleE could be proposed as targets for the development of new antimicrobial therapy against both typical and atypical EPEC infection in an attempt to exert less selective pressure leading to decreased rate of resistance and to preserve the host microbiome.

In conclusion, there is still much to understand about the activities of EPEC and *Salmonella* T3SS effector proteins, in particular where host binding targets and biological effects have not been confirmed in the context of infection. For example, the biological significance of the interaction between SseK3 and the DD of TNFR1 and TRIM32 will need to be investigated further *in vitro* and *in vivo*. The effect of SseK3 on the inhibition of host cell apoptosis upon TNFR1 stimulation has not been investigated in this study and could broaden the set of T3SS effectors with anti-apoptotic effects. In addition, the recent discovery of new enzymatic activities for

several EPEC effector proteins warrants the re-examination of other effectors in a variety of pathogens that may also be novel enzymes.

References

References

1. **Liu L, Oza S, Hogan D, Perin J, Rudan I, Lawn JE, Cousens S, Mathers C, Black RE.** 2015. Global, regional, and national causes of child mortality in 2000-13, with projections to inform post-2015 priorities: an updated systematic analysis. Lancet **385:**430-440.

2. **Walker CL, Rudan I, Liu L, Nair H, Theodoratou E, Bhutta ZA, O'Brien KL, Campbell H, Black RE.** 2013. Global burden of childhood pneumonia and diarrhoea. Lancet **381:**1405-1416.

3. **The United Nations Inter-agency Group for Child Mortality Estimation.** 2013. Levels and trends in child mortality: Report 2013. New York: UNICEF.

4. **Guerrant RL, Hughes JM, Lima NL, Crane J.** 1990. Diarrhea in developed and developing countries: magnitude, special settings, and etiologies. Reviews of Infectious Diseases **12** S41-50.

5. **DuPont HL, Hornick RB, Snyder MJ, Libonati JP, Formal SB, Gangarosa EJ.** 1972. Immunity in shigellosis. II. Protection induced by oral live vaccine or primary infection. The Journal of Infectious Diseases **125:**12-16.

6. **Levine MM, DuPont HL, Formal SB, Hornick RB, Takeuchi A, Gangarosa EJ, Snyder MJ, Libonati JP.** 1973. Pathogenesis of *Shigella dysenteriae* 1 (Shiga) dysentery. The Journal of Infectious Diseases **127:**261-270.

7. **Cash RA, Music SI, Libonati JP, Snyder MJ, Wenzel RP, Hornick RB.** 1974. Response of man to infection with *Vibrio cholerae*. I. Clinical, serologic, and bacteriologic responses to a known inoculum. The Journal of Infectious Diseases **129:**45-52.

8. **Escherich T.** 1989. The intestinal bacteria of the neonate and breast-fed infant. 1885. Reviews of Infectious Diseases **11:**352-356.

9. **Eckburg PB, Bik EM, Bernstein CN, Purdom E, Dethlefsen L, Sargent M, Gill SR, Nelson KE, Relman DA.** 2005. Diversity of the human intestinal microbial flora. Science **308:**1635-1638.

10. **Gao YD, Zhao Y, Huang J.** 2014. Metabolic modeling of common *Escherichia coli* strains in human gut microbiome. BioMed Research International **2014:**694967.

11. **Reid G, Howard J, Gan BS.** 2001. Can bacterial interference prevent infection? Trends in Microbiology **9:**424-428.

12. **Laurelle L.** 1889. Etude bactériologique sur les péritonites par perforation. La Céllule **5:**60-123.

13. **Lesage AA.** 1897. **Contribution à l'étude des entérites infantiles-sero-diagnostic des races de Bacterium coli**. Comptes Rendus des Sociétés Biologiques (Paris) **49:**900-901.

14. **Creighton C.** 1975. A history of epidemics in Britain, vol. 2. Barnes and Noble, New York.

15. **Baldwin TJ.** 1998. The 18th C.L. Oakley Lecture. Pathogenicity of enteropathogenic *Escherichia coli*. Journal of Medical Microbiology **47:**283-293.

16. **Finlay HVL.** 1973. Bray's discovery of pathogenic *Esch. coli* as a cause of infantile gastroenteritis. Archives of Disease in Childhood **48:**923-926.

17. **Bray J.** 1945. Isolation of antigenically homogeneous strains of Bact. coli neapolitanum from summer diarrhoea of infants. Journal of Pathology and Bacteriology **57:**239-247.

18. **Bray J, Beavan TED.** 1948. Slide agglutination of *Bacterium coli var. neapolitanum* in summer diarrhoea. Journal of Pathology and Bacteriology **60:**395-401.

19. **Giles C, Sangster G.** 1948. Outbreak of infantile gastro-enteritis in Aberdeen: association of special type of *Bact. coli* with infection. Journal of Hygiene (Cambridge) **46:**1.

20. **Giles C, Sangster G, Smith J.** 1949. Epidemic gastro-enteritis of infants in Aberdeen during 1947. Archives of Disease in Childhood **24:**45-53.

21. **Taylor J, Powell BW, Wright J.** 1949. Infantile diarrhoea and vomiting. A clinical and bacteriological investigation. British Medical Journal **2:**117-125.

22. **Smith J.** 1949. The association of certain types (α and β) of *Bact. coli* with infantile gastro-enteritis. Journal of Hygiene (Cambridge) **47:**221.

23. **Kauffmann F.** 1947. The serology of the Coli group. The Journal of Immunology **57:**71-100.

24. ***The Salmonella* Subcommittee of the Nomenclature Committee of the International Society for Microbiology.** 1934. The Genus *Salmonella* Lignières, 1900. Journal of Hygiene (London) **34:**333-350.

25. **Brenner FW, Villar RG, Angulo FJ, Tauxe R, Swaminathan B.** 2000. *Salmonella* nomenclature. Journal of Clinical Microbiology **38:**2465-2467.

26. **Euzéby JP.** 1999. Revised *Salmonella* nomenclature: designation of *Salmonella enterica* (ex Kauffmann and Edwards 1952) Le Minor and Popoff 1987 sp. nov., nom. rev. as the neotype species of the genus *Salmonella* Lignieres 1900 (approved lists 1980), rejection of the name *Salmonella choleraesuis* (Smith 1894) Weldin 1927 (approved lists 1980), and conservation of the name *Salmonella typhi* (Schroeter 1886) Warren and Scott 1930 (approved lists 1980). Request for an opinion. International Journal of Systematic Bacteriology **49 Pt 2:**927-930.

27. **Ewing WH.** 1956. Enteropathogenic *Escherichia coli* serotypes. Annals of the New York Academy of Sciences **66:**61-70.

28. **Levine MM, Bergquist EJ, Nalin DR, Waterman DH, Hornick RB, Young CR, Sotman S.** 1978. *Escherichia coli* strains that cause diarrhoea but do not produce heat-labile or heat-stable enterotoxins and are non-invasive. Lancet **1:**1119-1122.

29. **Neter E, Westphal O, Luderitz O, Gino RM, Gorzynski EA.** 1955. Demonstration of antibodies against enteropathogenic *Escherichia coli* in sera of children of various ages. Pediatrics **16:**801-808.

30. **Cravioto A, Gross RJ, Scotland SM, Rowe B.** 1979. An adhesive factor found in strains of *Escherichia coli* belonging to the traditional infantile enteropathogenic serotypes. Current Microbiology **3:**95-99.

31. **Scaletsky IC, Silva ML, Trabulsi LR.** 1984. Distinctive patterns of adherence of enteropathogenic *Escherichia coli* to HeLa cells. Infection and Immunity **45:**534-536.

32. **Staley TE, Jones EW, Corley LD.** 1969. Attachment and penetration of *Escherichia coli* into intestinal epithelium of the ileum in newborn pigs. The American Journal of Pathology **56:**371-392.

33. **Polotsky YE, Dragunskaya EM, Seliverstova VG, Avdeeva TA, Chakhutinskaya MG, Ketyi I, Vertenyl A, Ralovich B, Emody L, Malovics I, Safonova NV, Snigirevskaya ES, Karyagina EI.** 1977. Pathogenic effect of enterotoxigenic *Escherichia coli* and *Escherichia coli* causing infantile diarrhoea. Acta Microbiologica Academiae Scientiarum Hungaricae **24:**221-236.

34. **Peeters JE, Charlier GJ, Halen PH.** 1984. Pathogenicity of attaching effacing enteropathogenic *Escherichia coli* isolated from diarrheic suckling and weanling rabbits for newborn rabbits. Infection and Immunity **46:**690-696.

35. **Peeters JE, Pohl P, Okerman L, Devriese LA.** 1984. Pathogenic properties of *Escherichia coli* strains isolated from diarrheic commercial rabbits. Journal of Clinical Microbiology **20:**34-39.

36. **Moon HW, Whipp SC, Argenzio RA, Levine MM, Giannella RA.** 1983. Attaching and effacing activities of rabbit and human enteropathogenic *Escherichia coli* in pig and rabbit intestines. Infection and Immunity **41:**1340-1351.

37. **Rothbaum R, McAdams AJ, Giannella R, Partin JC.** 1982. A clinicopathologic study of enterocyte-adherent *Escherichia coli*: a cause of protracted diarrhea in infants. Gastroenterology **83:**441-454.

38. **Rothbaum RJ, Partin JC, Saalfield K, McAdams AJ.** 1983. An ultrastructural study of enteropathogenic *Escherichia coli* infection in human infants. Ultrastructural Pathology **4:**291-304.

39. **Taylor CJ, Hart A, Batt RM, McDougall C, McLean L.** 1986. Ultrastructural and biochemical changes in human jejunal mucosa associated with enteropathogenic *Escherichia coli* (0111) infection. Journal of Pediatric Gastroenterology and Nutrition **5:**70-73.

40. **Ulshen MH, Rollo JL.** 1980. Pathogenesis of *Escherichia coli* gastroenteritis in man--another mechanism. The New England Journal of Medicine **302:**99-101.

41. **Knutton S, Baldwin T, Williams PH, McNeish AS.** 1989. Actin accumulation at sites of bacterial adhesion to tissue culture cells: basis of a new diagnostic test for enteropathogenic and enterohemorrhagic *Escherichia coli*. Infection and Immunity **57:**1290-1298.

42. **Levine MM.** 1987. *Escherichia coli* that cause diarrhea: enterotoxigenic, enteropathogenic, enteroinvasive, enterohemorrhagic, and enteroadherent. The Journal of Infectious Diseases **155:**377-389.

43. **Lumish RM, Ryder RW, Anderson DC, Wells JG, Puhr ND.** 1980. Heat-labile enterotoxigenic *Escherichia coli* induced diarrhea aboard a Miami-based cruise ship. American Journal of Epidemiology **111:**432-436.

44. **Schultsz C, Pool GJ, van Ketel R, de Wever B, Speelman P, Dankert J.** 1994. Detection of enterotoxigenic *Escherichia coli* in stool samples by using nonradioactively labeled oligonucleotide DNA probes and PCR. Journal of Clinical Microbiology **32:**2393-2397.

45. **Kaper JB, Nataro JP, Mobley HL.** 2004. Pathogenic *Escherichia coli*. Nature Reviews Microbiology **2:**123-140.

46. **Girao DM, Girao VB, Irino K, Gomes TA.** 2006. Classifying *Escherichia coli*. Emerging Infectious Diseases **12:**1297-1299.

47. **Nataro JP, Kaper JB.** 1998. Diarrheagenic *Escherichia coli*. Clinical Microbiology Reviews **11:**142-201.

48. **Roe AJ, Gally DL.** 2000. Enteropathogenic and enterohaemorrhagic *Escherichia coli* and diarrhoea. Current Opinion in Infectious Diseases **13:**511-517.

49. **Donnenberg MS, Whittam TS.** 2001. Pathogenesis and evolution of virulence in enteropathogenic and enterohemorrhagic *Escherichia coli*. The Journal of Clinical Investigation **107:**539-548.

50. **Croxen MA, Law RJ, Scholz R, Keeney KM, Wlodarska M, Finlay BB.** 2013. Recent advances in understanding enteric pathogenic *Escherichia coli*. Clinical Microbiology Reviews **26:**822-880.

51. **Sizemore DR, Roland KL, Ryan US.** 2004. Enterotoxigenic *Escherichia coli* virulence factors and vaccine approaches. Expert Review of Vaccines **3:**585-595.

52. **Qadri F, Svennerholm AM, Faruque AS, Sack RB.** 2005. Enterotoxigenic *Escherichia coli* in developing countries: epidemiology, microbiology, clinical features, treatment, and prevention. Clinical Microbiology Reviews **18:**465-483.

53. **Al-Abri SS, Beeching NJ, Nye FJ.** 2005. Traveller's diarrhoea. The Lancet. Infectious Diseases **5:**349-360.

54. **Jiang ZD, Lowe B, Verenkar MP, Ashley D, Steffen R, Tornieporth N, von Sonnenburg F, Waiyaki P, DuPont HL.** 2002. Prevalence of enteric pathogens among international travelers with diarrhea acquired in Kenya (Mombasa), India (Goa), or Jamaica (Montego Bay). The Journal of Infectious Diseases **185:**497-502.

55. **Gaastra W, Svennerholm AM.** 1996. Colonization factors of human enterotoxigenic *Escherichia coli* (ETEC). Trends in Microbiology **4:**444-452.

56. **Evans DG, Evans DJ, Jr., Tjoa WS, DuPont HL.** 1978. Detection and characterization of colonization factor of enterotoxigenic *Escherichia coli* isolated from adults with diarrhea. Infection and Immunity **19:**727-736.

57. **Levine MM, Ferreccio C, Prado V, Cayazzo M, Abrego P, Martinez J, Maggi L, Baldini MM, Martin W, Maneval D, et al.** 1993. Epidemiologic studies of *Escherichia coli* diarrheal infections in a low socioeconomic level

peri-urban community in Santiago, Chile. American Journal of Epidemiology **138:**849-869.

58. **Svennerholm AM, Wenneras C, Holmgren J, McConnell MM, Rowe B.** 1990. Roles of different coli surface antigens of colonization factor antigen II in colonization by and protective immunogenicity of enterotoxigenic *Escherichia coli* in rabbits. Infection and Immunity **58:**341-346.

59. **Wolf MK.** 1997. Occurrence, distribution, and associations of O and H serogroups, colonization factor antigens, and toxins of enterotoxigenic *Escherichia coli*. Clinical Microbiology Reviews **10:**569-584.

60. **Gill DM, Richardson SH.** 1980. Adenosine diphosphate-ribosylation of adenylate cyclase catalyzed by heat-labile enterotoxin of *Escherichia coli*: comparison with cholera toxin. The Journal of Infectious Diseases **141:**64-70.

61. **Tauschek M, Gorrell RJ, Strugnell RA, Robins-Browne RM.** 2002. Identification of a protein secretory pathway for the secretion of heat-labile enterotoxin by an enterotoxigenic strain of *Escherichia coli*. Proceedings of the National Academy of Sciences of the United States of America **99:**7066-7071.

62. **Sears CL, Kaper JB.** 1996. Enteric bacterial toxins: mechanisms of action and linkage to intestinal secretion. Microbiological Reviews **60:**167-215.

63. **Currie MG, Fok KF, Kato J, Moore RJ, Hamra FK, Duffin KL, Smith CE.** 1992. Guanylin: an endogenous activator of intestinal guanylate cyclase. Proceedings of the National Academy of Sciences of the United States of America **89:**947-951.

64. **Nataro JP, Steiner T, Guerrant RL.** 1998. Enteroaggregative *Escherichia coli*. Emerging Infectious Diseases **4:**251-261.

65. **Nataro JP, Kaper JB, Robins-Browne R, Prado V, Vial P, Levine MM.** 1987. Patterns of adherence of diarrheagenic *Escherichia coli* to HEp-2 cells. The Pediatric Infectious Disease Journal **6:**829-831.

66. **Huang DB, DuPont HL, Jiang ZD, Carlin L, Okhuysen PC.** 2004. Interleukin-8 response in an intestinal HCT-8 cell line infected with enteroaggregative and enterotoxigenic *Escherichia coli*. Clinical and Diagnostic Laboratory Immunology **11:**548-551.

67. **Huang DB, Okhuysen PC, Jiang ZD, DuPont HL.** 2004. Enteroaggregative *Escherichia coli*: an emerging enteric pathogen. The American Journal of Gastroenterology **99:**383-389.

68. **Okeke IN, Nataro JP.** 2001. Enteroaggregative *Escherichia coli*. The Lancet. Infectious Diseases **1:**304-313.

69. **Mayer HB, Wanke CA.** 1995. Enteroaggregative *Escherichia coli* as a possible cause of diarrhea in an HIV-infected patient. The New England Journal of Medicine **332:**273-274.

70. **Thea DM, St Louis ME, Atido U, Kanjinga K, Kembo B, Matondo M, Tshiamala T, Kamenga C, Davachi F, Brown C, et al.** 1993. A prospective study of diarrhea and HIV-1 infection among 429 Zairian infants. The New England Journal of Medicine **329:**1696-1702.

71. **Wanke CA, Schorling JB, Barrett LJ, Desouza MA, Guerrant RL.** 1991. Potential role of adherence traits of *Escherichia coli* in persistent diarrhea in an urban Brazilian slum. The Pediatric Infectious Disease Journal **10:**746-751.

72. **Nataro JP, Deng Y, Maneval DR, German AL, Martin WC, Levine MM.** 1992. Aggregative adherence fimbriae I of enteroaggregative *Escherichia coli* mediate adherence to HEp-2 cells and hemagglutination of human erythrocytes. Infection and Immunity **60:**2297-2304.

73. **Germani Y, Minssart P, Vohito M, Yassibanda S, Glaziou P, Hocquet D, Berthelemy P, Morvan J.** 1998. Etiologies of acute, persistent, and dysenteric diarrheas in adults in Bangui, Central African Republic, in relation to human immunodeficiency virus serostatus. The American Journal of Tropical Medicine and Hygiene **59:**1008-1014.

74. **Huppertz HI, Rutkowski S, Aleksic S, Karch H.** 1997. Acute and chronic diarrhoea and abdominal colic associated with enteroaggregative *Escherichia coli* in young children living in western Europe. Lancet **349:**1660-1662.

75. **Nataro JP, Deng Y, Cookson S, Cravioto A, Savarino SJ, Guers LD, Levine MM, Tacket CO.** 1995. Heterogeneity of enteroaggregative *Escherichia coli* virulence demonstrated in volunteers. The Journal of Infectious Diseases **171:**465-468.

76. **Steiner TS, Lima AA, Nataro JP, Guerrant RL.** 1998. Enteroaggregative *Escherichia coli* produce intestinal inflammation and growth impairment and cause interleukin-8 release from intestinal epithelial cells. The Journal of Infectious Diseases **177:**88-96.

77. **Steiner TS, Nataro JP, Poteet-Smith CE, Smith JA, Guerrant RL.** 2000. Enteroaggregative *Escherichia coli* expresses a novel flagellin that causes IL-8 release from intestinal epithelial cells. The Journal of Clinical Investigation **105:**1769-1777.

78. **Henderson IR, Czeczulin J, Eslava C, Noriega F, Nataro JP.** 1999. Characterization of Pic, a secreted protease of *Shigella flexneri* and enteroaggregative *Escherichia coli*. Infection and Immunity **67:**5587-5596.

79. **Navarro-Garcia F, Eslava C, Villaseca JM, Lopez-Revilla R, Czeczulin JR, Srinivas S, Nataro JP, Cravioto A.** 1998. *In vitro* effects of a high-molecular-weight heat-labile enterotoxin from enteroaggregative *Escherichia coli*. Infection and Immunity **66:**3149-3154.

80. **Noriega FR, Liao FM, Formal SB, Fasano A, Levine MM.** 1995. Prevalence of *Shigella* enterotoxin 1 among *Shigella* clinical isolates of diverse serotypes. The Journal of Infectious Diseases **172:**1408-1410.

81. **Savarino SJ, Fasano A, Watson J, Martin BM, Levine MM, Guandalini S, Guerry P.** 1993. Enteroaggregative *Escherichia coli* heat-stable enterotoxin 1 represents another subfamily of *E. coli* heat-stable toxin. Proceedings of the National Academy of Sciences of the United States of America **90:**3093-3097.

82. **Menard LP, Dubreuil JD.** 2002. Enteroaggregative *Escherichia coli* heat-stable enterotoxin 1 (EAST1): a new toxin with an old twist. Critical Reviews in Microbiology **28:**43-60.

83. **Czeczulin JR, Balepur S, Hicks S, Phillips A, Hall R, Kothary MH, Navarro-Garcia F, Nataro JP.** 1997. Aggregative adherence fimbria II, a second fimbrial antigen mediating aggregative adherence in enteroaggregative *Escherichia coli*. Infection and Immunity **65:**4135-4145.

84. **Nataro JP, Yikang D, Yingkang D, Walker K.** 1994. AggR, a transcriptional activator of aggregative adherence fimbria I expression in enteroaggregative *Escherichia coli*. Journal of Bacteriology **176:**4691-4699.

85. **Sheikh J, Czeczulin JR, Harrington S, Hicks S, Henderson IR, Le Bouguenec C, Gounon P, Phillips A, Nataro JP.** 2002. A novel dispersin protein in enteroaggregative *Escherichia coli*. The Journal of Clinical Investigation **110:**1329-1337.

86. **Nishi J, Sheikh J, Mizuguchi K, Luisi B, Burland V, Boutin A, Rose DJ, Blattner FR, Nataro JP.** 2003. The export of coat protein from enteroaggregative *Escherichia coli* by a specific ATP-binding cassette transporter system. Journal of Biological Chemistry **278:**45680-45689.

87. **Morin N, Santiago AE, Ernst RK, Guillot SJ, Nataro JP.** 2013. Characterization of the AggR regulon in enteroaggregative *Escherichia coli*. Infection and Immunity **81:**122-132.

88. **Jiang ZD, Greenberg D, Nataro JP, Steffen R, DuPont HL.** 2002. Rate of occurrence and pathogenic effect of enteroaggregative *Escherichia coli* virulence factors in international travelers. Journal of Clinical Microbiology **40:**4185-4190.

89. **Boll EJ, Struve C, Boisen N, Olesen B, Stahlhut SG, Krogfelt KA.** 2013. Role of enteroaggregative *Escherichia coli* virulence factors in uropathogenesis. Infection and Immunity **81:**1164-1171.

90. **Rasko DA, Webster DR, Sahl JW, Bashir A, Boisen N, Scheutz F, Paxinos EE, Sebra R, Chin CS, Iliopoulos D, Klammer A, Peluso P, Lee L, Kislyuk AO, Bullard J, Kasarskis A, Wang S, Eid J, Rank D, Redman JC, Steyert SR, Frimodt-Moller J, Struve C, Petersen AM, Krogfelt KA, Nataro JP, Schadt EE, Waldor MK.** 2011. Origins of the *E. coli* strain causing an outbreak of hemolytic-uremic syndrome in Germany. The New England Journal of Medicine **365:**709-717.

91. **Brenner DJ, Fanning GR, Steigerwalt AG, Orskov I, Orskov F.** 1972. Polynucleotide sequence relatedness among three groups of pathogenic *Escherichia coli* strains. Infection and Immunity **6:**308-315.

92. **Engelkirk PG, Duben-Engelkirk JL.** 2008. Selected non-lactose-fermenting members of the family Enterobacteriaceae, Laboratory Diagnosis of Infectious Diseases: Essentials of Diagnostic Microbiology. Lippincott Williams & Wilkins.

93. **Pupo GM, Lan R, Reeves PR.** 2000. Multiple independent origins of *Shigella* clones of *Escherichia coli* and convergent evolution of many of their characteristics. Proceedings of the National Academy of Sciences of the United States of America **97:**10567-10572.

94. **Doyle MP, Padhye VV.** 1989. Enteroinvasive *E. coli*. *In* Doyle MP (ed.), Foodborne Bacterial Pathogens CRC Press.

95. **Sansonetti PJ.** 1992. Molecular and cellular biology of *Shigella flexneri* invasiveness: from cell assay systems to shigellosis. Current Topics in Microbiology and Immunology **180:**1-19.

96. **Sansonetti PJ.** 1992. *Escherichia coli*, *Shigella*, antibiotic-associated diarrhea and prevention and treatment of gastroenteritis. Current Opinion in Infectious Diseases **5**.

97. **Goldberg MB, Sansonetti PJ.** 1993. *Shigella* subversion of the cellular cytoskeleton: a strategy for epithelial colonization. Infection and Immunity **61:**4941-4946.

98. **Taylor DN, Echeverria P, Sethabutr O, Pitarangsi C, Leksomboon U, Blacklow NR, Rowe B, Gross R, Cross J.** 1988. Clinical and microbiologic features of *Shigella* and enteroinvasive *Escherichia coli* infections detected by DNA hybridization. Journal of Clinical Microbiology **26:**1362-1366.

99. **Baudry B, Maurelli AT, Clerc P, Sadoff JC, Sansonetti PJ.** 1987. Localization of plasmid loci necessary for the entry of *Shigella flexneri* into HeLa cells, and characterization of one locus encoding four immunogenic polypeptides. Journal of General Microbiology **133:**3403-3413.

100. **Sasakawa C, Buysse JM, Watanabe H.** 1992. The large virulence plasmid of *Shigella*. Current Topics in Microbiology and Immunology **180:**21-44.

101. **Small PL, Falkow S.** 1988. Identification of regions on a 230-kilobase plasmid from enteroinvasive *Escherichia coli* that are required for entry into HEp-2 cells. Infection and Immunity **56:**225-229.

102. **Allaoui A, Sansonetti PJ, Menard R, Barzu S, Mounier J, Phalipon A, Parsot C.** 1995. MxiG, a membrane protein required for secretion of *Shigella* spp. Ipa invasins: involvement in entry into epithelial cells and in intercellular dissemination. Molecular Microbiology **17:**461-470.

103. **Andrews GP, Hromockyj AE, Coker C, Maurelli AT.** 1991. Two novel virulence loci, mxiA and mxiB, in *Shigella flexneri* 2a facilitate excretion of invasion plasmid antigens. Infection and Immunity **59:**1997-2005.

104. **Maurelli AT.** 1994. Virulence protein export systems in *Salmonella* and *Shigella*: a new family or lost relatives? Trends in Cell Biology **4:**240-242.

105. **Hale TL, Oaks EV, Formal SB.** 1985. Identification and antigenic characterization of virulence-associated, plasmid-coded proteins of *Shigella* spp. and enteroinvasive *Escherichia coli*. Infection and Immunity **50:**620-629.

106. **Menard R, Prevost MC, Gounon P, Sansonetti P, Dehio C.** 1996. The secreted Ipa complex of *Shigella flexneri* promotes entry into mammalian cells. Proceedings of the National Academy of Sciences of the United States of America **93:**1254-1258.

107. **Menard R, Sansonetti PJ, Parsot C.** 1993. Nonpolar mutagenesis of the *ipa* genes defines IpaB, IpaC, and IpaD as effectors of *Shigella flexneri* entry into epithelial cells. Journal of Bacteriology **175:**5899-5906.

108. **Nataro JP, Scaletsky IC, Kaper JB, Levine MM, Trabulsi LR.** 1985. Plasmid-mediated factors conferring diffuse and localized adherence of enteropathogenic *Escherichia coli*. Infection and Immunity **48:**378-383.

109. **Bilge SS, Apostol JM, Jr., Aldape MA, Moseley SL.** 1993. mRNA processing independent of RNase III and RNase E in the expression of the F1845 fimbrial adhesin of *Escherichia coli*. Proceedings of the National Academy of Sciences of the United States of America **90:**1455-1459.

110. **Bilge SS, Apostol JM, Jr., Fullner KJ, Moseley SL.** 1993. Transcriptional organization of the F1845 fimbrial adhesin determinant of *Escherichia coli*. Molecular Microbiology **7:**993-1006.

111. **Bilge SS, Clausen CR, Lau W, Moseley SL.** 1989. Molecular characterization of a fimbrial adhesin, F1845, mediating diffuse adherence of diarrhea-associated Escherichia coli to HEp-2 cells. Journal of Bacteriology **171:**4281-4289.

112. **Peiffer I, Servin AL, Bernet-Camard MF.** 1998. Piracy of decay-accelerating factor (CD55) signal transduction by the diffusely adhering strain *Escherichia coli* C1845 promotes cytoskeletal F-actin rearrangements in cultured human intestinal INT407 cells. Infection and Immunity **66:**4036-4042.

113. **Scaletsky IC, Fabbricotti SH, Carvalho RL, Nunes CR, Maranhao HS, Morais MB, Fagundes-Neto U.** 2002. Diffusely adherent *Escherichia coli* as a cause of acute diarrhea in young children in Northeast Brazil: a case-control study. Journal of Clinical Microbiology **40:**645-648.

114. **Mansan-Almeida R, Pereira AL, Giugliano LG.** 2013. Diffusely adherent *Escherichia coli* strains isolated from children and adults constitute two different populations. BMC Microbiology **13:**22.

115. **Riley LW, Remis RS, Helgerson SD, McGee HB, Wells JG, Davis BR, Hebert RJ, Olcott ES, Johnson LM, Hargrett NT, Blake PA, Cohen ML.** 1983. Hemorrhagic colitis associated with a rare *Escherichia coli* serotype. The New England Journal of Medicine **308:**681-685.

116. **Karmali MA, Gannon V, Sargeant JM.** 2010. Verocytotoxin-producing *Escherichia coli* (VTEC). Veterinary Microbiology **140:**360-370.

117. **Karmali MA.** 1989. Infection by verocytotoxin-producing *Escherichia coli*. Clinical Microbiology Reviews **2:**15-38.

118. **Karmali MA, Steele BT, Petric M, Lim C.** 1983. Sporadic cases of haemolytic-uraemic syndrome associated with faecal cytotoxin and cytotoxin-producing *Escherichia coli* in stools. Lancet **1:**619-620.

119. **Karmali MA, Petric M, Lim C, Fleming PC, Steele BT.** 1983. *Escherichia coli* cytotoxin, haemolytic-uraemic syndrome, and haemorrhagic colitis. Lancet **2:**1299-1300.

120. **O'Brien AD, Holmes RK.** 1987. Shiga and Shiga-like toxins. Microbiological Reviews **51:**206-220.

121. **O'Brien AD, Tesh VL, Donohue-Rolfe A, Jackson MP, Olsnes S, Sandvig K, Lindberg AA, Keusch GT.** 1992. Shiga toxin: biochemistry, genetics, mode of action, and role in pathogenesis. Current Topics in Microbiology and Immunology **180:**65-94.

122. **Scotland SM, Smith HR, Willshaw GA, Rowe B.** 1983. Vero cytotoxin production in strain of *Escherichia coli* is determined by genes carried on bacteriophage. Lancet **2:**216.

123. **Betz J, Bielaszewska M, Thies A, Humpf HU, Dreisewerd K, Karch H, Kim KS, Friedrich AW, Muthing J.** 2011. Shiga toxin glycosphingolipid receptors in microvascular and macrovascular endothelial cells: differential association with membrane lipid raft microdomains. Journal of Lipid Research **52:**618-634.

124. **Hofmann SL.** 1993. Southwestern Internal Medicine Conference: Shiga-like toxins in hemolytic-uremic syndrome and thrombotic thrombocytopenic purpura. The American Journal of the Medical Sciences **306:**398-406.

125. **Sandvig K, van Deurs B.** 1996. Endocytosis, intracellular transport, and cytotoxic action of Shiga toxin and ricin. Physiological Reviews **76:**949-966.

126. **Jackson MP.** 1990. Structure-function analyses of Shiga toxin and the Shiga-like toxins. Microbial Pathogenesis **8:**235-242.

127. **Meyers KE, Kaplan BS.** 2000. Many cell types are Shiga toxin targets. Kidney international **57:**2650-2651.

128. **Griffin PM.** 1995. Escherichia coli O157:H7 and other enterohemorrhagic Escherichia coli, p. 739-761, Infections of the gastrointestinal tract, New York, N.Y.

129. **Griffin PM, Tauxe RV.** 1991. The epidemiology of infections caused by *Escherichia coli* O157:H7, other enterohemorrhagic *E. coli*, and the associated hemolytic uremic syndrome. Epidemiologic Reviews **13:**60-98.

130. **Rangel JM, Sparling PH, Crowe C, Griffin PM, Swerdlow DL.** 2005. Epidemiology of *Escherichia coli* O157:H7 outbreaks, United States, 1982-2002. Emerging Infectious Diseases **11:**603-609.

131. **Tilden J, Jr., Young W, McNamara AM, Custer C, Boesel B, Lambert-Fair MA, Majkowski J, Vugia D, Werner SB, Hollingsworth J, Morris JG, Jr.** 1996. A new route of transmission for *Escherichia coli*: infection from dry fermented salami. American Journal of Public Health **86:**1142-1145.

132. **Tuttle J, Gomez T, Doyle MP, Wells JG, Zhao T, Tauxe RV, Griffin PM.** 1999. Lessons from a large outbreak of *Escherichia coli* O157:H7 infections: insights into the infectious dose and method of widespread contamination of hamburger patties. Epidemiology and Infection **122:**185-192.

133. **Carter AO, Borczyk AA, Carlson JA, Harvey B, Hockin JC, Karmali MA, Krishnan C, Korn DA, Lior H.** 1987. A severe outbreak of *Escherichia coli* O157:H7--associated hemorrhagic colitis in a nursing home. The New England Journal of Medicine **317:**1496-1500.

134. **Rowe PC, Orrbine E, Lior H, Wells GA, McLaine PN.** 1993. Diarrhoea in close contacts as a risk factor for childhood haemolytic uraemic syndrome. The CPKDRC co-investigators. Epidemiology and Infection **110:**9-16.

135. **Spika JS, Parsons JE, Nordenberg D, Wells JG, Gunn RA, Blake PA.** 1986. Hemolytic uremic syndrome and diarrhea associated with *Escherichia coli* O157:H7 in a day care center. The Journal of Pediatrics **109:**287-291.

136. **Smith KE, Wilker PR, Reiter PL, Hedican EB, Bender JB, Hedberg CW.** 2012. Antibiotic treatment of *Escherichia coli* O157 infection and the risk of hemolytic uremic syndrome, Minnesota. The Pediatric Infectious Disease Journal **31:**37-41.

137. **Wong CS, Jelacic S, Habeeb RL, Watkins SL, Tarr PI.** 2000. The risk of the hemolytic-uremic syndrome after antibiotic treatment of *Escherichia coli* O157:H7 infections. The New England Journal of Medicine **342:**1930-1936.

138. **Kimmitt PT, Harwood CR, Barer MR.** 2000. Toxin gene expression by shiga toxin-producing *Escherichia coli*: the role of antibiotics and the bacterial SOS response. Emerging Infectious Diseases **6:**458-465.

139. **Bell BP, Griffin PM, Lozano P, Christie DL, Kobayashi JM, Tarr PI.** 1997. Predictors of hemolytic uremic syndrome in children during a large outbreak of *Escherichia coli* O157:H7 infections. Pediatrics **100:**E12.

140. **Cimolai N, Basalyga S, Mah DG, Morrison BJ, Carter JE.** 1994. A continuing assessment of risk factors for the development of *Escherichia coli* O157:H7-associated hemolytic uremic syndrome. Clinical Nephrology **42:**85-89.

141. **Clarke MB, Sperandio V.** 2005. Transcriptional autoregulation by quorum sensing *Escherichia coli* regulators B and C (QseBC) in enterohaemorrhagic *E. coli* (EHEC). Molecular Microbiology **58:**441-455.

142. **Robins-Browne RM, Yam WC, O'Gorman LE, Bettelheim KA.** 1993. Examination of archetypal strains of enteropathogenic *Escherichia coli* for properties associated with bacterial virulence. Journal of Medical Microbiology **38:**222-226.

143. **Trabulsi LR, Keller R, Tardelli Gomes TA.** 2002. Typical and atypical enteropathogenic *Escherichia coli*. Emerging Infectious Diseases **8:**508-513.

144. **Bieber D, Ramer SW, Wu CY, Murray WJ, Tobe T, Fernandez R, Schoolnik GK.** 1998. Type IV pili, transient bacterial aggregates, and virulence of enteropathogenic *Escherichia coli*. Science **280:**2114-2118.

145. **Frankel G, Phillips AD, Rosenshine I, Dougan G, Kaper JB, Knutton S.** 1998. Enteropathogenic and enterohaemorrhagic *Escherichia coli*: more subversive elements. Molecular Microbiology **30:**911-921.

146. **Gomez-Duarte OG, Kaper JB.** 1995. A plasmid-encoded regulatory region activates chromosomal *eaeA* expression in enteropathogenic *Escherichia coli*. Infection and Immunity **63:**1767-1776.

147. **Nguyen RN, Taylor LS, Tauschek M, Robins-Browne RM.** 2006. Atypical enteropathogenic *Escherichia coli* infection and prolonged diarrhea in children. Emerging Infectious Diseases **12:**597-603.

148. **Robins-Browne RM, Bordun AM, Tauschek M, Bennett-Wood VR, Russell J, Oppedisano F, Lister NA, Bettelheim KA, Fairley CK, Sinclair MI, Hellard ME.** 2004. *Escherichia coli* and community-acquired gastroenteritis, Melbourne, Australia. Emerging Infectious Diseases **10:**1797-1805.

149. **Afset JE, Bevanger L, Romundstad P, Bergh K.** 2004. Association of atypical enteropathogenic *Escherichia coli* (EPEC) with prolonged diarrhoea. Journal of Medical Microbiology **53:**1137-1144.

150. **Scaletsky IC, Pedroso MZ, Oliva CA, Carvalho RL, Morais MB, Fagundes-Neto U.** 1999. A localized adherence-like pattern as a second pattern of adherence of classic enteropathogenic *Escherichia coli* to HEp-2 cells that is associated with infantile diarrhea. Infection and Immunity **67:**3410-3415.

151. **Moffet HL, Shulenberger HK, Burkholder ER.** 1968. Epidemiology and etiology of severe infantile diarrhea. The Journal of Pediatrics **72:**1-14.

152. **Levine MM, Edelman R.** 1984. Enteropathogenic *Escherichia coli* of classic serotypes associated with infant diarrhea: epidemiology and pathogenesis. Epidemiologic Reviews **6:**31-51.

153. **Kotloff KL, Nataro JP, Blackwelder WC, Nasrin D, Farag TH, Panchalingam S, Wu Y, Sow SO, Sur D, Breiman RF, Faruque AS, Zaidi AK, Saha D, Alonso PL, Tamboura B, Sanogo D, Onwuchekwa U, Manna B, Ramamurthy T, Kanungo S, Ochieng JB, Omore R, Oundo JO, Hossain A, Das SK, Ahmed S, Qureshi S, Quadri F, Adegbola RA, Antonio M, Hossain MJ, Akinsola A, Mandomando I, Nhampossa T, Acacio S, Biswas K, O'Reilly CE, Mintz ED, Berkeley LY, Muhsen K, Sommerfelt H, Robins-Browne RM, Levine MM.** 2013. Burden and aetiology of diarrhoeal disease in infants and young children in developing countries (the Global Enteric Multicenter Study, GEMS): a prospective, case-control study. Lancet **382:**209-222.

154. **Lozer DM, Souza TB, Monfardini MV, Vicentini F, Kitagawa SS, Scaletsky IC, Spano LC.** 2013. Genotypic and phenotypic analysis of diarrheagenic *Escherichia coli* strains isolated from Brazilian children living in low socioeconomic level communities. BMC Infectious Diseases **13:**418.

155. **Hill SM, Phillips AD, Walker-Smith JA.** 1991. Enteropathogenic *Escherichia coli* and life threatening chronic diarrhoea. Gut **32:**154-158.

156. **Phillips AD, Frankel G.** 2000. Intimin-mediated tissue specificity in enteropathogenic *Escherichia coli* interaction with human intestinal organ cultures. The Journal of Infectious Diseases **181:**1496-1500.

157. **Donnenberg MS, Kaper JB.** 1992. Enteropathogenic *Escherichia coli*. Infection and Immunity **60:**3953-3961.

158. **Diniz-Santos DR, Silva LR, Silva N.** 2006. Antibiotics for the empirical treatment of acute infectious diarrhea in children. The Brazilian journal of infectious diseases : an official publication of the Brazilian Society of Infectious Diseases **10:**217-227.

159. **Tarr PI, Gordon CA, Chandler WL.** 2005. Shiga-toxin-producing *Escherichia coli* and haemolytic uraemic syndrome. Lancet **365:**1073-1086.

160. **Levine MM, Nataro JP, Karch H, Baldini MM, Kaper JB, Black RE, Clements ML, O'Brien AD.** 1985. The diarrheal response of humans to some classic serotypes of enteropathogenic *Escherichia coli* is dependent on a plasmid encoding an enteroadhesiveness factor. The Journal of Infectious Diseases **152:**550-559.

161. **Iguchi A, Thomson NR, Ogura Y, Saunders D, Ooka T, Henderson IR, Harris D, Asadulghani M, Kurokawa K, Dean P, Kenny B, Quail MA, Thurston S, Dougan G, Hayashi T, Parkhill J, Frankel G.** 2009. Complete genome sequence and comparative genome analysis of enteropathogenic *Escherichia coli* O127:H6 strain E2348/69. Journal of Bacteriology **191:**347-354.

162. **Schmidt MA.** 2010. LEEways: tales of EPEC, ATEC and EHEC. Cellular Microbiology **12:**1544-1552.

163. **Mellies JL, Elliott SJ, Sperandio V, Donnenberg MS, Kaper JB.** 1999. The *Per* regulon of enteropathogenic *Escherichia coli* : identification of a regulatory cascade and a novel transcriptional activator, the locus of enterocyte effacement (LEE)-encoded regulator (Ler). Molecular Microbiology **33:**296-306.

164. **Müller D, Benz I, Liebchen A, Gallitz I, Karch H, Schmidt MA.** 2009. Comparative analysis of the locus of enterocyte effacement and its flanking regions. Infection and Immunity **77:**3501-3513.

165. **Borenshtein D, McBee ME, Schauer DB.** 2008. Utility of the *Citrobacter rodentium* infection model in laboratory mice. Current Opinion in Gastroenterology **24:**32-37.

166. **Mundy R, Girard F, FitzGerald AJ, Frankel G.** 2006. Comparison of colonization dynamics and pathology of mice infected with enteropathogenic *Escherichia coli*, enterohaemorrhagic *E. coli* and *Citrobacter rodentium*. FEMS Microbiology Letters **265:**126-132.

167. **Mundy R, Pickard D, Wilson RK, Simmons CP, Dougan G, Frankel G.** 2003. Identification of a novel type IV pilus gene cluster required for gastrointestinal colonization of *Citrobacter rodentium*. Molecular Microbiology **48:**795-809.

168. **Luperchio SA, Schauer DB.** 2001. Molecular pathogenesis of *Citrobacter rodentium* and transmissible murine colonic hyperplasia. Microbes and Infection **3:**333-340.

169. **Petty NK, Bulgin R, Crepin VF, Cerdeno-Tarraga AM, Schroeder GN, Quail MA, Lennard N, Corton C, Barron A, Clark L, Toribio AL, Parkhill J, Dougan G, Frankel G, Thomson NR.** 2010. The *Citrobacter rodentium* genome sequence reveals convergent evolution with human pathogenic *Escherichia coli*. Journal of Bacteriology **192:**525-538.

170. **Barthold SW, Coleman GL, Bhatt PN, Osbaldiston GW, Jonas AM.** 1976. The etiology of transmissible murine colonic hyperplasia. Laboratory Animal Science **26:**889-894.

171. **Barthold SW, Coleman GL, Jacoby RO, Livestone EM, Jonas AM.** 1978. Transmissible murine colonic hyperplasia. Veterinary Pathology **15:**223-236.

172. **Deng W, Vallance BA, Li Y, Puente JL, Finlay BB.** 2003. *Citrobacter rodentium* translocated intimin receptor (Tir) is an essential virulence factor needed for actin condensation, intestinal colonization and colonic hyperplasia in mice. Molecular Microbiology **48:**95-115.

173. **Frankel G, Phillips AD, Novakova M, Field H, Candy DC, Schauer DB, Douce G, Dougan G.** 1996. Intimin from enteropathogenic *Escherichia coli* restores murine virulence to a *Citrobacter rodentium* eaeA mutant: induction of an immunoglobulin A response to intimin and EspB. Infection and Immunity **64:**5315-5325.

174. **Luperchio SA, Newman JV, Dangler CA, Schrenzel MD, Brenner DJ, Steigerwalt AG, Schauer DB.** 2000. *Citrobacter rodentium*, the causative agent of transmissible murine colonic hyperplasia, exhibits clonality: synonymy of C. rodentium and mouse-pathogenic *Escherichia coli*. Journal of Clinical Microbiology **38:**4343-4350.

175. **Mundy R, MacDonald TT, Dougan G, Frankel G, Wiles S.** 2005. *Citrobacter rodentium* of mice and man. Cellular Microbiology **7:**1697-1706.

176. **Vallance BA, Deng W, Jacobson K, Finlay BB.** 2003. Host susceptibility to the attaching and effacing bacterial pathogen *Citrobacter rodentium*. Infection and Immunity **71:**3443-3453.

177. **Ochman H, Elwyn S, Moran NA.** 1999. Calibrating bacterial evolution. Proceedings of the National Academy of Sciences of the United States of America **96:**12638-12643.

178. **Ochman H, Soncini FC, Solomon F, Groisman EA.** 1996. Identification of a pathogenicity island required for *Salmonella* survival in host cells. Proceedings of the National Academy of Sciences of the United States of America **93:**7800-7804.

179. **Le Minor L, Popoff MY.** 1987. Designation of *Salmonella enterica* sp. nov., nom. rev., as the Type and Only Species of the Genus *Salmonella*: Request for an Opinion. International Journal of Sytematic Bacteriology **37:**465-468.

180. **Reeves MW, Evins GM, Heiba AA, Plikaytis BD, Farmer JJ, 3rd.** 1989. Clonal nature of *Salmonella typhi* and its genetic relatedness to other

salmonellae as shown by multilocus enzyme electrophoresis, and proposal of *Salmonella bongori* comb. nov. Journal of Clinical Microbiology **27:**313-320.

181. **Su LH, Chiu CH.** 2007. *Salmonella*: clinical importance and evolution of nomenclature. Chang Gung Medical Journal **30:**210-219.

182. **Popoff MY, Bockemuhl J, Gheesling LL.** 2004. Supplement 2002 (no. 46) to the Kauffmann-White scheme. Research in Microbiology **155:**568-570.

183. **Crump JA, Luby SP, Mintz ED.** 2004. The global burden of typhoid fever. Bulletin of the World Health Organization **82:**346-353.

184. **Raffatellu M, Wilson RP, Winter SE, Baumler AJ.** 2008. Clinical pathogenesis of typhoid fever. Journal of infection in Developing Countries **2:**260-266.

185. **Stuart BM, Pullen RL.** 1946. Typhoid; clinical analysis of 360 cases. Archives of Internal Medicine **78:**629-661.

186. **Humphrey D.** 2006. *Salmonella* Infections: Clinical, Immunological and Molecular Aspects.

187. **Rabsch W, Tschäpe H, Bäumler AJ.** 2001. Non-typhoidal salmonellosis: emerging problems. Microbes Infect **3:**237-247.

188. **Hohmann EL.** 2001. Nontyphoidal salmonellosis. Clinical infectious diseases : an official publication of the Infectious Diseases Society of America **32:**263-269.

189. **Nelson JD, Kusmiesz H, Jackson LH, Woodman E.** 1980. Treatment of *Salmonella* gastroenteritis with ampicillin, amoxicillin, or placebo. Pediatrics **65:**1125-1130.

190. **Creagh EM, O'Neill LA.** 2006. TLRs, NLRs and RLRs: a trinity of pathogen sensors that co-operate in innate immunity. Trends in immunology **27:**352-357.

191. **Schwandner R, Dziarski R, Wesche H, Rothe M, Kirschning CJ.** 1999. Peptidoglycan- and lipoteichoic acid-induced cell activation is mediated by toll-like receptor 2. Journal of Biological Chemistry **274:**17406-17409.

192. **Takeuchi O, Hoshino K, Kawai T, Sanjo H, Takada H, Ogawa T, Takeda K, Akira S.** 1999. Differential roles of TLR2 and TLR4 in recognition of gram-negative and gram-positive bacterial cell wall components. Immunity **11:**443-451.

193. **Yoshimura A, Lien E, Ingalls RR, Tuomanen E, Dziarski R, Golenbock D.** 1999. Cutting edge: recognition of Gram-positive bacterial cell wall components by the innate immune system occurs via Toll-like receptor 2. Journal of Immunology **163:**1-5.

194. **Medzhitov R, Preston-Hurlburt P, Janeway CA, Jr.** 1997. A human homologue of the Drosophila Toll protein signals activation of adaptive immunity. Nature **388:**394-397.

195. **Park BS, Song DH, Kim HM, Choi BS, Lee H, Lee JO.** 2009. The structural basis of lipopolysaccharide recognition by the TLR4-MD-2 complex. Nature **458:**1191-1195.

196. **Shimazu R, Akashi S, Ogata H, Nagai Y, Fukudome K, Miyake K, Kimoto M.** 1999. MD-2, a molecule that confers lipopolysaccharide responsiveness on Toll-like receptor 4. The Journal of Experimental Medicine **189:**1777-1782.

197. **Hayashi F, Smith KD, Ozinsky A, Hawn TR, Yi EC, Goodlett DR, Eng JK, Akira S, Underhill DM, Aderem A.** 2001. The innate immune response to bacterial flagellin is mediated by Toll-like receptor 5. Nature **410:**1099-1103.

198. **Bauer S, Kirschning CJ, Hacker H, Redecke V, Hausmann S, Akira S, Wagner H, Lipford GB.** 2001. Human TLR9 confers responsiveness to bacterial DNA via species-specific CpG motif recognition. Proceedings of the National Academy of Sciences of the United States of America **98:**9237-9242.

199. **Hemmi H, Takeuchi O, Kawai T, Kaisho T, Sato S, Sanjo H, Matsumoto M, Hoshino K, Wagner H, Takeda K, Akira S.** 2000. A Toll-like receptor recognizes bacterial DNA. Nature **408:**740-745.

200. **Kawai T, Akira S.** 2010. The role of pattern-recognition receptors in innate immunity: update on Toll-like receptors. Nature immunology **11:**373-384.

201. **Ting JP, Lovering RC, Alnemri ES, Bertin J, Boss JM, Davis BK, Flavell RA, Girardin SE, Godzik A, Harton JA, Hoffman HM, Hugot JP, Inohara N, Mackenzie A, Maltais LJ, Nunez G, Ogura Y, Otten LA, Philpott D, Reed JC, Reith W, Schreiber S, Steimle V, Ward PA.** 2008. The NLR gene family: a standard nomenclature. Immunity **28:**285-287.

202. **Franchi L, Eigenbrod T, Munoz-Planillo R, Nunez G.** 2009. The inflammasome: a caspase-1-activation platform that regulates immune responses and disease pathogenesis. Nature Immunology **10:**241-247.

203. **Miao EA, Rajan JV, Aderem A.** 2011. Caspase-1-induced pyroptotic cell death. Immunological Reviews **243:**206-214.

204. **Schroder K, Tschopp J.** 2010. The inflammasomes. Cell **140:**821-832.

205. **Allen IC, Scull MA, Moore CB, Holl EK, McElvania-TeKippe E, Taxman DJ, Guthrie EH, Pickles RJ, Ting JP.** 2009. The NLRP3 inflammasome mediates *in vivo* innate immunity to influenza A virus through recognition of viral RNA. Immunity **30:**556-565.

206. **Burckstummer T, Baumann C, Bluml S, Dixit E, Durnberger G, Jahn H, Planyavsky M, Bilban M, Colinge J, Bennett KL, Superti-Furga G.** 2009. An orthogonal proteomic-genomic screen identifies AIM2 as a cytoplasmic DNA sensor for the inflammasome. Nature Immunology **10:**266-272.

207. **Davis BK, Roberts RA, Huang MT, Willingham SB, Conti BJ, Brickey WJ, Barker BR, Kwan M, Taxman DJ, Accavitti-Loper MA, Duncan JA, Ting JP.** 2011. Cutting edge: NLRC5-dependent activation of the inflammasome. Journal of Immunology **186:**1333-1337.

208. **Hise AG, Tomalka J, Ganesan S, Patel K, Hall BA, Brown GD, Fitzgerald KA.** 2009. An essential role for the NLRP3 inflammasome in host defense against the human fungal pathogen *Candida albicans*. Cell Host & Microbe **5:**487-497.

209. **Miao EA, Alpuche-Aranda CM, Dors M, Clark AE, Bader MW, Miller SI, Aderem A.** 2006. Cytoplasmic flagellin activates caspase-1 and secretion of interleukin 1beta via Ipaf. Nature immunology **7:**569-575.

210. **Lamkanfi M, Dixit VM.** 2014. Mechanisms and Functions of Inflammasomes. Cell **157:**1013-1022.

211. **Lawrence T.** 2009. The nuclear factor NF-κB pathway in inflammation. Cold Spring Harbor perspectives in biology **1:**a001651.

212. **Ghosh S, May MJ, Kopp EB.** 1998. NF-κB and Rel proteins: evolutionarily conserved mediators of immune responses. Annual Review of Immunology **16:**225-260.

213. **Nishikori M.** 2005. Classical and Alternative NF-κB Activation Pathways and Their Roles in Lymphoid Malignancies. Journal of Clinical and Experimental Hematopathology **45:**15-24.

214. **Vallabhapurapu S, Karin M.** 2009. Regulation and function of NF-κB transcription factors in the immune system. Annual Review of Immunology **27:**693-733.

215. **Hayden MS, Ghosh S.** 2012. NF-κB, the first quarter-century: remarkable progress and outstanding questions. Genes & Development **26:**203-234.

216. **Mogensen TH.** 2009. Pathogen recognition and inflammatory signaling in innate immune defenses. Clinical Microbiology Reviews **22:**240-273, Table of Contents.

217. **Liu S, Chen ZJ.** 2011. Expanding role of ubiquitination in NF-κB signaling. Cell Research **21:**6-21.

218. **Bonizzi G, Karin M.** 2004. The two NF-κB activation pathways and their role in innate and adaptive immunity. Trends in Immunology **25:**280-288.

219. **Dejardin E, Droin NM, Delhase M, Haas E, Cao Y, Makris C, Li ZW, Karin M, Ware CF, Green DR.** 2002. The lymphotoxin-β receptor induces different patterns of gene expression via two NF-κB pathways. Immunity **17:**525-535.

220. **Senftleben U, Cao Y, Xiao G, Greten FR, Krahn G, Bonizzi G, Chen Y, Hu Y, Fong A, Sun SC, Karin M.** 2001. Activation by IKKα of a second, evolutionary conserved, NF-κB signaling pathway. Science **293:**1495-1499.

221. **Krens SF, Spaink HP, Snaar-Jagalska BE.** 2006. Functions of the MAPK family in vertebrate-development. FEBS letters **580:**4984-4990.

222. **Kyriakis JM, Avruch J.** 2001. Mammalian mitogen-activated protein kinase signal transduction pathways activated by stress and inflammation. Physiological Reviews **81:**807-869.

223. **Schaeffer HJ, Weber MJ.** 1999. Mitogen-activated protein kinases: specific messages from ubiquitous messengers. Molecular and Cellular Biology **19:**2435-2444.

224. **Broom OJ, Widjaya B, Troelsen J, Olsen J, Nielsen OH.** 2009. Mitogen activated protein kinases: a role in inflammatory bowel disease? Clinical and Experimental Immunology **158:**272-280.

225. **Coulombe P, Meloche S.** 2007. Atypical mitogen-activated protein kinases: structure, regulation and functions. Biochimica et Biophysica Acta **1773:**1376-1387.

226. **Chen Z, Gibson TB, Robinson F, Silvestro L, Pearson G, Xu B, Wright A, Vanderbilt C, Cobb MH.** 2001. MAP kinases. Chemical Reviews **101:**2449-2476.

227. **Thalhamer T, McGrath MA, Harnett MM.** 2008. MAPKs and their relevance to arthritis and inflammation. Rheumatology **47:**409-414.

228. **Ralph JA, Morand EF.** 2008. MAPK phosphatases as novel targets for rheumatoid arthritis. Expert Opinion on Therapeutic Targets **12:**795-808.

229. **Aud D, Peng SL.** 2006. Mechanisms of disease: Transcription factors in inflammatory arthritis. Nature clinical practice. Rheumatology **2:**434-442.

230. **Roy PK, Rashid F, Bragg J, Ibdah JA.** 2008. Role of the JNK signal transduction pathway in inflammatory bowel disease. World journal of Gastroenterology **14:**200-202.

231. **Vandenabeele P, Galluzzi L, Vanden Berghe T, Kroemer G.** 2010. Molecular mechanisms of necroptosis: an ordered cellular explosion. Nature Reviews Molecular Cell Biology **11:**700-714.

232. **Ashida H, Mimuro H, Ogawa M, Kobayashi T, Sanada T, Kim M, Sasakawa C.** 2011. Cell death and infection: a double-edged sword for host and pathogen survival. The Journal of Cell Biology **195:**931-942.

233. **Elliott MR, Ravichandran KS.** 2010. Clearance of apoptotic cells: implications in health and disease. The Journal of Cell Biology **189:**1059-1070.

234. **Carneiro LA, Travassos LH, Soares F, Tattoli I, Magalhaes JG, Bozza MT, Plotkowski MC, Sansonetti PJ, Molkentin JD, Philpott DJ, Girardin SE.** 2009. *Shigella* induces mitochondrial dysfunction and cell death in nonmyleoid cells. Cell Host & Microbe **5:**123-136.

235. **Clark CS, Maurelli AT.** 2007. *Shigella flexneri* inhibits staurosporine-induced apoptosis in epithelial cells. Infection and Immunity **75:**2531-2539.

236. **Faherty CS, Maurelli AT.** 2009. Spa15 of *Shigella flexneri* is secreted through the type III secretion system and prevents staurosporine-induced apoptosis. Infection and Immunity **77:**5281-5290.

237. **Kerr JF, Wyllie AH, Currie AR.** 1972. Apoptosis: a basic biological phenomenon with wide-ranging implications in tissue kinetics. British Journal of Cancer **26:**239-257.

238. **Maderna P, Godson C.** 2003. Phagocytosis of apoptotic cells and the resolution of inflammation. Biochimica et Biophysica Acta **1639:**141-151.

239. **Bratton DL, Fadok VA, Richter DA, Kailey JM, Guthrie LA, Henson PM.** 1997. Appearance of phosphatidylserine on apoptotic cells requires calcium-mediated nonspecific flip-flop and is enhanced by loss of the aminophospholipid translocase. Journal of Biological Chemistry **272:**26159-26165.

240. **Savill J, Fadok V.** 2000. Corpse clearance defines the meaning of cell death. Nature **407:**784-788.

241. **Kurosaka K, Takahashi M, Watanabe N, Kobayashi Y.** 2003. Silent cleanup of very early apoptotic cells by macrophages. Journal of Immunology **171:**4672-4679.

242. **Salvesen GS, Dixit VM.** 1997. Caspases: intracellular signaling by proteolysis. Cell **91:**443-446.

243. **Iyer SS, Pulskens WP, Sadler JJ, Butter LM, Teske GJ, Ulland TK, Eisenbarth SC, Florquin S, Flavell RA, Leemans JC, Sutterwala FS.** 2009. Necrotic cells trigger a sterile inflammatory response through the Nlrp3 inflammasome. Proceedings of the National Academy of Sciences of the United States of America **106:**20388-20393.

244. **Fink SL, Cookson BT.** 2005. Apoptosis, pyroptosis, and necrosis: mechanistic description of dead and dying eukaryotic cells. Infection and Immunity **73:**1907-1916.

245. **Igney FH, Krammer PH.** 2002. Death and anti-death: tumour resistance to apoptosis. Nature reviews. Cancer **2:**277-288.

246. **Ashkenazi A, Dixit VM.** 1998. Death receptors: signaling and modulation. Science **281:**1305-1308.

247. **Banner DW, D'Arcy A, Janes W, Gentz R, Schoenfeld HJ, Broger C, Loetscher H, Lesslauer W.** 1993. Crystal structure of the soluble human 55 kd TNF receptor-human TNF beta complex: implications for TNF receptor activation. Cell **73:**431-445.

248. **Gruss HJ, Dower SK.** 1995. Tumor necrosis factor ligand superfamily: involvement in the pathology of malignant lymphomas. Blood **85:**3378-3404.

249. **Peter ME, Krammer PH.** 1998. Mechanisms of CD95 (APO-1/Fas)-mediated apoptosis. Current Opinion in Immunology **10:**545-551.

250. **Suliman A, Lam A, Datta R, Srivastava RK.** 2001. Intracellular mechanisms of TRAIL: apoptosis through mitochondrial-dependent and -independent pathways. Oncogene **20:**2122-2133.

251. **Chicheportiche Y, Bourdon PR, Xu H, Hsu YM, Scott H, Hession C, Garcia I, Browning JL.** 1997. TWEAK, a new secreted ligand in the tumor necrosis factor family that weakly induces apoptosis. Journal of Biological Chemistry **272:**32401-32410.

252. **Rubio-Moscardo F, Blesa D, Mestre C, Siebert R, Balasas T, Benito A, Rosenwald A, Climent J, Martinez JI, Schilhabel M, Karran EL, Gesk S, Esteller M, deLeeuw R, Staudt LM, Fernandez-Luna JL, Pinkel D, Dyer MJ, Martinez-Climent JA.** 2005. Characterization of 8p21.3 chromosomal deletions in B-cell lymphoma: TRAIL-R1 and TRAIL-R2 as candidate dosage-dependent tumor suppressor genes. Blood **106:**3214-3222.

253. **Schneider P, Holler N, Bodmer JL, Hahne M, Frei K, Fontana A, Tschopp J.** 1998. Conversion of membrane-bound Fas(CD95) ligand to its soluble form is associated with downregulation of its proapoptotic activity and loss of liver toxicity. The Journal of Experimental Medicine **187:**1205-1213.

254. **O' Reilly LA, Tai L, Lee L, Kruse EA, Grabow S, Fairlie WD, Haynes NM, Tarlinton DM, Zhang JG, Belz GT, Smyth MJ, Bouillet P, Robb L, Strasser A.** 2009. Membrane-bound Fas ligand only is essential for Fas-induced apoptosis. Nature **461:**659-663.

255. **Strasser A, Jost PJ, Nagata S.** 2009. The many roles of FAS receptor signaling in the immune system. Immunity **30:**180-192.

256. **Leithauser F, Dhein J, Mechtersheimer G, Koretz K, Bruderlein S, Henne C, Schmidt A, Debatin KM, Krammer PH, Moller P.** 1993. Constitutive and induced expression of APO-1, a new member of the nerve growth factor/tumor necrosis factor receptor superfamily, in normal and neoplastic cells. Laboratory Investigation; a journal of technical methods and pathology **69:**415-429.

257. **Moller P, Koretz K, Leithauser F, Bruderlein S, Henne C, Quentmeier A, Krammer PH.** 1994. Expression of APO-1 (CD95), a member of the NGF/TNF receptor superfamily, in normal and neoplastic colon epithelium. International journal of cancer. Journal International du Cancer **57:**371-377.

258. **Lee KH, Feig C, Tchikov V, Schickel R, Hallas C, Schutze S, Peter ME, Chan AC.** 2006. The role of receptor internalization in CD95 signaling. EMBO Journal **25:**1009-1023.

259. **Kischkel FC, Hellbardt S, Behrmann I, Germer M, Pawlita M, Krammer PH, Peter ME.** 1995. Cytotoxicity-dependent APO-1 (Fas/CD95)-associated proteins form a death-inducing signaling complex (DISC) with the receptor. EMBO Journal **14:**5579-5588.

260. **Li H, Zhu H, Xu CJ, Yuan J.** 1998. Cleavage of BID by caspase 8 mediates the mitochondrial damage in the Fas pathway of apoptosis. Cell **94:**491-501.

261. **Yin XM, Wang K, Gross A, Zhao Y, Zinkel S, Klocke B, Roth KA, Korsmeyer SJ.** 1999. Bid-deficient mice are resistant to Fas-induced hepatocellular apoptosis. Nature **400:**886-891.

262. **Jost PJ, Grabow S, Gray D, McKenzie MD, Nachbur U, Huang DC, Bouillet P, Thomas HE, Borner C, Silke J, Strasser A, Kaufmann T.** 2009. XIAP discriminates between type I and type II FAS-induced apoptosis. Nature **460:**1035-1039.

263. **Kuang AA, Diehl GE, Zhang J, Winoto A.** 2000. FADD is required for DR4- and DR5-mediated apoptosis: lack of trail-induced apoptosis in FADD-deficient mouse embryonic fibroblasts. Journal of Biological Chemistry **275:**25065-25068.

264. **Tartaglia LA, Goeddel DV.** 1992. Two TNF receptors. Immunology Today **13:**151-153.

265. **Tartaglia LA, Weber RF, Figari IS, Reynolds C, Palladino MA, Jr., Goeddel DV.** 1991. The two different receptors for tumor necrosis factor mediate distinct cellular responses. Proceedings of the National Academy of Sciences of the United States of America **88:**9292-9296.

266. **Vandenabeele P, Declercq W, Beyaert R, Fiers W.** 1995. Two tumour necrosis factor receptors: structure and function. Trends in Cell Biology **5:**392-399.

267. **Pfeffer K, Matsuyama T, Kundig TM, Wakeham A, Kishihara K, Shahinian A, Wiegmann K, Ohashi PS, Kronke M, Mak TW.** 1993. Mice deficient for the 55 kd tumor necrosis factor receptor are resistant to endotoxic shock, yet succumb to L. monocytogenes infection. Cell **73:**457-467.

268. **Zhao YX, Lajoie G, Zhang H, Chiu B, Payne U, Inman RD.** 2000. Tumor necrosis factor receptor p55-deficient mice respond to acute *Yersinia enterocolitica* infection with less apoptosis and more effective host resistance. Infection and Immunity **68:**1243-1251.

269. **Legler DF, Micheau O, Doucey MA, Tschopp J, Bron C.** 2003. Recruitment of TNF receptor 1 to lipid rafts is essential for TNFα-mediated NF-κB activation. Immunity **18:**655-664.

270. **Harper N, Hughes M, MacFarlane M, Cohen GM.** 2003. Fas-associated death domain protein and caspase-8 are not recruited to the tumor necrosis factor receptor 1 signaling complex during tumor necrosis factor-induced apoptosis. Journal of Biological Chemistry **278:**25534-25541.

271. **Micheau O, Tschopp J.** 2003. Induction of TNF receptor I-mediated apoptosis via two sequential signaling complexes. Cell **114:**181-190.

272. **Schneider-Brachert W, Tchikov V, Merkel O, Jakob M, Hallas C, Kruse ML, Groitl P, Lehn A, Hildt E, Held-Feindt J, Dobner T, Kabelitz D, Kronke M, Schutze S.** 2006. Inhibition of TNF receptor 1 internalization by adenovirus 14.7K as a novel immune escape mechanism. The Journal of Clinical Investigation **116:**2901-2913.

273. **Schneider-Brachert W, Tchikov V, Neumeyer J, Jakob M, Winoto-Morbach S, Held-Feindt J, Heinrich M, Merkel O, Ehrenschwender M, Adam D, Mentlein R, Kabelitz D, Schutze S.** 2004. Compartmentalization of TNF receptor 1 signaling: internalized TNF receptosomes as death signaling vesicles. Immunity **21:**415-428.

274. **Remijsen Q, Goossens V, Grootjans S, Van den Haute C, Vanlangenakker N, Dondelinger Y, Roelandt R, Bruggeman I, Goncalves A, Bertrand MJ, Baekelandt V, Takahashi N, Berghe TV, Vandenabeele P.** 2014. Depletion of RIPK3 or MLKL blocks TNF-driven necroptosis and switches towards a delayed RIPK1 kinase-dependent apoptosis. Cell Death & Disease **5:**e1004.

275. **Murphy JM, Czabotar PE, Hildebrand JM, Lucet IS, Zhang JG, Alvarez-Diaz S, Lewis R, Lalaoui N, Metcalf D, Webb AI, Young SN, Varghese LN, Tannahill GM, Hatchell EC, Majewski IJ, Okamoto T, Dobson RC, Hilton DJ, Babon JJ, Nicola NA, Strasser A, Silke J, Alexander WS.** 2013. The pseudokinase MLKL mediates necroptosis via a molecular switch mechanism. Immunity **39:**443-453.

276. **Li H, Kobayashi M, Blonska M, You Y, Lin X.** 2006. Ubiquitination of RIP is required for tumor necrosis factor α-induced NF-κB activation. Journal of Biological Chemistry **281:**13636-13643.

277. **Ea CK, Deng L, Xia ZP, Pineda G, Chen ZJ.** 2006. Activation of IKK by TNFalpha requires site-specific ubiquitination of RIP1 and polyubiquitin binding by NEMO. Molecular Cell **22:**245-257.

278. **Wang CY, Mayo MW, Korneluk RG, Goeddel DV, Baldwin AS, Jr.** 1998. NF-κB antiapoptosis: induction of TRAF1 and TRAF2 and c-IAP1 and c-IAP2 to suppress caspase-8 activation. Science **281:**1680-1683.

279. **Van Antwerp DJ, Martin SJ, Kafri T, Green DR, Verma IM.** 1996. Suppression of TNF-α-induced apoptosis by NF-κB. Science **274:**787-789.

280. **Strasser A, Harris AW, Huang DC, Krammer PH, Cory S.** 1995. Bcl-2 and Fas/APO-1 regulate distinct pathways to lymphocyte apoptosis. EMBO Journal **14:**6136-6147.

281. **Czabotar PE, Lessene G, Strasser A, Adams JM.** 2014. Control of apoptosis by the BCL-2 protein family: implications for physiology and therapy. Nature Reviews Molecular Cell Biology **15:**49-63.

282. **Chinnaiyan AM.** 1999. The apoptosome: heart and soul of the cell death machine. Neoplasia **1:**5-15.

283. **Zhou X, Giron JA, Torres AG, Crawford JA, Negrete E, Vogel SN, Kaper JB.** 2003. Flagellin of enteropathogenic *Escherichia coli* stimulates interleukin-8 production in T84 cells. Infection and Immunity **71:**2120-2129.

284. **Tzipori S, Gibson R, Montanaro J.** 1989. Nature and distribution of mucosal lesions associated with enteropathogenic and enterohemorrhagic *Escherichia coli* in piglets and the role of plasmid-mediated factors. Infection and Immunity **57:**1142-1150.

285. **Tzipori S, Robins-Browne RM, Gonis G, Hayes J, Withers M, McCartney E.** 1985. Enteropathogenic *Escherichia coli* enteritis: evaluation of the gnotobiotic piglet as a model of human infection. Gut **26:**570-578.

286. **Gewirtz AT, Navas TA, Lyons S, Godowski PJ, Madara JL.** 2001. Cutting edge: bacterial flagellin activates basolaterally expressed TLR5 to induce epithelial proinflammatory gene expression. Journal of Immunology **167:**1882-1885.

287. **McNamara BP, Koutsouris A, O'Connell CB, Nougayrede JP, Donnenberg MS, Hecht G.** 2001. Translocated EspF protein from enteropathogenic *Escherichia coli* disrupts host intestinal barrier function. The Journal of Clinical Investigation **107:**621-629.

288. **Muza-Moons MM, Koutsouris A, Hecht G.** 2003. Disruption of cell polarity by enteropathogenic *Escherichia coli* enables basolateral membrane proteins to migrate apically and to potentiate physiological consequences. Infection and Immunity **71:**7069-7078.

289. **Kinnebrew MA, Buffie CG, Diehl GE, Zenewicz LA, Leiner I, Hohl TM, Flavell RA, Littman DR, Pamer EG.** 2012. Interleukin 23 production by intestinal CD103(+)CD11b(+) dendritic cells in response to bacterial flagellin enhances mucosal innate immune defense. Immunity **36:**276-287.

290. **Khan MA, Bouzari S, Ma C, Rosenberger CM, Bergstrom KS, Gibson DL, Steiner TS, Vallance BA.** 2008. Flagellin-dependent and -independent

inflammatory responses following infection by enteropathogenic *Escherichia coli* and *Citrobacter rodentium*. Infection and Immunity **76:**1410-1422.

291. **Wang Y, Xiang GS, Kourouma F, Umar S.** 2006. *Citrobacter rodentium*-induced NF-κB activation in hyperproliferating colonic epithelia: role of p65 (Ser536) phosphorylation. British Journal of Pharmacology **148:**814-824.

292. **Khan MA, Ma C, Knodler LA, Valdez Y, Rosenberger CM, Deng W, Finlay BB, Vallance BA.** 2006. Toll-like receptor 4 contributes to colitis development but not to host defense during *Citrobacter rodentium* infection in mice. Infection and Immunity **74:**2522-2536.

293. **Higgins LM, Frankel G, Douce G, Dougan G, MacDonald TT.** 1999. *Citrobacter rodentium* infection in mice elicits a mucosal Th1 cytokine response and lesions similar to those in murine inflammatory bowel disease. Infection and Immunity **67:**3031-3039.

294. **Zheng Y, Valdez PA, Danilenko DM, Hu Y, Sa SM, Gong Q, Abbas AR, Modrusan Z, Ghilardi N, de Sauvage FJ, Ouyang W.** 2008. Interleukin-22 mediates early host defense against attaching and effacing bacterial pathogens. Nature Medicine **14:**282-289.

295. **Liang SC, Tan XY, Luxenberg DP, Karim R, Dunussi-Joannopoulos K, Collins M, Fouser LA.** 2006. Interleukin (IL)-22 and IL-17 are coexpressed by Th17 cells and cooperatively enhance expression of antimicrobial peptides. The Journal of Experimental Medicine **203:**2271-2279.

296. **Geddes K, Rubino SJ, Magalhaes JG, Streutker C, Le Bourhis L, Cho JH, Robertson SJ, Kim CJ, Kaul R, Philpott DJ, Girardin SE.** 2011. Identification of an innate T helper type 17 response to intestinal bacterial pathogens. Nature Medicine **17:**837-844.

297. **Gibson DL, Ma C, Rosenberger CM, Bergstrom KS, Valdez Y, Huang JT, Khan MA, Vallance BA.** 2008. Toll-like receptor 2 plays a critical role in maintaining mucosal integrity during *Citrobacter rodentium*-induced colitis. Cellular Microbiology **10:**388-403.

298. **Long KZ, Rosado JL, Santos JI, Haas M, Al Mamun A, DuPont HL, Nanthakumar NN, Estrada-Garcia T.** 2010. Associations between mucosal innate and adaptive immune responses and resolution of diarrheal pathogen infections. Infection and Immunity **78:**1221-1228.

299. **Zheng Y, Danilenko DM, Valdez P, Kasman I, Eastham-Anderson J, Wu J, Ouyang W.** 2007. Interleukin-22, a T(H)17 cytokine, mediates IL-23-induced dermal inflammation and acanthosis. Nature **445:**648-651.

300. **Sacks D, Kamhawi S.** 2001. Molecular aspects of parasite-vector and vector-host interactions in leishmaniasis. Annual Review of Microbiology **55:**453-483.

301. **Sonnenberg GF, Fouser LA, Artis D.** 2011. Border patrol: regulation of immunity, inflammation and tissue homeostasis at barrier surfaces by IL-22. Nature Immunology **12:**383-390.

302. **Spits H, Di Santo JP.** 2011. The expanding family of innate lymphoid cells: regulators and effectors of immunity and tissue remodeling. Nature Immunology **12:**21-27.

303. **Cella M, Fuchs A, Vermi W, Facchetti F, Otero K, Lennerz JK, Doherty JM, Mills JC, Colonna M.** 2009. A human natural killer cell subset provides an innate source of IL-22 for mucosal immunity. Nature **457:**722-725.

304. **Colonna M.** 2009. Interleukin-22-producing natural killer cells and lymphoid tissue inducer-like cells in mucosal immunity. Immunity **31:**15-23.

305. **Satoh-Takayama N, Vosshenrich CA, Lesjean-Pottier S, Sawa S, Lochner M, Rattis F, Mention JJ, Thiam K, Cerf-Bensussan N, Mandelboim O, Eberl G, Di Santo JP.** 2008. Microbial flora drives interleukin 22 production in intestinal NKp46+ cells that provide innate mucosal immune defense. Immunity **29:**958-970.

306. **Zenewicz LA, Yancopoulos GD, Valenzuela DM, Murphy AJ, Stevens S, Flavell RA.** 2008. Innate and adaptive interleukin-22 protects mice from inflammatory bowel disease. Immunity **29:**947-957.

307. **Cash HL, Whitham CV, Behrendt CL, Hooper LV.** 2006. Symbiotic bacteria direct expression of an intestinal bactericidal lectin. Science **313:**1126-1130.

308. **Bry L, Brenner MB.** 2004. Critical role of T cell-dependent serum antibody, but not the gut-associated lymphoid tissue, for surviving acute mucosal infection with *Citrobacter rodentium*, an attaching and effacing pathogen. Journal of Immunology **172:**433-441.

309. **Eckmann L, Kagnoff MF.** 2001. Cytokines in host defense against *Salmonella*. Microbes and Infection **3:**1191-1200.

310. **Gewirtz AT, Rao AS, Simon PO, Jr., Merlin D, Carnes D, Madara JL, Neish AS.** 2000. *Salmonella typhimurium* induces epithelial IL-8 expression via Ca(2+)-mediated activation of the NF-κB pathway. The Journal of Clinical Investigation **105:**79-92.

311. **Gewirtz AT, Simon PO, Jr., Schmitt CK, Taylor LJ, Hagedorn CH, O'Brien AD, Neish AS, Madara JL.** 2001. *Salmonella typhimurium* translocates flagellin across intestinal epithelia, inducing a proinflammatory response. The Journal of Clinical Investigation **107:**99-109.

312. **McCormick BA, Hofman PM, Kim J, Carnes DK, Miller SI, Madara JL.** 1995. Surface attachment of *Salmonella typhimurium* to intestinal epithelia imprints the subepithelial matrix with gradients chemotactic for neutrophils. The Journal of Cell Biology **131:**1599-1608.

313. **Monack DM, Navarre WW, Falkow S.** 2001. *Salmonella*-induced macrophage death: the role of caspase-1 in death and inflammation. Microbes and Infection **3:**1201-1212.

314. **Franchi L, Amer A, Body-Malapel M, Kanneganti TD, Ozoren N, Jagirdar R, Inohara N, Vandenabeele P, Bertin J, Coyle A, Grant EP, Nunez G.** 2006. Cytosolic flagellin requires Ipaf for activation of caspase-1 and interleukin 1β in *Salmonella*-infected macrophages. Nature Immunology **7:**576-582.

315. **Morrissey PJ, Charrier K, Vogel SN.** 1995. Exogenous tumor necrosis factor α and interleukin-1α increase resistance to *Salmonella typhimurium*: efficacy is influenced by the *Ity* and *Lps* loci. Infection and Immunity **63:**3196-3198.

316. **Gulig PA, Doyle TJ, Clare-Salzler MJ, Maiese RL, Matsui H.** 1997. Systemic infection of mice by wild-type but not Spv- *Salmonella typhimurium* is enhanced by neutralization of gamma interferon and tumor necrosis factor alpha. Infection and Immunity **65:**5191-5197.

317. **Nauciel C, Espinasse-Maes F.** 1992. Role of gamma interferon and tumor necrosis factor alpha in resistance to *Salmonella typhimurium* infection. Infection and Immunity **60:**450-454.

318. **Eckmann L, Fierer J, Kagnoff MF.** 1996. Genetically resistant (Ityr) and susceptible (Itys) congenic mouse strains show similar cytokine responses following infection with *Salmonella dublin*. Journal of Immunology **156:**2894-2900.

319. **Ramarathinam L, Shaban RA, Niesel DW, Klimpel GR.** 1991. Interferon gamma (IFN-γ) production by gut-associated lymphoid tissue and spleen following oral *Salmonella typhimurium* challenge. Microbial Pathogenesis **11:**347-356.

320. **Bao S, Beagley KW, France MP, Shen J, Husband AJ.** 2000. Interferon-gamma plays a critical role in intestinal immunity against *Salmonella typhimurium* infection. Immunology **99:**464-472.

321. **Kincy-Cain T, Clements JD, Bost KL.** 1996. Endogenous and exogenous interleukin-12 augment the protective immune response in mice orally challenged with *Salmonella dublin*. Infection and Immunity **64:**1437-1440.

322. **Mastroeni P, Harrison JA, Robinson JH, Clare S, Khan S, Maskell DJ, Dougan G, Hormaeche CE.** 1998. Interleukin-12 is required for control of the growth of attenuated aromatic-compound-dependent *salmonellae* in BALB/c mice: role of gamma interferon and macrophage activation. Infection and Immunity **66:**4767-4776.

323. **Dybing JK, Walters N, Pascual DW.** 1999. Role of endogenous interleukin-18 in resolving wild-type and attenuated *Salmonella typhimurium* infections. Infection and Immunity **67:**6242-6248.

324. **Mastroeni P, Clare S, Khan S, Harrison JA, Hormaeche CE, Okamura H, Kurimoto M, Dougan G.** 1999. Interleukin 18 contributes to host resistance and gamma interferon production in mice infected with virulent *Salmonella typhimurium*. Infection and Immunity **67:**478-483.

325. **Forbes JR, Gros P.** 2001. Divalent-metal transport by NRAMP proteins at the interface of host-pathogen interactions. Trends in Microbiology **9:**397-403.

326. **Nairz M, Fritsche G, Crouch ML, Barton HC, Fang FC, Weiss G.** 2009. Slc11a1 limits intracellular growth of *Salmonella enterica* sv. Typhimurium by promoting macrophage immune effector functions and impairing bacterial iron acquisition. Cellular Microbiology **11:**1365-1381.

327. **Mulero V, Searle S, Blackwell JM, Brock JH.** 2002. Solute carrier 11a1 (Slc11a1; formerly Nramp1) regulates metabolism and release of iron acquired by phagocytic, but not transferrin-receptor-mediated, iron uptake. The Biochemical Journal **363:**89-94.

328. **Valdez Y, Grassl GA, Guttman JA, Coburn B, Gros P, Vallance BA, Finlay BB.** 2009. Nramp1 drives an accelerated inflammatory response during *Salmonella*-induced colitis in mice. Cellular Microbiology **11:**351-362.

329. **Brown DE, Libby SJ, Moreland SM, McCoy MW, Brabb T, Stepanek A, Fang FC, Detweiler CS.** 2013. *Salmonella enterica* causes more severe inflammatory disease in C57/BL6 *Nramp1G169* mice than Sv129S6 mice. Veterinary Pathology **50:**867-876.

330. **Knutton S, Baldini MM, Kaper JB, McNeish AS.** 1987. Role of plasmid-encoded adherence factors in adhesion of enteropathogenic *Escherichia coli* to HEp-2 cells. Infection and Immunity **55:**78-85.

331. **Anantha RP, Stone KD, Donnenberg MS.** 2000. Effects of *bfp* mutations on biogenesis of functional enteropathogenic *Escherichia coli* type IV pili. Journal of Bacteriology **182:**2498-2506.

332. **Girón JA, Ho AS, Schoolnik GK.** 1991. An inducible bundle-forming pilus of enteropathogenic *Escherichia coli*. Science **254:**710-713.

333. **Sohel I, Puente JL, Ramer SW, Bieber D, Wu CY, Schoolnik GK.** 1996. Enteropathogenic *Escherichia coli*: identification of a gene cluster coding for bundle-forming pilus morphogenesis. Journal of Bacteriology **178:**2613-2628.

334. **Stone KD, Zhang HZ, Carlson LK, Donnenberg MS.** 1996. A cluster of fourteen genes from enteropathogenic *Escherichia coli* is sufficient for the biogenesis of a type IV pilus. Molecular Microbiology **20:**325-337.

335. **Girón JA, Donnenberg MS, Martin WC, Jarvis KG, Kaper JB.** 1993. Distribution of the bundle-forming pilus structural gene (*bfpA*) among enteropathogenic *Escherichia coli*. The Journal of Infectious Diseases **168:**1037-1041.

336. **Zhang HZ, Lory S, Donnenberg MS.** 1994. A plasmid-encoded prepilin peptidase gene from enteropathogenic *Escherichia coli*. Journal of Bacteriology **176:**6885-6891.

337. **Anantha RP, Stone KD, Donnenberg MS.** 1998. Role of BfpF, a member of the PilT family of putative nucleotide-binding proteins, in type IV pilus biogenesis and in interactions between enteropathogenic *Escherichia coli* and host cells. Infection and Immunity **66:**122-131.

338. **Khursigara C, Abul-Milh M, Lau B, Giron JA, Lingwood CA, Barnett Foster DE.** 2001. Enteropathogenic *Escherichia coli* virulence factor bundle-forming pilus has a binding specificity for phosphatidylethanolamine. Infection and Immunity **69:**6573-6579.

339. **McDaniel TK, Jarvis KG, Donnenberg MS, Kaper JB.** 1995. A genetic locus of enterocyte effacement conserved among diverse enterobacterial pathogens. Proceedings of the National Academy of Sciences of the United States of America **92:**1664-1668.

340. **Wieler LH, McDaniel TK, Whittam TS, Kaper JB.** 1997. Insertion site of the locus of enterocyte effacement in enteropathogenic and enterohemorrhagic

Escherichia coli differs in relation to the clonal phylogeny of the strains. FEMS Microbiology Letters **156:**49-53.

341. **Elliott SJ, Wainwright LA, McDaniel TK, Jarvis KG, Deng YK, Lai LC, McNamara BP, Donnenberg MS, Kaper JB.** 1998. The complete sequence of the locus of enterocyte effacement (LEE) from enteropathogenic *Escherichia coli* E2348/69. Molecular Microbiology **28:**1-4.

342. **Perna NT, Mayhew GF, Posfai G, Elliott S, Donnenberg MS, Kaper JB, Blattner FR.** 1998. Molecular evolution of a pathogenicity island from enterohemorrhagic *Escherichia coli* O157:H7. Infection and Immunity **66:**3810-3817.

343. **Coburn B, Sekirov I, Finlay BB.** 2007. Type III secretion systems and disease. Clinical Microbiology Reviews **20:**535-549.

344. **Gophna U, Ron EZ, Graur D.** 2003. Bacterial type III secretion systems are ancient and evolved by multiple horizontal-transfer events. Gene **312:**151-163.

345. **Nguyen L, Paulsen IT, Tchieu J, Hueck CJ, Saier MH, Jr.** 2000. Phylogenetic analyses of the constituents of Type III protein secretion systems. Journal of Molecular Microbiology and Biotechnology **2:**125-144.

346. **Kubori T, Matsushima Y, Nakamura D, Uralil J, Lara-Tejero M, Sukhan A, Galan JE, Aizawa SI.** 1998. Supramolecular structure of the *Salmonella typhimurium* type III protein secretion system. Science **280:**602-605.

347. **Kubori T, Sukhan A, Aizawa SI, Galan JE.** 2000. Molecular characterization and assembly of the needle complex of the *Salmonella typhimurium* type III protein secretion system. Proceedings of the National Academy of Sciences of the United States of America **97:**10225-10230.

348. **Sekiya K, Ohishi M, Ogino T, Tamano K, Sasakawa C, Abe A.** 2001. Supermolecular structure of the enteropathogenic *Escherichia coli* type III secretion system and its direct interaction with the EspA-sheath-like structure. Proceedings of the National Academy of Sciences of the United States of America **98:**11638-11643.

349. **Wilson RK, Shaw RK, Daniell S, Knutton S, Frankel G.** 2001. Role of EscF, a putative needle complex protein, in the type III protein translocation system of enteropathogenic *Escherichia coli*. Cellular Microbiology **3:**753-762.

350. **Tamano K, Aizawa S, Katayama E, Nonaka T, Imajoh-Ohmi S, Kuwae A, Nagai S, Sasakawa C.** 2000. Supramolecular structure of the *Shigella* type III

secretion machinery: the needle part is changeable in length and essential for delivery of effectors. EMBO Journal **19:**3876-3887.

351. **Daniell SJ, Kocsis E, Morris E, Knutton S, Booy FP, Frankel G.** 2003. 3D structure of EspA filaments from enteropathogenic *Escherichia coli*. Molecular Microbiology **49:**301-308.

352. **Yip CK, Kimbrough TG, Felise HB, Vuckovic M, Thomas NA, Pfuetzner RA, Frey EA, Finlay BB, Miller SI, Strynadka NC.** 2005. Structural characterization of the molecular platform for type III secretion system assembly. Nature **435:**702-707.

353. **Gauthier A, Puente JL, Finlay BB.** 2003. Secretin of the enteropathogenic *Escherichia coli* type III secretion system requires components of the type III apparatus for assembly and localization. Infection and Immunity **71:**3310-3319.

354. **Creasey EA, Delahay RM, Daniell SJ, Frankel G.** 2003. Yeast two-hybrid system survey of interactions between LEE-encoded proteins of enteropathogenic *Escherichia coli*. Microbiology **149:**2093-2106.

355. **Akeda Y, Galan JE.** 2004. Genetic analysis of the *Salmonella enterica* type III secretion-associated ATPase InvC defines discrete functional domains. Journal of Bacteriology **186:**2402-2412.

356. **Hueck CJ.** 1998. Type III protein secretion systems in bacterial pathogens of animals and plants. Microbiology and Molecular Biology Reviews : MMBR **62:**379-433.

357. **Woestyn S, Allaoui A, Wattiau P, Cornelis GR.** 1994. YscN, the putative energizer of the *Yersinia* Yop secretion machinery. Journal of Bacteriology **176:**1561-1569.

358. **Gauthier A, Finlay BB.** 2003. Translocated intimin receptor and its chaperone interact with ATPase of the type III secretion apparatus of enteropathogenic *Escherichia coli*. Journal of Bacteriology **185:**6747-6755.

359. **Galan JE, Wolf-Watz H.** 2006. Protein delivery into eukaryotic cells by type III secretion machines. Nature **444:**567-573.

360. **Giogha C, Wong Fok Lung T, Pearson JS, Hartland EL.** 2014. Inhibition of death receptor signaling by bacterial gut pathogens. Cytokine & Growth Factor Reviews **25:**235-243.

361. **Kenny B, DeVinney R, Stein M, Reinscheid DJ, Frey EA, Finlay BB.** 1997. Enteropathogenic *E. coli* (EPEC) transfers its receptor for intimate adherence into mammalian cells. Cell **91:**511-520.

362. **de Grado M, Abe A, Gauthier A, Steele-Mortimer O, DeVinney R, Finlay BB.** 1999. Identification of the intimin-binding domain of Tir of enteropathogenic *Escherichia coli*. Cellular Microbiology **1:**7-17.

363. **Hartland EL, Batchelor M, Delahay RM, Hale C, Matthews S, Dougan G, Knutton S, Connerton I, Frankel G.** 1999. Binding of intimin from enteropathogenic *Escherichia coli* to Tir and to host cells. Molecular Microbiology **32:**151-158.

364. **Kenny B.** 1999. Phosphorylation of tyrosine 474 of the enteropathogenic *Escherichia coli* (EPEC) Tir receptor molecule is essential for actin nucleating activity and is preceded by additional host modifications. Molecular Microbiology **31:**1229-1241.

365. **Liu H, Magoun L, Luperchio S, Schauer DB, Leong JM.** 1999. The Tir-binding region of enterohaemorrhagic *Escherichia coli* intimin is sufficient to trigger actin condensation after bacterial-induced host cell signalling. Molecular Microbiology **34:**67-81.

366. **Campellone KG, Leong JM.** 2003. Tails of two Tirs: actin pedestal formation by enteropathogenic *E. coli* and enterohemorrhagic *E. coli* O157:H7. Current Opinion in Microbiology **6:**82-90.

367. **Campellone KG, Giese A, Tipper DJ, Leong JM.** 2002. A tyrosine-phosphorylated 12-amino-acid sequence of enteropathogenic *Escherichia coli* Tir binds the host adaptor protein Nck and is required for Nck localization to actin pedestals. Molecular Microbiology **43:**1227-1241.

368. **Gruenheid S, DeVinney R, Bladt F, Goosney D, Gelkop S, Gish GD, Pawson T, Finlay BB.** 2001. Enteropathogenic *E. coli* Tir binds Nck to initiate actin pedestal formation in host cells. Nature Cell Biology **3:**856-859.

369. **Campellone KG, Leong JM.** 2005. Nck-independent actin assembly is mediated by two phosphorylated tyrosines within enteropathogenic *Escherichia coli* Tir. Molecular Microbiology **56:**416-432.

370. **Campellone KG, Rankin S, Pawson T, Kirschner MW, Tipper DJ, Leong JM.** 2004. Clustering of Nck by a 12-residue Tir phosphopeptide is sufficient to trigger localized actin assembly. The Journal of Cell Biology **164:**407-416.

371. **DeVinney R, Puente JL, Gauthier A, Goosney D, Finlay BB.** 2001. Enterohaemorrhagic and enteropathogenic *Escherichia coli* use a different Tir-based mechanism for pedestal formation. Molecular Microbiology **41:**1445-1458.

372. **DeVinney R, Stein M, Reinscheid D, Abe A, Ruschkowski S, Finlay BB.** 1999. Enterohemorrhagic *Escherichia coli* O157:H7 produces Tir, which is translocated to the host cell membrane but is not tyrosine phosphorylated. Infection and Immunity **67:**2389-2398.

373. **Kenny B.** 2001. The enterohaemorrhagic *Escherichia coli* (serotype O157:H7) Tir molecule is not functionally interchangeable for its enteropathogenic *E. coli* (serotype O127:H6) homologue. Cellular Microbiology **3:**499-510.

374. **Garmendia J, Phillips AD, Carlier MF, Chong Y, Schuller S, Marches O, Dahan S, Oswald E, Shaw RK, Knutton S, Frankel G.** 2004. TccP is an enterohaemorrhagic *Escherichia coli* O157:H7 type III effector protein that couples Tir to the actin-cytoskeleton. Cellular Microbiology **6:**1167-1183.

375. **Donnenberg MS, Tzipori S, McKee ML, O'Brien AD, Alroy J, Kaper JB.** 1993. The role of the *eae* gene of enterohemorrhagic *Escherichia coli* in intimate attachment *in vitro* and in a porcine model. The Journal of Clinical Investigation **92:**1418-1424.

376. **Nadler C, Baruch K, Kobi S, Mills E, Haviv G, Farago M, Alkalay I, Bartfeld S, Meyer TF, Ben-Neriah Y, Rosenshine I.** 2010. The type III secretion effector NleE inhibits NF-κB activation. PLoS Pathogens **6:**e1000743.

377. **Newton HJ, Pearson JS, Badea L, Kelly M, Lucas M, Holloway G, Wagstaff KM, Dunstone MA, Sloan J, Whisstock JC, Kaper JB, Robins-Browne RM, Jans DA, Frankel G, Phillips AD, Coulson BS, Hartland EL.** 2010. The type III effectors NleE and NleB from enteropathogenic *E. coli* and OspZ from *Shigella* block nuclear translocation of NF-κB p65. PLoS Pathogens **6:**e1000898.

378. **Vossenkamper A, Marches O, Fairclough PD, Warnes G, Stagg AJ, Lindsay JO, Evans PC, Luong le A, Croft NM, Naik S, Frankel G, MacDonald TT.** 2010. Inhibition of NF-κB signaling in human dendritic cells by the enteropathogenic *Escherichia coli* effector protein NleE. Journal of Immunology **185:**4118-4127.

379. **Zhang L, Ding X, Cui J, Xu H, Chen J, Gong YN, Hu L, Zhou Y, Ge J, Lu Q, Liu L, Chen S, Shao F.** 2012. Cysteine methylation disrupts ubiquitin-chain sensing in NF-κB activation. Nature **481:**204-208.

380. **Kanayama A, Seth RB, Sun L, Ea CK, Hong M, Shaito A, Chiu YH, Deng L, Chen ZJ.** 2004. TAB2 and TAB3 activate the NF-κB pathway through binding to polyubiquitin chains. Molecular Cell **15:**535-548.

381. **Kelly M, Hart E, Mundy R, Marches O, Wiles S, Badea L, Luck S, Tauschek M, Frankel G, Robins-Browne RM, Hartland EL.** 2006. Essential role of the type III secretion system effector NleB in colonization of mice by *Citrobacter rodentium*. Infection and Immunity **74:**2328-2337.

382. **Wickham ME, Lupp C, Vazquez A, Mascarenhas M, Coburn B, Coombes BK, Karmali MA, Puente JL, Deng W, Finlay BB.** 2007. *Citrobacter rodentium* virulence in mice associates with bacterial load and the type III effector NleE. Microbes and Infection **9:**400-407.

383. **Royan SV, Jones RM, Koutsouris A, Roxas JL, Falzari K, Weflen AW, Kim A, Bellmeyer A, Turner JR, Neish AS, Rhee KJ, Viswanathan VK, Hecht GA.** 2010. Enteropathogenic *E. coli* non-LEE encoded effectors NleH1 and NleH2 attenuate NF-κB activation. Molecular Microbiology **78:**1232-1245.

384. **Gao X, Wan F, Mateo K, Callegari E, Wang D, Deng W, Puente J, Li F, Chaussee MS, Finlay BB, Lenardo MJ, Hardwidge PR.** 2009. Bacterial effector binding to ribosomal protein s3 subverts NF-κB function. PLoS Pathogens **5:**e1000708.

385. **Feuerbacher LA, Hardwidge PR.** 2014. Influence of NleH effector expression, host genetics, and inflammation on *Citrobacter rodentium* colonization of mice. Microbes and Infection **16:**429-433.

386. **Wan F, Anderson DE, Barnitz RA, Snow A, Bidere N, Zheng L, Hegde V, Lam LT, Staudt LM, Levens D, Deutsch WA, Lenardo MJ.** 2007. Ribosomal protein S3: a KH domain subunit in NF-κB complexes that mediates selective gene regulation. Cell **131:**927-939.

387. **Wan F, Weaver A, Gao X, Bern M, Hardwidge PR, Lenardo MJ.** 2011. IKKβ phosphorylation regulates RPS3 nuclear translocation and NF-κB function during infection with *Escherichia coli* strain O157:H7. Nature Immunology **12:**335-343.

388. **Pham TH, Gao X, Singh G, Hardwidge PR.** 2013. *Escherichia coli* virulence protein NleH1 interaction with the v-Crk sarcoma virus CT10 oncogene-like protein (CRKL) governs NleH1 inhibition of the ribosomal protein S3 (RPS3)/nuclear factor κB (NF-κB) pathway. Journal of Biological Chemistry **288:**34567-34574.

389. **Pham TH, Gao X, Tsai K, Olsen R, Wan F, Hardwidge PR.** 2012. Functional differences and interactions between the *Escherichia coli* type III secretion system effectors NleH1 and NleH2. Infection and Immunity **80:**2133-2140.

390. **Hemrajani C, Berger CN, Robinson KS, Marches O, Mousnier A, Frankel G.** 2010. NleH effectors interact with Bax inhibitor-1 to block apoptosis during enteropathogenic *Escherichia coli* infection. Proceedings of the National Academy of Sciences of the United States of America **107:**3129-3134.

391. **Perna NT, Plunkett G, 3rd, Burland V, Mau B, Glasner JD, Rose DJ, Mayhew GF, Evans PS, Gregor J, Kirkpatrick HA, Posfai G, Hackett J, Klink S, Boutin A, Shao Y, Miller L, Grotbeck EJ, Davis NW, Lim A, Dimalanta ET, Potamousis KD, Apodaca J, Anantharaman TS, Lin J, Yen G, Schwartz DC, Welch RA, Blattner FR.** 2001. Genome sequence of enterohaemorrhagic *Escherichia coli* O157:H7. Nature **409:**529-533.

392. **Baruch K, Gur-Arie L, Nadler C, Koby S, Yerushalmi G, Ben-Neriah Y, Yogev O, Shaulian E, Guttman C, Zarivach R, Rosenshine I.** 2011. Metalloprotease type III effectors that specifically cleave JNK and NF-κB. EMBO Journal **30:**221-231.

393. **Mühlen S, Ruchaud-Sparagano MH, Kenny B.** 2011. Proteasome-independent degradation of canonical NFkB complex components by the NleC protein of pathogenic *Escherichia coli*. Journal of Biological Chemistry **286:**5100-5107.

394. **Pearson JS, Riedmaier P, Marches O, Frankel G, Hartland EL.** 2011. A type III effector protease NleC from enteropathogenic *Escherichia coli* targets NF-κB for degradation. Molecular Microbiology **80:**219-230.

395. **Yen H, Ooka T, Iguchi A, Hayashi T, Sugimoto N, Tobe T.** 2010. NleC, a type III secretion protease, compromises NF-κB activation by targeting p65/RelA. PLoS Pathogens **6:**e1001231.

396. **Marchès O, Wiles S, Dziva F, La Ragione RM, Schuller S, Best A, Phillips AD, Hartland EL, Woodward MJ, Stevens MP, Frankel G.** 2005. Characterization of two non-locus of enterocyte effacement-encoded type III-translocated effectors, NleC and NleD, in attaching and effacing pathogens. Infection and Immunity **73:**8411-8417.

397. **Hodgson A, Wier EM, Fu K, Sun X, Yu H, Zheng W, Sham HP, Johnson K, Bailey S, Vallance BA, Wan F.** 2015. Metalloprotease NleC suppresses host NF-κB/inflammatory responses by cleaving p65 and interfering with the p65/RPS3 interaction. PLoS Pathogens **11:**e1004705.

398. **Turco MM, Sousa MC.** 2014. The structure and specificity of the type III secretion system effector NleC suggest a DNA mimicry mechanism of substrate recognition. Biochemistry **53:**5131-5139.

399. **Giogha C, Wong Fok Lung T, Muhlen S, Pearson JS, Hartland EL.** 2015. Substrate recognition by the zinc metalloprotease effector NleC from enteropathogenic *Escherichia coli*. Cellular Microbiology.

400. **Sham HP, Shames SR, Croxen MA, Ma C, Chan JM, Khan MA, Wickham ME, Deng W, Finlay BB, Vallance BA.** 2011. Attaching and effacing bacterial effector NleC suppresses epithelial inflammatory responses by inhibiting NF-κB and p38 mitogen-activated protein kinase activation. Infection and Immunity **79:**3552-3562.

401. **Pearson JS, Giogha C, Ong SY, Kennedy CL, Kelly M, Robinson KS, Wong Fok Lung T, Mansell A, Riedmaier P, Oates CV, Zaid A, Mühlen S, Crepin VF, Marchès O, Ang CS, Williamson NA, O'Reilly LA, Bankovacki A, Nachbur U, Infusini G, Webb AI, Silke J, Strasser A, Frankel G, Hartland EL.** 2013. A type III effector antagonizes death receptor signalling during bacterial gut infection. Nature **501:**247-251.

402. **Yan D, Wang X, Luo L, Cao X, Ge B.** 2012. Inhibition of TLR signaling by a bacterial protein containing immunoreceptor tyrosine-based inhibitory motifs. Nature Immunology **13:**1063-1071.

403. **Neel BG, Gu H, Pao L.** 2003. The 'Shp'ing news: SH2 domain-containing tyrosine phosphatases in cell signaling. Trends in Biochemical Sciences **28:**284-293.

404. **Zhang Q, Raghunath PN, Vonderheid E, Odum N, Wasik MA.** 2000. Lack of phosphotyrosine phosphatase SHP-1 expression in malignant T-cell lymphoma cells results from methylation of the SHP-1 promoter. The American Journal of Pathology **157:**1137-1146.

405. **Yan D, Quan H, Wang L, Liu F, Liu H, Chen J, Cao X, Ge B.** 2013. Enteropathogenic *Escherichia coli* Tir recruits cellular SHP-2 through ITIM motifs to suppress host immune response. Cellular Signalling **25:**1887-1894.

406. **Ruchaud-Sparagano MH, Muhlen S, Dean P, Kenny B.** 2011. The enteropathogenic *E. coli* (EPEC) Tir effector inhibits NF-κB activity by targeting TNFα receptor-associated factors. PLoS Pathogens **7:**e1002414.

407. **Shaulian E, Karin M.** 2001. AP-1 in cell proliferation and survival. Oncogene **20:**2390-2400.

408. **Eferl R, Wagner EF.** 2003. AP-1: a double-edged sword in tumorigenesis. Nature reviews. Cancer **3:**859-868.

409. **Kallunki T, Su B, Tsigelny I, Sluss HK, Derijard B, Moore G, Davis R, Karin M.** 1994. JNK2 contains a specificity-determining region responsible

for efficient c-Jun binding and phosphorylation. Genes & Development **8:**2996-3007.

410. **Kayagaki N, Warming S, Lamkanfi M, Vande Walle L, Louie S, Dong J, Newton K, Qu Y, Liu J, Heldens S, Zhang J, Lee WP, Roose-Girma M, Dixit VM.** 2011. Non-canonical inflammasome activation targets caspase-11. Nature **479:**117-121.

411. **Liu Z, Zaki MH, Vogel P, Gurung P, Finlay BB, Deng W, Lamkanfi M, Kanneganti TD.** 2012. Role of inflammasomes in host defense against *Citrobacter rodentium* infection. Journal of Biological Chemistry **287:**16955-16964.

412. **Rathinam VA, Vanaja SK, Waggoner L, Sokolovska A, Becker C, Stuart LM, Leong JM, Fitzgerald KA.** 2012. TRIF licenses caspase-11-dependent NLRP3 inflammasome activation by gram-negative bacteria. Cell **150:**606-619.

413. **Yen H, Sugimoto N, Tobe T.** 2015. Enteropathogenic *Escherichia coli* Uses NleA to Inhibit NLRP3 Inflammasome Activation. PLoS Pathogens **11:**e1005121.

414. **Malladi V, Shankar B, Williams PH, Balakrishnan A.** 2004. Enteropathogenic *Escherichia coli* outer membrane proteins induce changes in cadherin junctions of Caco-2 cells through activation of PKCa. Microbes and Infection **6:**38-50.

415. **Shankar B, Krishnan S, Malladi V, Balakrishnan A, Williams PH.** 2009. Outer membrane proteins of wild-type and intimin-deficient enteropathogenic *Escherichia coli* induce Hep-2 cell death through intrinsic and extrinsic pathways of apoptosis. International Journal of Medical Microbiology : IJMM **299:**121-132.

416. **Abul-Milh M, Wu Y, Lau B, Lingwood CA, Barnett Foster D.** 2001. Induction of epithelial cell death including apoptosis by enteropathogenic *Escherichia coli* expressing bundle-forming pili. Infection and Immunity **69:**7356-7364.

417. **Flynn AN, Buret AG.** 2008. Caspases-3, -8, and -9 are required for induction of epithelial cell apoptosis by enteropathogenic *E. coli* but are dispensable for increased paracellular permeability. Microbial Pathogenesis **44:**311-319.

418. **Crane JK, Majumdar S, Pickhardt DF, 3rd.** 1999. Host cell death due to enteropathogenic *Escherichia coli* has features of apoptosis. Infection and Immunity **67:**2575-2584.

419. **Kenny B, Jepson M.** 2000. Targeting of an enteropathogenic *Escherichia coli* (EPEC) effector protein to host mitochondria. Cellular Microbiology **2:**579-590.

420. **Ma C, Wickham ME, Guttman JA, Deng W, Walker J, Madsen KL, Jacobson K, Vogl WA, Finlay BB, Vallance BA.** 2006. *Citrobacter rodentium* infection causes both mitochondrial dysfunction and intestinal epithelial barrier disruption *in vivo*: role of mitochondrial associated protein (Map). Cellular Microbiology **8:**1669-1686.

421. **Nougayrede JP, Donnenberg MS.** 2004. Enteropathogenic *Escherichia coli* EspF is targeted to mitochondria and is required to initiate the mitochondrial death pathway. Cellular Microbiology **6:**1097-1111.

422. **Nougayrede JP, Foster GH, Donnenberg MS.** 2007. Enteropathogenic *Escherichia coli* effector EspF interacts with host protein Abcf2. Cellular Microbiology **9:**680-693.

423. **Dean P, Maresca M, Schuller S, Phillips AD, Kenny B.** 2006. Potent diarrheagenic mechanism mediated by the cooperative action of three enteropathogenic *Escherichia coli*-injected effector proteins. Proceedings of the National Academy of Sciences of the United States of America **103:**1876-1881.

424. **Dean P, Kenny B.** 2004. Intestinal barrier dysfunction by enteropathogenic *Escherichia coli* is mediated by two effector molecules and a bacterial surface protein. Molecular Microbiology **54:**665-675.

425. **Raymond B, Young JC, Pallett M, Endres RG, Clements A, Frankel G.** 2013. Subversion of trafficking, apoptosis, and innate immunity by type III secretion system effectors. Trends in Microbiology **21:**430-441.

426. **Holmes A, Muhlen S, Roe AJ, Dean P.** 2010. The EspF effector, a bacterial pathogen's Swiss army knife. Infection and Immunity **78:**4445-4453.

427. **Maddocks OD, Scanlon KM, Donnenberg MS.** 2013. An *Escherichia coli* effector protein promotes host mutation via depletion of DNA mismatch repair proteins. mBio **4:**e00152-00113.

428. **Marchès O, Ledger TN, Boury M, Ohara M, Tu X, Goffaux F, Mainil J, Rosenshine I, Sugai M, De Rycke J, Oswald E.** 2003. Enteropathogenic and enterohaemorrhagic *Escherichia coli* deliver a novel effector called Cif, which blocks cell cycle G2/M transition. Molecular Microbiology **50:**1553-1567.

429. **Samba-Louaka A, Nougayrede JP, Watrin C, Jubelin G, Oswald E, Taieb F.** 2008. Bacterial cyclomodulin Cif blocks the host cell cycle by stabilizing

the cyclin-dependent kinase inhibitors p21 and p27. Cellular Microbiology **10:**2496-2508.

430. **Taieb F, Nougayrede JP, Watrin C, Samba-Louaka A, Oswald E.** 2006. *Escherichia coli* cyclomodulin Cif induces G2 arrest of the host cell cycle without activation of the DNA-damage checkpoint-signalling pathway. Cellular Microbiology **8:**1910-1921.

431. **Morikawa H, Kim M, Mimuro H, Punginelli C, Koyama T, Nagai S, Miyawaki A, Iwai K, Sasakawa C.** 2010. The bacterial effector Cif interferes with SCF ubiquitin ligase function by inhibiting deneddylation of Cullin1. Biochemical and Biophysical Research Communications **401:**268-274.

432. **Cui J, Yao Q, Li S, Ding X, Lu Q, Mao H, Liu L, Zheng N, Chen S, Shao F.** 2010. Glutamine deamidation and dysfunction of ubiquitin/NEDD8 induced by a bacterial effector family. Science **329:**1215-1218.

433. **Wong AR, Clements A, Raymond B, Crepin VF, Frankel G.** 2012. The interplay between the *Escherichia coli* Rho guanine nucleotide exchange factor effectors and the mammalian RhoGEF inhibitor EspH. mBio **3**.

434. **Dong N, Liu L, Shao F.** 2010. A bacterial effector targets host DH-PH domain RhoGEFs and antagonizes macrophage phagocytosis. EMBO Journal **29:**1363-1376.

435. **Fagundes-Neto U, Freymuller E, Gandolfi Schimitz L, Scaletsky I.** 1996. Nutritional impact and ultrastructural intestinal alterations in severe infections due to enteropathogenic *Escherichia coli* strains in infants. Journal of the American College of Nutrition **15:**180-185.

436. **Monack DM, Mecsas J, Ghori N, Falkow S.** 1997. *Yersinia* signals macrophages to undergo apoptosis and YopJ is necessary for this cell death. Proceedings of the National Academy of Sciences of the United States of America **94:**10385-10390.

437. **Monack DM, Raupach B, Hromockyj AE, Falkow S.** 1996. *Salmonella typhimurium* invasion induces apoptosis in infected macrophages. Proceedings of the National Academy of Sciences of the United States of America **93:**9833-9838.

438. **Xu Q, Reed JC.** 1998. Bax inhibitor-1, a mammalian apoptosis suppressor identified by functional screening in yeast. Molecular Cell **1:**337-346.

439. **Matarrese P, Falzano L, Fabbri A, Gambardella L, Frank C, Geny B, Popoff MR, Malorni W, Fiorentini C.** 2007. *Clostridium difficile* toxin B causes apoptosis in epithelial cells by thrilling mitochondria. Involvement of

ATP-sensitive mitochondrial potassium channels. Journal of Biological Chemistry **282:**9029-9041.

440. **Xu H, Yang J, Gao W, Li L, Li P, Zhang L, Gong YN, Peng X, Xi JJ, Chen S, Wang F, Shao F.** 2014. Innate immune sensing of bacterial modifications of Rho GTPases by the Pyrin inflammasome. Nature.

441. **Li S, Zhang L, Yao Q, Li L, Dong N, Rong J, Gao W, Ding X, Sun L, Chen X, Chen S, Shao F.** 2013. Pathogen blocks host death receptor signalling by arginine GlcNAcylation of death domains. Nature **501:**242-246.

442. **Gao X, Wang X, Pham TH, Feuerbacher LA, Lubos ML, Huang M, Olsen R, Mushegian A, Slawson C, Hardwidge PR.** 2013. NleB, a bacterial effector with glycosyltransferase activity, targets GAPDH function to inhibit NF-κB activation. Cell Host & Microbe **13:**87-99.

443. **Imtiyaz HZ, Zhang Y, Zhang J.** 2005. Structural requirements for signal-induced target binding of FADD determined by functional reconstitution of FADD deficiency. Journal of Biological Chemistry **280:**31360-31367.

444. **Wang L, Yang JK, Kabaleeswaran V, Rice AJ, Cruz AC, Park AY, Yin Q, Damko E, Jang SB, Raunser S, Robinson CV, Siegel RM, Walz T, Wu H.** 2010. The Fas-FADD death domain complex structure reveals the basis of DISC assembly and disease mutations. Nature Structural & Molecular Biology **17:**1324-1329.

445. **Imtiyaz HZ, Zhou X, Zhang H, Chen D, Hu T, Zhang J.** 2009. The death domain of FADD is essential for embryogenesis, lymphocyte development, and proliferation. Journal of Biological Chemistry **284:**9917-9926.

446. **Blasche S, Mortl M, Steuber H, Siszler G, Nisa S, Schwarz F, Lavrik I, Gronewold TM, Maskos K, Donnenberg MS, Ullmann D, Uetz P, Kogl M.** 2013. The *E. coli* effector protein NleF is a caspase inhibitor. PloS ONE **8:**e58937.

447. **Shi J, Zhao Y, Wang Y, Gao W, Ding J, Li P, Hu L, Shao F.** 2014. Inflammatory caspases are innate immune receptors for intracellular LPS. Nature.

448. **Deng W, Puente JL, Gruenheid S, Li Y, Vallance BA, Vazquez A, Barba J, Ibarra JA, O'Donnell P, Metalnikov P, Ashman K, Lee S, Goode D, Pawson T, Finlay BB.** 2004. Dissecting virulence: systematic and functional analyses of a pathogenicity island. Proceedings of the National Academy of Sciences of the United States of America **101:**3597-3602.

449. **Berger CN, Crepin VF, Baruch K, Mousnier A, Rosenshine I, Frankel G.** 2012. EspZ of enteropathogenic and enterohemorrhagic *Escherichia coli* regulates type III secretion system protein translocation. mBio **3**.

450. **Shames SR, Deng W, Guttman JA, de Hoog CL, Li Y, Hardwidge PR, Sham HP, Vallance BA, Foster LJ, Finlay BB.** 2010. The pathogenic *E. coli* type III effector EspZ interacts with host CD98 and facilitates host cell prosurvival signalling. Cellular Microbiology **12:**1322-1339.

451. **Cai S, Bulus N, Fonseca-Siesser PM, Chen D, Hanks SK, Pozzi A, Zent R.** 2005. CD98 modulates integrin beta1 function in polarized epithelial cells. Journal of Cell Science **118:**889-899.

452. **Feral CC, Nishiya N, Fenczik CA, Stuhlmann H, Slepak M, Ginsberg MH.** 2005. CD98hc (SLC3A2) mediates integrin signaling. Proceedings of the National Academy of Sciences of the United States of America **102:**355-360.

453. **Kim M, Ogawa M, Fujita Y, Yoshikawa Y, Nagai T, Koyama T, Nagai S, Lange A, Fassler R, Sasakawa C.** 2009. Bacteria hijack integrin-linked kinase to stabilize focal adhesions and block cell detachment. Nature **459:**578-582.

454. **Mitra SK, Hanson DA, Schlaepfer DD.** 2005. Focal adhesion kinase: in command and control of cell motility. Nature Reviews Molecular Cell Biology **6:**56-68.

455. **Morita-Ishihara T, Miura M, Iyoda S, Izumiya H, Watanabe H, Ohnishi M, Terajima J.** 2013. EspO1-2 regulates EspM2-mediated RhoA activity to stabilize formation of focal adhesions in enterohemorrhagic *Escherichia coli*-infected host cells. PloS ONE **8:**e55960.

456. **Santos RL, Zhang SP, Tsolis RM, Kingsley RA, Adams LG, Baumler AJ.** 2001. Animal models of *Salmonella* infections: enteritis versus typhoid fever. Microbes and Infection **3:**1335-1344.

457. **Barthel M, Hapfelmeier S, Quintanilla-Martinez L, Kremer M, Rohde M, Hogardt M, Pfeffer K, Russmann H, Hardt WD.** 2003. Pretreatment of mice with streptomycin provides a *Salmonella enterica* serovar Typhimurium colitis model that allows analysis of both pathogen and host. Infection and Immunity **71:**2839-2858.

458. **Kaiser P, Diard M, Stecher B, Hardt WD.** 2012. The streptomycin mouse model for *Salmonella* diarrhea: functional analysis of the microbiota, the pathogen's virulence factors, and the host's mucosal immune response. Immunological Reviews **245:**56-83.

459. **Foster JW.** 1995. Low pH adaptation and the acid tolerance response of *Salmonella typhimurium*. Critical Reviews in Microbiology **21:**215-237.

460. **Rolfe MD, Rice CJ, Lucchini S, Pin C, Thompson A, Cameron AD, Alston M, Stringer MF, Betts RP, Baranyi J, Peck MW, Hinton JC.** 2012. Lag phase is a distinct growth phase that prepares bacteria for exponential growth and involves transient metal accumulation. Journal of Bacteriology **194:**686-701.

461. **Kröger C, Colgan A, Srikumar S, Händler K, Sivasankaran SK, Hammarlöf DL, Canals R, Grissom JE, Conway T, Hokamp K, Hinton JC.** 2013. An infection-relevant transcriptomic compendium for *Salmonella enterica* Serovar Typhimurium. Cell Host & Microbe **14:**683-695.

462. **Prouty AM, Brodsky IE, Falkow S, Gunn JS.** 2004. Bile-salt-mediated induction of antimicrobial and bile resistance in *Salmonella typhimurium*. Microbiology-Sgm **150:**775-783.

463. **Prouty AM, Brodsky IE, Manos J, Belas R, Falkow S, Gunn JS.** 2004. Transcriptional regulation of *Salmonella enterica* serovar Typhimurium genes by bile. FEMS Immunology and Medical Microbiology **41:**177-185.

464. **Raffatellu M, Bäumler AJ.** 2010. Salmonella's iron armor for battling the host and its microbiota. Gut Microbes **1:**70-72.

465. **Santos RL, Raffatellu M, Bevins CL, Adams LG, Tukel C, Tsolis RM, Baumler AJ.** 2009. Life in the inflamed intestine, *Salmonella* style. Trends in Microbiology **17:**498-506.

466. **Blaser MJ, Newman LS.** 1982. A review of human salmonellosis: I. Infective dose. Reviews of Infectious Diseases **4:**1096-1106.

467. **Bajaj V, Hwang C, Lee CA.** 1995. *hilA* is a novel *ompR/toxR* family member that activates the expression of *Salmonella typhimurium* invasion genes. Molecular Microbiology **18:**715-727.

468. **Bajaj V, Lucas RL, Hwang C, Lee CA.** 1996. Co-ordinate regulation of *Salmonella typhimurium* invasion genes by environmental and regulatory factors is mediated by control of *hilA* expression. Molecular Microbiology **22:**703-714.

469. **Eichelberg K, Galan JE.** 1999. Differential regulation of *Salmonella typhimurium* type III secreted proteins by pathogenicity island 1 (SPI-1)-encoded transcriptional activators InvF and HilA. Infection and Immunity **67:**4099-4105.

470. **Lostroh CP, Lee CA.** 2001. The HilA box and sequences outside it determine the magnitude of HilA-dependent activation of P*prgH* from *Salmonella* pathogenicity island 1. Journal of Bacteriology **183:**4876-4885.

471. **Jensen VB, Harty JT, Jones BD.** 1998. Interactions of the invasive pathogens *Salmonella typhimurium*, *Listeria monocytogenes*, and *Shigella flexneri* with M cells and murine Peyer's patches. Infection and Immunity **66:**3758-3766.

472. **Jepson MA, Clark MA.** 2001. The role of M cells in *Salmonella* infection. Microbes and Infection **3:**1183-1190.

473. **Jones BD, Ghori N, Falkow S.** 1994. *Salmonella typhimurium* initiates murine infection by penetrating and destroying the specialized epithelial M cells of the Peyer's patches. The Journal of Experimental Medicine **180:**15-23.

474. **Penheiter KL, Mathur N, Giles D, Fahlen T, Jones BD.** 1997. Non-invasive *Salmonella typhimurium* mutants are avirulent because of an inability to enter and destroy M cells of ileal Peyer's patches. Molecular Microbiology **24:**697-709.

475. **Chieppa M, Rescigno M, Huang AY, Germain RN.** 2006. Dynamic imaging of dendritic cell extension into the small bowel lumen in response to epithelial cell TLR engagement. The Journal of Experimental medicine **203:**2841-2852.

476. **Niess JH, Brand S, Gu X, Landsman L, Jung S, McCormick BA, Vyas JM, Boes M, Ploegh HL, Fox JG, Littman DR, Reinecker HC.** 2005. CX3CR1-mediated dendritic cell access to the intestinal lumen and bacterial clearance. Science **307:**254-258.

477. **Rescigno M, Urbano M, Valzasina B, Francolini M, Rotta G, Bonasio R, Granucci F, Kraehenbuhl JP, Ricciardi-Castagnoli P.** 2001. Dendritic cells express tight junction proteins and penetrate gut epithelial monolayers to sample bacteria. Nature Immunology **2:**361-367.

478. **Harris JC, Dupont HL, Hornick RB.** 1972. Fecal leukocytes in diarrheal illness. Annals of Internal Medicine **76:**697-703.

479. **Thiennimitr P, Winter SE, Winter MG, Xavier MN, Tolstikov V, Huseby DL, Sterzenbach T, Tsolis RM, Roth JR, Baümler AJ.** 2011. Intestinal inflammation allows *Salmonella* to use ethanolamine to compete with the microbiota. Proceedings of the National Academy of Sciences of the United States of America **108:**17480-17485.

480. **Galan JE, Curtiss R, 3rd.** 1989. Cloning and molecular characterization of genes whose products allow *Salmonella typhimurium* to penetrate tissue culture cells. Proceedings of the National Academy of Sciences of the United States of America **86:**6383-6387.

481. **Shea JE, Hensel M, Gleeson C, Holden DW.** 1996. Identification of a virulence locus encoding a second type III secretion system in *Salmonella typhimurium*. Proceedings of the National Academy of Sciences of the United States of America **93:**2593-2597.

482. **McGhie EJ, Brawn LC, Hume PJ, Humphreys D, Koronakis V.** 2009. *Salmonella* takes control: effector-driven manipulation of the host. Current Opinion in Microbiology **12:**117-124.

483. **Ramos-Morales F.** 2012. Impact of *Salmonella enterica* Type III Secretion System Effectors on the Eukaryotic Host Cell. International Scholarly Research Network **2012:**36.

484. **McGhie EJ, Hayward RD, Koronakis V.** 2001. Cooperation between actin-binding proteins of invasive *Salmonella*: SipA potentiates SipC nucleation and bundling of actin. EMBO Journal **20:**2131-2139.

485. **McGhie EJ, Hayward RD, Koronakis V.** 2004. Control of actin turnover by a S*almonella* invasion protein. Molecular Cell **13:**497-510.

486. **Chang J, Chen J, Zhou D.** 2005. Delineation and characterization of the actin nucleation and effector translocation activities of *Salmonella* SipC. Molecular Microbiology **55:**1379-1389.

487. **Myeni SK, Zhou D.** 2010. The C terminus of SipC binds and bundles F-actin to promote *Salmonella* invasion. Journal of Biological Chemistry **285:**13357-13363.

488. **Hardt WD, Chen LM, Schuebel KE, Bustelo XR, Galan JE.** 1998. *S. typhimurium* encodes an activator of Rho GTPases that induces membrane ruffling and nuclear responses in host cells. Cell **93:**815-826.

489. **Stender S, Friebel A, Linder S, Rohde M, Mirold S, Hardt WD.** 2000. Identification of SopE2 from *Salmonella typhimurium*, a conserved guanine nucleotide exchange factor for Cdc42 of the host cell. Molecular Microbiology **36:**1206-1221.

490. **Patel JC, Galan JE.** 2006. Differential activation and function of Rho GTPases during *Salmonella*-host cell interactions. The Journal of Cell Biology **175:**453-463.

491. **Fu Y, Galan JE.** 1999. A *Salmonella* protein antagonizes Rac-1 and Cdc42 to mediate host-cell recovery after bacterial invasion. Nature **401:**293-297.

492. **Baumler AJ, Tsolis RM, Valentine PJ, Ficht TA, Heffron F.** 1997. Synergistic effect of mutations in *invA* and *lpfC* on the ability of Salmonella typhimurium to cause murine typhoid. Infection and Immunity **65:**2254-2259.

493. **Vazquez-Torres A, Jones-Carson J, Baumler AJ, Falkow S, Valdivia R, Brown W, Le M, Berggren R, Parks WT, Fang FC.** 1999. Extraintestinal dissemination of *Salmonella* by CD18-expressing phagocytes. Nature **401:**804-808.

494. **Gordon MA.** 2011. Invasive nontyphoidal *Salmonella* disease: epidemiology, pathogenesis and diagnosis. Current Opinion in Infectious Diseases **24:**484-489.

495. **Gordon MA, Graham SM, Walsh AL, Wilson L, Phiri A, Molyneux E, Zijlstra EE, Heyderman RS, Hart CA, Molyneux ME.** 2008. Epidemics of invasive *Salmonella enterica* serovar Enteritidis and *S. enterica* serovar Typhimurium infection associated with multidrug resistance among adults and children in Malawi. Clinical infectious diseases : an official publication of the Infectious Diseases Society of America **46:**963-969.

496. **Gordon MA, Kankwatira AM, Mwafulirwa G, Walsh AL, Hopkins MJ, Parry CM, Faragher EB, Zijlstra EE, Heyderman RS, Molyneux ME.** 2010. Invasive non-typhoid *Salmonellae* establish systemic intracellular infection in HIV-infected adults: an emerging disease pathogenesis. Clinical infectious diseases : an official publication of the Infectious Diseases Society of America **50:**953-962.

497. **Kingsley RA, Msefula CL, Thomson NR, Kariuki S, Holt KE, Gordon MA, Harris D, Clarke L, Whitehead S, Sangal V, Marsh K, Achtman M, Molyneux ME, Cormican M, Parkhill J, MacLennan CA, Heyderman RS, Dougan G.** 2009. Epidemic multiple drug resistant *Salmonella* Typhimurium causing invasive disease in sub-Saharan Africa have a distinct genotype. Genome Research **19:**2279-2287.

498. **Gordon MA.** 2008. *Salmonella* infections in immunocompromised adults. The Journal of Infection **56:**413-422.

499. **Gordon MA, Gordon SB, Musaya L, Zijlstra EE, Molyneux ME, Read RC.** 2007. Primary macrophages from HIV-infected adults show dysregulated cytokine responses to *Salmonella*, but normal internalization and killing. Aids **21:**2399-2408.

500. **Dougan G, John V, Palmer S, Mastroeni P.** 2011. Immunity to salmonellosis. Immunological Reviews **240:**196-210.

501. **McSorley SJ, Asch S, Costalonga M, Reinhardt RL, Jenkins MK.** 2002. Tracking *Salmonella*-specific CD4 T cells *in vivo* reveals a local mucosal response to a disseminated infection. Immunity **16:**365-377.

502. **Mittrücker HW, Kaufmann SH.** 2000. Immune response to infection with *Salmonella typhimurium* in mice. Journal of Leukocyte Biology **67:**457-463.

503. **Watson KG, Holden DW.** 2010. Dynamics of growth and dissemination of *Salmonella in vivo*. Cellular Microbiology **12:**1389-1397.

504. **Hensel M, Shea JE, Gleeson C, Jones MD, Dalton E, Holden DW.** 1995. Simultaneous identification of bacterial virulence genes by negative selection. Science **269:**400-403.

505. **Fields PI, Swanson RV, Haidaris CG, Heffron F.** 1986. Mutants of *Salmonella typhimurium* that cannot survive within the macrophage are avirulent. Proceedings of the National Academy of Sciences of the United States of America **83:**5189-5193.

506. **Leung KY, Finlay BB.** 1991. Intracellular replication is essential for the virulence of *Salmonella typhimurium*. Proceedings of the National Academy of Sciences of the United States of America **88:**11470-11474.

507. **Wijburg OL, Simmons CP, van Rooijen N, Strugnell RA.** 2000. Dual role for macrophages *in vivo* in pathogenesis and control of murine *Salmonella enterica* var. Typhimurium infections. European Journal of Immunology **30:**944-953.

508. **Ochman H, Groisman EA.** 1996. Distribution of pathogenicity islands in *Salmonella* spp. Infection and Immunity **64:**5410-5412.

509. **Garcia-del Portillo F, Zwick MB, Leung KY, Finlay BB.** 1993. *Salmonella* induces the formation of filamentous structures containing lysosomal membrane glycoproteins in epithelial cells. Proceedings of the National Academy of Sciences of the United States of America **90:**10544-10548.

510. **Figueira R, Holden DW.** 2012. Functions of the *Salmonella* pathogenicity island 2 (SPI-2) type III secretion system effectors. Microbiology **158:**1147-1161.

511. **Beuzón CR, Meresse S, Unsworth KE, Ruiz-Albert J, Garvis S, Waterman SR, Ryder TA, Boucrot E, Holden DW.** 2000. *Salmonella* maintains the integrity of its intracellular vacuole through the action of SifA. EMBO Journal **19:**3235-3249.

512. **Stein MA, Leung KY, Zwick M, Garcia-del Portillo F, Finlay BB.** 1996. Identification of a *Salmonella* virulence gene required for formation of filamentous structures containing lysosomal membrane glycoproteins within epithelial cells. Molecular Microbiology **20:**151-164.

513. **Henry T, Couillault C, Rockenfeller P, Boucrot E, Dumont A, Schroeder N, Hermant A, Knodler LA, Lecine P, Steele-Mortimer O, Borg JP, Gorvel JP, Meresse S.** 2006. The *Salmonella* effector protein PipB2 is a linker for kinesin-1. Proceedings of the National Academy of Sciences of the United States of America **103:**13497-13502.

514. **Knodler LA, Steele-Mortimer O.** 2005. The *Salmonella* effector PipB2 affects late endosome/lysosome distribution to mediate Sif extension. Molecular Biology of the Cell **16:**4108-4123.

515. **Ruiz-Albert J, Yu XJ, Beuzon CR, Blakey AN, Galyov EE, Holden DW.** 2002. Complementary activities of SseJ and SifA regulate dynamics of the *Salmonella typhimurium* vacuolar membrane. Molecular Microbiology **44:**645-661.

516. **Kuhle V, Hensel M.** 2002. SseF and SseG are translocated effectors of the type III secretion system of *Salmonella* pathogenicity island 2 that modulate aggregation of endosomal compartments. Cellular Microbiology **4:**813-824.

517. **Salcedo SP, Holden DW.** 2003. SseG, a virulence protein that targets *Salmonella* to the Golgi network. EMBO Journal **22:**5003-5014.

518. **Buchmeier NA, Heffron F.** 1991. Inhibition of macrophage phagosome-lysosome fusion by *Salmonella typhimurium*. Infection and Immunity **59:**2232-2238.

519. **Drecktrah D, Knodler LA, Howe D, Steele-Mortimer O.** 2007. *Salmonella* trafficking is defined by continuous dynamic interactions with the endolysosomal system. Traffic **8:**212-225.

520. **Oh YK, Alpuche-Aranda C, Berthiaume E, Jinks T, Miller SI, Swanson JA.** 1996. Rapid and complete fusion of macrophage lysosomes with phagosomes containing *Salmonella typhimurium*. Infection and Immunity **64:**3877-3883.

521. **Coombes BK, Wickham ME, Brown NF, Lemire S, Bossi L, Hsiao WW, Brinkman FS, Finlay BB.** 2005. Genetic and molecular analysis of GogB, a phage-encoded type III-secreted substrate in *Salmonella enterica* serovar typhimurium with autonomous expression from its associated phage. Journal of Molecular Biology **348:**817-830.

522. **Pilar AV, Reid-Yu SA, Cooper CA, Mulder DT, Coombes BK.** 2012. GogB is an anti-inflammatory effector that limits tissue damage during *Salmonella* infection through interaction with human FBXO22 and Skp1. PLoS Pathogens **8:**e1002773.

523. **Winston JT, Strack P, Beer-Romero P, Chu CY, Elledge SJ, Harper JW.** 1998. The $SCF^{b\text{-}TRCP}$–ubiquitin ligase complex associates specifically with phosphorylated destruction motifs in IkBa and b-catenin and stimulates IkBa ubiquitination in vitro. Genes and Development **13:**270-283.

524. **Kaniga K, Uralil J, Bliska JB, Galan JE.** 1996. A secreted protein tyrosine phosphatase with modular effector domains in the bacterial pathogen Salmonella *typhimurium*. Molecular Microbiology **21:**633-641.

525. **Fu Y, Galan JE.** 1998. The *Salmonella typhimurium* tyrosine phosphatase SptP is translocated into host cells and disrupts the actin cytoskeleton. Molecular Microbiology **27:**359-368.

526. **Murli S, Watson RO, Galan JE.** 2001. Role of tyrosine kinases and the tyrosine phosphatase SptP in the interaction of *Salmonella* with host cells. Cellular Microbiology **3:**795-810.

527. **Lin SL, Le TX, Cowen DS.** 2003. SptP, a *Salmonella typhimurium* type III-secreted protein, inhibits the mitogen-activated protein kinase pathway by inhibiting Raf activation. Cellular Microbiology **5:**267-275.

528. **Figueroa-Bossi N, Uzzau S, Maloriol D, Bossi L.** 2001. Variable assortment of prophages provides a transferable repertoire of pathogenic determinants in *Salmonella*. Molecular Microbiology **39:**260-271.

529. **Miao EA, Scherer CA, Tsolis RM, Kingsley RA, Adams LG, Baumler AJ, Miller SI.** 1999. *Salmonella typhimurium* leucine-rich repeat proteins are targeted to the SPI1 and SPI2 type III secretion systems. Molecular Microbiology **34:**850-864.

530. **Haraga A, Miller SI.** 2006. A *Salmonella* type III secretion effector interacts with the mammalian serine/threonine protein kinase PKN1. Cellular Microbiology **8:**837-846.

531. **Haraga A, Miller SI.** 2003. A *Salmonella enterica* serovar typhimurium translocated leucine-rich repeat effector protein inhibits NF-κB-dependent gene expression. Infection and Immunity **71:**4052-4058.

532. **Mazurkiewicz P, Thomas J, Thompson JA, Liu M, Arbibe L, Sansonetti P, Holden DW.** 2008. SpvC is a *Salmonella* effector with phosphothreonine

lyase activity on host mitogen-activated protein kinases. Molecular Microbiology **67:**1371-1383.

533. **Haneda T, Ishii Y, Shimizu H, Ohshima K, Iida N, Danbara H, Okada N.** 2012. *Salmonella* type III effector SpvC, a phosphothreonine lyase, contributes to reduction in inflammatory response during intestinal phase of infection. Cellular Microbiology **14:**485-499.

534. **Li H, Xu H, Zhou Y, Zhang J, Long C, Li S, Chen S, Zhou JM, Shao F.** 2007. The phosphothreonine lyase activity of a bacterial type III effector family. Science **315:**1000-1003.

535. **Le Negrate G, Faustin B, Welsh K, Loeffler M, Krajewska M, Hasegawa P, Mukherjee S, Orth K, Krajewski S, Godzik A, Guiney DG, Reed JC.** 2008. *Salmonella* secreted factor L deubiquitinase of *Salmonella typhimurium* inhibits NF-κB, suppresses IkBα ubiquitination and modulates innate immune responses. Journal of Immunology **180:**5045-5056.

536. **Mesquita FS, Holden DW, Rolhion N.** 2013. Lack of effect of the *Salmonella* deubiquitinase SseL on the NF-κB pathway. PloS ONE **8:**e53064.

537. **Guiney DG.** 2005. The role of host cell death in *Salmonella* infections. Current Topics in Microbiology and Immunology **289:**131-150.

538. **Brennan MA, Cookson BT.** 2000. *Salmonella* induces macrophage death by caspase-1-dependent necrosis. Molecular Microbiology **38:**31-40.

539. **van der Velden AW, Velasquez M, Starnbach MN.** 2003. *Salmonella* rapidly kill dendritic cells via a caspase-1-dependent mechanism. Journal of Immunology **171:**6742-6749.

540. **Hersh D, Monack DM, Smith MR, Ghori N, Falkow S, Zychlinsky A.** 1999. The *Salmonella* invasin SipB induces macrophage apoptosis by binding to caspase-1. Proceedings of the National Academy of Sciences of the United States of America **96:**2396-2401.

541. **Miao EA, Mao DP, Yudkovsky N, Bonneau R, Lorang CG, Warren SE, Leaf IA, Aderem A.** 2010. Innate immune detection of the type III secretion apparatus through the NLRC4 inflammasome. Proceedings of the National Academy of Sciences of the United States of America **107:**3076-3080.

542. **Libby SJ, Lesnick M, Hasegawa P, Weidenhammer E, Guiney DG.** 2000. The *Salmonella* virulence plasmid *spv* genes are required for cytopathology in human monocyte-derived macrophages. Cellular Microbiology **2:**49-58.

543. **Rytkönen A, Poh J, Garmendia J, Boyle C, Thompson A, Liu M, Freemont P, Hinton JC, Holden DW.** 2007. SseL, a *Salmonella*

deubiquitinase required for macrophage killing and virulence. Proceedings of the National Academy of Sciences of the United States of America **104:**3502-3507.

544. **van der Velden AW, Lindgren SW, Worley MJ, Heffron F.** 2000. *Salmonella* pathogenicity island 1-independent induction of apoptosis in infected macrophages by *Salmonella enterica* serotype typhimurium. Infection and Immunity **68:**5702-5709.

545. **Broz P, Newton K, Lamkanfi M, Mariathasan S, Dixit VM, Monack DM.** 2010. Redundant roles for inflammasome receptors NLRP3 and NLRC4 in host defense against *Salmonella*. The Journal of Experimental Medicine **207:**1745-1755.

546. **Kim JM, Eckmann L, Savidge TC, Lowe DC, Witthoft T, Kagnoff MF.** 1998. Apoptosis of human intestinal epithelial cells after bacterial invasion. The Journal of Clinical Investigation **102:**1815-1823.

547. **Hong KH, Miller VL.** 1998. Identification of a novel *Salmonella* invasion locus homologous to *Shigella ipgDE*. Journal of Bacteriology **180:**1793-1802.

548. **Wood MW, Jones MA, Watson PR, Hedges S, Wallis TS, Galyov EE.** 1998. Identification of a pathogenicity island required for *Salmonella* enteropathogenicity. Molecular Microbiology **29:**883-891.

549. **Galyov EE, Wood MW, Rosqvist R, Mullan PB, Watson PR, Hedges S, Wallis TS.** 1997. A secreted effector protein of *Salmonella dublin* is translocated into eukaryotic cells and mediates inflammation and fluid secretion in infected ileal mucosa. Molecular Microbiology **25:**903-912.

550. **Knodler LA, Finlay BB, Steele-Mortimer O.** 2005. The *Salmonella* effector protein SopB protects epithelial cells from apoptosis by sustained activation of Akt. Journal of Biological Chemistry **280:**9058-9064.

551. **Steele-Mortimer O, Knodler LA, Marcus SL, Scheid MP, Goh B, Pfeifer CG, Duronio V, Finlay BB.** 2000. Activation of Akt/protein kinase B in epithelial cells by the *Salmonella typhimurium* effector sigD. Journal of Biological Chemistry **275:**37718-37724.

552. **Zhang HM, Rao JN, Guo X, Liu L, Zou T, Turner DJ, Wang JY.** 2004. Akt kinase activation blocks apoptosis in intestinal epithelial cells by inhibiting caspase-3 after polyamine depletion. Journal of Biological Chemistry **279:**22539-22547.

553. **Hardt WD, Galan JE.** 1997. A secreted *Salmonella* protein with homology to an avirulence determinant of plant pathogenic bacteria. Proceedings of the National Academy of Sciences of the United States of America **94:**9887-9892.

554. **Collier-Hyams LS, Zeng H, Sun J, Tomlinson AD, Bao ZQ, Chen H, Madara JL, Orth K, Neish AS.** 2002. Cutting edge: *Salmonella* AvrA effector inhibits the key proinflammatory, anti-apoptotic NF-κB pathway. Journal of Immunology **169:**2846-2850.

555. **Ye Z, Petrof EO, Boone D, Claud EC, Sun J.** 2007. *Salmonella* effector AvrA regulation of colonic epithelial cell inflammation by deubiquitination. The American Journal of Pathology **171:**882-892.

556. **Jones RM, Wu H, Wentworth C, Luo L, Collier-Hyams L, Neish AS.** 2008. *Salmonella* AvrA Coordinates Suppression of Host Immune and Apoptotic Defenses via JNK Pathway Blockade. Cell Host & Microbe **3:**233-244.

557. **Wu H, Jones RM, Neish AS.** 2012. The *Salmonella* effector AvrA mediates bacterial intracellular survival during infection in vivo. Cellular Microbiology **14:**28-39.

558. **Sansonetti PJ, Di Santo JP.** 2007. Debugging how bacteria manipulate the immune response. Immunity **26:**149-161.

559. **Brown NF, Coombes BK, Bishop JL, Wickham ME, Lowden MJ, Gal-Mor O, Goode DL, Boyle EC, Sanderson KL, Finlay BB.** 2011. Salmonella phage ST64B encodes a member of the SseK/NleB effector family. PloS ONE **6:**e17824.

560. **Kujat Choy SL, Boyle EC, Gal-Mor O, Goode DL, Valdez Y, Vallance BA, Finlay BB.** 2004. SseK1 and SseK2 are novel translocated proteins of *Salmonella enterica* serovar typhimurium. Infection and Immunity **72:**5115-5125.

561. **Wong Fok Lung T, Pearson JS, Schuelein R, Hartland EL.** 2014. The cell death response to enteropathogenic *Escherichia coli* infection. Cellular Microbiology **16:**1736-1745.

562. **Wong AR, Pearson JS, Bright MD, Munera D, Robinson KS, Lee SF, Frankel G, Hartland EL.** 2011. Enteropathogenic and enterohaemorrhagic *Escherichia coli*: even more subversive elements. Molecular Microbiology **80:**1420-1438.

563. **Vaughan S, Jat PS.** 2011. Deciphering the role of nuclear factor-κB in cellular senescence. Aging **3:**913-919.

564. **Zhang W, Liu HT.** 2002. MAPK signal pathways in the regulation of cell proliferation in mammalian cells. Cell Research **12:**9-18.

565. **Ofengeim D, Yuan J.** 2013. Regulation of RIP1 kinase signalling at the crossroads of inflammation and cell death. Nature Reviews Molecular Cell Biology **14:**727-736.

566. **Ogino T, Ohno R, Sekiya K, Kuwae A, Matsuzawa T, Nonaka T, Fukuda H, Imajoh-Ohmi S, Abe A.** 2006. Assembly of the type III secretion apparatus of enteropathogenic *Escherichia coli*. Journal of Bacteriology **188:**2801-2811.

567. **Pallen MJ, Beatson SA, Bailey CM.** 2005. Bioinformatics, genomics and evolution of non-flagellar type-III secretion systems: a Darwinian perspective. FEMS Microbiology Reviews **29:**201-229.

568. **Stevens JM, Galyov EE, Stevens MP.** 2006. Actin-dependent movement of bacterial pathogens. Nature Reviews. Microbiology **4:**91-101.

569. **Hall TA.** 1999. BioEdit: a user-friendly biological sequence alignment editor and analysis program for Windows 95/98/NT. Nucleic Acids Symposium Series **41:**95-98.

570. **Edgar RC.** 2004. MUSCLE: multiple sequence alignment with high accuracy and high throughput. Nucleic Acids Research **32:**1792-1797.

571. **Kearse M, Moir R, Wilson A, Stones-Havas S, Cheung M, Sturrock S, Buxton S, Cooper A, Markowitz S, Duran C, Thierer T, Ashton B, Meintjes P, Drummond A.** 2012. Geneious Basic: an integrated and extendable desktop software platform for the organization and analysis of sequence data. Bioinformatics **28:**1647-1649.

572. **Tamura K, Peterson D, Peterson N, Stecher G, Nei M, Kumar S.** 2011. MEGA5: molecular evolutionary genetics analysis using maximum likelihood, evolutionary distance, and maximum parsimony methods. Molecular Biology and Evolution **28:**2731-2739.

573. **Huson DH, Richter DC, Rausch C, Dezulian T, Franz M, Rupp R.** 2007. Dendroscope: An interactive viewer for large phylogenetic trees. BMC Bioinformatics **8:**460.

574. **Altschul SF, Gish W, Miller W, Myers EW, Lipman DJ.** 1990. Basic local alignment search tool. Journal of Molecular Biology **215:**403-410.

575. **Hazen TH, Sahl JW, Fraser CM, Donnenberg MS, Scheutz F, Rasko DA.** 2013. Refining the pathovar paradigm via phylogenomics of the attaching and

effacing *Escherichia coli*. Proceedings of the National Academy of Sciences of the United States of America **110:**12810-12815.

576. **Wattam AR, Abraham D, Dalay O, Disz TL, Driscoll T, Gabbard JL, Gillespie JJ, Gough R, Hix D, Kenyon R, Machi D, Mao C, Nordberg EK, Olson R, Overbeek R, Pusch GD, Shukla M, Schulman J, Stevens RL, Sullivan DE, Vonstein V, Warren A, Will R, Wilson MJ, Yoo HS, Zhang C, Zhang Y, Sobral BW.** 2014. PATRIC, the bacterial bioinformatics database and analysis resource. Nucleic Acids Research **42:**D581-591.

577. **Rice P, Longden I, Bleasby A.** 2000. EMBOSS: the European Molecular Biology Open Software Suite. Trends in Genetics : TIG **16:**276-277.

578. **Stamatakis A.** 2014. RAxML version 8: a tool for phylogenetic analysis and post-analysis of large phylogenies. Bioinformatics **30:**1312-1313.

579. **Huson DH, Scornavacca C.** 2012. Dendroscope 3: an interactive tool for rooted phylogenetic trees and networks. Systematic Biology **61:**1061-1067.

580. **Charpentier X, Oswald E.** 2004. Identification of the secretion and translocation domain of the enteropathogenic and enterohemorrhagic *Escherichia coli* effector Cif, using TEM-1 b-lactamase as a new fluorescence-based reporter. Journal of Bacteriology **186:**5486-5495.

581. **Isono T.** 2011. *O*-GlcNAc-specific antibody CTD110.6 cross-reacts with *N*-GlcNAc2-modified proteins induced under glucose deprivation. PloS ONE **6:**e18959.

582. **Gietz RD, Schiestl RH, Willems AR, Woods RA.** 1995. Studies on the transformation of intact yeast cells by the LiAc/SS-DNA/PEG procedure. Yeast **11:**355-360.

583. **Kushnirov VV.** 2000. Rapid and reliable protein extraction from yeast. Yeast **16:**857-860.

584. **Hanahan D.** 1983. Studies on transformation of *Escherichia coli* with plasmids. Journal of Molecular Biology **166:**557-580.

585. **Breton C, Snajdrova L, Jeanneau C, Koca J, Imberty A.** 2006. Structures and mechanisms of glycosyltransferases. Glycobiology **16:**29R-37R.

586. **Lairson LL, Henrissat B, Davies GJ, Withers SG.** 2008. Glycosyltransferases: structures, functions, and mechanisms. Annual Review of Biochemistry **77:**521-555.

587. **Chou TY, Hart GW, Dang CV.** 1995. c-Myc is glycosylated at threonine 58, a known phosphorylation site and a mutational hot spot in lymphomas. Journal of Biological Chemistry **270:**18961-18965.

588. **Cole RN, Hart GW.** 1999. Glycosylation sites flank phosphorylation sites on synapsin I: O-linked N-acetylglucosamine residues are localized within domains mediating synapsin I interactions. Journal of Neurochemistry **73:**418-428.

589. **Cheng X, Cole RN, Zaia J, Hart GW.** 2000. Alternative O-glycosylation/O-phosphorylation of the murine estrogen receptor beta. Biochemistry **39:**11609-11620.

590. **Hart GW, Slawson C, Ramirez-Correa G, Lagerlof O.** 2011. Cross talk between O-GlcNAcylation and phosphorylation: roles in signaling, transcription, and chronic disease. Annual Review of Biochemistry **80:**825-858.

591. **Lehrman MA.** 1991. Biosynthesis of N-acetylglucosamine-P-P-dolichol, the committed step of asparagine-linked oligosaccharide assembly. Glycobiology **1:**553-562.

592. **Hart GW.** 1997. Dynamic O-linked glycosylation of nuclear and cytoskeletal proteins. Annual Review of Biochemistry **66:**315-335.

593. **Comer FI, Hart GW.** 2000. O-Glycosylation of nuclear and cytosolic proteins. Dynamic interplay between O-GlcNAc and O-phosphate. Journal of Biological Chemistry **275:**29179-29182.

594. **Marshall RD.** 1972. Glycoproteins. Annual Review of Biochemistry **41:**673-702.

595. **Burda P, Aebi M.** 1999. The dolichol pathway of *N*-linked glycosylation. Biochimica et Biophysica Acta **1426:**239-257.

596. **Kelleher DJ, Gilmore R.** 2006. An evolving view of the eukaryotic oligosaccharyltransferase. Glycobiology **16:**47R-62R.

597. **Grass S, Buscher AZ, Swords WE, Apicella MA, Barenkamp SJ, Ozchlewski N, St Geme JW, 3rd.** 2003. The *Haemophilus influenzae* HMW1 adhesin is glycosylated in a process that requires HMW1C and phosphoglucomutase, an enzyme involved in lipooligosaccharide biosynthesis. Molecular Microbiology **48:**737-751.

598. **Grass S, Lichti CF, Townsend RR, Gross J, St Geme JW, 3rd.** 2010. The *Haemophilus influenzae* HMW1C protein is a glycosyltransferase that

transfers hexose residues to asparagine sites in the HMW1 adhesin. PLoS Pathogens **6:**e1000919.

599. **Schwarz F, Fan YY, Schubert M, Aebi M.** 2011. Cytoplasmic *N*-glycosyltransferase of *Actinobacillus pleuropneumoniae* is an inverting enzyme and recognizes the NX(S/T) consensus sequence. Journal of Biological Chemistry **286:**35267-35274.

600. **Breton C, Bettler E, Joziasse DH, Geremia RA, Imberty A.** 1998. Sequence-function relationships of prokaryotic and eukaryotic galactosyltransferases. Journal of Biochemistry **123:**1000-1009.

601. **Wiggins CA, Munro S.** 1998. Activity of the yeast *MNN1* α-1,3-mannosyltransferase requires a motif conserved in many other families of glycosyltransferases. Proceedings of the National Academy of Sciences of the United States of America **95:**7945-7950.

602. **Pak JE, Arnoux P, Zhou S, Sivarajah P, Satkunarajah M, Xing X, Rini JM.** 2006. X-ray crystal structure of leukocyte type core 2 β1,6-*N*-acetylglucosaminyltransferase. Evidence for a convergence of metal ion-independent glycosyltransferase mechanism. Journal of Biological Chemistry **281:**26693-26701.

603. **Ünligil UM, Rini JM.** 2000. Glycosyltransferase structure and mechanism. Current Opinion in Structural Biology **10:**510-517.

604. **Qasba PK, Ramakrishnan B, Boeggeman E.** 2005. Substrate-induced conformational changes in glycosyltransferases. Trends in Biochemical Sciences **30:**53-62.

605. **Reinert DJ, Jank T, Aktories K, Schulz GE.** 2005. Structural basis for the function of *Clostridium difficile* toxin B. Journal of Molecular Biology **351:**973-981.

606. **Busch C, Hofmann F, Gerhard R, Aktories K.** 2000. Involvement of a conserved tryptophan residue in the UDP-glucose binding of large clostridial cytotoxin glycosyltransferases. Journal of Biological Chemistry **275:**13228-13234.

607. **Jank T, Giesemann T, Aktories K.** 2007. *Clostridium difficile* glucosyltransferase toxin B-essential amino acids for substrate binding. Journal of Biological Chemistry **282:**35222-35231.

608. **Lassak J, Keilhauer EC, Furst M, Wuichet K, Godeke J, Starosta AL, Chen JM, Sogaard-Andersen L, Rohr J, Wilson DN, Haussler S, Mann**

M, Jung K. 2015. Arginine-rhamnosylation as new strategy to activate translation elongation factor P. Nature Chemical Biology **11:**266-270.

609. **Jinek M, Rehwinkel J, Lazarus BD, Izaurralde E, Hanover JA, Conti E.** 2004. The superhelical TPR-repeat domain of *O*-linked GlcNAc transferase exhibits structural similarities to importin alpha. Nature Structural & Molecular Biology **11:**1001-1007.

610. **Kreppel LK, Blomberg MA, Hart GW.** 1997. Dynamic glycosylation of nuclear and cytosolic proteins. Cloning and characterization of a unique *O*-GlcNAc transferase with multiple tetratricopeptide repeats. Journal of Biological Chemistry **272:**9308-9315.

611. **Lubas WA, Frank DW, Krause M, Hanover JA.** 1997. *O*-Linked GlcNAc transferase is a conserved nucleocytoplasmic protein containing tetratricopeptide repeats. Journal of Biological Chemistry **272:**9316-9324.

612. **Mudgett MB, Chesnokova O, Dahlbeck D, Clark ET, Rossier O, Bonas U, Staskawicz BJ.** 2000. Molecular signals required for type III secretion and translocation of the *Xanthomonas campestris* AvrBs2 protein to pepper plants. Proceedings of the National Academy of Sciences of the United States of America **97:**13324-13329.

613. **Sory MP, Boland A, Lambermont I, Cornelis GR.** 1995. Identification of the YopE and YopH domains required for secretion and internalization into the cytosol of macrophages, using the cyaA gene fusion approach. Proceedings of the National Academy of Sciences of the United States of America **92:**11998-12002.

614. **Lara-Tejero M, Kato J, Wagner S, Liu X, Galan JE.** 2011. A sorting platform determines the order of protein secretion in bacterial type III systems. Science **331:**1188-1191.

615. **Lee SH, Galan JE.** 2004. *Salmonella* type III secretion-associated chaperones confer secretion-pathway specificity. Molecular Microbiology **51:**483-495.

616. **Söding J.** 2005. Protein homology detection by HMM-HMM comparison. Bioinformatics **21:**951-960.

617. **Söding J, Biegert A, Lupas AN.** 2005. The HHpred interactive server for protein homology detection and structure prediction. Nucleic Acids Research **33:**W244-248.

618. **Boix E, Swaminathan GJ, Zhang Y, Natesh R, Brew K, Acharya KR.** 2001. Structure of UDP complex of UDP-galactose:beta-galactoside-alpha -1,3-galactosyltransferase at 1.53-A resolution reveals a conformational change

in the catalytically important C terminus. Journal of Biological Chemistry **276:**48608-48614.

619. **Flint J, Taylor E, Yang M, Bolam DN, Tailford LE, Martinez-Fleites C, Dodson EJ, Davis BG, Gilbert HJ, Davies GJ.** 2005. Structural dissection and high-throughput screening of mannosylglycerate synthase. Nature Structural & Molecular Biology **12:**608-614.

620. **Gordon RD, Sivarajah P, Satkunarajah M, Ma D, Tarling CA, Vizitiu D, Withers SG, Rini JM.** 2006. X-ray crystal structures of rabbit N-acetylglucosaminyltransferase I (GnT I) in complex with donor substrate analogues. Journal of Molecular Biology **360:**67-79.

621. **Kubota T, Shiba T, Sugioka S, Furukawa S, Sawaki H, Kato R, Wakatsuki S, Narimatsu H.** 2006. Structural basis of carbohydrate transfer activity by human UDP-GalNAc: polypeptide alpha-N-acetylgalactosaminyltransferase (pp-GalNAc-T10). Journal of Molecular Biology **359:**708-727.

622. **Ramakrishnan B, Ramasamy V, Qasba PK.** 2006. Structural snapshots of beta-1,4-galactosyltransferase-I along the kinetic pathway. Journal of Molecular Biology **357:**1619-1633.

623. **Ziegler MO, Jank T, Aktories K, Schulz GE.** 2008. Conformational changes and reaction of clostridial glycosylating toxins. Journal of Molecular Biology **377:**1346-1356.

624. **Gastinel LN, Cambillau C, Bourne Y.** 1999. Crystal structures of the bovine beta4galactosyltransferase catalytic domain and its complex with uridine diphosphogalactose. EMBO Journal **18:**3546-3557.

625. **Ramasamy V, Ramakrishnan B, Boeggeman E, Qasba PK.** 2003. The role of tryptophan 314 in the conformational changes of beta1,4-galactosyltransferase-I. Journal of Molecular Biology **331:**1065-1076.

626. **Persson K, Ly HD, Dieckelmann M, Wakarchuk WW, Withers SG, Strynadka NC.** 2001. Crystal structure of the retaining galactosyltransferase LgtC from *Neisseria meningitidis* in complex with donor and acceptor sugar analogs. Nature Structural Biology **8:**166-175.

627. **Hart GW, Akimoto Y.** 2009. The O-GlcNAc Modification. *In* Varki A, Cummings RD, Esko JD, Freeze HH, Stanley P, Bertozzi CR, Hart GW, Etzler ME (ed.), Essentials of Glycobiology, 2nd ed, Cold Spring Harbor (NY).

628. **Cuff JA, Barton GJ.** 2000. Application of multiple sequence alignment profiles to improve protein secondary structure prediction. Proteins **40:**502-511.

629. **Akama TO, Nakagawa H, Sugihara K, Narisawa S, Ohyama C, Nishimura S, O'Brien DA, Moremen KW, Millan JL, Fukuda MN.** 2002. Germ cell survival through carbohydrate-mediated interaction with Sertoli cells. Science **295:**124-127.

630. **Talbot P, Shur BD, Myles DG.** 2003. Cell adhesion and fertilization: steps in oocyte transport, sperm-zona pellucida interactions, and sperm-egg fusion. Biology of Reproduction **68:**1-9.

631. **Varki A.** 1993. Biological roles of oligosaccharides: all of the theories are correct. Glycobiology **3:**97-130.

632. **Crocker PR, Feizi T.** 1996. Carbohydrate recognition systems: functional triads in cell-cell interactions. Current Opinion in Structural Biology **6:**679-691.

633. **Lowe JB.** 2003. Glycan-dependent leukocyte adhesion and recruitment in inflammation. Current Opinion in Cell Biology **15:**531-538.

634. **Rudd PM, Elliott T, Cresswell P, Wilson IA, Dwek RA.** 2001. Glycosylation and the immune system. Science **291:**2370-2376.

635. **Rudd PM, Wormald MR, Stanfield RL, Huang M, Mattsson N, Speir JA, DiGennaro JA, Fetrow JS, Dwek RA, Wilson IA.** 1999. Roles for glycosylation of cell surface receptors involved in cellular immune recognition. Journal of Molecular Biology **293:**351-366.

636. **Haines N, Irvine KD.** 2003. Glycosylation regulates Notch signalling. Nature Reviews Molecular Cell Biology **4:**786-797.

637. **Moran AP, Gupta A, Joshi L.** 2011. Sweet-talk: role of host glycosylation in bacterial pathogenesis of the gastrointestinal tract. Gut **60:**1412-1425.

638. **Belyi Y, Aktories K.** 2010. Bacterial toxin and effector glycosyltransferases. Biochimica et Biophysica Acta **1800:**134-143.

639. **Busch C, Aktories K.** 2000. Microbial toxins and the glycosylation of rho family GTPases. Current Opinion in Structural Biology **10:**528-535.

640. **Genth H, Dreger SC, Huelsenbeck J, Just I.** 2008. *Clostridium difficile* toxins: more than mere inhibitors of Rho proteins. The International Journal of Biochemistry & Cell Biology **40:**592-597.

641. **Jank T, Aktories K.** 2008. Structure and mode of action of clostridial glucosylating toxins: the ABCD model. Trends in Microbiology **16:**222-229.

642. **Schirmer J, Aktories K.** 2004. Large clostridial cytotoxins: cellular biology of Rho/Ras-glucosylating toxins. Biochimica et Biophysica Acta **1673:**66-74.

643. **Voth DE, Ballard JD.** 2005. *Clostridium difficile* toxins: mechanism of action and role in disease. Clinical Microbiology Reviews **18:**247-263.

644. **Selzer J, Hofmann F, Rex G, Wilm M, Mann M, Just I, Aktories K.** 1996. *Clostridium* novyi α-toxin-catalyzed incorporation of GlcNAc into Rho subfamily proteins. Journal of Biological Chemistry **271:**25173-25177.

645. **Bartlett JG, Moon N, Chang TW, Taylor N, Onderdonk AB.** 1978. Role of *Clostridium difficile* in antibiotic-associated pseudomembranous colitis. Gastroenterology **75:**778-782.

646. **George WL, Sutter VL, Goldstein EJ, Ludwig SL, Finegold SM.** 1978. Aetiology of antimicrobial-agent-associated colitis. Lancet **1:**802-803.

647. **Kelly CP, LaMont JT.** 2008. *Clostridium difficile*--more difficult than ever. The New England Journal of Medicine **359:**1932-1940.

648. **Lyerly DM, Saum KE, MacDonald DK, Wilkins TD.** 1985. Effects of *Clostridium difficile* toxins given intragastrically to animals. Infection and Immunity **47:**349-352.

649. **Lyras D, O'Connor JR, Howarth PM, Sambol SP, Carter GP, Phumoonna T, Poon R, Adams V, Vedantam G, Johnson S, Gerding DN, Rood JI.** 2009. Toxin B is essential for virulence of *Clostridium difficile*. Nature **458:**1176-1179.

650. **O'Connor JR, Lyras D, Farrow KA, Adams V, Powell DR, Hinds J, Cheung JK, Rood JI.** 2006. Construction and analysis of chromosomal *Clostridium difficile* mutants. Molecular Microbiology **61:**1335-1351.

651. **Razaq N, Sambol S, Nagaro K, Zukowski W, Cheknis A, Johnson S, Gerding DN.** 2007. Infection of hamsters with historical and epidemic BI types of *Clostridium difficile*. The Journal of Infectious Diseases **196:**1813-1819.

652. **Tsokos M, Schalinski S, Paulsen F, Sperhake JP, Puschel K, Sobottka I.** 2008. Pathology of fatal traumatic and nontraumatic clostridial gas gangrene: a histopathological, immunohistochemical, and ultrastructural study of six autopsy cases. International Journal of Legal Medicine **122:**35-41.

653. **Hofmann F, Rex G, Aktories K, Just I.** 1996. The ras-related protein Ral is monoglucosylated by *Clostridium sordellii* lethal toxin. Biochemical and Biophysical Research Communications **227:**77-81.

654. **Just I, Selzer J, Hofmann F, Green GA, Aktories K.** 1996. Inactivation of Ras by *Clostridium sordellii* lethal toxin-catalyzed glucosylation. Journal of Biological Chemistry **271:**10149-10153.

655. **Popoff MR, Chaves-Olarte E, Lemichez E, von Eichel-Streiber C, Thelestam M, Chardin P, Cussac D, Antonny B, Chavrier P, Flatau G, Giry M, de Gunzburg J, Boquet P.** 1996. Ras, Rap, and Rac small GTP-binding proteins are targets for *Clostridium sordellii* lethal toxin glucosylation. Journal of Biological Chemistry **271:**10217-10224.

656. **Vetter IR, Hofmann F, Wohlgemuth S, Herrmann C, Just I.** 2000. Structural consequences of mono-glucosylation of Ha-Ras by *Clostridium sordellii* lethal toxin. Journal of Molecular Biology **301:**1091-1095.

657. **Berger KH, Isberg RR.** 1993. Two distinct defects in intracellular growth complemented by a single genetic locus in *Legionella pneumophila*. Molecular Microbiology **7:**7-19.

658. **Berger KH, Merriam JJ, Isberg RR.** 1994. Altered intracellular targeting properties associated with mutations in the *Legionella pneumophila dotA* gene. Molecular Microbiology **14:**809-822.

659. **Ge J, Shao F.** 2011. Manipulation of host vesicular trafficking and innate immune defence by *Legionella* Dot/Icm effectors. Cellular Microbiology **13:**1870-1880.

660. **Luo ZQ.** 2012. *Legionella* secreted effectors and innate immune responses. Cellular Microbiology **14:**19-27.

661. **Belyi Y, Jank T, Aktories K.** 2011. Effector glycosyltransferases in *Legionella*. Frontiers in Microbiology **2:**76.

662. **Belyi Y, Niggeweg R, Opitz B, Vogelsgesang M, Hippenstiel S, Wilm M, Aktories K.** 2006. *Legionella pneumophila* glucosyltransferase inhibits host elongation factor 1A. Proceedings of the National Academy of Sciences of the United States of America **103:**16953-16958.

663. **Belyi Y, Tabakova I, Stahl M, Aktories K.** 2008. Lgt: a family of cytotoxic glucosyltransferases produced by *Legionella pneumophila*. Journal of Bacteriology **190:**3026-3035.

664. **Hurtado-Guerrero R, Zusman T, Pathak S, Ibrahim AF, Shepherd S, Prescott A, Segal G, van Aalten DM.** 2010. Molecular mechanism of

elongation factor 1A inhibition by a *Legionella pneumophila* glycosyltransferase. The Biochemical Journal **426:**281-292.

665. **Ramakrishnan V.** 2002. Ribosome structure and the mechanism of translation. Cell **108:**557-572.

666. **Mateyak MK, Kinzy TG.** 2010. eEF1A: thinking outside the ribosome. Journal of Biological Chemistry **285:**21209-21213.

667. **Hotokezaka Y, Tobben U, Hotokezaka H, Van Leyen K, Beatrix B, Smith DH, Nakamura T, Wiedmann M.** 2002. Interaction of the eukaryotic elongation factor 1A with newly synthesized polypeptides. Journal of Biological Chemistry **277:**18545-18551.

668. **Chuang SM, Chen L, Lambertson D, Anand M, Kinzy TG, Madura K.** 2005. Proteasome-mediated degradation of cotranslationally damaged proteins involves translation elongation factor 1A. Molecular and Cellular Biology **25:**403-413.

669. **Abbas W, Kumar A, Herbein G.** 2015. The eEF1A Proteins: At the Crossroads of Oncogenesis, Apoptosis, and Viral Infections. Frontiers in Oncology **5:**75.

670. **Blanch A, Robinson F, Watson IR, Cheng LS, Irwin MS.** 2013. Eukaryotic translation elongation factor 1-alpha 1 inhibits p53 and p73 dependent apoptosis and chemotherapy sensitivity. PloS ONE **8:**e66436.

671. **Deng W, Yu HB, de Hoog CL, Stoynov N, Li Y, Foster LJ, Finlay BB.** 2012. Quantitative proteomic analysis of type III secretome of enteropathogenic *Escherichia coli* reveals an expanded effector repertoire for attaching/effacing bacterial pathogens. Molecular & Cellular Proteomics : MCP **11:**692-709.

672. **Mills E, Baruch K, Aviv G, Nitzan M, Rosenshine I.** 2013. Dynamics of the type III secretion system activity of enteropathogenic *Escherichia coli*. mBio **4**.

673. **Mills E, Baruch K, Charpentier X, Kobi S, Rosenshine I.** 2008. Real-time analysis of effector translocation by the type III secretion system of enteropathogenic *Escherichia coli*. Cell Host & Microbe **3:**104-113.

674. **Burkinshaw BJ, Strynadka NC.** 2014. Assembly and structure of the T3SS. Biochimica et Biophysica Acta **1843:**1649-1663.

675. **Feldman MF, Cornelis GR.** 2003. The multitalented type III chaperones: all you can do with 15 kDa. FEMS Microbiology Letters **219:**151-158.

676. **Shi J, Blundell TL, Mizuguchi K.** 2001. FUGUE: sequence-structure homology recognition using environment-specific substitution tables and structure-dependent gap penalties. Journal of Molecular Biology **310:**243-257.

677. **Gerrard J, Waterfield N, Vohra R, ffrench-Constant R.** 2004. Human infection with *Photorhabdus asymbiotica*: an emerging bacterial pathogen. Microbes and Infection **6:**229-237.

678. **Jank T, Bogdanovic X, Wirth C, Haaf E, Spoerner M, Bohmer KE, Steinemann M, Orth JH, Kalbitzer HR, Warscheid B, Hunte C, Aktories K.** 2013. A bacterial toxin catalyzing tyrosine glycosylation of Rho and deamidation of Gq and Gi proteins. Nature Structural & Molecular Biology **20:**1273-1280.

679. **Anderson DM, Fouts DE, Collmer A, Schneewind O.** 1999. Reciprocal secretion of proteins by the bacterial type III machines of plant and animal pathogens suggests universal recognition of mRNA targeting signals. Proceedings of the National Academy of Sciences of the United States of America **96:**12839-12843.

680. **Anderson DM, Schneewind O.** 1997. A mRNA signal for the type III secretion of Yop proteins by *Yersinia enterocolitica*. Science **278:**1140-1143.

681. **Anderson DM, Schneewind O.** 1999. *Yersinia enterocolitica* type III secretion: an mRNA signal that couples translation and secretion of YopQ. Molecular Microbiology **31:**1139-1148.

682. **Ramamurthi KS, Schneewind O.** 2003. *Yersinia* yopQ mRNA encodes a bipartite type III secretion signal in the first 15 codons. Molecular Microbiology **50:**1189-1198.

683. **Sorg JA, Miller NC, Schneewind O.** 2005. Substrate recognition of type III secretion machines--testing the RNA signal hypothesis. Cellular Microbiology **7:**1217-1225.

684. **Buetow L, Smith TK, Dawson A, Fyffe S, Hunter WN.** 2007. Structure and reactivity of LpxD, the *N*-acyltransferase of lipid A biosynthesis. Proceedings of the National Academy of Sciences of the United States of America **104:**4321-4326.

685. **D'Urzo N, Malito E, Biancucci M, Bottomley MJ, Maione D, Scarselli M, Martinelli M.** 2012. The structure of *Clostridium difficile* toxin A glucosyltransferase domain bound to Mn2+ and UDP provides insights into glucosyltransferase activity and product release. The FEBS Journal **279:**3085-3097.

686. **Pruitt RN, Chumbler NM, Rutherford SA, Farrow MA, Friedman DB, Spiller B, Lacy DB.** 2012. Structural determinants of *Clostridium difficile* toxin A glucosyltransferase activity. Journal of Biological Chemistry **287:**8013-8020.

687. **Lazarus MB, Nam Y, Jiang J, Sliz P, Walker S.** 2011. Structure of human *O*-GlcNAc transferase and its complex with a peptide substrate. Nature **469:**564-567.

688. **Moréra S, Imberty A, Aschke-Sonnenborn U, Rüger W, Freemont PS.** 1999. T4 phage β-glucosyltransferase: substrate binding and proposed catalytic mechanism. Journal of Molecular Biology **292:**717-730.

689. **Raman J, Fritz TA, Gerken TA, Jamison O, Live D, Liu M, Tabak LA.** 2008. The catalytic and lectin domains of UDP-GalNAc:polypeptide α-*N*-Acetylgalactosaminyltransferase function in concert to direct glycosylation site selection. Journal of Biological Chemistry **283:**22942-22951.

690. **Soya N, Shoemaker GK, Palcic MM, Klassen JS.** 2009. Comparative study of substrate and product binding to the human ABO(H) blood group glycosyltransferases. Glycobiology **19:**1224-1234.

691. **Sun HY, Lin SW, Ko TP, Pan JF, Liu CL, Lin CN, Wang AH, Lin CH.** 2007. Structure and mechanism of *Helicobacter pylori* fucosyltransferase. A basis for lipopolysaccharide variation and inhibitor design. Journal of Biological Chemistry **282:**9973-9982.

692. **De Azevedo WF, Jr., Dias R.** 2008. Experimental approaches to evaluate the thermodynamics of protein-drug interactions. Current Drug Targets **9:**1071-1076.

693. **Ghai R, Falconer RJ, Collins BM.** 2012. Applications of isothermal titration calorimetry in pure and applied research--survey of the literature from 2010. Journal of Molecular Recognition : JMR **25:**32-52.

694. **Liang Y.** 2008. Applications of isothermal titration calorimetry in protein science. Acta Biochimica et Biophysica Sinica **40:**565-576.

695. **Figueroa-Bossi N, Bossi L.** 2004. Resuscitation of a defective prophage in *Salmonella* cocultures. Journal of Bacteriology **186:**4038-4041.

696. **McClelland M, Sanderson KE, Spieth J, Clifton SW, Latreille P, Courtney L, Porwollik S, Ali J, Dante M, Du F, Hou S, Layman D, Leonard S, Nguyen C, Scott K, Holmes A, Grewal N, Mulvaney E, Ryan E, Sun H, Florea L, Miller W, Stoneking T, Nhan M, Waterston R,**

Wilson RK. 2001. Complete genome sequence of *Salmonella enterica* serovar Typhimurium LT2. Nature **413:**852-856.

697. **Wilmes-Riesenberg MR, Foster JW, Curtiss R, 3rd.** 1997. An altered *rpoS* allele contributes to the avirulence of Salmonella typhimurium LT2. Infection and Immunity **65:**203-210.

698. **Jiang X, Rossanese OW, Brown NF, Kujat-Choy S, Galan JE, Finlay BB, Brumell JH.** 2004. The related effector proteins SopD and SopD2 from *Salmonella enterica* serovar Typhimurium contribute to virulence during systemic infection of mice. Molecular Microbiology **54:**1186-1198.

699. **Brumell JH, Kujat-Choy S, Brown NF, Vallance BA, Knodler LA, Finlay BB.** 2003. SopD2 is a novel type III secreted effector of *Salmonella typhimurium* that targets late endocytic compartments upon delivery into host cells. Traffic **4:**36-48.

700. **D'Costa VM, Braun V, Landekic M, Shi R, Proteau A, McDonald L, Cygler M, Grinstein S, Brumell JH.** 2015. *Salmonella* Disrupts Host Endocytic Trafficking by SopD2-Mediated Inhibition of Rab7. Cell reports **12:**1508-1518.

701. **Bakshi CS, Singh VP, Wood MW, Jones PW, Wallis TS, Galyov EE.** 2000. Identification of SopE2, a *Salmonella* secreted protein which is highly homologous to SopE and involved in bacterial invasion of epithelial cells. Journal of Bacteriology **182:**2341-2344.

702. **Friebel A, Ilchmann H, Aepfelbacher M, Ehrbar K, Machleidt W, Hardt WD.** 2001. SopE and SopE2 from *Salmonella typhimurium* activate different sets of RhoGTPases of the host cell. Journal of Biological Chemistry **276:**34035-34040.

703. **Bishop AL, Hall A.** 2000. Rho GTPases and their effector proteins. The Biochemical Journal **348 Pt 2:**241-255.

704. **Van Aelst L, D'Souza-Schorey C.** 1997. Rho GTPases and signaling networks. Genes & Development **11:**2295-2322.

705. **Pelludat C, Mirold S, Hardt WD.** 2003. The SopEΦ phage integrates into the *ssrA* gene of *Salmonella enterica* serovar Typhimurium A36 and is closely related to the Fels-2 prophage. Journal of Bacteriology **185:**5182-5191.

706. **Mirold S, Rabsch W, Rohde M, Stender S, Tschape H, Russmann H, Igwe E, Hardt WD.** 1999. Isolation of a temperate bacteriophage encoding the type III effector protein SopE from an epidemic *Salmonella typhimurium* strain.

Proceedings of the National Academy of Sciences of the United States of America **96:**9845-9850.

707. **Brumell JH, Goosney DL, Finlay BB.** 2002. SifA, a type III secreted effector of *Salmonella typhimurium*, directs *Salmonella*-induced filament (Sif) formation along microtubules. Traffic **3:**407-415.

708. **Freeman JA, Ohl ME, Miller SI.** 2003. The *Salmonella enterica* serovar typhimurium translocated effectors SseJ and SifB are targeted to the Salmonella-containing vacuole. Infection and Immunity **71:**418-427.

709. **Knodler LA, Vallance BA, Hensel M, Jackel D, Finlay BB, Steele-Mortimer O.** 2003. *Salmonella* type III effectors PipB and PipB2 are targeted to detergent-resistant microdomains on internal host cell membranes. Molecular Microbiology **49:**685-704.

710. **Yang Z, Soderholm A, Wong Fok Lung T, Giogha C, Hill MM, Brown NF, Hartland E, Teasdale RD.** 2015. SseK3 Is a *Salmonella* Effector That Binds TRIM32 and Modulates the Host's NF-κB Signalling Activity. PloS ONE **10:**e0138529.

711. **Albor A, El-Hizawi S, Horn EJ, Laederich M, Frosk P, Wrogemann K, Kulesz-Martin M.** 2006. The interaction of Piasy with Trim32, an E3-ubiquitin ligase mutated in limb-girdle muscular dystrophy type 2H, promotes Piasy degradation and regulates UVB-induced keratinocyte apoptosis through NFkappaB. Journal of Biological Chemistry **281:**25850-25866.

712. **Kudryashova E, Kudryashov D, Kramerova I, Spencer MJ.** 2005. Trim32 is a ubiquitin ligase mutated in limb girdle muscular dystrophy type 2H that binds to skeletal muscle myosin and ubiquitinates actin. Journal of Molecular Biology **354:**413-424.

713. **Arango Duque G, Descoteaux A.** 2014. Macrophage cytokines: involvement in immunity and infectious diseases. Frontiers in Immunology **5:**491.

714. **Cavaillon JM.** 1994. Cytokines and macrophages. Biomedicine & pharmacotherapy = Biomedecine & Pharmacotherapie **48:**445-453.

715. **Nordgård O, Dahle Ø, Andersen TØ, Gabrielsen OS.** 2001. JAB1/CSN5 interacts with the GAL4 DNA binding domain: a note of caution about two-hybrid interactions. Biochimie **83:**969-971.

716. **Kidwai AS, Mushamiri I, Niemann GS, Brown RN, Adkins JN, Heffron F.** 2013. Diverse secreted effectors are required for *Salmonella* persistence in a mouse infection model. PloS ONE **8:**e70753.

717. **Vidal S, Tremblay ML, Govoni G, Gauthier S, Sebastiani G, Malo D, Skamene E, Olivier M, Jothy S, Gros P.** 1995. The Ity/Lsh/Bcg locus: natural resistance to infection with intracellular parasites is abrogated by disruption of the Nramp1 gene. The Journal of Experimental Medicine **182:**655-666.

718. **Vidal SM, Pinner E, Lepage P, Gauthier S, Gros P.** 1996. Natural resistance to intracellular infections: Nramp1 encodes a membrane phosphoglycoprotein absent in macrophages from susceptible (Nramp1 D169) mouse strains. Journal of Immunology **157:**3559-3568.

719. **Buckner MM, Croxen MA, Arena ET, Finlay BB.** 2011. A comprehensive study of the contribution of *Salmonella enterica* serovar Typhimurium SPI2 effectors to bacterial colonization, survival, and replication in typhoid fever, macrophage, and epithelial cell infection models. Virulence **2:**208-216.

720. **Ryu YS, Lee Y, Lee KW, Hwang CY, Maeng JS, Kim JH, Seo YS, You KH, Song B, Kwon KS.** 2011. TRIM32 protein sensitizes cells to tumor necrosis factor (TNFalpha)-induced apoptosis via its RING domain-dependent E3 ligase activity against X-linked inhibitor of apoptosis (XIAP). Journal of Biological Chemistry **286:**25729-25738.

721. **Schwamborn JC, Berezikov E, Knoblich JA.** 2009. The TRIM-NHL protein TRIM32 activates microRNAs and prevents self-renewal in mouse neural progenitors. Cell **136:**913-925.

722. **Gonzalez-Cano L, Hillje AL, Fuertes-Alvarez S, Marques MM, Blanch A, Ian RW, Irwin MS, Schwamborn JC, Marin MC.** 2013. Regulatory feedback loop between TP73 and TRIM32. Cell Death & Disease **4:**e704.

723. **Fridell RA, Harding LS, Bogerd HP, Cullen BR.** 1995. Identification of a novel human zinc finger protein that specifically interacts with the activation domain of lentiviral Tat proteins. Virology **209:**347-357.

724. **Fu B, Wang L, Ding H, Schwamborn JC, Li S, Dorf ME.** 2015. TRIM32 Senses and Restricts Influenza A Virus by Ubiquitination of PB1 Polymerase. PLoS Pathogens **11:**e1004960.

725. **Reymond A, Meroni G, Fantozzi A, Merla G, Cairo S, Luzi L, Riganelli D, Zanaria E, Messali S, Cainarca S, Guffanti A, Minucci S, Pelicci PG, Ballabio A.** 2001. The tripartite motif family identifies cell compartments. EMBO Journal **20:**2140-2151.

726. **Slack FJ, Ruvkun G.** 1998. A novel repeat domain that is often associated with RING finger and B-box motifs. Trends in Biochemical Sciences **23:**474-475.

727. **Horn EJ, Albor A, Liu Y, El-Hizawi S, Vanderbeek GE, Babcock M, Bowden GT, Hennings H, Lozano G, Weinberg WC, Kulesz-Martin M.** 2004. RING protein Trim32 associated with skin carcinogenesis has anti-apoptotic and E3-ubiquitin ligase properties. Carcinogenesis **25:**157-167.

728. **Shuai K, Liu B.** 2005. Regulation of gene-activation pathways by PIAS proteins in the immune system. Nature Reviews Immunology **5:**593-605.

729. **Liu J, Zhang C, Wang XL, Ly P, Belyi V, Xu-Monette ZY, Young KH, Hu W, Feng Z.** 2014. E3 ubiquitin ligase TRIM32 negatively regulates tumor suppressor p53 to promote tumorigenesis. Cell Death and Differentiation **21:**1792-1804.

730. **Park HH, Lo YC, Lin SC, Wang L, Yang JK, Wu H.** 2007. The death domain superfamily in intracellular signaling of apoptosis and inflammation. Annual Review of Immunology **25:**561-586.

731. **Fujita Y, Hayashi T, Kiyomitsu T, Toyoda Y, Kokubu A, Obuse C, Yanagida M.** 2007. Priming of centromere for CENP-A recruitment by human hMis18α, hMis18β, and M18BP1. Developmental Cell **12:**17-30.

732. **Naegeli A, Michaud G, Schubert M, Lin CW, Lizak C, Darbre T, Reymond JL, Aebi M.** 2014. Substrate specificity of cytoplasmic *N*-glycosyltransferase. Journal of Biological Chemistry **289:**24521-24532.

733. **Naegeli A, Neupert C, Fan YY, Lin CW, Poljak K, Papini AM, Schwarz F, Aebi M.** 2014. Molecular analysis of an alternative *N*-glycosylation machinery by functional transfer from *Actinobacillus pleuropneumoniae* to *Escherichia coli*. Journal of Biological Chemistry **289:**2170-2179.

734. **Gross J, Grass S, Davis AE, Gilmore-Erdmann P, Townsend RR, St Geme JW, 3rd.** 2008. The *Haemophilus influenzae* HMW1 adhesin is a glycoprotein with an unusual *N*-linked carbohydrate modification. Journal of Biological Chemistry **283:**26010-26015.

735. **Brimer CD, Montie TC.** 1998. Cloning and comparison of *fliC* genes and identification of glycosylation in the flagellin of *Pseudomonas aeruginosa* a-type strains. Journal of Bacteriology **180:**3209-3217.

736. **Castric P.** 1995. *pilO*, a gene required for glycosylation of *Pseudomonas aeruginosa* 1244 pilin. Microbiology **141 (Pt 5):**1247-1254.

737. **Stimson E, Virji M, Makepeace K, Dell A, Morris HR, Payne G, Saunders JR, Jennings MP, Barker S, Panico M, et al.** 1995. Meningococcal pilin: a glycoprotein substituted with digalactosyl 2,4-diacetamido-2,4,6-trideoxyhexose. Molecular Microbiology **17:**1201-1214.

738. **Szymanski CM, Yao R, Ewing CP, Trust TJ, Guerry P.** 1999. Evidence for a system of general protein glycosylation in *Campylobacter jejuni*. Molecular Microbiology **32:**1022-1030.

739. **Bedford MT, Clarke SG.** 2009. Protein arginine methylation in mammals: who, what, and why. Molecular Cell **33:**1-13.

740. **Najbauer J, Johnson BA, Young AL, Aswad DW.** 1993. Peptides with sequences similar to glycine, arginine-rich motifs in proteins interacting with RNA are efficiently recognized by methyltransferase(s) modifying arginine in numerous proteins. Journal of Biological Chemistry **268:**10501-10509.

741. **Smith BC, Denu JM.** 2009. Chemical mechanisms of histone lysine and arginine modifications. Biochimica et Biophysica Acta **1789:**45-57.

742. **Cuthbert GL, Daujat S, Snowden AW, Erdjument-Bromage H, Hagiwara T, Yamada M, Schneider R, Gregory PD, Tempst P, Bannister AJ, Kouzarides T.** 2004. Histone deimination antagonizes arginine methylation. Cell **118:**545-553.

743. **Singh DG, Lomako J, Lomako WM, Whelan WJ, Meyer HE, Serwe M, Metzger JW.** 1995. β-Glucosylarginine: a new glucose-protein bond in a self-glucosylating protein from sweet corn. FEBS Letters **376:**61-64.

744. **Brockhausen I.** 2014. Crossroads between Bacterial and Mammalian Glycosyltransferases. Frontiers in Immunology **5:**492.

745. **Martinez-Fleites C, Macauley MS, He Y, Shen DL, Vocadlo DJ, Davies GJ.** 2008. Structure of an *O*-GlcNAc transferase homolog provides insight into intracellular glycosylation. Nature Structural & Molecular Biology **15:**764-765.

746. **Clarke AJ, Hurtado-Guerrero R, Pathak S, Schuttelkopf AW, Borodkin V, Shepherd SM, Ibrahim AF, van Aalten DM.** 2008. Structural insights into mechanism and specificity of *O*-GlcNAc transferase. EMBO Journal **27:**2780-2788.

747. **Soya N, Fang Y, Palcic MM, Klassen JS.** 2011. Trapping and characterization of covalent intermediates of mutant retaining glycosyltransferases. Glycobiology **21:**547-552.

748. **McMurry J.** 2014. Organic Chemistry with Biological Applications. Cengage Learning.

749. **Imperiali B, Shannon KL, Unno M, Rickert KW.** 1992. A mechanistic proposal for asparagine-linked glycosylation. Journal of the American Chemical Society **114:**7944-7945.

750. **Lizak C, Gerber S, Numao S, Aebi M, Locher KP.** 2011. X-ray structure of a bacterial oligosaccharyltransferase. Nature **474:**350-355.

751. **Ghiviriga I, El-Gendy Bel D, Steel PJ, Katritzky AR.** 2009. Tautomerism of guanidines studied by (15)N NMR: 2-hydrazono-3-phenylquinazolin-4(3H)-ones and related compounds. Organic & Biomolecular Chemistry **7:**4110-4119.

752. **Lazarus MB, Jiang J, Kapuria V, Bhuiyan T, Janetzko J, Zandberg WF, Vocadlo DJ, Herr W, Walker S.** 2013. HCF-1 is cleaved in the active site of *O*-GlcNAc transferase. Science **342:**1235-1239.

753. **Pathak S, Alonso J, Schimpl M, Rafie K, Blair DE, Borodkin VS, Schuttelkopf AW, Albarbarawi O, van Aalten DM.** 2015. The active site of *O*-GlcNAc transferase imposes constraints on substrate sequence. Nature Structural & Molecular Biology **22:**744-750.

754. **Schimpl M, Zheng X, Borodkin VS, Blair DE, Ferenbach AT, Schuttelkopf AW, Navratilova I, Aristotelous T, Albarbarawi O, Robinson DA, Macnaughtan MA, van Aalten DM.** 2012. *O*-GlcNAc transferase invokes nucleotide sugar pyrophosphate participation in catalysis. Nature Chemical Biology **8:**969-974.

755. **Kawai F, Grass S, Kim Y, Choi KJ, St Geme JW, 3rd, Yeo HJ.** 2011. Structural insights into the glycosyltransferase activity of the *Actinobacillus pleuropneumoniae* HMW1C-like protein. Journal of Biological Chemistry **286:**38546-38557.

756. **Thomas NA, Deng W, Puente JL, Frey EA, Yip CK, Strynadka NC, Finlay BB.** 2005. CesT is a multi-effector chaperone and recruitment factor required for the efficient type III secretion of both LEE- and non-LEE-encoded effectors of enteropathogenic *Escherichia coli*. Molecular Microbiology **57:**1762-1779.

757. **Colley KJ.** 1997. Golgi localization of glycosyltransferases: more questions than answers. Glycobiology **7:**1-13.

758. **Pan M, Li S, Li X, Shao F, Liu L, Hu HG.** 2014. Synthesis of and specific antibody generation for glycopeptides with arginine *N*-GlcNAcylation. Angewandte Chemie **53:**14517-14521.

759. **Chaudhuri RR, Morgan E, Peters SE, Pleasance SJ, Hudson DL, Davies HM, Wang J, van Diemen PM, Buckley AM, Bowen AJ, Pullinger GD, Turner DJ, Langridge GC, Turner AK, Parkhill J, Charles IG, Maskell DJ, Stevens MP.** 2013. Comprehensive assignment of roles for *Salmonella*

Typhimurium genes in intestinal colonization of food-producing animals. PLoS Genetics **9:**e1003456.

760. **Cai Z, Jitkaew S, Zhao J, Chiang HC, Choksi S, Liu J, Ward Y, Wu LG, Liu ZG.** 2014. Plasma membrane translocation of trimerized MLKL protein is required for TNF-induced necroptosis. Nature Cell Biology **16:**55-65.

761. **Ogura Y, Ooka T, Iguchi A, Toh H, Asadulghani M, Oshima K, Kodama T, Abe H, Nakayama K, Kurokawa K, Tobe T, Hattori M, Hayashi T.** 2009. Comparative genomics reveal the mechanism of the parallel evolution of O157 and non-O157 enterohemorrhagic *Escherichia coli*. Proceedings of the National Academy of Sciences of the United States of America **106:**17939-17944.

762. **Ingle DJ, Tauschek M, Edwards DJ, Hocking DM, Pickard DJ, Azzopardi KI, Amarasena T, Bennett-Wood V, Pearson JS, Tamboura B, Antonio M, Ochieng JB, Oundo J, Mandomando I, Qureshi S, Ramamurthy T, Hossain A, Kotloff KL, Nataro JP, Dougan G, Levine MM, Robins-Browne RM, Holt KE.** 2016. Evolution of atypical enteropathogenic *E. coli* by repeated acquisition of LEE pathogenicity island variants. Nature Microbiology**:**15010.

763. **Heczko U, Carthy CM, O'Brien BA, Finlay BB.** 2001. Decreased apoptosis in the ileum and ileal Peyer's patches: a feature after infection with rabbit enteropathogenic *Escherichia coli* O103. Infection and Immunity **69:**4580-4589.

764. **Melo AR, Lasunskaia EB, de Almeida CM, Schriefer A, Kipnis TL, Dias da Silva W.** 2005. Expression of the virulence factor, BfpA, by enteropathogenic *Escherichia coli* is essential for apoptosis signalling but not for NF-κB activation in host cells. Scandinavian Journal of Immunology **61:**511-519.

Appendix

Supplementary Table 1. List of accession numbers used in the construction of the phylogenetic tree shown in Figure 5.2

Strain	Accession number	Genus	Pathotype/serovar
86-24	AIAK01000000	*Escherichia*	EHEC
11128	NC_013364	*Escherichia*	EHEC
12009	NC_013353	*Escherichia*	EHEC
14028S	CP001363	*Salmonella*	Typhimurium
2362-75-1	ADUL01000000	*Escherichia*	EPEC
B171	AAJX02000000	*Escherichia*	EPEC
C12_92-1	AIAE01000000	*Escherichia*	EPEC
C1214_90	AIAD01000000	*Escherichia*	EPEC
C154_11	AIAF01000000	*Escherichia*	EPEC
C155_11	AIAG01000000	*Escherichia*	EPEC
C157_11	AIAH01000000	*Escherichia*	EPEC
C161_11	AIAI01000000	*Escherichia*	EPEC
C166_11	AICF01000000	*Escherichia*	EPEC
C213_10	AIAL01000000	*Escherichia*	EPEC
C2130	AIAL01000000	*Escherichia*	EPEC
C2139_99	AIAM01000000	*Escherichia*	EPEC
C238_91	AIAN01000000	*Escherichia*	EPEC
C260_92	AIAO01000000	*Escherichia*	EPEC
C262	AIAP01000000	*Escherichia*	EPEC
C283_09	AIAQ01000000	*Escherichia*	EPEC
C295_10	AKNI01000000	*Escherichia*	EPEC
C342	AKNI01000000	*Escherichia*	EPEC
C343_08	AIAT01000000	*Escherichia*	EPEC
C347_93	AIAU01000000	*Escherichia*	EPEC
C354_03B	AIAW01000000	*Escherichia*	EPEC
C40_11	AIAX01000000	*Escherichia*	EPEC
C458_10	AIAZ01000000	*Escherichia*	EPEC
C496_10	AIBB01000000	*Escherichia*	EPEC
C497_10	AIBC01000000	*Escherichia*	EPEC
C527_94	AIBD01000000	*Escherichia*	EPEC
C58_11	AIBF01000000	*Escherichia*	EPEC
C581_05	AIBE01000000	*Escherichia*	EPEC
C586_05	AIBG01000000	*Escherichia*	EPEC
C639_08	AIBH01000000	*Escherichia*	EPEC
C652_10	AIBI01000000	*Escherichia*	EPEC
C654_09	AIBJ01000000	*Escherichia*	EPEC
C717_10	AIBK01000000	*Escherichia*	EPEC
C725_88	AIBL01000000	*Escherichia*	EPEC
C732_98	AIBM01000000	*Escherichia*	EPEC
C743_03	AIBN01000000	*Escherichia*	EPEC
C78_09C	AIBP01000000	*Escherichia*	EPEC

C792_92	AIBR01000000	*Escherichia*	EPEC
C799_92	AIBT01000000	*Escherichia*	EPEC
C80_08	AIBU0100000	*Escherichia*	EPEC
C82_11	AIBW01000000	*Escherichia*	EPEC
C842_97	AIBY01000000	*Escherichia*	EPEC
C87_11	AICA01000000	*Escherichia*	EPEC
C9_92	AICE0100000	*Escherichia*	EPEC
CB9615	CAS10779	*Escherichia*	EPEC
CT_02021853	CP001144	*Salmonella*	Dublin
CT_02021853	CP001144	*Salmonella*	Dublin
D23580	FN424405	*Salmonella*	Typhimurium
DEC11A	AIGV01000000	*Escherichia*	EPEC
DEC11B	AIGW01000000	*Escherichia*	EPEC
DEC11C	AIGX01000000	*Escherichia*	EHEC
DEC11C	AIGX01000000	*Escherichia*	EHEC
DEC11D	AIGY01000000	*Escherichia*	EPEC
DEC11E	AIGZ01000000	*Escherichia*	EPEC
DEC11E	AIGZ01000000	*Escherichia*	EPEC
DEC12A	AIHA01000000	*Escherichia*	EPEC
DEC12B	AIHB01000000	*Escherichia*	EPEC
DEC12C	AIHC01000000	*Escherichia*	EPEC
DEC12D	AIHD01000000	*Escherichia*	EPEC
DEC12E	AIHE01000000	*Escherichia*	EPEC
DEC1A	AIEV01000000	*Escherichia*	EPEC
DEC1B	AIEW01000000	*Escherichia*	EPEC
DEC1C	AIEX01000000	*Escherichia*	EPEC
DEC1D	AIEY01000000	*Escherichia*	EPEC
DEC1E	AIEZ01000000	*Escherichia*	EPEC
DEC2A	AIFA01000000	*Escherichia*	EPEC
DEC2B	AFJB01000000	*Escherichia*	EPEC
DEC2C	AIFB01000000	*Escherichia*	EPEC
DEC2E	AIFD01000000	*Escherichia*	EPEC
DEC4A	AIFK01000000	*Escherichia*	EPEC
DEC4B	AIFL01000000	*Escherichia*	EHEC
DEC4C	AIFM01000000	*Escherichia*	EPEC
DEC4D	AIFN01000000	*Escherichia*	EHEC
DEC4E	AIFO01000000	*Escherichia*	EPEC
DEC5A	AIFQ01000000	*Escherichia*	EPEC
DEC5B	AIFR01000000	*Escherichia*	EPEC
DEC5C	AIFS01000000	*Escherichia*	EPEC
DEC5D	AIFT01000000	*Escherichia*	EPEC
DEC5E	AIFU01000000	*Escherichia*	EPEC
DEC9A	AIGK01000000	*Escherichia*	EPEC
DEC9B	AIGL01000000	*Escherichia*	EPEC
DEC9C	AIGM01000000	*Escherichia*	EPEC

DEC9D	AIGN01000000	*Escherichia*	EPEC
DEC9E	AIGO01000000	*Escherichia*	EPEC
E22	AAJV02000000	*Escherichia*	EPEC
E2348/69	NC_011601	*Escherichia*	EPEC
EC4115	NC_011353	*Escherichia*	EHEC
EDL933	NC_002655	*Escherichia*	EHEC
EPECa14	ADUN01000000	*Escherichia*	EHEC
ICC168	WP_012905389	*Citrobacter*	*C. rodentium*
LT2	AE006468	*Salmonella*	Typhimurium
O26-H11	CAS10779	*Escherichia*	EHEC
OK1114	AICG01000000	*Escherichia*	EHEC
OK1180	ADUQ01000000	*Escherichia*	EHEC
P125109	AM933172	*Salmonella*	Enteritidis
RKS4594	CP000857	*Salmonella*	Paratyphi C
RM12579	CP003109	*Escherichia*	EPEC
RN587	ADUS01000000	*Escherichia*	EPEC
Sakai	NC_002695	*Escherichia*	EHEC
SARB27-1	CM001274	*Salmonella*	Infantis
SC-B67	AE017220	*Salmonella*	Choleraesuis
serovar62	CP000880.1	*Salmonella*	Arizonae
SL1344	FQ312003	*Salmonella*	Typhimurium
SL254	CP001113	*Salmonella*	Newport
SL476	CP001120	*Salmonella*	Heidelberg
SL483	CP001138	*Salmonella*	Agona
SPB7	CP000886	*Salmonella*	Paratyphi B
STEC_H.1.8	AFDY01000000	*Escherichia*	EHEC
TW14359	NC_013008	*Escherichia*	EHEC
Xuzhou21	CP001925	*Escherichia*	EHEC